ENGINEERED INFLATED SPHERICAL LACTOSE PARTICLE AND ITS POTENTIAL USE AS A CARRIER FOR DRY POWDER FORMULATION AEROSOLS

Ursula Thevarajah

A thesis submitted to the University of Huddersfield in partial fulfilment of the requirements for the award of the degree of Doctor of Philosophy

University of HUDDERSFIELD

JUNE 2018

Copyright statement

i. The author of this thesis (including any appendices and/or schedules to this thesis) owns any copyright in it (the "Copyright") and s/he has given The University of Huddersfield the right to use such copyright for any administrative, promotional, educational and/or teaching purposes.

ii. Copies of this thesis, either in full or in extracts, may be made only in accordance with the regulations of the University Library. Details of these regulations may be obtained from the Librarian. This page must form part of any such copies made.

iii. The ownership of any patents, designs, trademarks and any and all other intellectual property rights except for the Copyright (the "Intellectual Property Rights") and any reproductions of copyright works, for example graphs and tables ("Reproductions"), which may be described in this thesis, may not be owned by the author and may be owned by third parties. Such Intellectual Property Rights and Reproductions cannot and must not be made available for use without the prior written permission of the owner(s) of the relevant Intellectual Property Rights and/or Reproductions.

Abstract

Dry powder inhalation aerosol is usually formed by blending lactose carrier with micronized drug particles using an order mix. In this thesis, blends of either Salbutamol Sulphate (SS), Beclomethasone Dipropionate (BDP) or Fluticasone Propionate (FP) and coarse lactose particles were employed to investigate the effects of lactose morphological features on drug delivery by dry powder aerosols *in-vitro* or *ex-vivo* using recorded patients' inhalation profiles. Two lactose carriers were used in this study namely Lactohale and engineered lactose. Engineered lactose was prepared by a novel crystallisation technique from solid state using spray dried amorphous lactose prepared from lactose solution alone (10% w/v) or in the presence of additives (1% w/v) such as Polyvinyl Pyrrolidone (PVP K90) or sodium chloride (NaCl). A 10 g of amorphous spray dried particles (< 5 μm) were introduced to a boiled ethanolic solution (100 mL) under stirring for 10 seconds or 30 seconds to form crystalline spherical porous hollow particles at least 10-fold larger in size compared to spray dried particles. The increase in size was possibly due to a combination of factors; crystal growth and the ethanol vapour pressure increase inside the hollow volume facilitating particles inflation causing an increase in the hollow volume of the particles. This method of crystallisation is predictable in forming spherical particles irrespective of the additive. The particles contacted with ethanol for 30 seconds ($PSDL_{30}$) were more crystalline and rougher than those exposed for 10 seconds ($PSDL_{10}$) to ethanolic solution. The same process was successfully applied to lactose spray dried from a suspension to form large spherical particles with rougher surface compared to those spray dried from solution. The engineered lactose particles were rougher than Lactohale lactose and were found to mix rapidly to stabilize the DPI formulations against segregation when compared to smooth Lactohale as confirmed by drug content uniformity and tribo-electrification study. Drug deposition in-vitro was dependent on the physico-chemical properties of drug particles. For SS, high drug deposition was obtained when smooth lactose was used, thus the fine particle dose (FPD) was higher for Lactohale followed by $PSDL_{10}$ and finally $PSDL_{30}$ suggesting that drug deposition increased with surface smoothness. A different trend was observed with hydrophobic drugs such as BDP and FP. A nano-surface roughness was favourable for both hydrophobic drugs BDP and FP and the order of FPD was $PSDL_{10}$ > Lactohale > $PSDL_{30}$. A balanced drug roughness is needed for hydrophobic drugs to improve drug content uniformity and to facilitate drug detachment during aerosolisation. *Ex-vivo* study using four patient profiles having the same inhaled volume (Vin) and acceleration (ACIM) at the start of the inhalation manoeuvre but having different maximum inhalation flow (MIF) were used to study the aerodynamic dose emission characteristics of SS with lactohale and engineered lactose carrier produced from spray dried lactose formed from spray dried suspension of lactose, which is commercially available (PSDL com). PSDL com had the highest roughness in comparison to all carriers highlighted above and showed low FPD at all MIFs in comparison to Lactohale. This study confirmed again that smooth carrier such as Lactohale provides better drug deposition for hydrophilic drugs such as SS. In conclusion, the drug deposition study showed that there is no ideal carrier for all drugs with different physico-chemical properties such as hydrophilicity. To improve drug deposition from DPIs, hydrophilic

drugs are better formulated with a smooth carrier and hydrophobic drugs require a moderate surface roughness.

Acknowledgment

I would like to express my gratitude to everyone who guided and supported me throughout my Ph.D. I would like to express my most sincere appreciation to my supervisor, Dr. El Hassane Larhrib, for his guidance, support and trust during my research. I would also like to thank Prof. Barbara Conway for her support throughout my PhD. In addition, special thanks go to Dr. Richard Hughes and Ms Hayley Markham for their technical support and assistance.

I would like to thank all my friends for creating such a fun atmosphere and for the support given throughout my studies.

Finally, I would like to thank my parents and my siblings. You have been an amazing support system and no words can describe how grateful I am for everything you have done for me. Thank you.

Dedication

I would like to dedicate this thesis to my niece, Akshaya. You have always looked up to me and I would like to thank you for giving me the motivation to always do better.

Table of Contents

List of Figures

List of Tables

List of Abbreviations

°C	Degree Celcius
ΔP	Pressure Drop
ACI	Andersen Cascade Impactor
ACIM	Initial acceleration Rate of Inhalation Manoeuvre
AIT	Alberta Idealised Throat
AUC	Area Under Curve
BP	British Pharmacopoeia
BRS	Breath Simulator
BDP	Beclomethasone Dipropionate
cmH_20	Centimetre of water
CFC	Chlorofluorocarbons
COPD	Chronic Obstructive Pulmonary Disease
CV	Coefficient Variation
DPIs	Dry Powder Inhalers
EFPD	Extra Fine Particle Dose
EP	European Pharmacopoeia
FP	Fluticasone Propionate
FPD	Fine Particle Dose
FPF	Fine Particle Fraction
g	Gram
GSD	Geometric Standard Deviation
HFA	Hydrofluoro-alkanes
HPLC	High Performance Liquid Chromatography
IP	Inhalation Profile

kPa	Kilopascal
L	Litre
L/min	Litre per Minute
LOD	Limit of Detection
LOQ	Limit of Quantification
LPM	Large Particle Mass
L/s^2	Litre per Second Square
MDI	Meter Dose Inhaler
m^2	Meter Squared
mm	Millimetre
mM	Millimolar
mg	Milligram
MgSt	Magnesium Stearate
MIF	Maximum Inhalation Flow
MMAD	Mass Median Aerodynamic Diameter
MP	Mouth Piece
mL	Millilitre
mL/min	Millilitre per Minute
m/s	Metre per Second
NaCl	Sodium Chloride
NGI	Next Generation Impactor
pMDIs	Pressurized Meter Dose Inhalers
PIF	Peak Inhalation Flow
PIL	Patient Information Leaflet
PS	Pre-Separator

PSDL	Processed Spray Dried Lactohale
PVP	Polyvinylpyrrolidone
Q	Flow Rate
R	Resistance
R^2	Correlation Coefficient
Re	Reynolds Number
RA_{cap}	Residual Amount in Capsule
RA_{dev}	Residual Amount in Device
RSD	Relative Standard Deviation
RV	Residual Volume
S	Second
SD	Standard Deviation
SDL	Spray-Dried Lactohale
SS	Salbutamol Sulphate
TED	Total Emitted Dose
TRA	Total Residual Amount
TRD	Total Recovered Dose
USP	United States Pharmacopoeia
v/w	Volume per Weight
V_{in}	Inhaled Volume
µg	Microgram
µg/mL	Microgram per Millilitre
µL	Microlitre
µm	Micrometre

Chapter 1. Introduction

1.1 Background

Pulmonary drug delivery is the preferred mode of drug delivery for numerous conditions such as asthma and chronic obstructive pulmonary disease (COPD). An advantage of pulmonary drug delivery is the direct targeting of the drug to the lungs, which is why it has become one of the preferred routes to administer large molecules that are subject to first-pass metabolism in the liver. Pulmonary drug delivery also requires a relatively low drug dose to produce the desired effect and offers a rapid onset with minimal side effects (Byron and Patton., 1994)

Drug delivery to the lungs is not only applicable for pulmonary diseases but can also be used to treat cancer; diabetes; cystic fibrosis that can also affect the liver, pancreas and kidney; osteoporosis and thrombosis (Brocklebank et al., 2002; Chougule et al., 2006; Haynes et al., 2003; Laube et al., 2011; Thomas et al., 1991; Hickey et al., 2004; Kawashima et al., 2005; Yang et al., 2004). Islam et al. evaluated the potential to use pulmonary drug delivery for the management of some neurological diseases such as Parkinson and Alzheimer's disorders (Islam & Rahman, 2008).

Several devices are available to target the delivery of drugs to the lungs. There are three main types of inhalers present in the market for that purpose, which are nebulizers, metered-dose inhalers (MDIs) and dry powder inhalers (DPIs). The difference between these devices lies in their mechanisms of delivering the drug into the lungs (Groneberg et al., 2003)

Most DPIs are breath-actuated devices (Brocklebank et al., 2001). They do not require coordination between actuation and inhalation, which makes them easy to use for the patient. As opposed to other inhalers, DPIs do not use liquid propellants. They are patient friendly, environmentally friendly and portable (not requiring the use of spacers) (Bunnag et al., 2007; Siddiqui & Plosker, 2005).

DPI formulations are made of drug particles blended with a suitable large carrier such as lactose. The main advantage of adding carrier particles to the formulation is to increase the bulk of the formulation improving the reproducibility of dose delivery. It also aids in reducing the cohesiveness of the micronized drug particle and improves the flow properties of the drug-carrier formulation (Prime, 1997). The drug particles usually adhere onto the surface of lactose (Hersey, 1974). In order to achieve an efficient delivery of the aerosol into the lungs from DPI formulations, adhesive forces between the drug and carrier have to be overcome, resulting in dispersion of the particles and deposition of the drug particles in the deep regions of the lungs Islam et al., 2004b). Three inter-related parameters play a significant role in efficient delivery of drug via the pulmonary route: the design of the device, the powder formulation and the inhalation manoeuvers of the patient (Chougule et al., 2007; Frijlink and de Boer, 2005).

Most DPI formulations available on the market are only able to deliver about 20-30% of the total dose to the lungs (Smith and Parry-Billings, 2003; Steckel and Müller, 1997). This low efficacy is caused by the complicated physiology of the respiratory tract, the physico-chemical properties of the components in the powder formulation and the inhalation device. There can be inefficient separation of the drug from the carrier because the micronized drug particles, which are adhered onto the surface of the carrier, produce agglomerates. To deliver the drug efficiently, the drug has to be dispersed from these agglomerates Islam et al., 2004b).
Commercially available inhalation grade lactose is irregular in shape and has asperities in its surface, which affects separation of drug from carrier during aerosolisation. Controlling the particle size, shape and surface roughness of the carrier particles is important in order to achieve an efficient drug detachment from the carrier particles (French et al., 1996; Steckel & Müller, 1997; Zeng et al., 2000).

Many studies have investigated factors that impact the delivery of drugs into the lungs. These studies mainly focused on improving dispersion of the pharmaceutical active ingredient (API) by optimizing the physico-chemical properties of the lactose carrier such as particle size (Larhrib et al., 1999), shape and surface texture (Kawashima et al., 1998b; Zeng et al., 2000), and mixing different grades of lactose (Bergström et al., 2000; Steckel & Müller, 1997). Some studies demonstrated that modifying the carrier surfaces improved the dispersibility of the drug from the surface of lactose. Many approaches have been used to achieve this result: one of the techniques used was to coat the surface of the lactose carrier by physically blending it with fine lactose particles, magnesium stearate or L-leucine (Grosvenor & Staniforth, 1996; Staniforth et al., 1999; Staniforth, 1997; Staniforth, 1995).

Common techniques used to modify the shape of the carrier particles include spray drying (Chew et al., 2005), encapsulation (Yue et al., 2004) and mechanofusion (Begat et al., 2005). It is well known that particles with curved surfaces, small asperities and low surface energy tend to reduce the contact area between particles (Katainen et al., 2006; Li et al., 2006; Podczeck, 1999).

Particles with irregular shapes, such as commercially available Lactohale®, have many contact points leading to more cohesive forces than spherical particles. Irregular particles tend to interlock, which can compromise powder flow properties. Spherical particles have fewer contact points, which usually results in improved powder fluidity and potentially can be suitable shape for carrier particles in DPI formulations. Spherical particles produced by spray drying have been shown to achieve a higher deposition of the drug, Prankulast Hydrate, with a fine particle fraction of 17.8% compared to irregular lactose, which only achieved FPF of 3.4-14.7% (Kawashima et al., 1998a).

Therefore, producing carrier particles with a specific shape and surface texture may have potential in improving the efficacy of drug delivery with DPIs (Zeng et al., 2000).

1.2 Aims and objectives

1.2.1 Aims

The principal aim of this thesis is to investigate the potential of engineered particles (processed spray-dried Lactohale: PSDL) produced from solid-state crystallization as an alternative carrier to α-lactose monohydrate. A further aim was to investigate the influence of the carrier surface properties on their interaction with drug particles for the development of dry powder formulations and to target maximum drug delivery to the deepest regions of the lung. Furthermore, it was the purpose of this thesis to extend this crystallization process to produce lactose carrier particles coated with a ternary component in particles suitable for inhalation. In addition, triboelectrification studies were performed to study the magnitude of the interactions between drug and carrier particles.

Another aim of this study was to investigate the effect of the inhalation manoeuver parameters such as maximum inhalation flow rate (MIF), inhaled volume (Vin) and the initial acceleration rate of inhalation manoeuver (ACIM) on the aerodynamic characteristics of the emitted dose of SS from Onbrez Breezhaler® using patient profiles.

1.2.2 Objectives

The objectives of this study were:

- ✓ To modify and validate a High-Performance Liquid Chromatography (HPLC) method for salbutamol sulphate based on the USP method
- ✓ To engineer a novel lactose carrier in the presence of an inflating agent in the crystallisation medium to produce large hollow spherical carrier particles for inhalation (PSDL)
- ✓ To investigate the mechanism by which PSDL particles are formed
- ✓ To characterize PSDL particles using various analytical techniques.

- ✓ To assess the effect of a ternary component in DPI formulations (NaCl and PVP) and determine their effect on the dose emission characteristics of SS formulation from MacHaler®.
- ✓ To assess the difference in aerosolisation behavior between the Andersen Cascade Impactor (ACI) and the Next Generation Impactor (NGI)
- ✓ To assess the difference between the dose emission characteristics using two different impactors (ACI and NGI) at different MIF and Vin.
- ✓ To measure the drug content uniformity of SS, FP and BDP in both Lactohale and PSDL formulations and investigate the effect of mixing time on the deposition performance of the DPI formulation.
- ✓ To evaluate the effect of MIF and Vin on the dose emission of SS emitted from a MacHaler® using two different MIFs and Vins with both lactohale and PSDL formulations.
- ✓ To use an ex-vivo method with inhalation profiles to assess the effects of the inhalation manoeuver parameter (MIF, Vin, ACIM) on the aerodynamic dose emission characteristics of SS from a low resistance device: BreezeHaler®.

1.3 Thesis structure

This thesis consists of eight chapters:

Chapter 1 is a general introduction on pulmonary drug delivery with a focus on DPIs and the factors affecting drug de-aggregation and deposition. It also outlines the importance of carrier parameters selection during particle engineering and formulation.

Chapter 2 offers an overview of the respiratory system, the related pulmonary diseases, different types of inhalers used in the treatment of such diseases. The chapter will focus more on DPIs and their dose emission, it also outlines the factors that can affect drug de-aggregation and deposition into the lung. In addition, previous studies are reviewed to demonstrate the flow

dependency of DPIs, and recent modified pharmacopoeia methodology and patient inhalation characteristics are highlighted.

Chapter 3 reviews the materials and equipment which were used during the experimental studies. It also describes the HPLC method development and validation for the quantification of salbutamol sulphate.

Chapter 4 describes the solid-state crystallisation method used to produce PSDL particles. It also provides a detailed characterisation of the lactose carrier particles used in this study as well as the *in-vitro* dose emission performance of SS formulations with both Lactohale and PSDL carriers using two different MIFs (60 L/min and 90L/min) and different Vins (1L and 2L) using both ACI and NGI.

Chapter 5 presents an *in-vitro* comparison between SS formulations with PSDL and with PSDL formulated with a ternary component (NaCl and PVP). The impact of adding a ternary component in the DPI formulation was assessed.

Chapter 6 discusses the effects of mixing time on the homogeneity and dispersion performance of DPI formulations as well as the impact of the carrier surface morphology. Furthermore, the impact of triboelectric forces on in-vitro drug deposition was studied.

Chapter 7 explores the effect of inhalation profiles characteristics on the *ex-vivo* dose emission characteristics for two DPI formulations.

Chapter 8 provides a general conclusion for this thesis and finally some suggestions for future work.

Chapter 2. Literature Review

This chapter provides a review of the literature related to pulmonary drug delivery. It summaries the structure of the respiratory system and outlines the mechanisms of drug deposition in the lungs. It also emphasizes the importance of the carrier in DPI formulations. This chapter also introduces the aspects of drug delivery from DPI systems, which include the device and the formulation properties. This chapter highlights the importance of lactose particles' surface characteristics, which can potentially affect drug delivery and outlines the ternary components used in DPI formulations discussing the use of engineered lactose particles as carriers for DPIs.

2.1 Introduction to inhalation drug delivery

The lung is considered as being ideal to deliver drugs systemically because it has a large surface area (about 100 m^2), it is well-vascularized (5L/min of blood supply), the epithelium of the alveolar are thin (0.1-0.2μm), which allows good solute exchange (Rahimpour & Hamishehkar, 2012), and also because inhalation generates a rapid systemic onset.

The common advantages of pulmonary drug delivery are listed below (Chrystyn, 2006).

- Low doses of drugs used (typical salbutamol inhaled dose is 200μg whereas salbutamol dose orally is 4mg)
- High local targeting
- Low systemic concentration, decreasing toxicity
- Bypass first-pass metabolism
- Effective and rapid onset of action
- Low enzymatic activity as opposed to the liver, making the lungs suitable for protein and peptide delivery
- High specific surface area

Drug deposition via the pulmonary route is primarily controlled by the aerodynamic diameter of the drug particles (Wolff & Dorato, 1993), where particles with an aerodynamic diameter in the range of 1-5 μm are expected to be deposited in the lung periphery. The performance of dry-powder products highly depends on the formulation, the inhaler device and on the patient. Dry powder mixtures are usually prepared by blending the micronized drug particles with larger carrier particles. The carrier characteristics play an important role on the aerosolization efficiency of the formulation; such characteristics include the particle size distribution, particle shape and surface properties. The main goal in the inhalation field is to achieve high and reproducible deposition in the lung. To do so, there is a need to select successfully the carrier particles and optimise processes carefully (Pilcer et al., 2012).

2.2 Pulmonary Delivery

2.2.1 Organization of the respiratory system

The lung is the main organ of breathing in humans. A schematic representation of the respiratory system is illustrated in Figure 2.1. The respiratory system can be classified into two components: the upper respiratory tract and lower respiratory tract (Fig. 2.1). The former comprises the nasal cavity, nose, larynx and pharynx. The main functions of the upper respiratory tract are to filter and clear unwanted particles, warm and humidify the inhaled air. When air is inspired, it is heated from the normal atmospheric air conditions of 20 °C and 50 % moisture to 37°C and 99% moisture (Waldron, 2007). The lower respiratory system consists of the trachea, bronchi, bronchioles and alveoli, which cool and dehumidifies the air being exhaled (Martini & Nath, 2009).

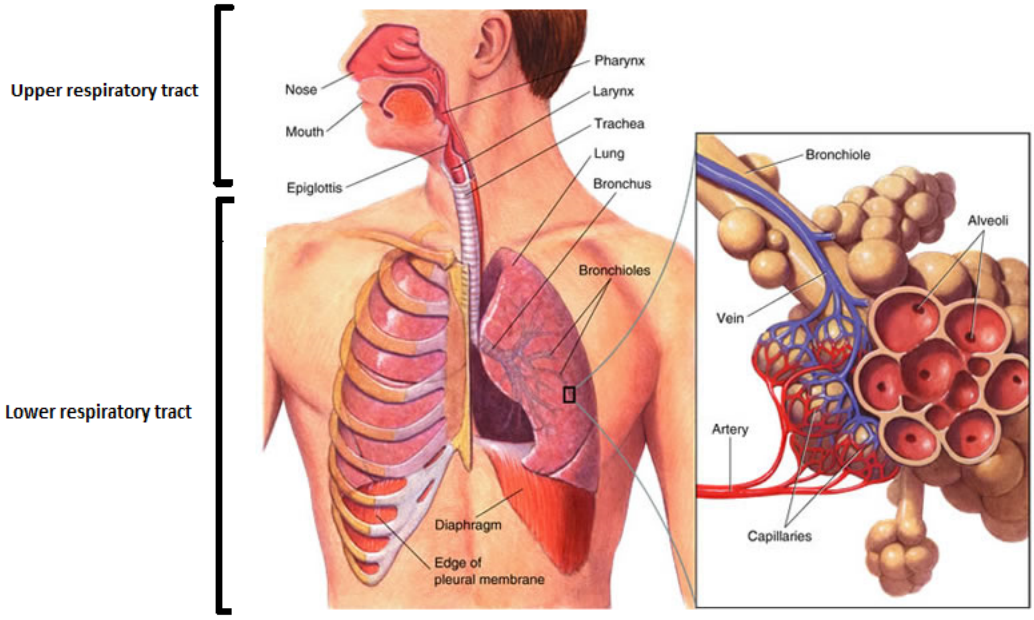

Figure 2.1 Schematic illustration of the human respiratory system (modified from https://www.pdhpe.net/the-body-in-motion/how-do-the-musculoskeletal-and-cardiorespiratory-systems-of-the-body-influence-and-respond-to-movement/respiratory-system/structure-and-function, accessed October 2017)

The respiratory tract is made of a conduction tract and a respiratory tract. According to Weibel's tracheobronchial organization (Fig. 2.2), the first 16 branches (or generations) characterise the conductive airways and branches 17 to 23 represent the respiratory portion where most of gas exchanges between air and blood occurs (Weibel, 1963).

The 23 divisions increase significantly the airways' total cross-sectional area from the trachea to the alveoli (2.5 to 11800 cm^2, respectively) which consequently produces a lower velocity of airflow in the small airways. The conducting airways are shaped like an inverted tree composed of branches and tubes.

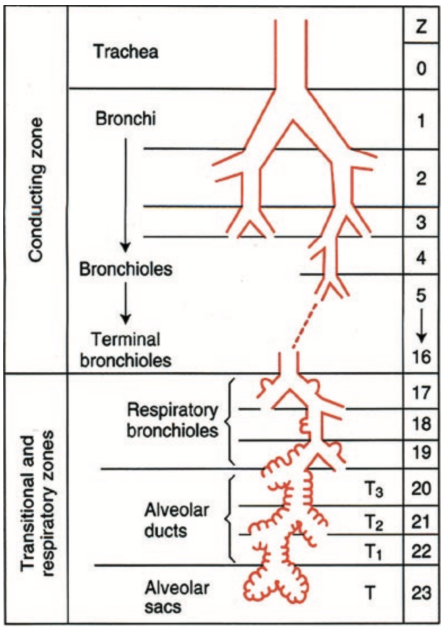

Figure 2.2 Structure of the Lungs showing the branching airways and their characteristics (Weibel, 1963)

As they go deeper in the lungs, the branches and tubes are more abundant, get narrower in diameter and have a thinner bronchial epithelium; these features allow gas exchanges to happen efficiently as the distance that separates the blood in alveolar capillary and the air inside an alveolus is only 1µm. Because filtering of the incoming air occurs in the upper respiratory tract, by the time the air gets to the alveoli, most pathogens and foreign particles would have been cleared out (Martini & Nath, 2009).

The principal role of the respiratory system is to offer a high surface area for gas exchanges between air and circulating blood through the respiratory passageways (Martini & Nath, 2009). On the other hand, the conducting tract consists of the area from the trachea and the terminal bronchioles down to branch 16. No gaseous exchange occurs in this zone due to the absence of alveoli. The conducting tract has two important functions; firstly, the inhaled air gets humidified and warmed, which will protect the alveoli by avoiding contact with dry cold air. Secondly, it allows air to be conducted down to the alveoli where gas exchange occurs. The muscles are situated in the conducting region where inflammation of the airways typically

happens. However, inflammations are also expected to occur in the respiratory region (Thomas et al., 2009) hence, particles less than 5μm are necessary to target these sites.

2.2.2 Brief overview of pulmonary diseases

Respiratory disorders, such as asthma and COPD, are characterized by a reduced rate of air into the lungs causing inflammation (Welte, 2009). Airway obstruction can be reversible for asthmatic patients; however, the airway obstruction of COPD patients is not fully reversible (Yawn, 2009). Asthma most commonly starts during childhood and the clinical symptoms vary between constant wheezing, cough or shortness of breath. In some cases, asthmatic symptoms reduce after childhood (Jenkins et al., 1994). On the other hand, COPD does not occur in children and young adults. Its prevalence increases substantially after the age of 40. Generally, COPD is related to intensive smoking habits, exposure to inhaled toxins or irritants (Yawn, 2009), Table 2.1 summarises the differences between asthma and COPD. Airway obstruction in asthma is associated with bronchial smooth muscle constriction and inflammation. In COPD, the airways obstruction results from cellular damage and mucus hypersecretion with more prominent inflammation (Decramer et al., 2005).

The acute symptoms related to asthma are usually treated with bronchodilators (β_2 adrenoreceptor agonists which can be classified in two categories: short-acting (e.g. Salbutamol and Terbutaline) and long-acting (e.g. salmeterol), Xanthines (e.g. theophylline, theobromine and caffeine), Muscarinic receptor antagonist (e.g. ipratropium) and corticosteroids (such as fluticasone, budesonide and bechlomethasone) (Yawn, 2009). A day-to-day variability is observed for COPD patients and the most common approach to reduce inflammation is to give them fast-acting bronchodilators and corticosteroids as combination drugs of either two long-acting bronchodilators or inhaled corticosteroid and a long-acting bronchodilator.

Table 2.1 Summary of some differences between asthma and COPD disease. (Adapted from NHS improvement program asthma, available at https://www.pharmaceutical-journal.com/learning/learning-article/knowing-the-differences-between-copd-and-asthma-is-vital-to-good-practice/11085597.article)

	Asthma	**COPD**
age	any age	40 years +
causes	genetic and environmental factors	result from smoking, genetic and environmental factors too
prognosis	symptoms are controlled, daily activities possible until old age	symptoms get worse over time. Patient rely on intensive health care services
predictability	disease progression not predictable	lung function deteriorates over time
aim of treatment	avoid asthma attacks, ameliorate normal lung function	slow down deterioration of lung function
treatments	inhaled corticosteroids, long acting bronchodilators, anti-inflammatory and anti-allergy drugs	combination therapy, bronchodilators with steroids, long term oxygen therapy
triggers	patient exposed to allergens, under-treatment	poor control of the disease

2.3 Drug deposition mechanisms

A pharmacological effect is observed only when inhaled drug particles are deposited at the site of action (Byron and Patton., 1994). The deposition of inhaled drug particles in the lungs is usually dependent on the aerodynamic particle size of the particles and is regulated by three physiological factors: inertial impaction, gravitational sedimentation and diffusion (via Brownian motion).

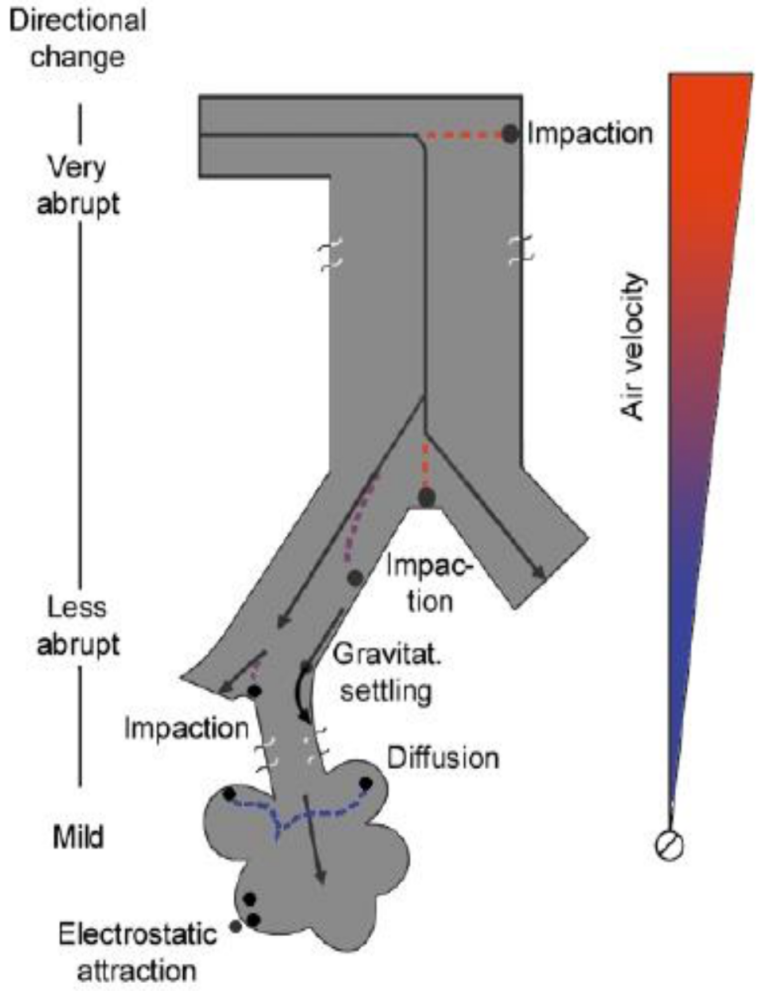

Figure 2.3 Schematic of the three mechanisms responsible for inhaled particle deposition in the respiratory airways (with permission from Hussain et al., 2011)

Inertial impaction is the primary mode of deposition of particles larger than 5μm, such as lactose carrier particles, in the oropharynx (Hinds, 1982). Such deposition primarily occurs when the gas airstream is rapid, changing direction (e.g. in the throat) or turbulent.

Sedimentation occurs for smaller particles between 1 to 5 μm in the lower respiratory tract (i.e. bronchial tree and alveoli). Inertial impaction occurs less and gravity become the main force in the deposition mechanism. The sedimentation efficiency is a function of aerodynamic diameter and residence time and occurs at low air velocity in the respiratory tract and when the residence time is great (Hinds, 1999). To be able to reach the alveolus tissue, the particle aerodynamic diameter needs to be between 1 to 3 μm.

Diffusion is the mode of deposition for particles below 0.5μm that cannot be deposited in the respiratory tract by sedimentation during normal breathing. These particles are subjected to diffusion forces (Brain and Blanchard, 1993; Zeng et al., 2000) but are mostly exhaled by the expiratory flow. The efficiency of diffusion and sedimentation is enhanced by high residence times that may be achieved by the patient when they are required to hold their breath (Hatch and Gross, 1964; Hinds, 1999).

Drug particles may acquire an electrostatic charge during aerosolisation (Yeomans et al., 1949). The charging of particles may have an effect on the deposition mechanisms either by attractive electrostatic forces between dissimilar charges on drug particles and the respiratory surface, or by repulsive forces between like-charged aerosol particles directing them towards the surface of the respiratory surface (Balásházy & Hofmann, 1995).

2.4 Expression used in inhaled drug delivery

2.4.1 Particle aerodynamic diameter

The deposition of the particles in the different levels of the respiratory tract is based on the aerodynamic size distribution of the particles. The aerodynamic diameter (d_{ae}) is defined as the diameter of a spherical particle with a density of 1000 kg/m^2 and same settling velocity as the irregular particle. It is usually used to express the particle size because it takes into account the particle dynamic behaviour in the airflow which is dependent on the size, shape and density of the particles and also is representative of the deposition mechanisms of the particles (i.e. inertial impaction and gravitational sedimentation (Hinds, 1999; Telko & Hickey, 2005)

2.4.2 Mass median aerodynamic diameter

To assess the *in-vitro* performance of a DPI formulation, the American and European pharmacopoeias have designated methods that are based on inertial impaction to evaluate the fraction of fine inhalable particles (EP, 2010).

The mass median aerodynamic diameter (MMAD) corresponds to the particle diameter that has 50% of the aerosol mass being present above and 50% below it. MMAD is a crucial parameter as its control certifies reproducibility and indicates that the particles have been retained in the desired regions of the lungs. On the cumulative curve, MMAD is read at the 50% point. In order to achieve the required particle size of the drugs delivered by DPIs, numerous processes are available. Drug particles size reduction can most commonly be achieved by micronisation (Thibert & Tawashi, 1999). Other techniques are also available: spray-drying (Li et al., 2005) or supercritical fluid technologies (Chow et al., 2003).

Most of the therapeutic aerosol formulations comprise a wide range of particle sizes, they are said to be polydisperse.

Geometric standard deviation (GSD) is a representation of the particle diameter variations within the aerosol and is calculated from the ratio of the particle diameter at the 84.1% point on the cumulative distribution to the MMAD. A GSD of 1 signifies that the aerosol is mono-dispersed; when GSD is higher than 1.2 the aerosol is polydisperse.

To achieve good drug distribution in the lungs, particles are required to have an aerodynamic diameter between 1 and 5 μm (Atkins, 2005). The aerosol droplet diameter should be less than 3μm to be able to target the alveolar region. Particles larger than 5μm are deposited in the oropharynx while particles smaller than 1μm are exhaled during tidal breathing.

2.4.3 Fine particle dose and fine particle fraction

The fine particle dose (FPD) corresponds to the mass of drug particles that have a d_{ae} less than 5 μm. Such particles are theoretically proven to deposit in the deepest regions of the lungs after inhalation.

The fine particle fraction (FPF) is the percentage of the fine particle dose related to either the total drug mass contained in the inhaler device (nominal dose) or the recovered drug (collected from all the parts of the impactor after inhalation). FPF can also be calculated as a function of the emitted dose instead of the total recovered dose (Rahimpour & Hamishehkar, 2012)

2.4.4 Total emitted dose

The total emitted dose (TED) corresponds to the total mass of drug exiting the inhaler device after the patient inhales. This parameter allows a better understanding on the fluidisation properties of the powder through the device, whereas FPF and FPD express the ability of the powder blend to be fluidised and de-agglomerated so that the drug and carrier detach from each

other to allow the drug to be deposited in distal parts of the impactor. The dispersibility is worked out as the ratio of FPD to emitted dose (Rahimpour & Hamishehkar, 2012)

2.5 Drug delivery from Dry powder inhalers

2.5.1 DPI formulation

'Top-down' methods have been used to engineer DPI formulations, where drug particles with large particle size are micronized to generate particles with a median geometric diameter of 1-5μm (Telko & Hickey, 2005). The resulting fine drug particles are then mixed with large lactose monohydrate carrier particles (50-100μm) (Figure 2.4) to improve the flow properties of the powder blend (Dunbar et al, 2000).

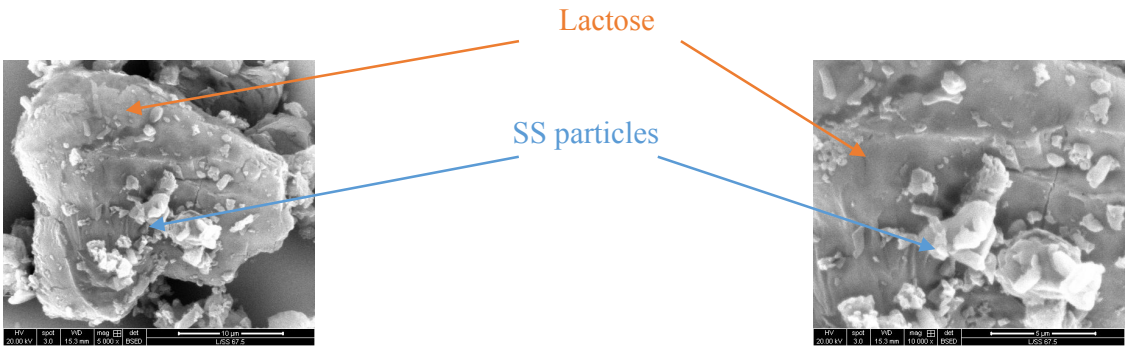

Figure 2.4a SEM images of a DPI formulation containing lactose carrier and salbutamol sulphate particles at x5000 and x10 000 magnifications

Only 20-30% of the nominal dose is generally delivered to the lungs, this poor delivery efficiency is due to the strong adhesive and cohesive forces between drug and carrier particles. To allow dispersion of the particles, the adhesive forces between the particles need to be overcome. Hence, deposition of drug particles in the airways is highly dependent on the balance of the forces between components of DPI formulations (Young, et al., 2008).

DPIs are a widely accepted dosage form used to deliver drugs via the inhalation route and are commonly used to treat respiratory diseases. The interactions between the DPI formulation and

the inhalation device are responsible for successful delivery of the drug in the lungs. For the drug to be delivered in the deepest regions of the lung, drugs particles are required to be in the size range of 1 to 5 μm; this size is usually achieved by micronizing the drug particles. However, small drug particles are known to have poor flow properties and tend to be highly cohesive, which would compromise the dispersion of the particles in the airstream (Atkins, 2005). Because of their cohesive nature, the drug particles tend to remain in the capsule and DPI device during dose emission, resulting in a poor and unreproducible dose emission (York et al.,1998)

Thus, to improve flow dispersion, coarse particles within the size range of 50 μm to 100 μm are added to the formulation. These particles will act as a carrier onto which the drug particles will adhere during blending (Tian et al., 2004). Lactose is the most commonly used carrier because it is inert, safe to use, non-toxic, widely available, inexpensive and has physicochemical properties that are compatible with most active pharmaceutical ingredients APIs (Pilcer & Amighi, 2010; Steckel & Bolzen, 2004). Lactose has been extensively used as an excipient in solid dosage forms, and is available on the market in various grades with various physicochemical properties.

DPI formulations, also called adhesive mixtures, usually require a few milligrams of the API, as most commercially available medications contain between 20 μg to 500 μg of drug for asthma therapy; lactose acts as a bulking agent to ease the handling and dosing processes during manufacturing. Typically, the drug-to-carrier ratio is 1:67.5 (Flament et al., 2004; Larhrib et al., 1999; Zeng, et al., 2000).

2.5.2 Dry powder inhaler devices

While metered dose inhalers (MDIs) are the most commonly used devices, the number of MDI products dropped due to the gradual removal of chlorofluorocarbons use and the limited availability of substitute products with hydrofluorocarbon propellants (Steckel & Bolzen, 2004).

DPIs entered the market in the 1950s to overcome the drawbacks associated with pMDIs, such as the use of CFC-propellants and poor patient coordination techniques (Roche et al., 2013; Chrystyn et al., 2006). DPIs are commonly used to treat asthma and lung infections and has some key features which make inhalation an attractive route of delivery: rapid onset of action, reduction of side effects, and direct target of drug to the site of action.

There are different types of DPIs available: single-dose inhalers or multi-dose inhalers. A list of the DPIs available in the market is displayed below in Table 2.2.

Table 2.2 Types of DPI devices available in the market (Chrystyn, 2007)

Inhaler Device (Manufacturer)	Dosage forms
Single Dose Inhalers	
Spinhaler® (Aventis)	Spincaps
Rotahaler® (GlaxoSmithKline)	Rotacaps
Aerolizer® (Novartis Pharma)	Capsules
Breezhaler® (Novartis, Pharma)	Capsules
Handihaler® (Boehringer Ingelheim)	Capsules
Multi-dose inhalers	
Multiple Unit-Dose Inhaler	
Diskhaler® (GlaxoSmithKline)	Rotadisk (4-8 doses)
Elipta® (GlaxoSmithKline)	Powder on strip
Accuhaler® (GlaxoSmithKline)	Powder on strip
Reservoir Systems	
Turbuhaler® (AstraZeneca)	Reservoir
Clickhaler® (Innovata Biomed)	Reservoir
Easyhaler® (Orion Pharma)	Reservoir
Novolizer® (Meda)	Reservoir
Genuair® (AstraZeneca)	Reservoir
Twisthaler® (Merk)	Reservoir
NEXThaler® (Cheisi)	Reservoir

Single-dose DPIs are usually required to be filled with capsules which are pierced by the patient prior to inhalation to allow the aerosolisation of the dose (Chrystyn, 2007). Breezhaler® (Novartis, Basel, Switzerland) is a single dose, capsule-based DPI that delivers both LABA indacaterol and anticholinergic glycopyrronium bromide for the treatment of COPD (Lavorini et al., 2017).

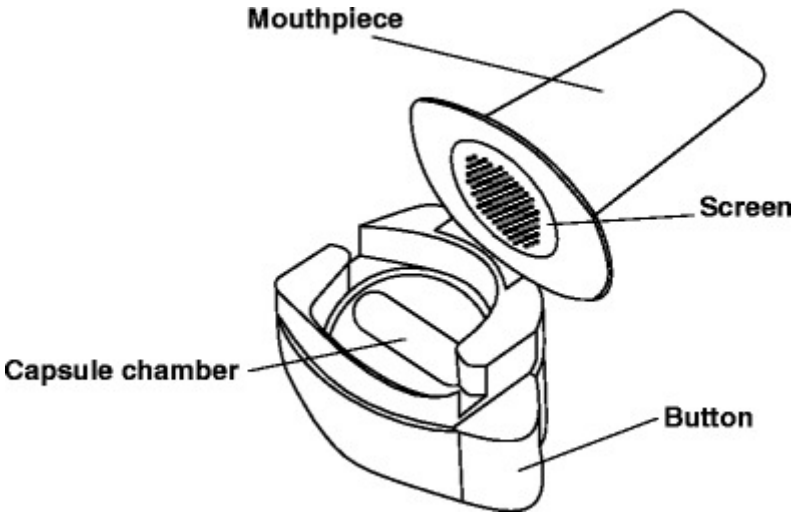

Figure. 2.4b Schematic diagram of the Breezhaler (Berkenfeld et al., 2015)

BreezHaler's® mouthpiece and capsule chamber are built with acrylonitrile butadiene styrene, push buttons are made from methyl methacrylate acrylonitrile butadiene styrene. The needles located inside the capsule camber and springs (in the buttons) are made from stainless steel. Prior to inhalation manoeuvre, the patient has to open the device, insert the capsule in the capsule chamber (Figure. 2.4b) and pierce the gelatine capsule by pressing the buttons located on both sides of the inhaler. The piercing sound of the capsule is an indicator that the device is primed and during the inhalation manoeuver a whirring noise should indicate to the patient that the dose has been emitted from the capsule (Berkenfeld et al., 2015; Buhl & Banerji, 2012). Breezhaler® is a low resistance device with an airflow resistance of 0.017 $kPa^{0.5}$ min/L and an inhalation flow of 111 L/min is typically required to achieve 4KPa (Dal Negro, 2015; Pavkov et al., 2010).

The majority of DPIs are said to be passive breath-actuated devices which rely on the inspiration of the patient in order to operate. The efficacy of inhaled drugs is dependent on the patient's age, inhalation technique and disease severity. One of the major disadvantage of DPIs is the requirement for a moderate inspiratory flow to draw the formulation from the device, however some patients are unable to achieve such effort. Several studies demonstrated that the patient failure to achieve the threshold inspiratory flow resulted in incomplete dose de-aggregation, thus poor drug deposition in the lungs (Palander et al., 2000).

Nevertheless, recently introduced DPIs have been shown to require low inspiratory flow rate (approximately 30 L/min) and are able to produce higher FPF (>40% of the nominal dose) (Colthorpe et al., 2013).

Since the velocity distribution of air inside the lungs depends on the tidal volume and breathing frequency parameters, the amount of drug delivered to the alveoli can be improved by increasing the inspiratory volume (Sbirlea-Apiou et al., 2007). At a constant flow rate, particle de-agglomeration can be favoured by increasing the time of breathings, i.e. increasing the inspiratory volume. It has been demonstrated that for DPI formulations to be deposited deep in the lungs, not only the peak flow rate was important, but also the flow- increase rate. Studies have shown that a high peak flow does not always result in high aerosol deposition if the initial flow-increase rate was not high enough to disperse the drug particles, thus resulting in drug particles not reaching the deep lung (De Boer et al., 2003; Martini & Nath, 2009).

The flow rate and inhaled volume through the DPI is determined by the lung volume of the patient, the force that the patient can generate and the resistance of the device.

The design of DPIs results in an inhaler specific resistance to airflow. The specific resistance can be calculated by the following equation:

$$\sqrt{\Delta p}=R.Q \qquad \text{Eq 2.1}$$

where $\sqrt{\Delta p}$ is the square root of pressure drop; R is the specific resistance and Q is the inhalation flow.

The main forces resulting in drug particles de-agglomeration is believed to be achieved by three key mechanisms within the device: particle interaction with shear flow and turbulence, particle-device impaction and particle-particle impaction (Coates et al., 2004).

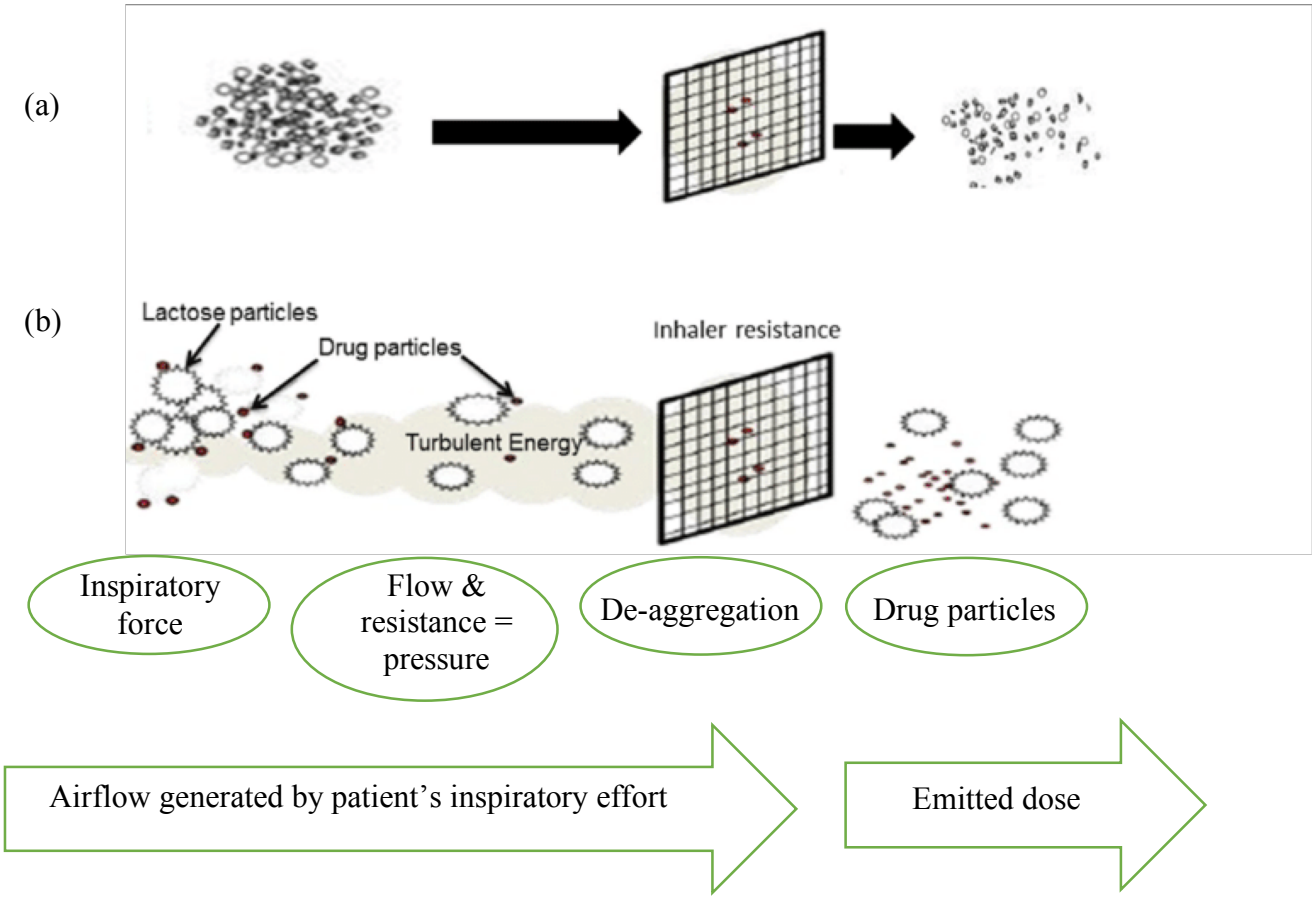

Figure 2.5. Schematic diagram of the dose de-aggregation mechanism of DPI powders formulations. (a) drug-only formulation (b) carrier-drug formulation (Lavorini et al., 2017)

The de-aggregating forces increase as turbulence forces in the device increase (Voss et al., 2002). The turbulence energy is represented by the pressure drop occurring inside the device, this energy is responsible for the disintegration of the formulation into the emitted dose containing the drug particles (Figure 2.5) (Chrystyn, 2003; Chrystyn, 2009).

Thus, DPIs are designed in such a way that the device produces enough turbulence for particles to collide with other particles, resulting in drug detachment from the carrier surface. The interaction between the powder and the device is poorly understood as well as the effects of such interactions on powder dispersion. Recently, computational dynamic fluids have allowed a better knowledge on particle-device impaction and its effects and has demonstrated that the performance of DPIs can be enhanced by making small changes in the device design (Chan et al., 2006; Coates et al., 2004).

Most DPIs are made of short tubes through which an airflow, consisting of a turbulent core surrounded by a laminar envelope, passes (Dunbar et al., 2000). The inspiratory effort of the patient along with the inhaler specific resistance yield a flow rate that allows formation of an aerosol and deposition of drug particles in the lung. Generally, devices with high-specific resistance generate high turbulent forces that lead to higher drug dispersibility and higher FPF as opposed to lower resistance devices (Srichana et al., 1998). However, high resistance devices require a high inspiratory force from the patient to reach the desired air flow. Consequently, a balance between the design of the inhaler device (resistance and turbulence), the inspiratory flow of the patient, as well as the drug formulation is required.

2.6 Inter-particulate forces

During inhalation, the drug particles usually detach from the surface of the carrier particles, this phenomenon occurs only when the energy of the inspired flow is sufficient to overcome the adhesion forces between the drug and carrier particles (Zeng et al., 2000). The large lactose

carrier particles tend to impact in the upper airways, while the micron-sized drug particles are able penetrate into the lungs. The adhesion forces between drug and carrier particles should be such that the drug particles are not too strongly adhered to the surface of the carrier particles preventing dispersion and leading to the drug-carrier agglomerates depositing in the upper airways.

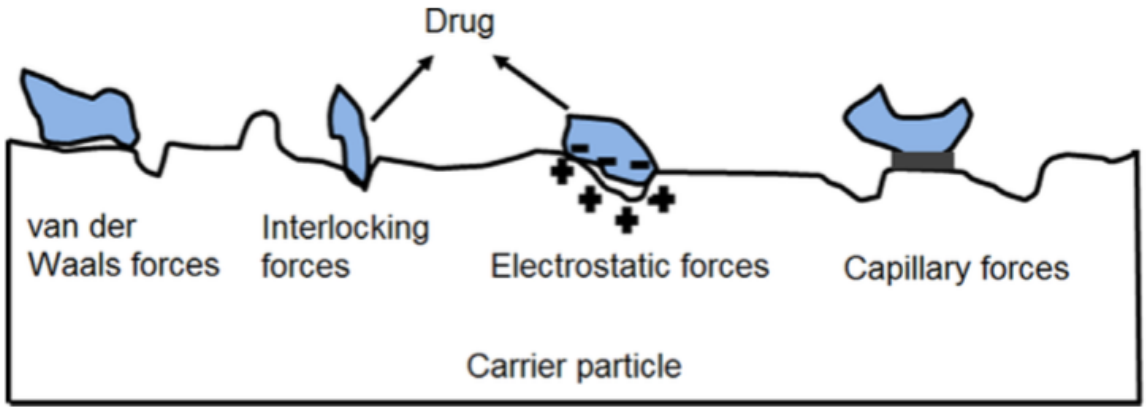

Figure 2.6 Physical forces occurring between drug and carrier particles (Peng et al., 2016)

The stability of the formulation, the good homogeneity of the mixture and good content uniformity depend on the optimal balance between the adhesive and cohesive forces between drug and carrier particles. Ideally, the right balance would provide a stable formulation with no powder segregation, yet allow easy separation of the particles during inhalation. The lactose particle size, quality of the lactose particles as well as the surface roughness have been described to have a major influence on the aerosol properties (Flament et al., 2004; Zeng et al., 2000a; Zeng et al., 2000b). This is why selecting the right carrier is pivotal during formulation to enhance the performance of the DPI.

The interactions between particles (cohesion (drug-drug) and adhesion (drug-carrier)) are governed by physical forces such as van der Waals forces, capillary forces, electrostatic charges and mechanical interlocking (Telko & Hickey, 2005). Some other interactions are dominated by chemical forces such as acid-base interactions and hydrogen bonding (Fowkes, 1964). The degree of magnitude of the physical forces differs depending on the particle size, surface properties, surface roughness, press-on forces during mixing and relative humidity (RH) (De Boer et al., 2003).

Capillary forces occur due to the formation of a liquid bridge (concave-shaped meniscus) around the contact area of two adjacent particles (Figure 2.6) (Butt & Kappl, 2009). The attractive force caused by the concave-shaped meniscus is cause by the surface tension of the liquid around the border of the meniscus which pull particles towards one another. Also, the difference in pressure between the inside of the meniscus and the outer pressure pulls the particles together (Butt & Kappl, 2009). Capillary forces can be involved in adhesion and cohesion and their magnitude depends on the physicochemical properties of the particles such as shape, size, RH and surface roughness (Butt & Kappl, 2009).

Electrostatic charges arise when two particles with dissimilar surfaces get in contact with each other and then separate quickly. This result in a charge transfer between a donor and an acceptor (Figure 2.6). The collision is generally short or can happen as an intense friction between the particles and a charging phenomenon called triboelectrification as a result. Contact charges are categorized into three types: metal-metal, metal-insulator and insulator-insulator (Bailey, 1993; Matsusaka et al., 2010).

Pharmaceutical drugs and excipients behave as insulators under ambient conditions. The contact surface can either be metal (such as the mixer vessel) or insulating materials (device's

plastic components and excipient or drug during mixing and aerosolisation). Metal surfaces (stainless steel) and the device components (polypropylene and acetal) effect the magnitude and the polarity of the charges. A study showed that the addition of fine lactose (less than 10μm) to the coarse lactose particles resulted in a decrease in the magnitude of the triboelectrification charges during mixing process (Bennett et al., 1999).

Triboelectrification charges which appear during mixing, handling and filling, can be a drawback to powder aerosol performance as they limit powder flowability during manufacturing processes by increasing the inter-particle adhesive and cohesive forces. Studies have shown that the polarity and magnitude of triboelectric charges increase with increasing amorphous content in the sample as well as high particle size distribution of the carrier particles (Murtomaa et al., 2004; Murtomaa et al., 2002). Chow et al. (2008) studied the triboelectric forces arising during different stages of manufacturing and while aerosolizing the powder formulation through the inhaler using a coarse lactose (Inhalac® 230). They observed that the initial negative charges were not significant and decreased with increasing RH. They noted that during the mixing process and during handling powder in gelatin capsules there was an increase in the triboelectric charges. They did not see any changes in the sign of the charge of the lactose particles, however they noticed that the charge became much higher during aerosolisation and the polarity of the charge changed. This was believed to be due to the contact between the lactose particles (insulator) and the plastic of the inhaler device (insulator) (Chow et al., 2008). In DPI formulations, the net charge on the drug particles could occur during drug detachment from the carrier particles or from the surface of the capsule and/or from the device. Studies showed that the aerosolisation of the DPI formulation is influenced by the grade of lactose (sieved or milled), the type of device and the type of capsule as they have an effect on the

polarity and magnitude of the electrostatic charges arising during in-vitro aerodynamic performance (Hickey et al., 2007; Telko et al., 2007).

2.7 Influence of physical properties of carrier on the performance of DPIs

2.7.1 α-Lactose monohydrate

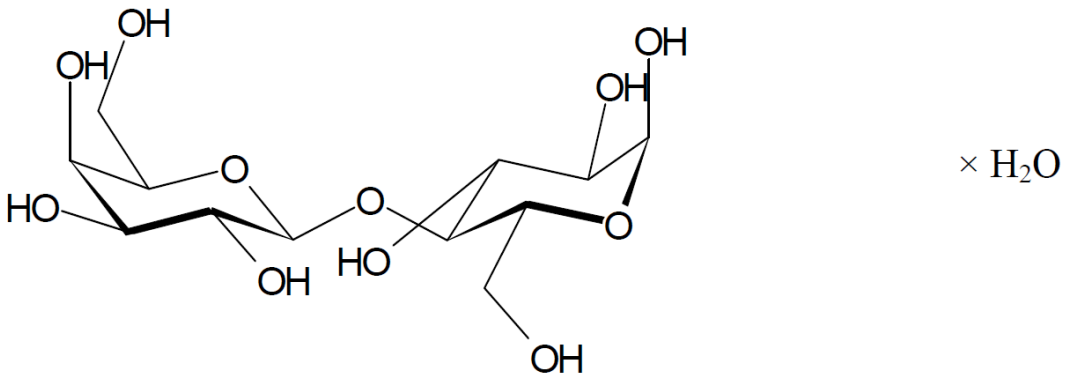

Figure 2.7: Structure of α-lactose monohydrate ($C_{12}H_{22}O_{11}H_2O$)

Lactose is a disaccharide found in the milk of most mammals and is made of galactose and glucose. Lactose is extracted from the whey of cow's milk (Chan et al., 2012). The production of lactose is achieved by several steps; the first step involves producing raw lactose which is obtained by de-proteinating the whey using heat or acid treatment, then the remaining super-saturated solution is further cooled, dissolved, re-cooled and recrystallized. There are different grades of lactose available in the pharmaceutical market: below 93.5ºC α-lactose is produced, whereas above 93.5ºC β-lactose crystals are formed. Lactose can also exist as anhydrous lactose (containing 70-80% β-lactose anhydrous and 20-30% α-anhydrous lactose) (Kaialy et al., 2012).

Lactose is soluble in 2.04 parts of water at 50°C. α-lactose monohydrate is the most stable form due to its less hygroscopic properties, cheap cost, wide availability and high compatibility with drug substances. α-lactose particles shape can vary from pyramid, prism to tomahawk.

All the grades differ in their physical characteristics and flow properties. The different physical forms of lactose have been demonstrated to affect the adhesive forces between the particles. For example, the crystalline form of lactose reduced the adhesion forces which resulted in a better dispersion with the drug being released more easily from the lactose surfaces. Lactose can be either processed by micronizing, spray-drying or sieving, resulting in different surface morphologies.

Many researchers focus their work on modifying the surface characteristics of lactose by 'particle engineering'. The disadvantage of particle engineering is that the resulting modified lactose particles are characterized by a heterogeneous surface with non-homogenous energy distribution and morphology on the surface of the particles, leading to batch to batch variations which could compromise the performance of the formulations (Young et al., 2008).

2.7.2 Particle size

It is well accepted that particle size of the carrier has a great influence on the aerosolisation performance of the DPI formulation. Authors have published contradictory reports about the suitable size for carriers in DPIs. Some previous studies have reported that decreasing the particle size of the carrier increased the fraction of respirable drug delivered from a DPI (Gilani et al., 2004; Kaialy et al., 2012; Louey et al., 2003; Steckel & Müller, 1997), however this has a negative effect on drug content uniformity and resulted in a higher amount of drug deposited in the oropharyngeal region (Kaialy et al., 2012). It was suggested that smaller agglomerates

are subjected to more forceful shear in the turbulent airstream which resulted in better de-agglomeration (Islama et al., 2012).

However, Zeng et al., suggested that the addition of a coarse carrier in the formulation was due to the poor powder flow properties of small carriers (Zeng et al., 2001a).

Another study demonstrated that larger carrier particles have larger gaps on the surface than fine crystals (De Boer et al., 2003). These discontinuities offered shelter to drug particles when press-on forces occurred during mixing (De Boer et al., 2005), enhancing the drug deposition profiles after inhalation (Hamishehkar et al., 2010). The contradictory results could be due to the interdependence of physical characteristics of the particles. It is therefore very important to optimize the particle size to achieve efficient aerosolization.

To achieve the optimum particle size of carrier particles, other physical properties need to be taken into consideration, such as their shape, surface roughness, density and geometric diameter (Sahane et al., 2012)

2.7.3 Particle shape

It is recognized that the attractive forces between drug and carrier particles depend on the shape of the particles, thus this will affect the aerosolisation and dispersibility of the drug (Crowder, et al., 2001; Kaialy et al., 2011; Mullins et al., 1992). Shape modification has been used to try to improve drug deposition.

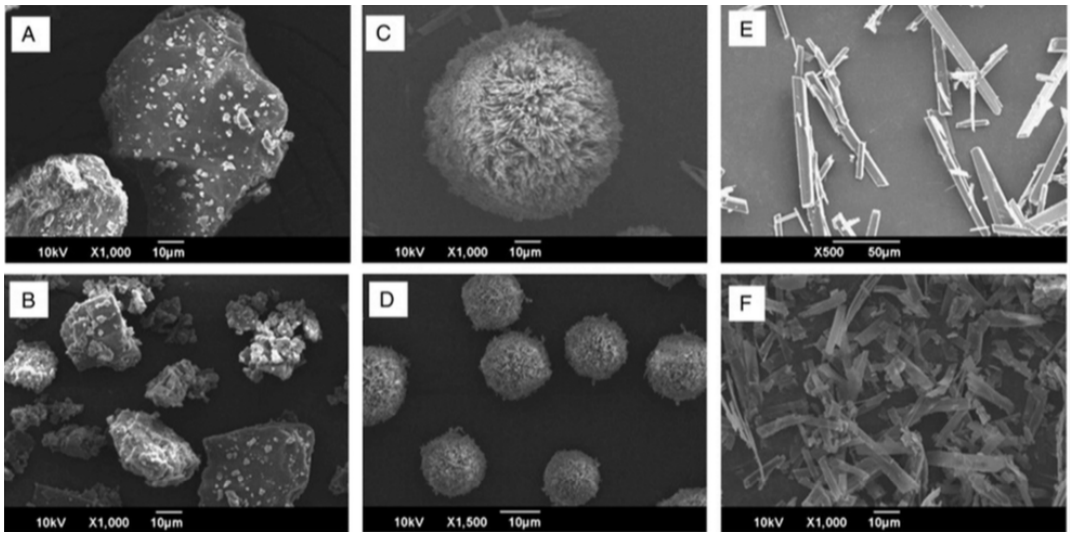

Figure 2.8 Scanning electron microscopy images of different lactose shapes obtained from crystallization (Kho et al., 2013)

When particles have different shapes, they are exposed to different drag forces and velocities during aerosolisation, which affects drug deposition (Kaialy & Nokhodchi, 2013). Most carrier particles generally used in DPI formulations have irregular shapes (image A from Figure 2.8). Several authors have shown that carriers with different shapes resulted in improved drug deposition, such shapes include elongated particles (image F from Figure 2.8) (Larhrib et al., 2003; Zeng et al., 2000a), porous and wrinkled particles (images C and D from Figure 2.8) (Chew et al., 2005) and needle-like particles (image E from Figure 2.8) (Ikegami et al., 2002). An increase in the elongation ratio of the lactose carrier also resulted in a higher FPF of salbutamol sulphate (Zeng et al., 2000). More recent studies reported an increase in the dispersibility of budesonide particles when using pollen-shape like hydroxyapatite carrier particles. This is due to the reduction in the interactions between the drug and carrier particles (Hassan & Lau, 2010a, 2010b). Additionally, particle shape was found to exert an effect on the aerodynamic diameter of the agglomerates. Elongated particles have a lower aerodynamic diameter than spherical particles, therefore they have a longer time of flight and remain for a longer distance in the airstream, enhancing de-agglomeration (Islama et al., 2012). Needle

shape particles, which have a high elongation ratio, result in more efficient drug deposition in the small airways of the lungs (Larhrib et al., 2003; Yang et al., 2014), however such particles have limitations because they tend to have an adverse effect when processing and handling due to their poor flowability (Kaialy et al., 2011).

2.7.4 Surface roughness

The surface roughness of carrier particles has been found to have a profound impact on the adhesion forces between drug and carrier particles (Podczeck, 1999). To achieve an efficient drug delivery deep into the lung, drug particles need to be adhered to the carrier and detach from the surface of the carrier particles. The magnitude of the adhesion forces between drug and carrier particles depends on the particles geometry (Figure 2.9), is directly proportional to the surface energies and inversely proportional to the contact area between them (Adi et al., 2008; Peng et al., 2016).

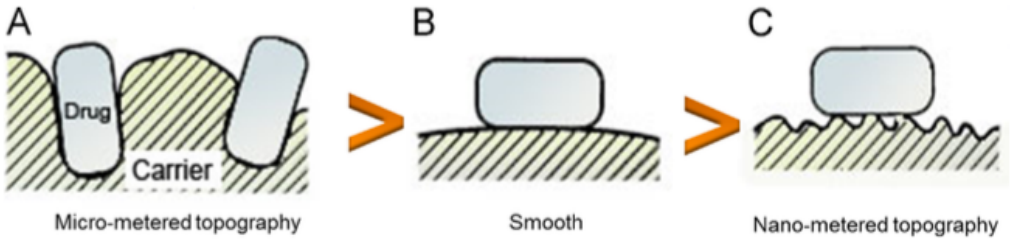

Figure 2.9 Carrier particles differing in their surface roughness: (a) micrometer topography, (B) smooth and (C) nano-metered topography (with permission from Peng et al., 2016)

Several attempts have been made by different research groups to modify the surface properties of the drug and carrier particles with the intent to improve aerosol performance (Peng et al., 2016). Increasing surface roughness can be done by re-crystallisation, coating the carrier particles, mechanofusion or also by spray drying (or adding micronized particles with spray

dried particles) (El-Sabawi et al., 2006; Kumon et al., 2008; Parlati et al., 2009). On the other hand, smoothing the surface of carrier particles in DPIs can be achieved by crystallization processes whereby carrier particles were partially dissolved in an ethanol-water mixture and then filtered and dried (Dickhoff et al., 2006; Iida et al., 2003; Steckel et al., 2004).

Smooth carrier particles can also be obtained by solution phase variable temperature dissolution, where an increase in the dissolution led to a decrease in the surface roughness of the particles (El-Sabawi et al., 2006). It has also been shown that applying direct shear stress to the bulk powder can smooth out carrier particles (Iida et al., 2004). However, numerous studies in the literature have contradictory findings with regards to the impact of smooth and rough carrier particles on drug detachment and dispersion.

For example, a study showed that higher SS FPF was observed when lactose surface roughness was decreased (Timsina et al., 1994).

Other authors published studies where they reduced the roughness of lactose carrier particles which led to a reduction in the surface area and consequently a reduction in the van der Waals adhesion forces (Zeng et al., 2000)

(Iida et al., 2003). Similarly, Zeng et al. study showed that lactose crystals with higher surface smoothness resulted in higher respirable fraction of SS. A study by Heng et al. confirmed that less SS was detached from the surface of rougher lactose particles (Heng et al., 2000). A study by Larhrib et al. assessed the drug delivery efficiency of different batches of crystallised lactose with different morphologies. They found that smoother lactose delivered more SS as opposed to rougher surfaces (Larhrib et al., 2003).

Comparably, Young et al. demonstrated that “smoothing” lactose particles led to an increase in the respirable fraction of BDP (Young et al., 2002).

On the other hand, some conflicting results have been found in the literature, showing that surface roughness can be beneficial in drug delivery of DPIs. For example, Adi et al. demonstrated a direct relationship between roughness, particle adhesion and deposition of drugs *in-vitro*. They observed that adhesion forces between particles was reduced as the degree of corrugation increased, which resulted in a higher FPF value, thus the roughness of particles can greatly affect the aerodynamic performance of DPIs (Adi et al., 2008).

Some studies performed surface modification on the drug particles by increasing the surface roughness. This modification resulted in a decrease in the contact area between drug and carrier particles, which consequently reduced the van der Waals forces that were involved in the adhesion forces (Adi et al., 2008; Chew et al., 2005; Kawashima et al., 1998b). Chan et al. observed a more significant SS deposition with lactose carriers having higher surface roughness. They incorporated fine lactose particles on the surface of coarser lactose particles. The fine particles formed undulations that facilitated the detachment of SS from the carrier (Chan et al., 2003).

The lactose carrier surface is represented by a non-homogenous energy distribution which is characterized by the presence of low energy sites as well as active sites of high energy. Active sites generally arise in amorphous regions (resulting from milling or spray-drying processes), in the presence of impurities (protein and fat present in lactose extracted from milk), in polar/non-polar regions and in morphological regions (peaks and troughs). Active sites are generally occupied by small particles, therefore when low-drug dose formulations are made the drug particles tend to saturate the active sites and compromise the aerosol performance. Drug particles also lodge in non-active sites where a lower adhesion forces occur. Young et al., (2005) studied the relationship between drug/lactose ratio and the influence of drug dose on aerosolisation performance. They found that when higher doses of salbutamol sulphate were

used (from 135 μg to 450 μg) a significant increase in the FPD occurred. A possible explanation was that when a higher drug dose was used, some of the SS particles acted as a ternary component and lodged in the active sites of the carrier, allowing the other drug particles to adhere to lower energy sites on the carrier surface (Young et al., 2005).

On the other hand, Flament et al., found that FPF of tebutaline sulphate decrease with increasing surface roughness of lactose particles (Flament et al., 2004). It was suggested that due to the increase of contact points between the carrier and drug particles, the blend was stabilised but less deaggregation occurred during aerosolisation. These conflicting studies show that in order for DPIs to be efficient, a certain level of surface roughness needs to be achieved (Peng et al., 2016). This is why it has become a great challenge for researchers in the inhalation field to achieve high inhalable dose fraction delivery to the lung with high reproducibility. One of the main cause for great variability and poor deposition results is poor drug-carrier detachment (Zeng et al., 2000).

Thus, when developing DPI products, it is crucial to select carrier particle with suitable physicochemical properties to achieve efficient drug deposition deep in the lungs.

Four interrelated factors control drug delivery to the lungs: firstly, the physicochemical properties of the DPI formulation (powder flow, particle size and morphological features, drug-carrier interaction forces); the second factor is the DPI device (its performance, geometry, dosing method); another factor is that the patient should be trained to use the device properly and use correct inhalation technique and finally the last factor is the inspiratory flow and volume. All these parameters are essential and need to be taken into consideration when engineering new DPI formulations.

2.7.5 Lactose in ternary mixtures

The addition of ternary components into DPI formulations was intended to reduce the cohesion between particles. Researchers believed that incorporating additives would weaken the bond between fine particles and thus reduce adhesion. Studies demonstrated an improvement in the efficiency of inhaled drugs when fine particles were added to the formulation (Staniforth et al., 1998; Zeng et al., 1998). Islam et al. confirmed that when fine lactose particles were added to larger lactose particles or added as an excipient, they had a great impact on drug dispersion (Islam et al., 2004).

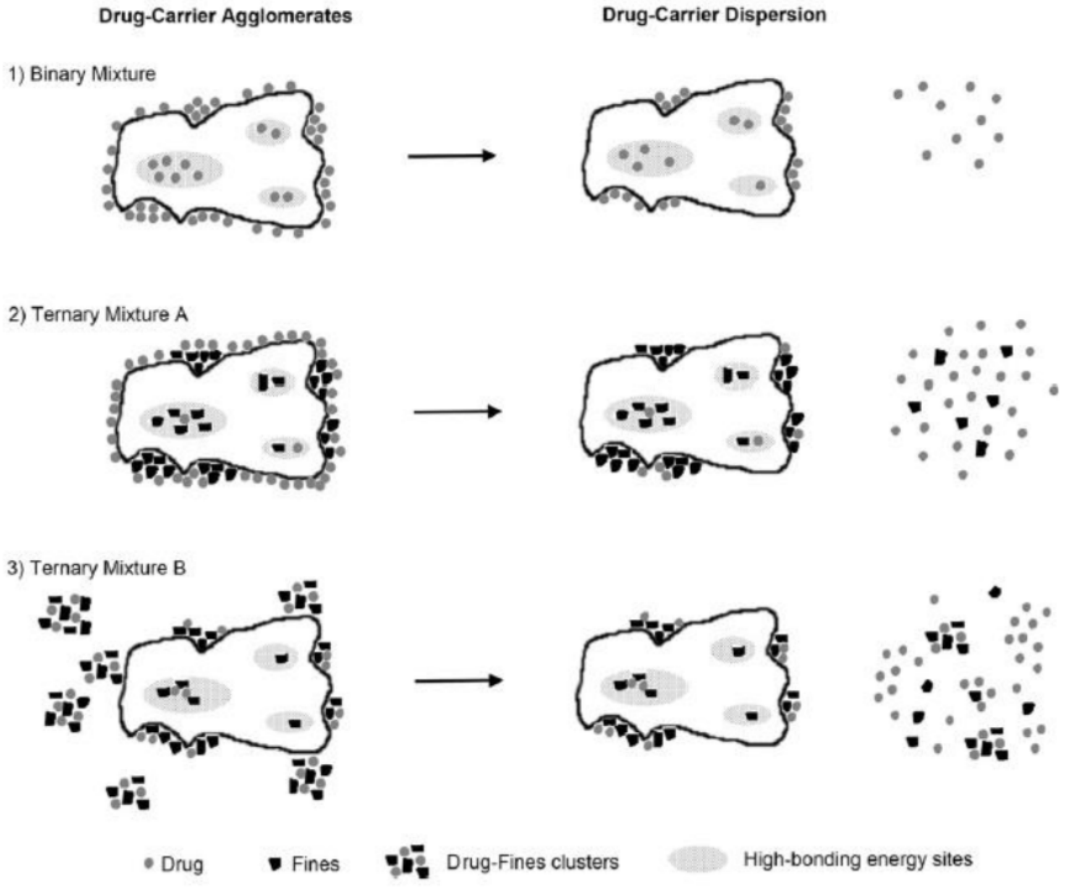

Figure 2.10 Drug dispersion in (1) binary mixtures and (2,3) ternary mixtures (Pilcer et al., 2012).

Drug dispersion was improved when a ternary component, such as Magnesium Stearate (MgSt) and Leucine, was added to the formulation (French et al., 1996; Grosvenor & Staniforth, 1996;

Islam et al., 2004b). The ternary component reduced the cohesive forces between drug-drug particles. The same conclusion was reached when 10% of fine carrier particles (lactose, glucose, mannitol or sorbitol) were added in the formulation containing Salmeterol Xinafoate and coarse carriers. This study showed that the addition of fines improved the detachment of the drug particles from the surface of the carrier (Adi et al., 2007) as represented in Figure 2.10(2) where fine lactose will lodge in the high energy areas on the lactose surface, forcing drug particles to adhere less to those active sites.

The 'active sites' theory was first introduced by Hersey (Hersey, 1975) suggesting that the carrier surface is characterized by the presence of sites of high energy, thus these areas are more adhesive than others. (Pilcer et al., 2012). The 'agglomeration theory' (Figure 2.10 (3)) is believed to improve DPI performance by the presence of fine particles resulting from the formation of drug-fine agglomerates. The fines are more likely to bind to the carrier due to high drag forces, allowing the API particles to detach from the carrier particle surface (Jones et al., 2008).

However, a few studies have shown the opposite effect with the impact of fines in DPI formulations. These studies stated that the concentration of added fine lactose particles has to be prudently measured so that the right dispersibility of the drug can be attained without decreasing the flow properties of the powder formulation (Zeng et al., 1998). The addition of lactose fines in the formulation is inclined to reduce the flow because fines can lodge into the empty spaces between larger particles and promote packing, thus resulting in a more densified powder, with fine particles having poor flow properties (Augsburger, 1974) due to several surface interactions (Hickey et al., 2007) and great cohesion between particles. Some recent studies demonstrated that the addition of fines in the DPI formulation caused a decrease in FPF (Hamishehkar et al., 2010; Steckel & Bolzen, 2004).

Furthermore, when micronised fine carrier particles are used, they usually have some amorphous content and may cause the formulation to be to thermodynamically unstable (Saleki-Gerhardt et al., 1994).

In order to reduce the cohesion between drug particles, force controlled agents (FCA) can be added to formulations. The most common FCA is magnesium stearate (Staniforth et al., 1982; Staniforth, 1997), a lubricant used to modify the properties of DPI formulations, such as the ability of the formulation to pick up moisture and the interaction between particles. Magnesium stearate can be added in the formulation by mechanofusion, where the particles are dispersed around the lactose carrier, forming nano-structured layers around the carrier particles (Begat et al., 2009).

The modifications of the lactose surface morphology allowed a reduction in the interaction forces between the drug and carrier particles in DPI formulations, allowing drug particles to be detached from the carrier more easily and improve aerosol generation.

The particle engineering processes described above were quite successful and encouraging for the optimization of DPI formulations, however, the safe use of hydrophobic excipients such as Mg St is still not fully understood as the way they are cleared from the lungs is still unclear.

2.8 Mixing process

Mixing is an important step in DPI powder formulation as the aerosolisation performance of the formulation depends on the balance between the adhesion forces between particles but also the detachment and dispersion of drug particles from the surface of carrier particles upon actuation. Although mixing remains a major source of variability in manufacturing processes, as batch-to-batch variations still occur (but are limited by controlled blending parameters), mixing remains a key operation in the formulation of adhesive mixtures as the blending of drug

particles with carrier particles is a crucial step that determines the homogeneity of the blend and is the first stage towards achieving the requirements of the final product.

The mixing of powder particles necessitates motion to be exerted on them. Hence, powder blenders induce motion by either rotating the container or by the aid of an impeller that moves within the powder. Powder mixing differs from fluid mixing as the latter is characterized by the diffusion of molecules from a high concentration area to a low concentration location. In the initial stages of the mixing process, drug particles are randomly allocated on the surface of carrier particles and they tend to locate and regroup on the carrier surface discontinuities as shown in Figure 2.11.

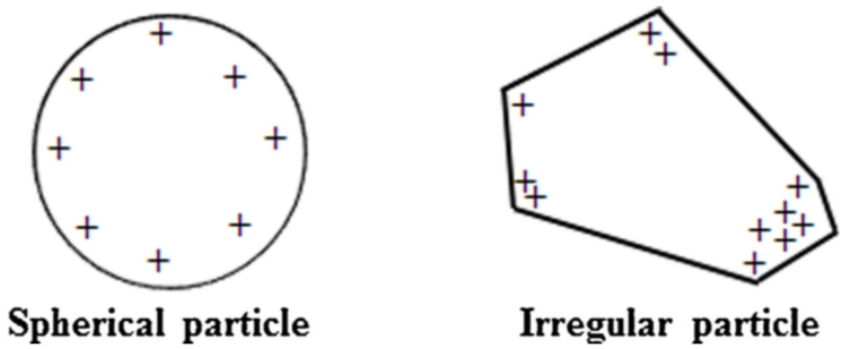

Figure 2.11 Schematic representation of drug distribution on the surface of a carrier particle during mixing (Kaialy, 2016)

The distribution of drug particles depends on the concentration of drug: if the concentration is low, the distribution is less effective as drug particles lodge into the discontinuities and are exempt from the frictional and initial forces, thus they remain strongly attached to the carrier (De Boer et al., 2005)

There are two types of blenders that have been utilised in the production of DPI formulations. These are tumbling blenders (e.g Turbula mixer, V-blender) and high-speed impeller mixers.

They differ in the range of energy inputs they have, which may play an important role on the mixing properties and adhesive properties of the drug to the carrier.

Powder mixing is accomplished by different mechanisms, namely convective, diffusive and shear mixing. Although all three tend to happen during mixing processes, the one that predominates will depend on the type of blender used, the blending parameters, such as fill weight, speed and percentage loading, and also the flow properties of the carrier used in the formulation. Shear mixing was reported to be the only mechanism efficient in engendering enough stress needed to de-agglomerate cohesive drug particles (Figure 2.12).

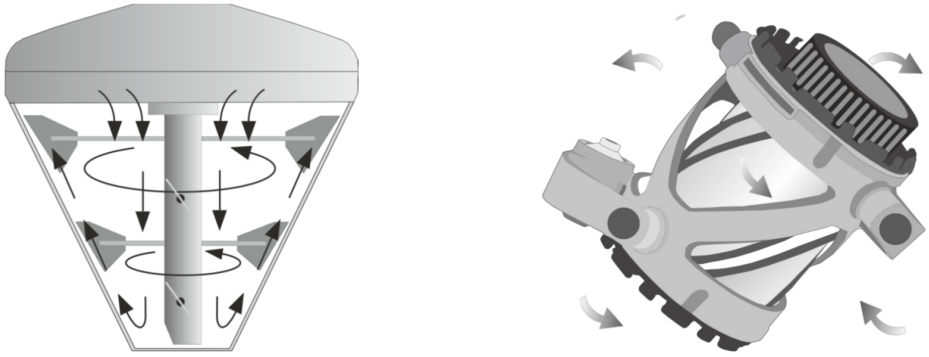

Picomix® high shear mixer module **Turbula® low shear tumble blender**

Figure 2.12 Schematic representation of a Picomix® and Turbula mixer (Hertel, 2016)

High stresses are required to break up the drug agglomerates, thus allowing individual drug particles to be distributed on the surface of the carrier. During mixing, each component of the DPI formulation collides with each other and with the walls of the container. The powder flow in the blender may cause friction between the particles, such friction forces are accountable for de-agglomerating drug particles. It has been demonstrated in the literature that drug agglomerates can still subsist after mixing. However, these agglomerates were weaker than the initial ones. They have been shown to be broken up into single particles at a relatively low pressure drop of 4 kPa in an inhaler (De Boer et al., 2004)

2.9 Particle engineering for lactose particles

2.9.1 Spray-drying

Spray-drying (SD) is a well-used particle engineering technique because it is rapid, continuous, straightforward, easy to operate, cost-effective, reproducible and is available for large scale batches.

SD consists of producing dry powders from a liquid feed by atomisation through an atomiser into hot air. The process involves four fundamental steps listed below (Master et al., 1998):

Step 1: Feed solution is atomised into a spray

Step 2: Drying of spray into drying medium (gas or air)

Step 3: Formation of dry particles

Step 4: Dried particles are separated from the air and collected.

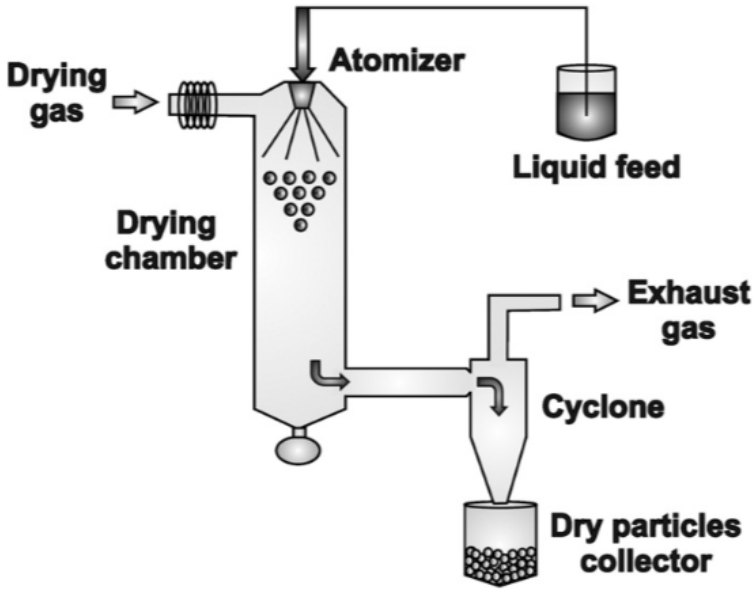

Figure 2.13 Diagram of the conventional spray drying equipment (with permission from (Sosnik & Seremeta, 2015).

Figure 2.13 shows a diagram of a conventional spray drying process. The process starts by introducing the liquid feed through a nozzle into the chamber using a peristatic pump. There

are three types of nozzles, namely rotary atomiser, pressure nozzle or a two-fluid nozzle, and the atomisation takes place by centrifugal, pressure or kinetic energy, respectively (Lee et al., 2011). The feed can either be a solution, a suspension, a colloidal dispersion, slurry, paste or emulsion (Gómez-Gaete et al., 2008; Rabbani & Seville, 2005). Following atomisation, the micro-droplets undergo fast solvent evaporation (Elversson et al., 2003; Fatnassi et al., 2014) forming dry particles.

The separation of the dry particles from the drying gas occurs in the cyclone, where the dried particles are deposited in a glass collector at the bottom end of the spray-drier (Schoubben et al., 2010; Ståhl et al., 2002). The solid dry particles generated show relatively narrow size distribution at the micron scale and the percentage yield is usually quite low and not optimal (20-70%) (Lee et al., 2011; Rabbani & Seville, 2005; Liu et al., 2006). A great loss of particles occurs in the cyclone due to the low capacity of the cyclone to separate particles that are less than 2 μm, which end up passing into the exhaust air, and because a lot of product is usually adhered to the walls of the drying chamber (Sosnik & Seremeta, 2015).

Several parameters can be adjusted to optimise the spray drying technique. The main adjustable parameters are listed in Table 2.3. The important drying parameters are inlet and outlet temperatures, the type of drying gas, the flow rate of the drying gas and residence time, all of which will affect the size, shape, crystallinity, density and residual solvent content of the final product.

Table 2.3 Main adjustable parameters for spray-drying (Modified from Sosnik & Seremeta, 2015)

Parameters		
Process	**Liquid feed**	**Equipment**
Flow rate of feed	Concentration	Co-current flow
Flow rate of drying gas	Viscosity	counter-current flow
inlet temperature (gas/air)	Density	Mixed flow
drying rate	Solvent boiling point	Atomiser size
pressure		
type of gas		

It is important to note that particles generated by spray-drying from solutions are spherical, small (less than 10 μm) and predominantly amorphous; however, suspensions can be processed to preserve the crystalline state of the material. For example, the crystallinity of spray-dried lactose can be adjusted depending on the ethanol-to-water ratio in the liquid feed solution. Because lactose is practically insoluble in ethanol, spray drying a lactose suspension from pure ethanol will produce 100% crystalline spray-dried lactose particles, but spray-drying a lactose solution from pure water will generate 100% amorphous lactose particles (Harjunen et al., 2002). It is interesting to note that commercial lactose (SuperTab®, DFE Pharma) generally used for direct compression is generated by spray-drying. SuperTab® particles are spherical, have a narrow size distribution and have an excellent flow and compactibility (DFE Pharma). Studies in the literature show that spray-dried lactose did not improve the inhalation efficiency of the DPI formulation containing pranlukast hydrate because the drug was strongly adhered to the surface of the smooth spray-dried lactose. However, it was found that spray-dried crystallised lactose, which had microscopical projections on its surfaces, had a higher fine particle fraction. The conclusion of this study was that a certain degree of roughness was needed to improve inhalation efficiency. As spray-dried lactose on its own is not optimal for efficient drug delivery in DPIs (Kawashima et al., 1998b). More recently, to improve the dispersibility of cohesive materials, additives such as amino acids (leucine and trileucine) were incorporated with the carrier particles to modify the inter-particulate forces (Vehring, 2008).

2.9.2 Milling

Micronisation or milling is a well-established and widely used technique to produce particles in numerous marketed inhaler formulations. Such particles are firstly crystallised, then filtered, dried and finally micronised. Particle size reduction is a result of either pressure, friction, attrition, impact or shear (Kalman, 2000). Ball-milling and jet-milling are widely used to produce particles intended for inhalation. In the jet-milling technique, particle-particle and particle-wall collisions occur before the separation of larger particles from smaller particles by inertial impaction. This categorisation guarantees that the particle size required is eventually obtained.

Unwanted changes in the physico-chemical properties of the material can occur due to intense milling. Such changes include the generation of amorphous domains at the surface, which compromise the stability of the material and the possibility of undergoing recrystallization, thus crystal growth on the amorphous regions; solid bridges can also be formed between particles. Milling is also known to induce electrostatic charging at the particle surface, thus making the material more cohesive and adhesive. Additionally, the micronisation process produces small, irregular lactose particles with highly flat surfaces which contributes to larger contact areas, promoting the adhesion between the particles and exhibiting poor flow properties (Mohammed et al., 2017). Despite micronisation being a convenient technique for size reduction, it offers only a limited opportunity to manipulate particle characteristics such as size distribution, shape and morphology. That is why it is necessary to develop other particle engineering methods capable of producing particles suitable for inhalation.

2.9.3 Crystallisation of solids

Crystallisation methods have been extensively used in particle engineering to produce carrier particles with different size, shapes (Section 2.7.3) and surface textures (Section 2.7.4 and 2.7.5).

This section will cover the mechanism of crystallisation as it is important to understand how each step during crystallisation can influence the morphological properties of the crystallised material.

Crystallisation processes are made of three important steps:

Step 1: Supersaturation

Step 2: Nucleation

Step 3: Crystal growth.

Supersaturation is the driving force of the crystallisation process because the second and third steps in crystallisation depend on the level of supersaturation in the solution (Davey and Garside, 2000). Supersaturated solutions are generally produced by cooling, evaporation, anti-solvent addition or a mixture of these processes.

Nucleation is defined by the development of small agglomerates in the supersaturated solution. Such agglomerates are formed by either bimolecular addition or can occur when molecules collide with each other (Mullin, 1993). Bimolecular addition is characterised by the coagulation of a molecule, with the lowest interaction energy amongst others in that particular zone, to another molecule which will act as a seed for others to bind to. Agglomerates form until a stable nucleus is formed. The formation of crystal nuclei is challenging because molecules have to coagulate but also fight dissolution (Kitaigorodsky & Ahmed, 1972).

Crystal growth is characterised by the increase in particle of size leading to a crystal state. The increase in particle size occurs by the formation of layers from loose particles that lodge themselves on the imperfections of the crystal's surface.

The mechanisms of nucleation and crystal growth are still a difficult phenomenon, however by optimising the crystallisation parameters, it is still possible to control some crystals features such as morphology and size, but this is quite limited, because several factors can affect the quality of the final crystals (e.g. induction time, cooling rate, level of supersaturation, type of solvent used, stirring rate, impurity levels) (Mullin, 1993; Storey, 1997; Raseneck and Muller, 2002).

2.10 Reasons for engineering new lactose carriers

Most commercially available dry powder inhalers are only able to deliver about 20-30% of the dose to the lungs (Figure 2.14)

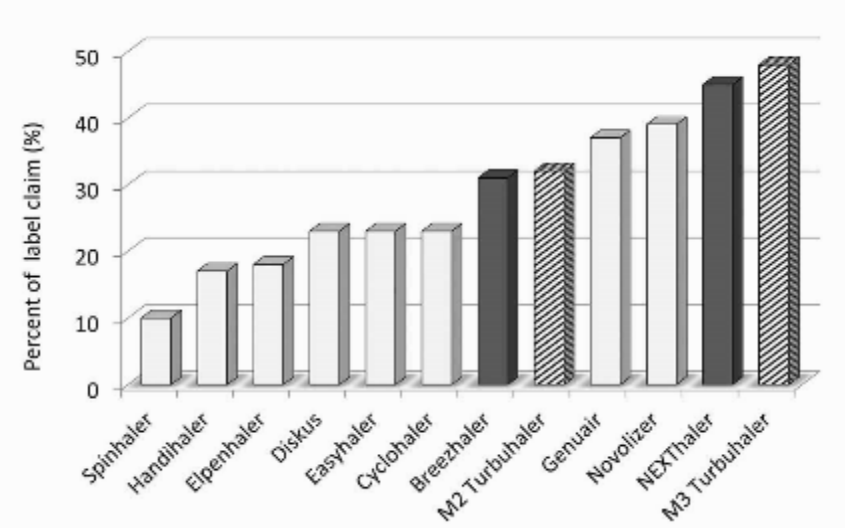

Figure 2.14 *In-vitro* %FPF of label claim from different DPIs tested at 4kPa using a next generation impactor (DeBoer et al. (2016)

The undelivered portion of the drug stays attached to the carrier surface (Steckel & Müller, 1997). The possible explanations for this ineffective delivery have not been completely understood. One of the reason is known to be the morphology of the commercially available

inhalation grade lactose such as its irregular shape and rough surface which may affect drug dispersion. Another reason for inefficient delivery is attributed to the sensitivity of the DPI formulations to high temperatures and humidity. α-lactose monohydrate is not hygroscopic; however, moisture can get into DPI formulations and may affect the performance of the powder blend. Because of the difference in particle size between lactose carriers (< 100 μm) and drug particles (1-5 μm), any moisture entering the particles will enhance the cohesion between particles in the DPI formulation. Lactose is usually produced by particle size reduction techniques which usually produce amorphous regions on the processed material. These amorphous regions are usually associated with high free energy sites which require higher energy to detach drug particles from the carrier surfaces (Malcolmson & Embleton, 1998).

A study by Larhrib et al. demonstrated that different grades of lactose exhibited different delivery profiles of SS, this suggests that the grade of lactose has a profound effect on the delivery of the drug (Larhrib et al., 1999).

All of the studies listed in this chapter suggest that modifications of the carrier particles are required to achieve satisfactory drug delivery.

Chapter 3. Materials

This chapter gives an outline of the laboratory materials, apparatus and methods used in the study.

3.1 General laboratory apparatus and materials

- 4 decimal places analytical balance (ADAM, AAA 160 LE)
- Ultrawave U300 benchtop bath (Scientific Laboratory Supplies, Ltd)
- Sealing Parafilm™ (Fisher Scientific Ltd, UK)
- 20 mL clear vials (Sigma Aldrich, UK)
- Syringe filter 0.45μm pore size (Fisher Scientific Ltd, UK)
- 5 mL plastic syringe (Fisher Scientific Ltd, UK)
- Glass Pasteur pipettes (Fisher Scientific Ltd, UK)
- Hot plate and magnetic stirrer (Cole-Parmer®, UK)

3.2 Measurement of the aerodynamic characteristics of the emitted dose using the in-vitro and ex-vivo methods

3.2.1 Apparatus and Software's

- Andersen Cascade Impactor (ACI) (Copley Scientific Ltd, UK)
- Next Generation Impactor (NGI) (Copley Scientific Ltd, UK)
- Breath Simulator (BRS) 3000 (Copley Scientific, Ltd, UK)
- Alberta Idealised Throat (AIT) (Copley Scientific Ltd, UK)
- Mixing Inlet (Copley Scientific Ltd, UK)
- Cyclohaler® and BreezHaler® Mouth Pieces (Copley Scientific Ltd, UK)
- Critical flow controller, TPK 2000 (Copley Scientific Ltd, UK)
- Vacuum Pump (HCP5 High capacity pump; Copley Scientific Ltd, UK)
- Digital flow meter 2000 (Copley Scientific Ltd, UK)

- Filter paper Grade 934-AH circle glass microfibre 47mm for DSU (Fisher Scientific Ltd, UK)
- Filter paper Grade 934-AH circle glass microfibre 82 mm Whatman (Fisher Scientific Ltd, UK)
- Silicone spray (Pro-Power Silicone Lubricant, Premier Farnell plc, UK)
- Copley Inhaler Testing Data Analysis Software (CITDAS) version 2.00 (Copley Scientific Ltd, Nottingham, UK)

3.2.2 Impactors set-up

The use of impactors allows the API to be quantified and differentiated from the other components of the formulation as these devices capture the entire dose and measure the aerodynamic diameter, which is relevant to particle behavior during inhalation (Mark Copley, 2008).

The aerodynamic properties of SS with Lactohale® and PSDL have been determined using an Andersen cascade impactor (ACI) and the next generation impactor (NGI) with maximum inhalation flows of 60 and 90 L/min and inhaled volumes of 1 and/or 2L.

The ACI configuration used for 60L/min was designed with collection stages -1A to 6 (Figure 3.1) and the pre-separator appropriate for 60 L/min was used. Similarly, the ACI configuration used for 90 L/min was with stages -2A to 5 with the pre-separator suited for 90 L/min.

(a)

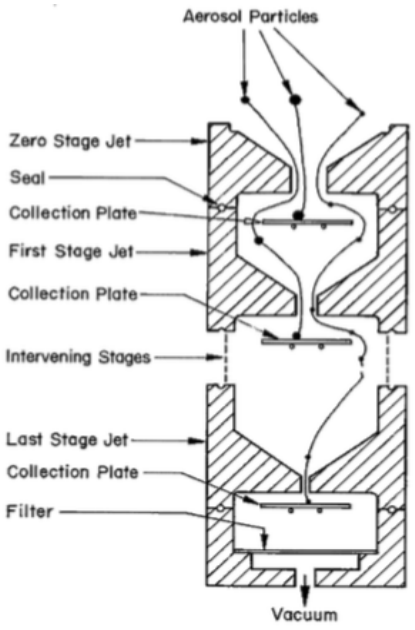

(b)

Figure 3.1 (a) Andersen Cascade Impactor set up for DPIs **(b)** Mechanism of operation of the Andersen Cascade Impactor (Adapted from Copley Scientific, 2016)

The next generation impactor (Copley Scientific Ltd, Nottingham, UK) comprises seven stages (Figure 3.2). The impactor was fitted with a pre-separator to prevent any powder boluses and larger carrier particles from overloading the collection plate of the first stage of the impactor. One of the differences between the NGI and the ACI is the arrangement of the different stages which are vertically organized for the ACI and horizontally set for the NGI. The airflow passes through the NGI in a "saw-tooth pattern" (Copley, 2008). Particles pass through a series of nozzles containing gradually reducing diameters.

All the NGI testing was first carried out with an airflow of 60 L/min with a sampling time of 1 second (corresponding to 1 L) and 2 seconds (corresponding to 2L). A secondary set of testing was carried out at 90 L/min for 0.7 seconds and 1.3 seconds corresponding to 1 L and 2 L respectively. The inhaler device was connected to the throat using a rubber mouthpiece adapter. 20 ml of the HPLC mobile phase (described in section 3.3.3) was added to the pre-separator and 10 ml was added to each collection cups. The collection cups were coated with a sprayed layer of silicone to reduce the chances of particles hitting the cup and bouncing

back into the airstream. The required airflow was generated from a vacuum pump. After each experiment, the NGI was cleaned with water and methanol and was left to air dry.

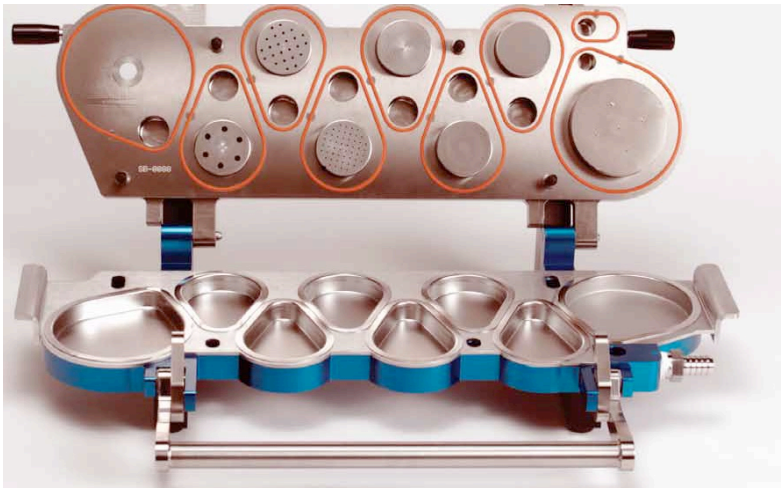

Figure 3.2 The Next Generation Impactor (with permission from Copley Scientific, 2014)

The NGI was operated at 60 and 90 L/min, which are within the calibration range from 30 to 100 L/min (Marple et al., 2003), with its appropriate pre-separator and the standard NGI collection cups (1 to 7).

Both cascade impactors were equipped with a United States Pharmacopeia (USP) throat. The collection cups and collection stages for NGI and ACI, respectively, were each coated with silicone lubricant (Pro-Power premier Farnell plc, UK) and left to dry at room temperature before use. The coating was done to ensure good API recovery and assay by avoiding bias from particle bounce and re-entrainment in the impactors.

The impactors were connected to a vacuum pump (HCP5, Copley Scientific Ltd, UK) via a TPK critical flow rate controller (Copley Scientific Ltd, UK). The cascade impactors were assembled with their appropriate pre-separator containing 10 ml of water and a glass fiber GF50 (Whatman, UK) filter positioned in the last stage and a Micro-Orifice Collector (MOC) for ACI and NGI, respectively.

A total of 27.4 mg of SS/lactose carrier (1:67.5 w/w) mixture were filled into three size 3 hard gelatine capsules for each formulation. The capsules were entered into the dry powder inhalation device (MacHaler®) which was fitted to the mouthpiece and attached to the USP throat. The pump was then switched on and allowed to run for 1 and 2 secs at 60 L/min and 0.7 and 1.3 sec at 90L/min, as the dose was being released from the device. The deposition test was repeated two more times in the same manner. The capsule shells were washed with 5ml of the washing solution. The inhaler device and the mouthpiece were washed with 10ml. Similarly, the inlet port was washed with 20 ml of the washing solution and the pre-separator with 25ml. All the stages/plates were washed separately with 10ml and finally the filter with 10 ml. Salbutamol sulphate was recovered from each component of the cascade impactor using a suitable solvent (Methanol) and then assayed by a validated high-performance liquid chromatography (HPLC) method described in section 3.3.3.

In order to calculate the aerodynamic dose emission parameters, the Copley Inhaler Testing Data System Analysis Software (CITDAS Version 2.0, Copley Scientific Ltd, UK) was used. The American and European pharmacopoeias have described methods based on inertial impaction in order to evaluate the in-vitro performance of formulations by studying the fine particles (Pilcer et al., 2012). The efficiency of drug delivery in the lung is mainly dependent on the delivered dose. High fractions of emitted dose and fine particle fraction are required for an optimized performance. Statistical analysis using two-way analysis of variance (ANOVA) was used to compare the different parameters obtained (%FPF; FPD; MMAD; TED) from the different inhalation volumes and inhalation flow rates used for all the formulations.

3.2.3 Inhalation profiles

Patient's inhalation profiles can be characterised by three important parameters which are the peak inspiratory flow rate (PIF), the inhalation volume, the initial acceleration rate.

One of the most important parameter for breath actuated DPIs to achieve sufficient dose de-aggregation is the PIF.

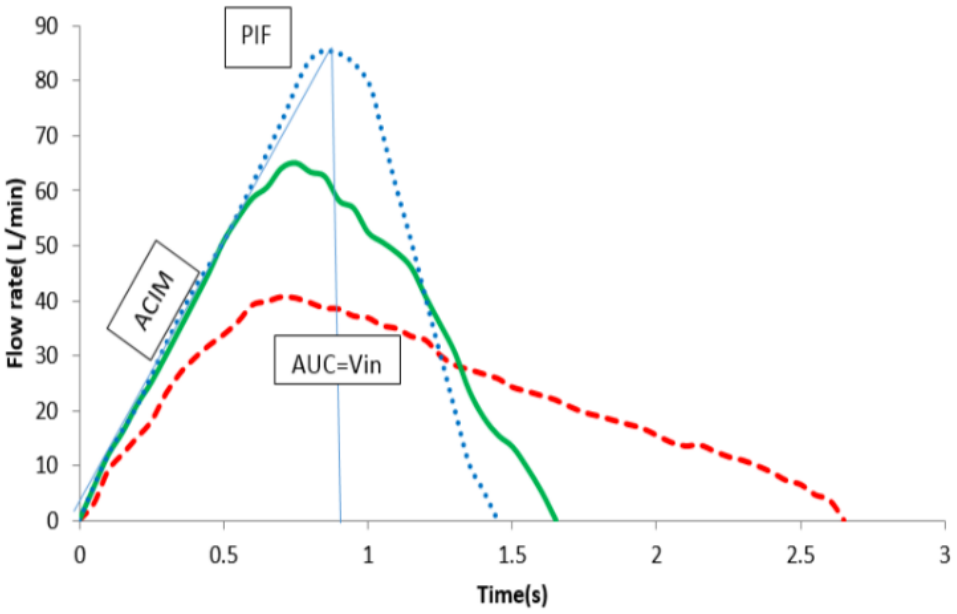

Figure 3.3 Schematic diagram displaying different COPD patients' inhalation profiles (Red: low profile; Green: medium profile; blue: high profile) (Abadelah, 2017)

3.2.4 Breath Simulator (BRS) 3000

The BRS 2000 was originally intended for being used by nebulisers. The launch of the BRS into the market in 2012 allowed the use of higher inhalation flows up to 240 L/min with a maximum acceleration rate of 25 L/s^2 and an inhalation volume capacity of up to 5 L (Copley Scientific, 2015). These new features allowed the BRS 3000 to be used in testing DPIs and MDIs in a more realistic manner as BRS 3000 is able to replicate inhalation profiles (Copley Scientific, 2014).

3.3 High Performance Liquid Chromatography (HPLC)

3.3.1 Materials

3.3.1.1 General materials

- ✓ Amber HPLC vials (2mL) (Fisher Scientific Ltd, UK)
- ✓ Filter membranes, 0.45μm pore size (Sigma Aldrich Ltd, UK)
- ✓ Supelco® mobile phase filtration apparatus (Sigma Aldrich Ltd, UK)
- ✓ Ultra-purified water apparatus (Thermo Scientific Ltd, UK)
- ✓ Glass Pasteur pipettes (Fisher Scientific Ltd, UK)
- ✓ Volumetric flasks and beakers (Fisher Scientific Ltd, UK)

3.3.1.2 Chemicals used for buffer preparation

- ✓ Hexanesulfonic acid (Sigma Aldrich Ltd, UK)
- ✓ Methanol, HPLC grade (Fisher Scientific Ltd, UK)
- ✓ Ultrapure water (Barnsted™ Nanopure ™, Thermo Scientific Ltd, UK)

3.3.2 Introduction

High performance liquid chromatography (HPLC) is a chromatographic technique highly used in the pharmaceutical field for the quantification of separate components of a mixture. It is both a qualitative and quantitative method in which the separation of components is dependent on the polarity of the compounds as well as the polarity of the aqueous phase and stationary phase. The separation is also driven by the affinity of the compound to the mobile and stationary phase, therefore the elution time will vary depending on their affinity (McPollin, 2009).

Reversed-phase HPLC (RP-HPLC) is most commonly used, the stationary phase is usually made of non-polar alkyl hydrocarbons bound to silica. On the other hand, the mobile phase is polar, creating a strong attraction between the polar molecules and solvent when the mixture

passes through the column (McPolin, 2009b). A schematic diagram of a HPLC system is illustrated in Figure 3.4 below.

The solvent constituting the mobile phase is water/buffer which is used in parallel with an organic solvent (miscible in water). The most commonly used solvents in HPLC are acetonitrile and methanol which are water miscible and easily accessible from suppliers in HPLC grade).

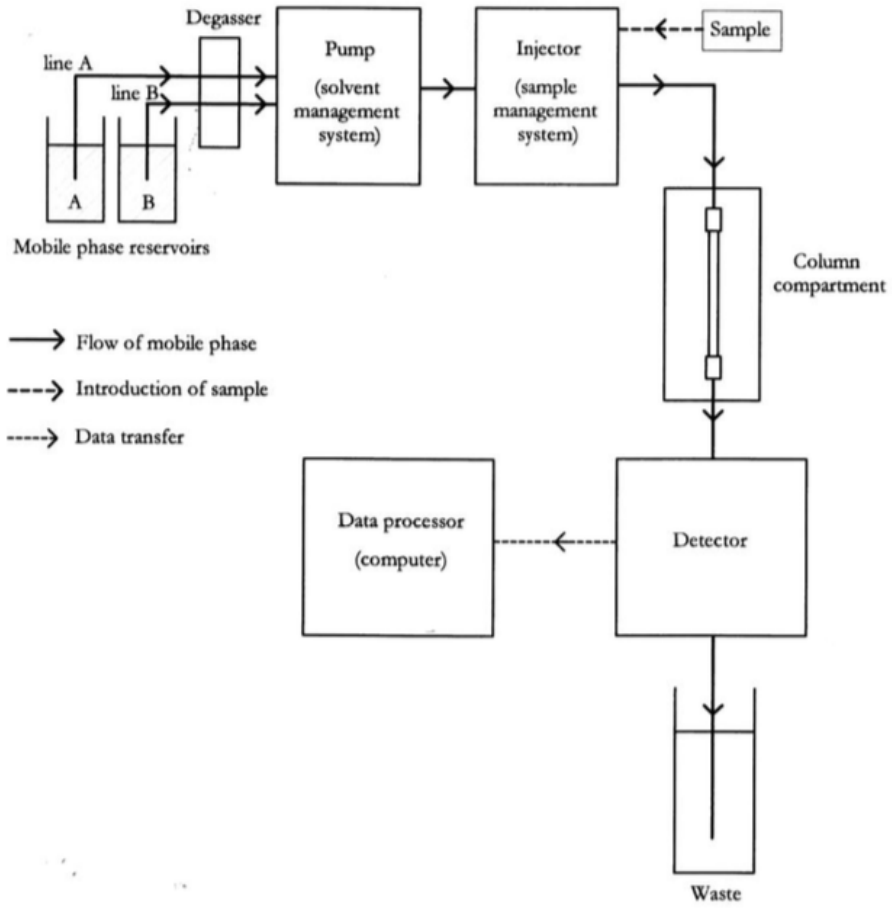

Figure 3.4 Configuration of a typical HPLC system (McPolin, 2009)

3.3.3 HPLC conditions

The concentration of SS solution was measured by a Shimadzu system consisting of a Prominence liquid chromatograph (LC-20AT) pump (Shimadzu Ltd, UK), a Prominence

degasser (DGU-20A5) (Shimadzu Ltd, UK) and a Photodiode Array detector (SPD-M20A). The column used was Luna® C18 100A (250mm x 4.6 mm) with a pore size of 5µm (Phenomenex, UK). The mobile phase consisting of a mixture of 30% v/v methanol and 70% v/v hexanesulfonic acid. This buffer was chosen to achieve maximum separation and sensitivity. The buffer (10 mM of hexanesulfonate buffer) was prepared by dissolving 0.941 g of sodium hexanesulfonate and 10 ml of glacial acetic acid in 1L of ultra-pure water (18.2 Ω). The buffer was then filtered under vacuum using 0.45µm nylon filter.

The mobile phase was filtered and degassed before use. The flow rate was 1mL/min. Samples were detected at 276nm using photodiode array detector. The data analysis was performed with Shimazu LC-solutions. All the calculations concerning the quantitative analysis were performed by measurement of peak areas. Results were expressed as the mean of three determinations.

The preparation of standard solutions is described below:

Eight standard solutions were prepared. Firstly, 10 mg of SS was dissolved in ultrapure water in a 10 mL volumetric flask to obtain solution A with concentration of 1 mg/mL. Solution B was made by withdrawing 1 mL of solution A and then topping up with water in a 10 mL volumetric flask. Its concentration was 100 µg/mL. Solutions C, D, E, F, G, H, I and J with concentrations 25 µg/mL, 20 µg/mL, 10 µg/mL, 5 µg/mL, 2.5 µg/mL, 1 µg/mL, 500 ng/mL and 250 ng/mL respectively were prepared using the same method using appropriate dilution factors.

The accuracy of HPLC methods can be inferred from the analytical parameters used in assay validation such as linearity and precision. In order to establish the linear detection range for SS, standard stock solutions were analyzed to determine the linearity.

Calibration ranges of 250 ng/mL to 25 mg/mL (solutions C to J) were prepared. Triplicate 10 µL injections were made for each standard solution to see the reproducibility of the detector response at each concentration level.

3.3.4 HPLC system suitability and validation

The suitability of the system is one of the parameters that must be checked to validate the HPLC method, according to the ICH guidelines (ICH, 2005). The system suitability test ensures that the HPLC system is performing as expected, including the mobile phases, pump, injector, column, detector, data processor and the operator (McPolin, 2009a).

The system suitability parameters are listed below:

- **Void volume determination:**

The void volume of the column was determined by using thiourea. Using the same HPLC conditions as described above, Thiourea was assayed at λmax= 240 nm with the working concentration range of 1 to 25ug/ml.

- **Capacity factor (k'):**

The capacity factor of the column was calculated using the formula $k' = (T_r T_0)/T_0$

Where T_0 being the initial retention time (solvent front), T_r being the retention time of the analyte (salbutamol sulphate in this study)

- **Tailing factor:**

Tailing factor was calculated by using the below formula

$T = W/2F$

Where W is the width of the peak, F is the flow rate (ml/min)

- **Number of theoretical plates:**

Number of theoretical plates was calculated by using the below formula

$N= 5.54[T_r/W_{0.5}]^2$

Where T_r is the retention time of the analyte, $W_{0.5}$ is half the peak width

3.3.5 Linearity

The linearity of the method is verified to establish a proportional relationship of response versus salbutamol concentration over the working range. The calibration curve was constructed and linearity was verified between inter and intra-day, all experiments were carried out in triplicate.

The peak area of each drug was plotted against the concentration to obtain the calibration graph. The eight concentrations were subjected to regression analysis to calculate calibration equation and correlation coefficients (Fig.3.6). The equation of the regression line formula is:

$$y = 3157.2 + 132.54$$

With correlation coefficient $r^2 = 0.99904$. The regression analysis indicated that there was an excellent linearity between the peak area and SS concentrations.

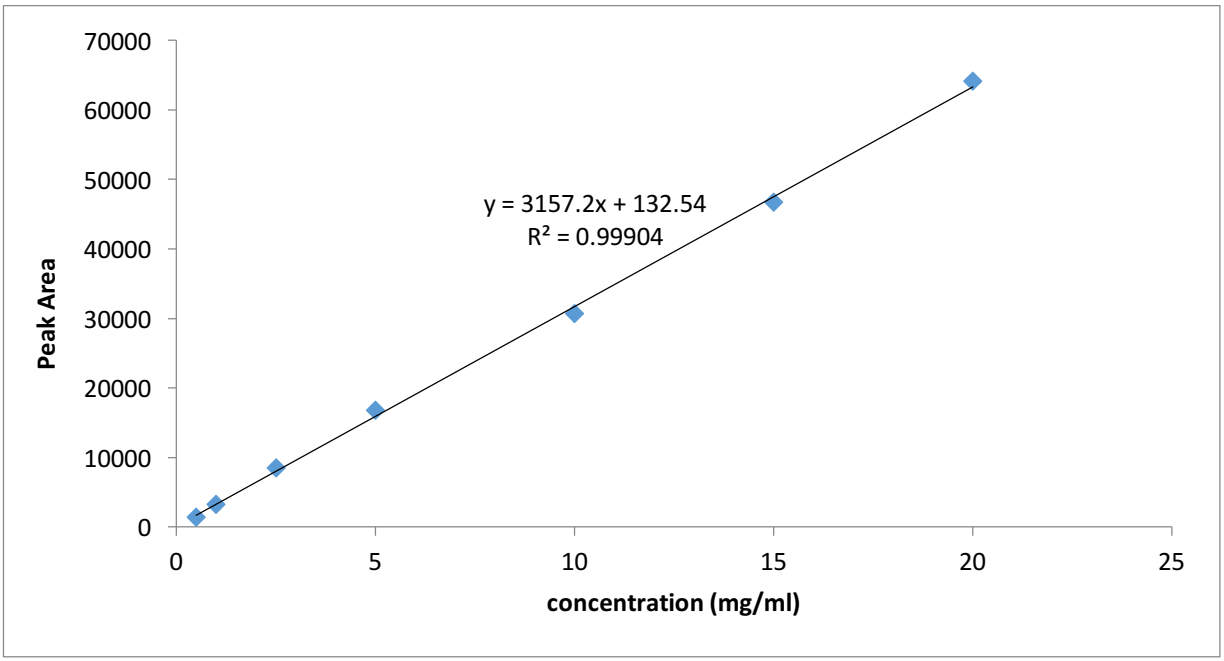

Figure 3.6 Calibration curve of salbutamol sulphate

The inter-day precision is defined as relative standard deviation (RSD) calculated from the values measured from three samples at SS concentrations of 0.25, 0.5, 1, 2.5, 5, 10, 20 and 25 mg/mL, respectively, in three different days. The calculated inter-day precision (RSD) values ranged from 2.56 % to 6.6 % indicated that the HPLC method is accurate for measurement of SS concentrations.

3.3.6 Precision

The precision is the measure of degree of repeatability of an analytical method under normal operation and it is expressed in relative standard deviation. The relative standard deviation of obtained in an experiment should be less than 1%. For salbutamol sulphate the developed method shows high degree of precision with relative standard deviation below 1% (n=6). Statistical significance was evaluated using One-way Anova, there was no significant difference ($P<0.05$), found in both the method. From these results, the developed method shows high degree of precision and compiles with ICH guidelines.

Table 3.1 Precision test for Salbutamol Sulphate

Log Concentration	Mean Peak Area 1	Mean Peak Area 2	Mean Peak Area 3	Mean Peak Area 4	Mean Peak Area 5	Mean Peak Area 6	Peak Area Mean	SD	RSD %
-0.30	3.40	3.41	3.40	3.40	3.40	3.41	3.40	0.00	0.09
0.00	3.70	3.70	3.71	3.71	3.71	3.70	3.70	0.00	0.04
0.40	4.09	4.09	4.09	4.09	4.09	4.09	4.09	0.00	0.02
0.70	4.40	4.40	4.40	4.40	4.40	4.40	4.40	0.00	0.01
1.00	4.70	4.70	4.70	4.70	4.70	4.70	4.70	0.00	0.01
1.30	5.00	5.00	5.00	5.00	5.00	5.00	5.00	0.00	0.00
1.40	5.09	5.09	5.09	5.09	5.09	5.09	5.09	0.00	0.01

3.3.7 Accuracy

The accuracy describes the closeness between the true values by the proposed analytical method. The Accuracy of the developed method was studied by adding a known amount of drug (10 mg) to the placebo formulation (30 mg of lactose). Accuracy studies were performed in the range of 500 ng/ml to 25 μg/ml; all experiments were carried out in triplicate. For all concentrations, RSD were calculated and statistical significance was tested using one-way ANOVA.

Accuracy of an analytical method is the closeness of test results obtained by the method to the true value. Accuracy is assessed by analysing the sample of known concentration and comparing it with measured true value. Seven different concentrations were used for accuracy test in a linear range. In both the methods recovery was found to be 99% with relative standard deviation below 1% confirms that the method is accurate and can be used to quantify analyte accurately within the specified range. Statistical significance was evaluated using One-way Anova ($P<0.05$), there was no significant difference found

Table 3.2 Accuracy test Salbutamol Sulphate

Number of Samples(n=7)	% Recovery	SD	RSD %
1	98.42	0.70	0.71
2	99.41	0.86	0.87
3	98.85	0.19	0.19
4	99.72	0.03	0.03
5	100.70	0.10	0.10
6	100.71	0.01	0.01
7	98.25	0.14	0.15
Mean recovery =99.44% RSD = 0.29%			

3.3.8 Limit of detection (LOD) and limit of quantification (LOQ)

The limit of quantification (LOQ) and limit of detection (LOD) were calculated for salbutamol sulphate. Three calibration runs were performed in triplicate and calibration curves were constructed using the least square method. The relative residual standard deviation of the y intercepts (δ) and the slope of the regression lines (S) was calculated from the calibration curves. The following equations were used to calculate LOQ and LOD (ICH guidelines, 1998)

$$LOD=10\delta/S$$

$$LOQ=3.3\delta/S$$

Limit of detection (LOD) is the lowest limit of the analyte that can be detected above the base line noise; typically, three times the noise level S/N =3.3. LOQ is defined as the lowest amount of the analyte which can be quantified accurately above the baseline noise i.e S/N=10.

In the current study, LOD and LOQ were calculated using the relative standard deviation obtained from the calibration curve. The LOD and LOQ for salbutamol sulphate found to be 30 ng/ml respectively.

3.3.9 Conclusion

The optimised HPLC method was found to be accurate, precise and robust.

Results and Discussion

Chapter 4

Study of aerosolisation performance of Untreated Lactose and Processed Spray-Dried Lactose formulations using Salbutamol Sulphate as a model drug aerosolized from a MacHaler® into an Andersen Cascade Impactor (ACI) and Next Generation Impactor (NGI) at two inhalation flow rates (60 and 90 L/min) and at inhaled volumes 1 litre and 2 litres.

Aim

The aim of this chapter was to engineer a new lactose carrier, namely Processed Spray-dried Lactose (PSDL) for dry powder inhalation aerosol using solid-state crystallization of spray dried Lactohale. Commercial Lactohale was used as a control in this study and was fractioned so that its size range (63-90 μm) matched that of PSDL. Both lactose carriers namely Lactohale and PSDL were characterized using scanning electron microscopy, differential scanning calorimetry and X-ray powder diffraction. Each of these carriers was then blended separately with micronized salbutamol sulphate in a drug to carrier ratio of 1:67.5 (w/w). The homogeneity of each formulation was assessed by measuring drug content uniformity of SS using a validated HPLC method. The SS drug deposition profiles were determined using an Andersen Cascade Impactor and Next Generation Impactor after aerosolisation at different maximum inhalation flow rates (MIFs: 60 and 90 L/min) and inhaled volumes (V_{in}: 1 L and 2L) via a low resistance inhaler device MacHaler®.

4.1 Introduction

Most dry powder formulations comprise lactose as a coarse carrier. α-lactose monohydrate has been used most commonly and it is usually fractionated to 63-90 μm (Timsina et al., 1994). The carrier particles are usually large particles with a good flow to ensure a proper filling of the powder formulation containing a consistent dose of the API into the dose cavity (i.e., capsule, blister compartment) or DPI reservoir, but also emitting a consistent dose during inhalation and to provide efficient emptying of the device using patient inhalation maneuver. When the patient inhales, the drug particles must be detached from the carrier and be dispersed into the airstream to be able to reach the lungs. The drug particles are generally present in low concentration, with a drug to carrier ratio of 1:67.5 w/w

The large carrier particles provide good flow to the powder formulation leading to an improvement in drug consistency when filling capsules and aerosolisation from an inhaler device (S.P Newman, 2002). The carrier is an important component in DPI formulations and any changes in the morphological features of the carrier particles such as particle size (Larhrib et al., 1999; Zeng et al., 2001a), particle surface roughness, particle shape (Larhrib et al., 2003; Larhrib et al., 1999; Zeng et al., 2000), crystallinity (Kawashima et al., 1998b; Zeng et al., 2001b) can have an impact on drug deposition. Several studies have reported an increase in the respirable dose of SS when delivered from DPI formulations comprising engineered lactose particles. For example, smoothing out the carrier surface irregularities by means of crystallization from solutions (Larhrib et al., 2003; Zeng et al., 2000) has resulted in an improvement in the amount of respirable fraction of SS. Particle smoothness was found to be a crucial factor in a study where two lactose grades of distinct morphological features, anhydrous and granulated lactose, were formulated with budesonide. The formulation with anhydrous lactose which had a smooth surface, gave a better drug delivery than the granulated lactose which had a rough surface (Heng et al., 2000).

A study of five different grades of lactose for use as a carrier for SS in DPI formulations showed that the grade of lactose had a great effect on the performance of the DPI formulation and drug delivery in-vitro. Anhydrous lactose provided more effective drug delivery when compared to the other grades of lactose (Larhrib et al., 1999). Kaialy et al. (2011) reported that SS formulated with recrystallized needle-shaped mannitol gave a fine particle fraction of 46% in comparison to commercial mannitol formulation. The addition of fine lactose particles to fill the active sites on the surfaces of coarse lactose particles has been shown to improve the dispersion and de-aggregation of SS (Zeng et al., 1998).

Current methods of engineering DPI carrier particles such as lactose (Zeng et al., 2000) or mannitol (Kaialy et al., 2011) use crystallization/precipitation from solution followed by

harvesting the crystals and drying. Crystallization from solution is unpredictable, firstly crystals may or may not form depending on the additives used, the nature of solvent(s) present in the crystallization medium, the size and shape of the crystallization vessel, stirring rate, stirring element and the temperature. Secondly the crystal shape, size and surface texture could not be predicted prior starting the crystallization process; furthermore, the harvested crystals are usually not uniform, product loss during the multistage processing sequence and batch to batch variation are not unusual causing problems in downstream processing and product uniformity. Crystallization from solution remains the process of choice for particles formation but has limited scope in particle engineering and design. Therefore, there is a need to provide a reliable crystallization method to form crystals with the desired shape, particle size, surface texture and crystallinity. All of which have been shown to affect the powder flow, drug content uniformity, physicochemical stability and drug deposition.

Spherical shape is desirable in many pharmaceutical solid dosage forms such as tablets, capsules, enteric coated granules/ pellets. Particles with spherical shape were useful in producing good flow, thus providing consistent filling of die cavity of the tableting machine and hence consistent dosing, in addition to reproducible drug release from pellets due to the uniformity of shape of the spherical particles. There are techniques available for producing spherical shaped particles such as spray drying, but the latter produces highly cohesive powder with some amorphous content hindering the stability and performance of the pharmaceutical product. The aim of this chapter was to overcome the above challenges by producing crystalline spherical shaped carrier lactose particles using a solid-state crystallization of spray dried lactose. The characterization of the engineered carrier and drug deposition will be carried out as discussed in the aim of the study.

The standard pharmacopoeial in-vitro methods for determining the aerosol aerodynamic particle size distribution from a DPI suggest using multistage cascade impactors such as the

ACI and NGI. These methods involve simulating a maximum inhalation flow rate (MIF) equivalent to a pressure drop of 4 kPa and an inhaled volume (Vin) of 4 L using a vacuum pump to emit a dose and collect it into the impactors (Council of Europe, 2014; United States Pharmacopeia, 2014). Humans are not able to replicate the square wave profile generated by a vacuum pump and the majority of patients are not able to achieve the pharmacopoeia recommended inhaled volume of 4 L (Chrystyn et al., 2015), thus making the *in-vitro* and *in-vivo* correlation between the impactor and clinical study difficult to achieve. Therefore, it is more appropriate to use an inhalation flow rate and volume when using an inertial impactor that a patient can achieve when using his inhaler device in real life. MacHaler® is a low resistance device with a specific resistance similar to the Onbrez Breezhaler® and many COPD patients were able to achieve a high inhalation flow from the latter and for this reason we carried out the SS deposition study using 60 and 90 L/min. ACI and NGI are routinely used for testing DPIs, the difference in their internal dead volumes ACI (1.155 L); NGI (2.025 L) can impact on the fractioning of the aerosol bolus emitted from an inhaler. The inhaled volume we choose for this work were 1 L and 2 L because the clinical study showed that 2 L is achievable by most of the asthmatic and COPD patients. This volume may be sufficient to pull the aerosol bolus to distal stages of the ACI and may not be sufficient for the NGI. Therefore, an investigation on the impact of the inhaled volume at 60 and 90 L/min on SS drug deposition from Lactohale® and engineered carrier will be carried out using ACI and NGI.

4.2 Material and Methods

4.2.1 Chemicals and solvents

Salbutamol Sulphate was obtained from GSK (UK). Hexane sulfonic acid; glacial acetic acid; methanol (HPLC grade) and absolute ethanol were purchased from Fischer Scientific (UK). Lactose was obtained from DFE Pharma (UK). The water was ultra-purified.

4.2.2 Production of spray-dried particles

Microparticles of lactohale were prepared by spray drying. A pre-calculated amount of lactohale was solubilized in water to obtain lactose concentration of 10% (w/v). Then the solution was spray dried using a laboratory scale spray dryer (Labplant SD-06, UK) with the following conditions: inlet temperature at 180 °C, solution feed rate at 4 rpm. The product was collected from the collecting chamber and transferred into a glass jar before storage in a desiccator before use.

4.2.3 Preparation of Processed Spray dried Lactohale

100 ml of absolute ethanol (Fisher, UK) was poured into a 600mL glass beaker and allowed to boil using a hot plate. This work was carried out in the fume-hood. 10g of spray-dried lactose particles were introduced to the boiling solvent under stirring for 30 secs at 250 rpm. The beaker was then removed and the content was passed through 500µm sieve into a collecting pan. The 500µm sieve was used to remove large agglomerates. The suspension recovered in the collecting pan was dispersed using a cool air generated by a hair drier. The cool air was preferred to the hot air in order not to affect the physicochemical stability of the particles such as polymorphic transformation, etc. This step was followed by drying in a ventilated oven at

45°C for 48 hours. The particles were easily removed from the collecting pan and stored in a clean glass jar until required.

4.2.4 Preparation of coarse Lactohale

The 63-90μm particle size fraction of lactohale was obtained by sieving. Approximately 50g of Lactohale was passed through a test sieve with an aperture width of 90 μm (Endecotts, UK) for 10 mins and the sieved powder fraction was then passed through a 63μm sieve for another 10 mins. The powder was then collected from the 63μm sieve and stored in a sealed jar until required for further use.

4.2.5 Characterisation of particle shape and size using scanning electron microscopy (SEM)

SEM was used to investigate the particle size, shape and surface structure of the lactose carriers used in the formulations. The lactose particles were mounted on an aluminium stub on which a double-sided carbon adhesive tape (Agar Scientific, UK) was first placed and after removing the protective covering, a few particles were scattered on the tape. The particles were then coated with gold for one minute using a Quorum SC7620 ion sputter coater (Quorum Technologies Ltd., UK) under vacuum of 0.09 mbar and a current of 40mA. Images were then obtained by a Jeol 6060LV SM scanning electron microscope (JEOL, Japan).

4.2.6 Characterisation of Salbutamol Sulphate and lactose carriers using thermal analysis techniques

Differential scanning calorimetry (DSC) was used to determine the crystal form of SS and lactose carriers. The experiment was carried out using a Mettler TA 4000 (Mettler, Toledo). Approximately 5mg of each sample was weighed into an aluminium pan (40μl) (Mettler AT

260 delta range weighing balance) and the lid was crimped into place. The samples were then heated from 25 to 250ºC at a heating rate of 10ºC per minute. The DSC was continuously flushed with nitrogen at a flow rate of 50ml/min.

Thermal gravimetric analysis (TGA) was carried out using a Mettler TA 4000 thermal analysis system, with a TG 50 thermo-balance. The sample of SS (10mg) was weighed into an aluminium crucible and placed into the furnace. The sample was heated from 25 to 250 ºC at a heating rate of 10 ºC min^{-1}. The weight change with temperature was recorded and analysed with Mettler GraphWare software.

4.2.7 Solid State Characterization of both lactose carriers using X-Ray Powder Diffraction (XRPD)

Single crystal XRD data was used to assess the crystallinity of lactose crystals. In this work, the surface forces can be predicted based on such data. Powder X-ray diffraction patterns were recorded after samples were spread uniformly over the sample holder using a D8 Advance powder X-Ray diffractometer with Cu $K_{\alpha l}$ radiation of $\lambda = 1.54$Å. (Bruker AXS). The voltage and current applied were 40 kV and 40 mA respectively. The sample powder was packed into the rotation sample holder and scanned in the 2θ range 5° to 40°. Lactose particles' morphologies were identified by comparing the characteristic 2θ peaks ("fingerprints") of the XRD pattern.

4.2.8 Blending lactose carrier particles with Salbutamol Sulphate

Salbutamol Sulphate was mixed separately with lactohale and processed spray dried lactose in a ratio of 1:67.5, w/w in accordance with the ratio employed in the commercial 'Ventolin®' formulations. Thus, salbutamol sulphate was weighed into a 15 mL vial which was followed by the addition of one spatula full of lactohale crystals. The powder blend was mixed manually

with a spatula. More lactose particles (similar to the amount of the blend) were added to the vial and the blend was mixed manually. This process was repeated until all the lactose (2.70 g) had been added into the salbutamol sulphate/lactose blend to obtain a ratio of drug to carrier of 1:67.5, w/w. The same process was done with salbutamol sulphate and processed spray dried lactose. The stoppered vials were then placed in a Turbula mixer and mixed for 30 min. Finally, the samples were stored in a vacuum desiccator over silica gel until required.

Hard gelatine capsules (size 3) were filled with 27.4mg (corresponding to the mass of the powder blend needed for the filling of 100 capsules) of the powder mixture so that each of the capsules contained 400μg salbutamol sulphate. The filling of capsules was completed manually.

4.2.9 Measurement of the homogeneity of the mixtures

Nine samples were taken randomly from each blend. The sample (approximately 27.4 mg) was weighed accurately and the amount of salbutamol sulphate was measured by HPLC. The coefficient of variation in the drug content was used to evaluate the homogeneity of the mixtures.

4.2.10 HPLC analysis of Salbutamol Sulphate

A mixture of methanol: 10mM of hexane sulfonic acid was used as the mobile phase in the ratio of 30:70 v/v. Hexane sulfonic acid was used as an ion pairing agent to mask the ionized secondary amine group and to improve the retention of salbutamol sulphate on the stationary phase of the HPLC column.

Methanol was chosen as organic modifier because the drug is soluble and stable in methanol.

4.2.11 Deposition test of Salbutamol sulphate

Salbutamol Sulphate was emitted from MacHaler device using an Andersen Cascade Impactor (see Section 3.2.2 for set-up and method)

4.3. Results and discussion

4.3.1 Morphological characterization of SS and lactose particles by SEM

Filling of DPI capsules and deposition of the drug in the lung is influenced by the quality of the carrier particles used in DPI formulations. Lactose is widely used for inhalation due to its safety, good physico-chemical stability, it acts as a marker after the aerosolisation of the dose that it has been taken by the patient and as lactose is a disaccharide it leaves a sweet taste in the mouth. Lactose is widely used as an excipient in solid dosage forms (capsules, tablets). It is widely recognized and accepted by all regulatory authorities as being safe and ideal to be used as a carrier for DPIs. In most DPI formulations, the lactose carrier is the most important in term of quantity and drug to carrier ratio of 1:67.5 is been typical. According to a large number of studies mentioned in the introduction part of this chapter, any changes in the lactose morphological features can have an effect on drug deposition performance from DPIs (Kaialy et al., 2011).

Lactose is available in various grades, particles sizes, shapes, polymorphic forms and surface properties and batch to batch variation is not unusual. Drug deposition from DPIs is generally considered poor with about 12–40% of the emitted dose is delivered to the lungs and 20–25% of the drug remains within the device (Labiris & Dolovich, 2003). A lot of effort has been made by researchers to manipulate lactose carrier, drug particles or the formulation as a whole to improve drug delivery to the lungs.

Such modifications include: altering carrier particle shape through crystallisation of lactose from solution to form needle-shaped lactose (Larhrib et al., 2003); smoothing out lactose surface irregularities by crystallising lactose in the presence of Carbopol gel (Zeng et al., 2000); adding a ternary agent to the formulation to cover the active sites of lactose (Colombo et al., 2012; Grosvenor & Staniforth, 1996; Tee et al., 2000; Zeng et al., 1998) such ternary components include fine lactose, magnesium stereate, L-leucine.

It is known that the attractive forces between drug and carrier particles can be influenced by shape, size of the carrier, surface texture and crystallinity (Mullins et al., 1992; Crowder et al., 2001).

Scanning electron micrographs of micronized salbutamol sulphate particles and Lactohale, spray-dried lactose (SDL) and PSDL are shown in Figure 4.1.

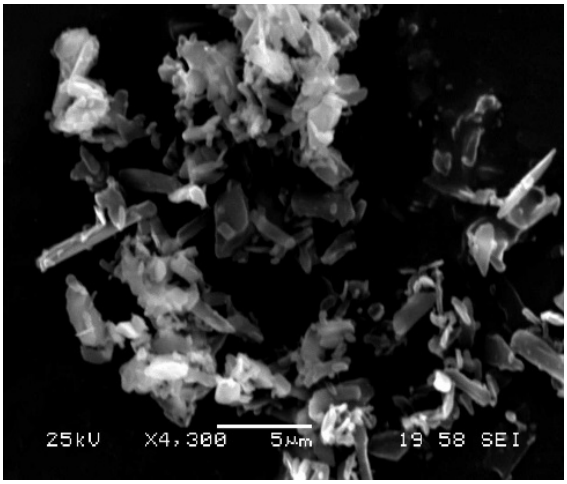

(a) Salbutamol Sulphate

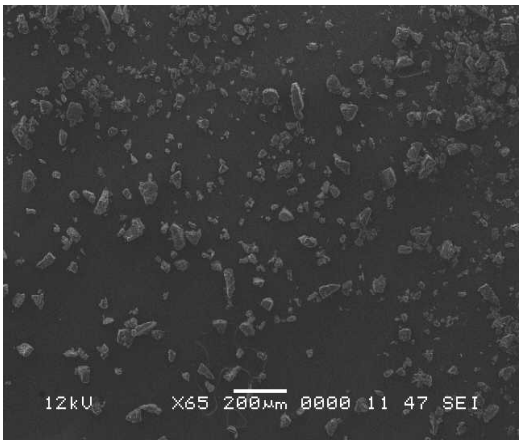

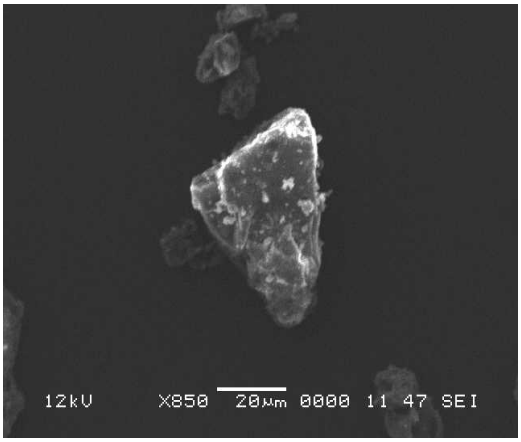

(b) Lactohale

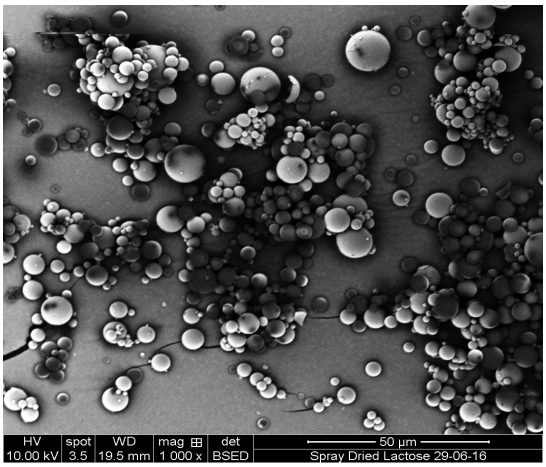

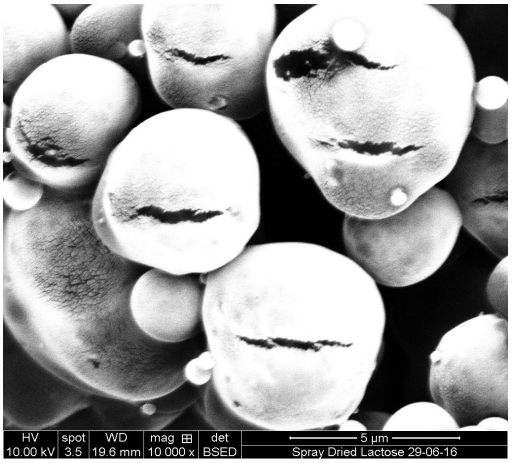

(c) Spray-dried Lactohale

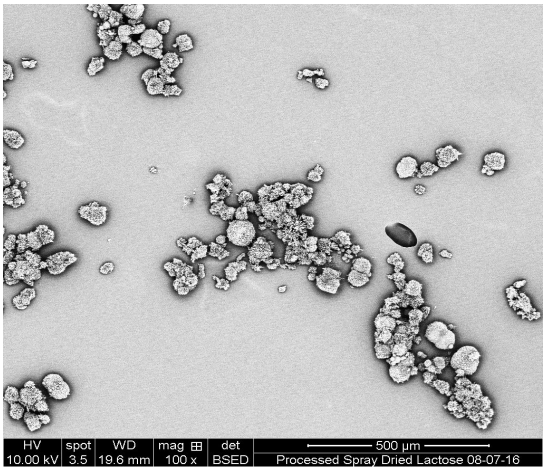

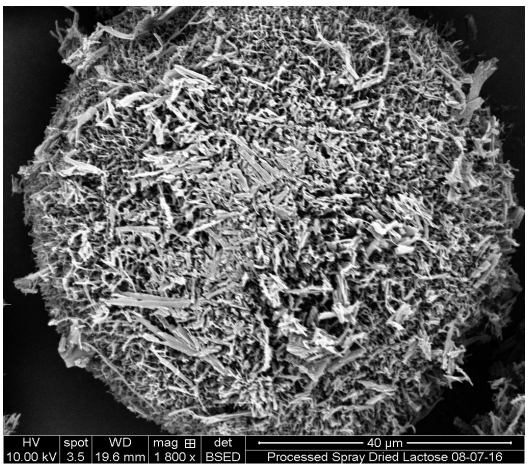

(d) Processed Spray-dried Lactohale

Figure 4.1. Scanning electron micrographs of SS (a); Lactohale (b); spray dried lactose(c) and processed spray dried Lactohale (d)

From the visual examination of the SE micrographs, SS was observed to be elongated with a size range between 1 to 5 μm as shown from the scale bar on the SS micrograph (Figure 4.1(a)). SS was donated by GSK Ware, UK and has a Volumetric Median Diameter (VMD) value of 2.4 μm suggesting its suitability for inhalation.

Lactohale showed a tomahawk shape with some surface roughness (Figure 4.1(b)) and this is in accordance with the literature (Larhrib et al., 1999). On the other hand, the spray-dried Lactohale particles are spherical with a smooth and fractured surface as shown in Figure 4.1(c).

Spray drying is a single-step process used to yield dry and potentially respirable dry powder formulations suitable for inhalation. It offers control over parameters such as particle size and morphology, and also provides the choice of incorporating additives in one particle. In spray drying, many parameters can be adjusted to design powders suitable for effective delivery to the lungs. This process usually provides uniform particles with a geometric mean particle size below 10 μm. However, the main problem of spray-drying is the formation of amorphous material due to the rapid transition from liquid to solid state. Although the particles are of suitable size for inhalation, they are usually cohesive and difficult to disperse into individual particles making them to deposit in the upper airways or to stick to the wall of the inhaler device. These drawbacks can have a negative impact on the usability of spray-drying as a main process of forming particles for inhalation. In this study, we took on board some of the advantages of spray-drying such as the spherical shape and the hollowness of the particles which have been shown to enhance drug deposition to the lungs (Hassan & Lau, 2010b) and we tried to convert the disadvantages of the particles formed by this process into more useful particles by reducing the cohesiveness, improving their stability and flowability by processing the spray dried particles.

The method to produce the processed spray-dried particles is detailed in Section 4.2.3 and the resulting particles are shown in SE micrographs in Figure 4.1(d).

It is clear that the particles have increased in size reaching about 80 μm without deviating from spherical shape. Ethanol acted as an inflating agent promoting an increase in the lactose particle size. A possible explanation is that the spray-dried lactose particles are polydisperse with some very small particles (Figure 4.1(c)) and amorphous as shown from X-ray powder diffraction scan (Fig 4.2(a) and 4.2(b)). Although the solubility of lactose in ethanol is limited (0.0111 g at 40 °C and 0.027 g at 60 °C per 100 g solution), the small size lactose with high amorphous content, in the presence of heat, may have promoted the dissolution of some particles totally or partially, thus increasing the concentration of lactose solution into the crystallisation medium (ethanol). Therefore, the dissolved lactose can be easily transferred under the influence of stirring and heat to the undissolved particles which act as a nucleus for crystal growth. The engineered lactose is spherical in shape and crystalline. These properties are desirable to produce a stable performant solid dosage form. With regards to inhalation, the engineered particles may contribute to improved flow of the DPI formulation and to a better drug delivery consistency.

Larger carrier particles are usually used to improve dosing accuracy and to minimise the dose variability observed with drug formulations and making manufacturing operations easier to handle. (Hamishehkar, 2012).

The surface properties of the carrier particle can play an important role, as there should be sufficient adhesive forces to hold the drug particles to the surface of the carrier particle during formulation, but that force of adhesion should be low enough to enable the dispersion of the drug in the respiratory tract (Zeng et al., 2000; Zhou et al., 2012). The rough surface of the PSDL particles (Figure 4.1(d)) will contribute to the stability of the powder blend against segregation.

Differences can be observed between the surface textures of all lactose grades. Spray dried lactose exhibited a smooth surface compared to the processed spray dried lactose which appeared to show a rougher surface texture. The literature provides contradictory data on the effect of surface roughness and the aerosolisation performance of DPI formulations. For example, Kaialy et al showed that a better DPI performance was observed when the formulation contained more irregular particles with rougher surfaces, as the carrier particles exhibited smaller adhesion forces with salbutamol sulphate, as opposed to commercial lactose particles. (Kaialy et al., 2011). In contrast, Flament et al., demonstrated that the rougher the lactose particles, the lower the FPF as rough particles have more contacts points with the drug, thus allowing a greater adherence of the terbutaline sulphate to the carrier particles (Flament et al., 2004).

In a general aspect, the engineering process provided a method of producing suitable sized carrier particles, with a rougher surface while retaining the spherical shape of the spray-dried material which could potentially enhance drug deposition into deep lungs.

4.3.2 Characterization of the polymorphic forms of SS and lactose particles by thermal analysis

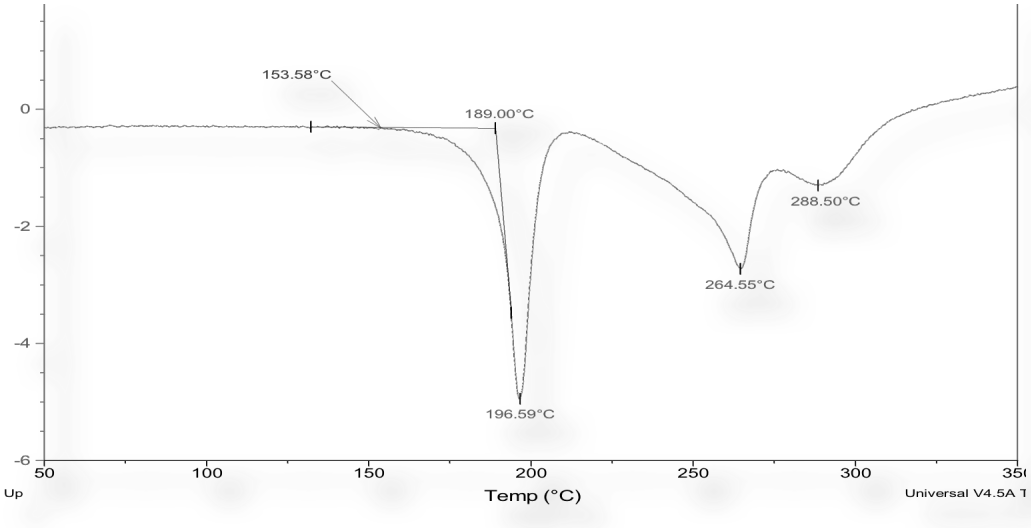

Figure 4.2a. Differential Scanning Calorimetry thermogram of Salbutamol sulphate

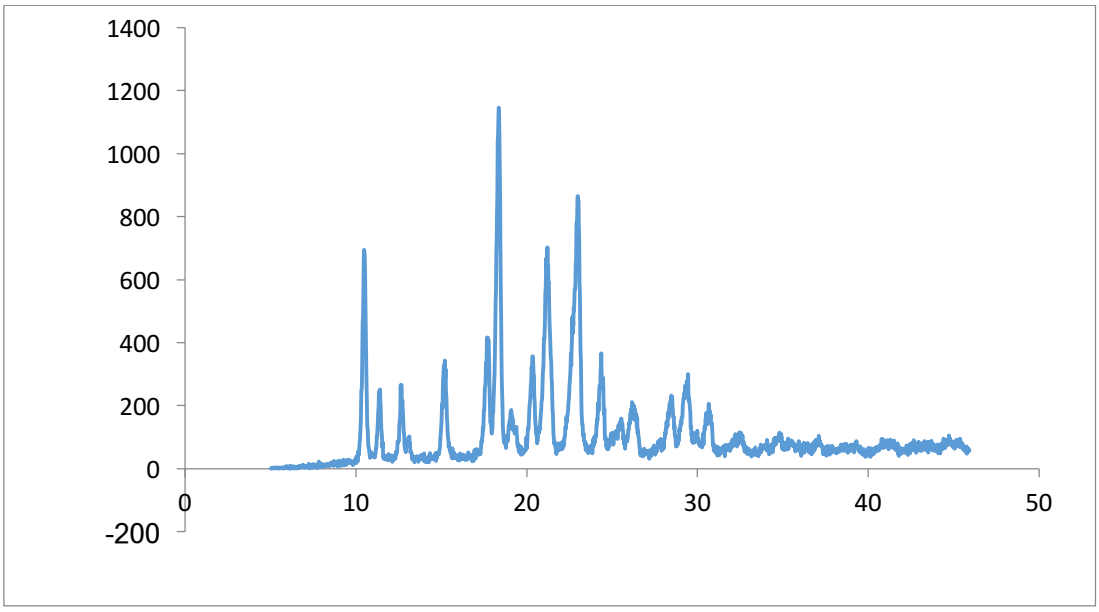

Figure 4.2b. X-Ray Diffraction pattern of Salbutamol Sulphate

Figure 4.2. Thermal analysis on Salbutamol sulphate: Differential Scanning Calorimetry thermogram of Salbutamol Sulphate (4.2a), X-Ray Diffraction pattern of Salbutamol Sulphate (4.2b)

On heating the sample (Figure 4.2a), no events occurred until around 153°C after which an endothermic peak was seen to start. This sharp peak had an extrapolated onset temperature of 189.15 ± 0.13 °C. The endothermic transition peaked at 196.67 ± 0.25 °C. This transition corresponds to the melting of Salbutamol Sulphate (Corrigan et al., 2006; Kauppinen et al., 2010). The offset of this initial endothermic peak overlapped with a broader endothermic event which in turn overlapped with a third endothermic event. These latter two endothermic events had peak temperatures at around 265 °C and 289 °C, respectively**.** However, a study carried out by Larhrib et al. (2003) suggested that the transition that was thought to correspond to melting of SS showed no transition from solid to liquid when SS sample was heated and observed under optical microscopy. The transition was suggested to correspond to the decomposition of SS. In order to confirm this result, an experiment with Hot Stage Microscopy

was carried out on SS to provide a visual representation of the effect of heating the sample and these are represented at 10°C intervals from 100°C to 200°C in the pictures below. A final picture of the residue is also shown (Fig. 4.3).

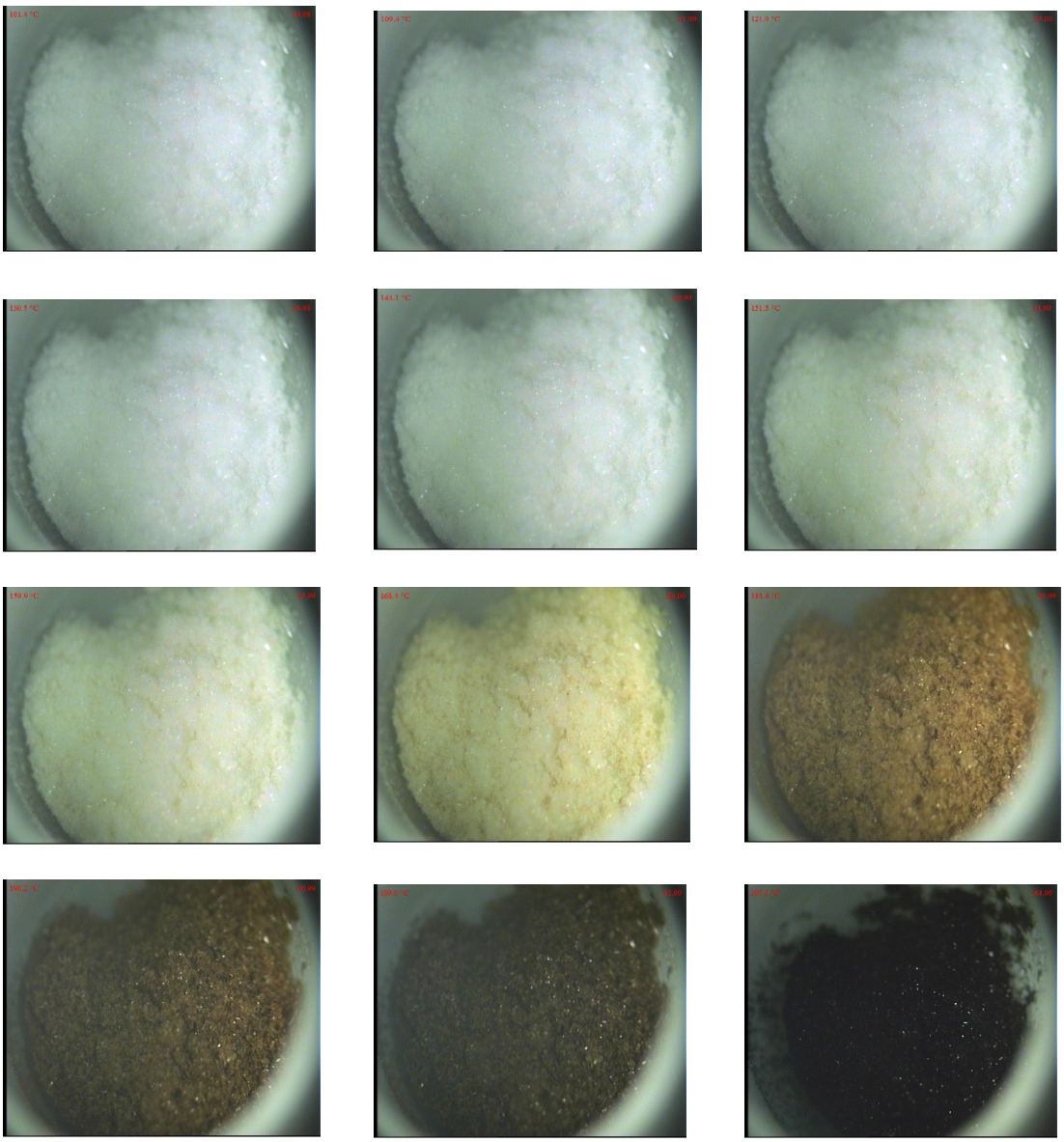

Figure 4.3. Hot stage microscopy of Salbutamol sulphate heated from 0 °C to 300°C

This study confirms that the sharp endothermic transition observed initially in the DSC thermogram at around 200 °C does not correspond to melting. Several studies indicated that SS melts at around 200°C but hot stage microscopy confirmed that no melting was observed but rather SS decomposed at higher temperatures.

It can be seen that there is no apparent change (from solid to liquid) in the appearance of the sample during heating until around 140°C when there is a slight yellowing of the sample. On further heating, the extent of discolouration continues until a mid-brown residue is seen at around 200°C. No molten phase indicating a melting reaction was observed throughout the heating cycle. Above 200°C, the decomposition reaction continued until a black carbonaceous residue was formed. The hot stage study on the sample is in agreement with the experiments using DSC.

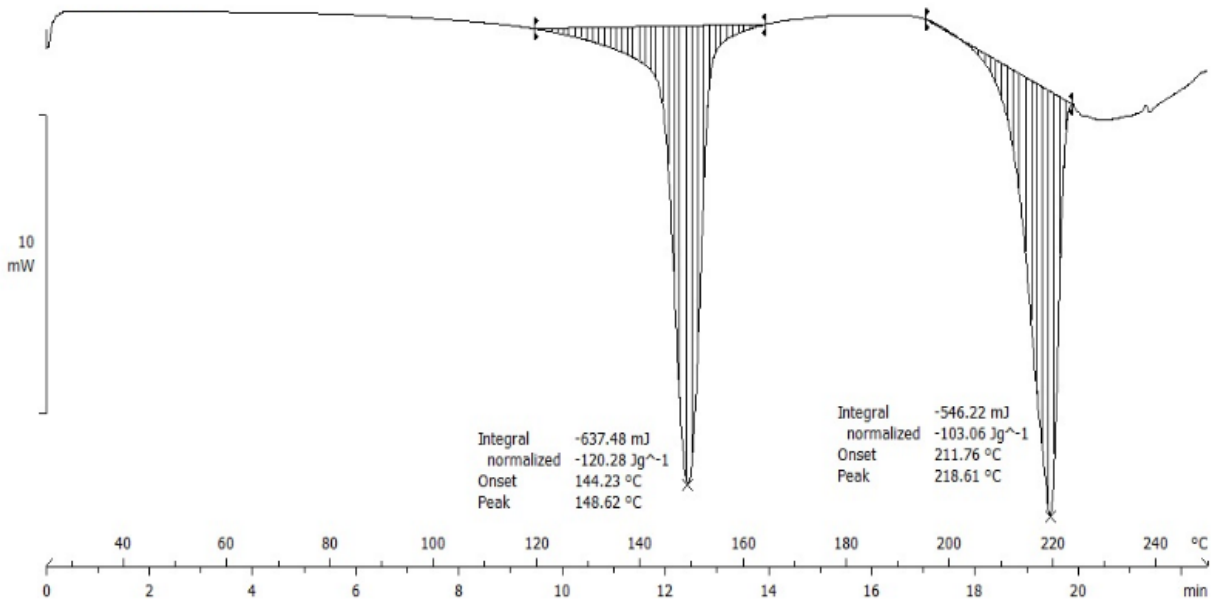

Figure 4.4. Differential scanning calorimetry thermogram of Lactohale

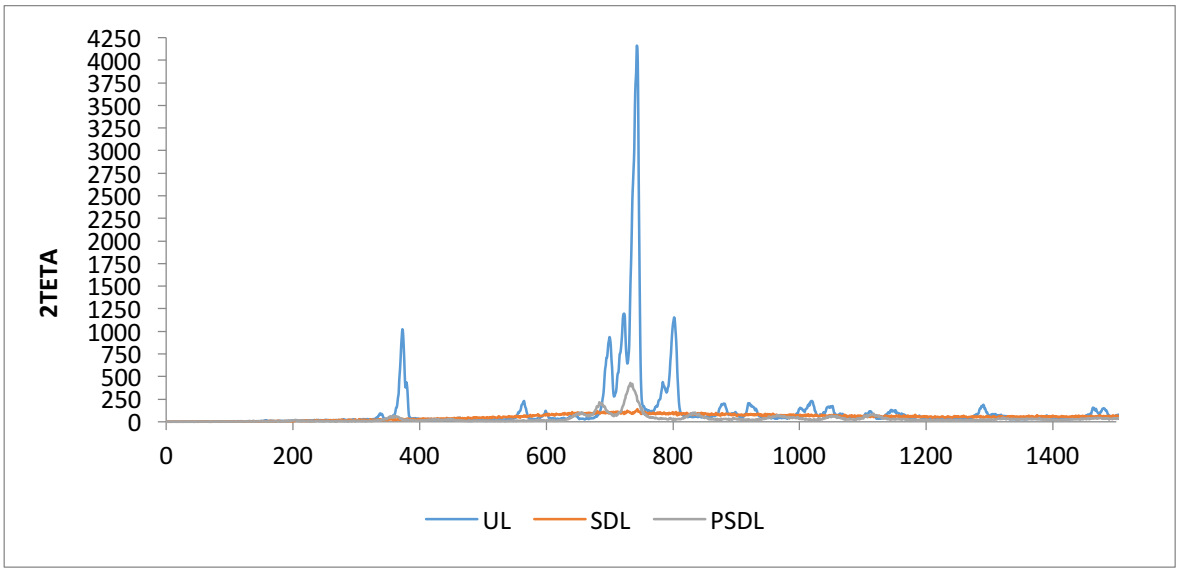

Figure 4.7: X-Ray Diffraction patterns of untreated lactose (UL), spray-dried lactose (SDL) and processed spray-dried lactose (PSDL)

Lactohale displayed DSC thermogram (Figure 4.4) which is representative of α-lactose monohydrate. This was justified by the presence of two typical endothermic transitions (Xian Ming Zeng, Pandhal, et al., 2000)

The first endothermic peak of the Lactohale DSC thermogram (Figure 4.4) at around 148ºC corresponds to the loss of water of crystallisation whereas the second endothermic transition starting at around 200ºC is due to the melting of α-lactose monohydrate followed by its decomposition. A slight deflection from the baseline was observed at around 190 ºC reflecting the small amount of amorphous content in the sample. Lactohale exhibited an X-ray Diffraction pattern (Figure 4.7) comparable to α-lactose monohydrate (Sebhatu et al., 1994). The presence of α-lactose monohydrate was supported by the presence of a peak at a diffraction angle of around 13º.

Spray-dried lactose exhibited a deflection of the baseline below 100 ºC suggesting that some amount of free water (surface water) was present in the sample. A small endothermic transition at around 115-120ºC (Figure 4.5) corresponded to the water of crystallisation. However, the

size of this transition was much smaller compared to the one in Lactohale sample suggesting that the drying phase during the spray-drying process removed most of the water of crystallisation, thus rendering the material anhydrous (due to the presence only of small amount of water of crystallisation). This transition was followed by an exothermic transition at around 180ºC which is representative of amorphous content. This non-crystalline portion is responsible for the improved compressibility of spray-dried lactose (José et al., 2000). The endothermic transition occurring at around 210ºC corresponded to the melting of α-lactose. The exothermic transition present in DSC thermogram is in agreement with the XRD data suggesting that spray-dried lactose is amorphous. The XRD pattern showed a dispersive scatter of X-rays confirming that the material was amorphous.

The processed spray-dried lactose thermogram (Figure 4.6) indicated that the material was completely anhydrous. The peak at 210 ºC suggested that the material was α-anhydrous lactose. The engineering process helped repair the defects present in the spray-dried lactose. One of the advantages resulting from this process was that the product was made to be more stable due to its crystallinity being restored. The XRD pattern in Figure 4.7 shows the evidence of crystalline peaks. There was a difference in peak intensity between the untreated lactose and the processed spray-dried lactose which might reveal a difference in degree of crystallinity. The relative degree of crystallinity of different samples of the same crystal form is said to be proportional to the ratio of the peak intensity (Zeng et al., 2000).

The obvious higher peak intensity for untreated lactose could be attributed to a higher crystallinity compared to the processed spray-dried lactose.

4.3.3 Homogeneity of the blends

Table 4.1. Drug content uniformity and coefficient of variation (%CV) of SS formulations containing either Lactohale or PSDL

formulation	Average drug content	SD	%CV
SS- Lactohale	*405.32*	*6.45*	*1.59*
SS-PSDL	*388.07*	*4.68*	*1.21*

Both formulations showed a low coefficient of variation, which were found to be less than 5%. This indicates that processing, formulating and order mixing of the binary blend formulation mixing as well as sampling and analysis of the samples were accurate and reproducible.

4.3.4 MacHaler® resistance to airflow

The relationship between pressure drop and flow rate is shown in Figure 4.8. It can be observed that this relationship is not linear. The relationship between pressure drop and flow rate can be made linear by plotting $\sqrt{\Delta P}$ against flow rate (Figure 4.9).

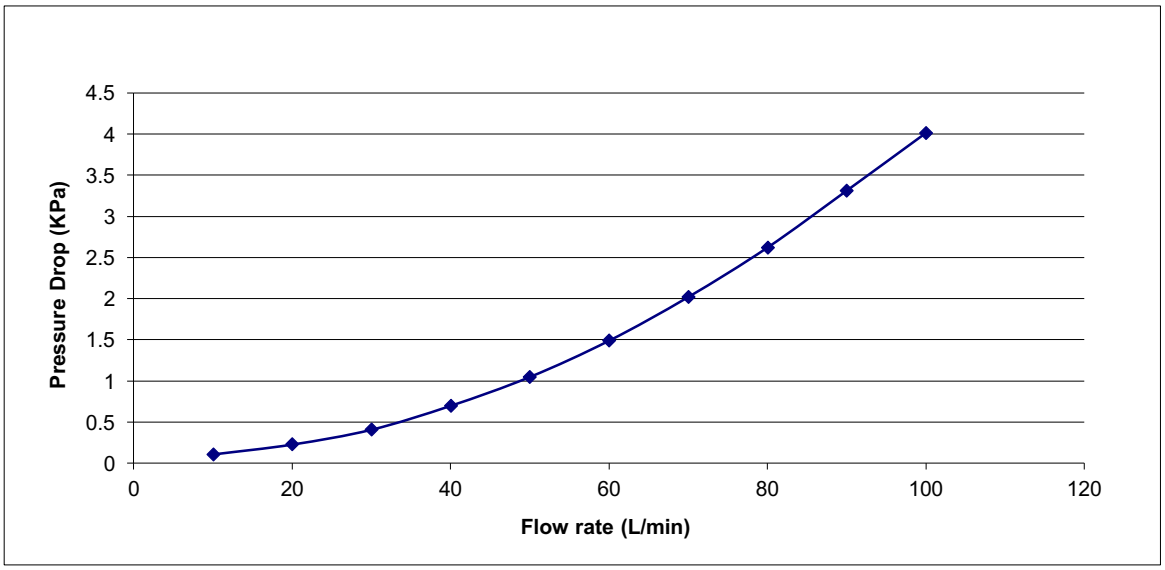

Figure 4.8 MacHaler® resistance to airflow

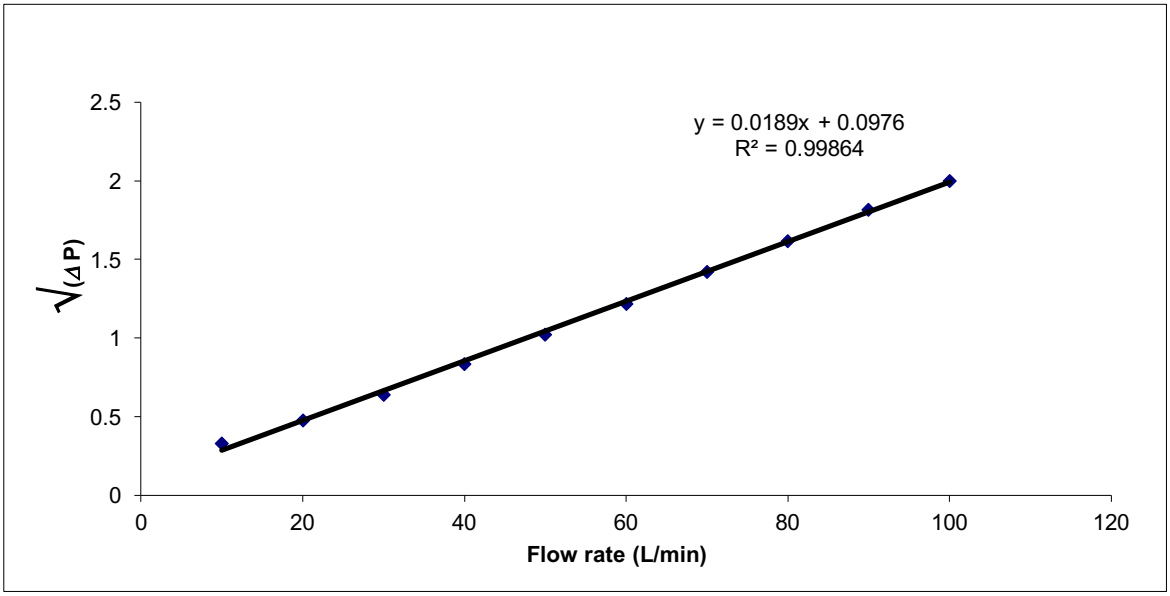

Figure 4.9 Relationship between pressure drop and flow rate of MacHaler®

The intrinsic resistance can be determined from the slope of the equation (Dal Negro, 2015). The pressure drops at different inhaled flow rates were measured for MacHaler device (Figure 4.9). DPI devices are categorised into four groups based on their resistance (Dal Negro, 2015). Patients with airflow limitation can still achieve a high flow with a low resistance device (Buttini et al., 2016). Azouz and Chrystyn (2012) demonstrated that an inhaler device with a low resistance and a high flow rate will have an equivalent turbulent energy as a device with

high resistance and low flow rate. It is clear that turbulent energy is more related to IFR for the MacHaler. Thus, dose delivery would be more dependent on the inspiratory flow. Sufficient inspiratory flow should be produced by the patient in order to release the powder and deaggregate the dose to generate respirable particles. The relationship between the pressure drop and the flow rate is not linear. To attain 4KPa pressure drop across the MacHaler, an inhalation flow of 102L/min was required (Figure I). The results suggested that MacHaler is a low resistance device and this is in agreement with the published data (Dal Negro, 2015; Laube et al., 2011). Therefore, patients can achieve a high inhalation flow from this device.

Figure 4.8 also showed that inhalation flow below 60 L/min caused only a little change in the pressure drop, hence turbulent energy. Above 60 L/min, a small change in the IFR caused a significant increase in pressure drop, thus 60 L/min can be considered as a threshold inhalation flow to successfully operate this device, suggesting that higher turbulence energy would be expected to occur inside the device above that flow rate. That is why flow rates of 60 and 90 L/min were chosen in this study.

4.3.5 Aerodynamic properties for both formulations:

Table 4.2. aerodynamic dose emission characteristics obtained from Lactohale-SS formulation using ACI

	60L/min-1L		60L/min- 2L			90L/min- 1L		90L/min-2L	
	mean	SD	mean	SD		mean	SD	mean	SD
S-1	5.35	0.19	4.06	0.12	S-2A	7.31	1.77	10.40	0.88
S-0	5.22	0.28	4.32	0.16	S-1A	4.47	0.03	3.74	0.06
S1	10.06	0.04	9.56	0.22	S-0	9.07	0.40	6.30	0.06
S2	17.45	0.55	18.74	0.14	S1	13.96	0.59	16.60	0.13
S3	39.28	0.82	41.99	2.73	S2	26.63	1.00	23.16	0.05
S4	18.73	0.18	26.66	0.32	S3	41.25	0.66	49.69	1.05
S5	2.56	0.02	4.92	0.14	S4	20.36	1.01	26.68	0.14
S6	0.00	0.00	0.00	0.00	S5	3.53	0.12	6.05	0.18
Filter	0.00	0.00	0.00	0.00	Filter	1.28	0.75	2.58	0.09
throat	42.13	1.58	37.19	0.13	throat	32.93	3.49	41.69	0.41
PreSep	201.33	4.16	207.73	7.88	PreSep	171.81	3.58	167.74	3.08
MP	6.52	0.04	6.76	0.17	MP	11.14	0.96	5.58	0.10
Device	42.13	1.42	36.25	0.95	Device	41.66	1.23	39.59	0.90
Cap	7.74	0.99	4.82	0.53	Cap	16.16	0.20	12.26	0.22
TED	348.62	2.35	361.93	2.17	TED	343.74	1.93	360.20	2.10
FPD	88.07	1.64	101.87	1.48	FPD	116.08	1.09	131.06	1.01
%FPF	25.26	1.23	28.15	0.76	%FPF	33.77	1.02	36.39	0.72
RA	49.87	0.96	41.07	0.92	RA	57.82	1.14	51.85	0.59
TRD	398.49	2.64	403.00	2.97	TRD	401.56	2.64	412.05	1.30
% Recovery	98.39		99.51		% Recovery	99.15		101.74	
LPM	243.46	3.73	244.92	2.47	LPM	204.74	2.08	209.43	1.72
EFPD (<3)	93.29	1.82	106.19	1.58	EFPD (<3)	120.55	1.27	134.80	1.11
MMAD	2.90	0.07	2.70	0.00	MMAD	2.00	0.02	1.80	0.01
GSD	1.80	0.00	1.80	0.00	GSD	2.40	0.04	2.50	0.03

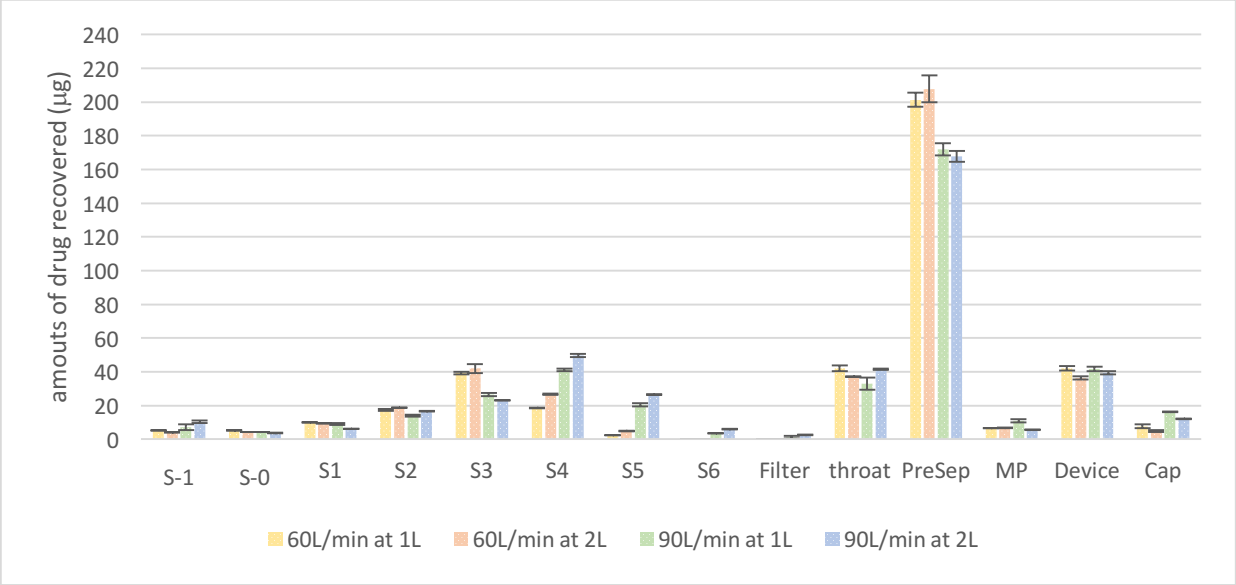

Figure 4.10 Amounts of SS found in each part of the ACI at 60 L/min, 90 L/min and 1 and 2L for Lactohale-SS formulation

Table 4.3 aerodynamic dose emission characteristics obtained from Lactohale-SS formulation using NGI

	60 L/min-1L		60 L/min- 2L		90 L/min-1L		90 L/min-2L	
	mean	SD	mean	SD	mean	SD	mean	SD
S1	25.62	1.06	14.17	0.23	36.61	0.76	28.73	1.15
S2	14.98	0.57	16.23	0.30	23.91	0.43	32.66	0.98
S3	15.80	0.54	20.68	1.35	23.93	0.12	35.87	1.94
S4	12.33	0.65	32.18	1.18	29.76	0.95	38.00	0.61
s5	3.28	0.28	12.71	0.62	5.07	0.76	13.58	1.02
S6	0.00	0.00	1.42	0.31	0.00	0.00	3.26	0.44
s7	0.00	0.00	0.00	0.00	0.00	0.00	0.00	0.00
MOC	0.00	0.00	0.00	0.00	0.00	0.00	0.00	0.00
throat	47.02	2.55	49.70	1.58	70.95	2.09	38.13	2.64
PreSep	217.91	3.88	207.39	2.43	144.42	3.52	163.54	3.20
MP	5.97	0.53	5.12	0.22	9.41	0.77	7.84	0.81
Device	42.90	1.59	32.70	1.38	44.24	0.28	32.13	0.70
Cap	17.51	1.41	13.95	0.11	11.85	0.93	7.93	0.62
TED	342.90	2.36	359.60	2.14	344.05	1.98	361.61	1.32
FPD	46.39	0.25	83.22	0.79	82.66	0.56	123.37	1.09
%FPF	13.53	0.69	23.14	0.94	24.03	1.17	34.12	0.25
RA	60.41	1.65	46.65	1.13	56.09	1.04	40.06	0.69
TRD	403.31	7.61	406.25	3.90	400.14	5.48	401.67	6.70
% Recovery	99.58		100.31		98.80		99.18	
LPM	264.93	1.34	257.09	1.61	215.37	1.35	201.67	2.46
EFPD (<3)	31.40	1.26	66.99	1.15	58.76	1.54	90.71	1.22
MMAD	5.40	0.49	3.00	0.07	4.60	0.70	3.70	0.35
GSD	2.20	0.07	2.60	0.21	2.00	1.55	1.90	0.00

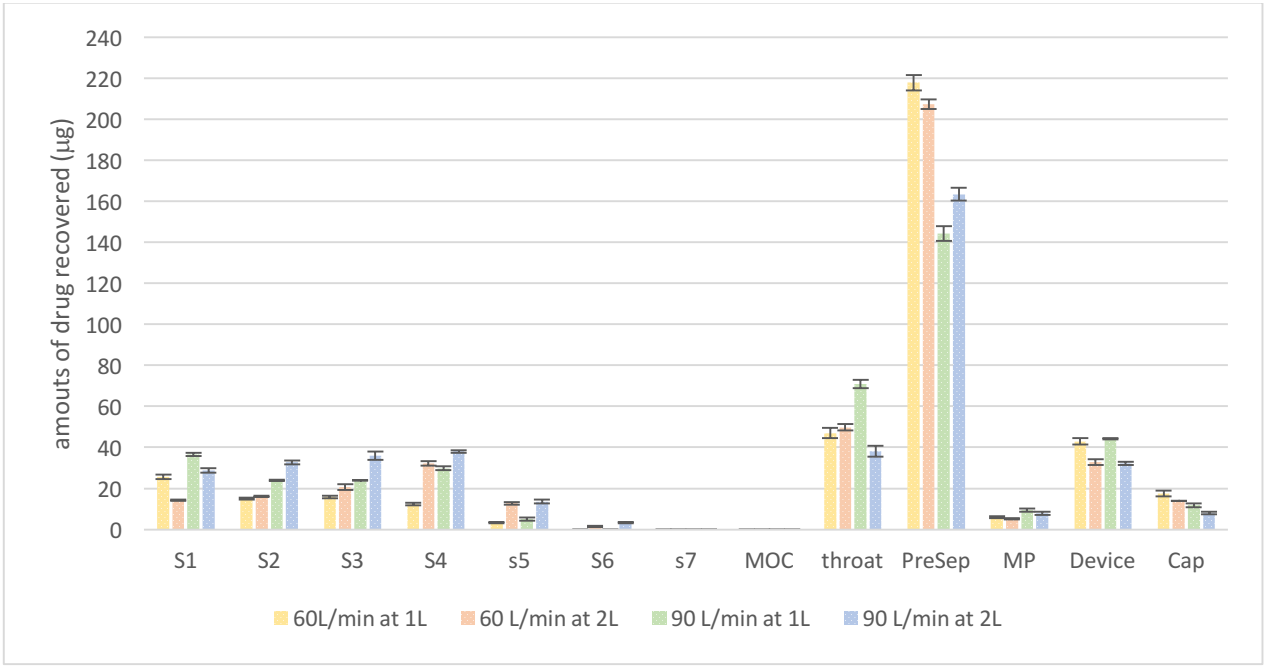

Figure 4.11 Amounts of SS found in each part of the NGI at 60 L/min, 90 L/min and 1 and 2L for Lactohale-SS formulation

Table 4.4 aerodynamic dose emission characteristics obtained from PSDL-SS formulation using ACI

	60L/min-1L		60L/min-2L			90L/min- 1L		90L/min- 2L	
	mean	SD	mean	SD		mean	SD	mean	SD
S-1	6.09	0.11	5.69	0.80	S-2A	13.99	0.50	9.89	0.76
S-0	4.97	0.20	4.57	0.04	S-1A	4.96	0.63	3.99	0.12
S1	8.78	1.51	10.31	0.14	S-0	6.26	0.78	4.98	0.41
S2	12.01	1.74	15.30	0.13	S1	14.65	0.90	15.02	0.11
S3	30.97	1.18	42.88	0.95	S2	23.05	0.58	29.63	0.30
S4	20.36	1.11	33.39	0.74	S3	45.60	1.36	53.44	1.93
S5	2.60	0.31	5.84	0.25	S4	19.69	1.27	27.45	1.97
S6	0.00	0.00	0.00	0.00	S5	1.61	0.33	2.98	0.17
Filter	0.00	0.00	0.00	0.00	Filter	1.28	0.09	2.81	0.51
throat	52.83	3.03	46.00	0.27	throat	59.56	1.48	46.58	1.03
PreSep	164.88	2.25	138.77	1.67	PreSep	151.11	3.55	141.04	0.91
MP	4.77	0.56	13.23	0.19	MP	4.46	0.29	12.39	1.53
Device	72.38	1.89	64.92	0.45	Device	45.46	1.71	50.24	0.63
Cap	9.61	0.12	3.15	0.19	Cap	2.11	0.13	5.85	0.30
TED	308.26	3.15	315.99	2.74	TED	346.22	2.19	350.19	2.15
FPD	74.72	2.43	107.72	1.39	FPD	112.14	1.26	136.30	1.34
%FPF	24.24	1.27	34.09	0.79	%FPF	32.39	0.98	38.92	0.79
RA	81.99	1.15	68.07	0.47	RA	47.57	0.37	56.09	0.36
TRD	390.25	2.42	384.06	3.25	TRD	393.79	2.22	406.28	5.46
% Recovery	97.56		96.01		% Recovery	98.45		101.57	
LPM	217.71	1.35	184.77	2.17	LPM	210.67	2.01	187.62	1.36
EFPD (<3)	53.93	0.95	82.11	1.12	EFPD (<3)	105.88	1.63	131.32	1.12
MMAD	2.80	0.07	2.60	0.02	MMAD	2.00	0.01	1.80	0.07
GSD	1.90	0.07	1.90	0.01	GSD	2.70	0.00	2.30	0.07

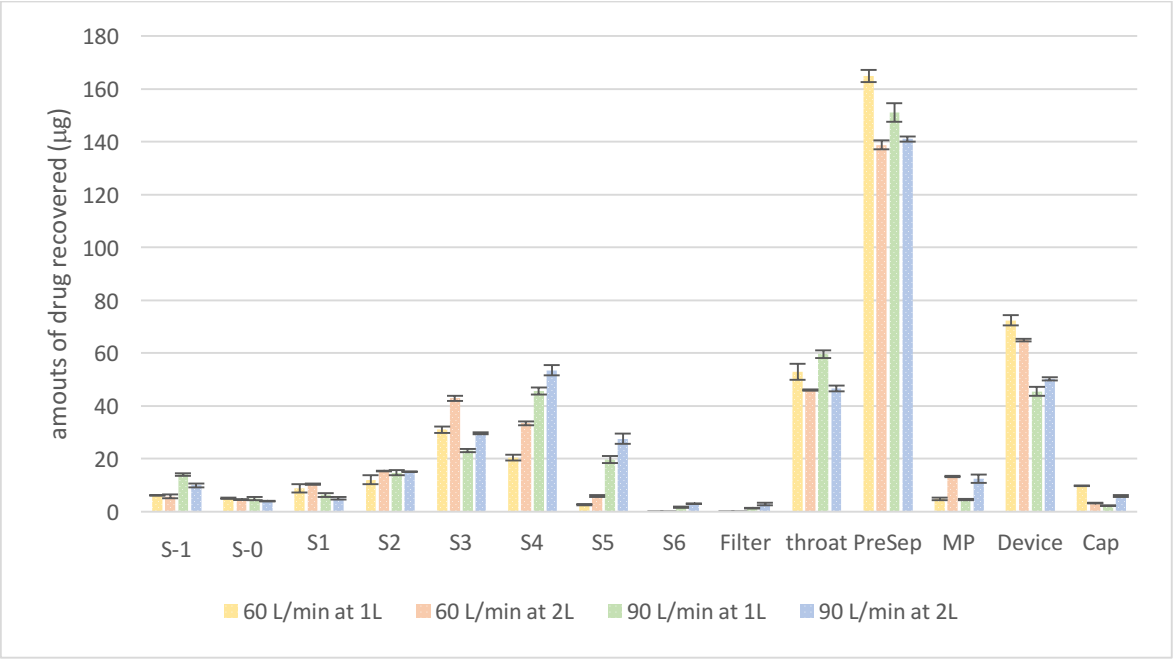

Figure 4.12 Amounts of SS found in each part of the ACI at 60 L/min, 90 L/min and 1 and 2L for PSDL-SS formulation

Table 4.5 aerodynamic dose emission characteristics obtained from PSDL-SS formulation using NGI

	60L/min-1L		60L/min-2L		90L/min-1L		60L/min-2L	
	mean	SD	mean	SD	mean	SD	mean	SD
S1	23.40	0.20	19.64	0.33	32.05	0.88	25.37	0.32
S2	14.91	0.71	20.13	1.04	22.98	0.03	24.97	0.49
S3	13.22	0.18	29.68	0.15	26.07	1.18	37.97	0.20
S4	13.76	0.64	43.68	0.58	21.42	1.60	44.37	0.87
s5	3.09	0.09	17.95	0.13	5.35	1.08	15.79	0.77
S6	0.00	0.00	3.53	0.24	0.00	0.00	3.42	0.03
s7	0.00	0.00	0.00	0.00	0.00	0.00	1.53	0.30
MOC	0.00	0.00	0.00	0.00	0.00	0.00	0.00	0.00
throat	51.02	4.84	49.62	3.32	56.54	2.06	47.30	2.21
PreSep	203.27	1.51	162.59	0.46	185.56	2.35	145.81	0.98
MP	6.03	0.12	6.78	0.52	5.92	0.16	11.05	0.26
Device	62.13	0.78	42.73	0.61	47.16	1.48	41.51	3.03
Cap	2.29	0.16	2.86	0.33	2.54	0.48	4.16	0.19
TED	328.70	3.56	353.60	2.90	355.89	2.96	357.58	3.18
FPD	44.98	1.14	114.97	1.76	75.83	1.15	128.05	1.63
%FPF	13.68	0.44	32.51	1.10	21.31	1.02	35.81	1.03
RA	64.42	0.58	45.59	1.23	49.70	1.56	45.67	0.72
TRD	393.12	6.86	399.19	6.50	405.59	9.21	403.25	3.37
% Recovery	98.28		99.80		101.40		100.81	
LPM	254.29	2.14	212.21	2.42	242.10	2.19	193.11	1.24
EFPD (<3)	30.07	1.34	94.84	1.47	52.85	0.79	103.08	1.02
MMAD	5.30	0.09	2.90	0.05	4.60	0.12	3.30	0.06
GSD	2.20	0.07	2.60	0.09	1.90	0.07	1.90	0.04

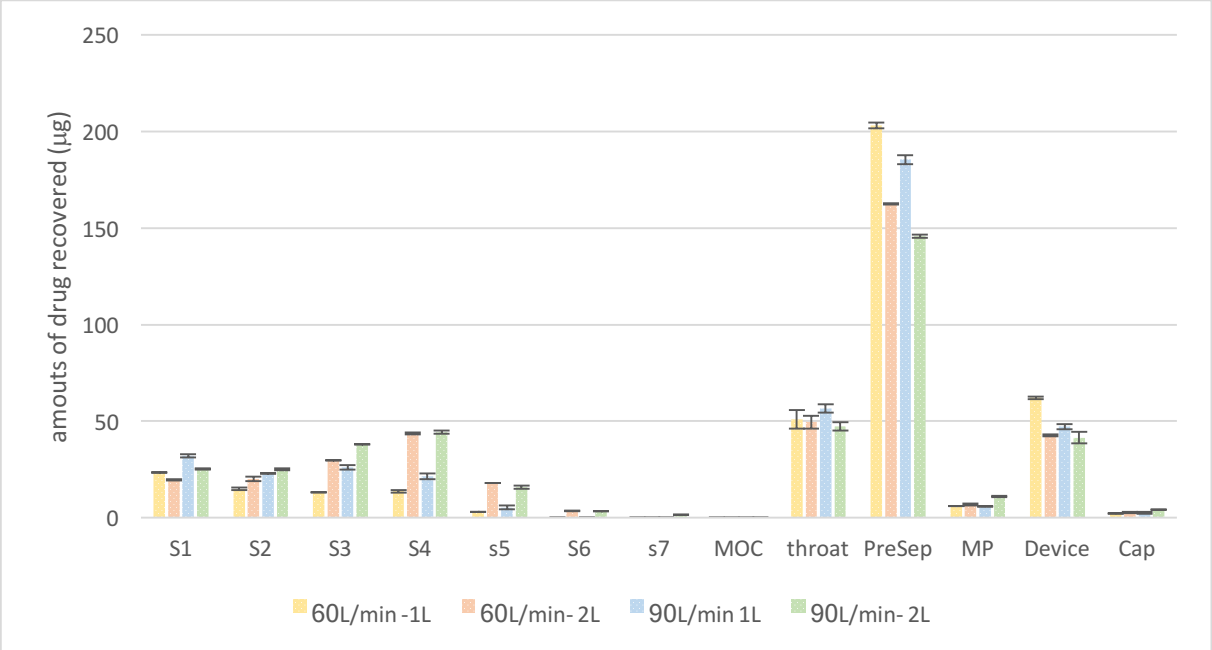

Figure 4.13 Amounts of SS found in each part of the NGI at 60 L/min, 90 L/min and 1 and 2L for PSDL-SS formulation

4.3.5.1 Comparison between ACI and NGI data with Lactohale-SS formulation

The aerodynamic dose emission results of SS with Lactohale formulations from ACI and NGI are summarised in Tables 4.2 and Table 4.3 and Figures 4.10 and 4.11. For both ACI and NGI, as the inhalation flow increased from 60 to 90 L/min, FPD increased significantly ($p<0.05$) while MMAD decreased ($p<0.05$). Also, irrespective of the inhalation flow for both impactors, as the inhaled volume (Vin) increased from 1 to 2 L, the EFPD increased significantly ($p<0.05$) resulting from an increase in the TED and an increased in the aerosol dispersion as suggested by the low MMAD values.

MMAD values ranged from 5.4 and 4.6 for 1L at 60 and 90 L/min respectively for NGI, implying that 1L was not sufficient enough to de-aggregate and disperse the drug particles. When increasing the V_{in} to 2L, at both flow rates a significant decrease in MMAD was observed ($p<0.05$) with MMAD values of 2.7 to 1.8 at 60 and 90L/min, respectively with ACI and 3.0 to 3.7 at 60 and 90 L/min respectively with NGI, suggesting that the patient should inhale for a longer time for more drug particles to be dispersed thus, drug agglomerates were broken into fine particles and reach lower stages of the lungs.

An increase in the inhalation volume promoted capsule and device emptying as shown from the decrease in the residual amount (RA) with increasing inhaled volume. This is in agreement with the TaskForce report statement (Laube et al., 2011). Furthermore, the increasing the inhaled volume would provide the dose emitted from the device with a longer time of flight to allow further drug detachment from the surface of the carrier but also dispersion of drug aggregates which may have contributed to the EFPD and reduction in MMAD. This result is in line with the literature which showed that dose emission from blisters and reservoir-based devices can occur at the start of the inhalation manoeuvre, whereas capsule-based devices such as MacHaler, require longer inhalation times to empty the capsule and the device (Abadelah et al., 2017)

LPM is superior or equal to 50% of the nominal dose (Tables 4.2 and 4.3) and was independent of the inhaled volume, this is in agreement with the studies carried out by Mohammed et al. (2012) and Abadelah et al. (2017).

Above the threshold in inhalation flow 60 L/min, little change was observed in TED when the inhalation flow rate increased from 60 to 90 L/min suggesting that TED reached its maximum value at 60 L/min.

Patients with low lung capacity may need to inhale twice to empty the capsule and device (Chrystyn et al., 2015; Laube et al., 2011). It is interesting to note that the highest TED values irrespective of the impactor was obtained at the highest inhaled volume coupled with the highest inhalation flow rate (90 L/min; 2 L) suggesting that a forceful inhalation coupled with deep breath are helpful in maximizing drug delivery to the lungs, as shown from the highest FPD values.

PIF and Vin are important parameters in the patient inhalation manoeuvre. It is clear from this study that by coupling a high inhalation flow rate with a high inhalation volume, drug delivery to the lungs is maximised as shown from FPD values.

The amount of drug lost during washing was negligible, almost all the drug was recovered as shown by the TRD values.

4.3.5.2 Comparison between ACI and NGI data with PSDL-SS formulation

The aerodynamic dose emission results of SS with PSDL formulations from ACI and NGI summarised in Tables 4.4 and 4.5 and Figures 4.12 and 4.13 respectively. The results showed a similar trend to Lactohale formulations deposition data. When using ACI, a significant increase ($p<0.05$) in TED, FPD and FPF was observed as the inhalation flow increased from 60 to 90 L/min at 1L and 2L while MMAD decreased ($p<0.05$). Also, irrespective of the inhalation flow with both impactors, as the V_{in} increased from 1 to 2 L, the EFPD increased

significantly ($p<0.05$).

When using NGI less SS was found in the lowest stages in comparison to the ACI as shown in Figures 4.12 and 4.13. ACI and NGI have dissimilar internal dead volumes which are 1.150L and 2.025L respectively. When an inhaled volume of 1L was used with the NGI less SS was retrieved in the distal stages as shown in Figure 4.13 in comparison to the ACI (Figure 4.12). The results suggest that an inhaled volume of 1L was not sufficient to pull the aerosol to deep stages of the NGI. These results are in agreement with Mohammed et al. (2012) study which showed that 1L was not generating sufficient turbulent airflow within the device to de-aggregate the powder and to overcome the dead volume of NGI.

At 60 L/min, there was a significant increase in TED when V_{in} was increased from 1 to 2L. At 90 L/min, no significant change was observed for TED when increasing the V_{in} from 1 to 2 L (Table 4.5). The result show that for this type of device, an increase in V_{in} is important, as there is an improvement in FPD and an increase in drug dispersion as suggested by a reduction in MMAD (Table 4.5), indicating further de-agglomeration had taken place.

The total residual amount (TRA) significantly reduced ($P<0.05$) with increasing V_{in} suggesting that less drug impacted in the upper stages. From this observation, V_{in} plays an important role in maximizing drug delivery in-vitro.

4.3.5.3 Comparison between Lactohale and PSDL

The emitted dose consistency was calculated as the difference in the emitted dose between high volume (2 L) and low volume (1 L). With ACI for example, the difference in the emitted dose between 1 L and 2 L inhalation volumes for Lactohale was 13 ±0.18 µg at 60L/min and this difference increased to 17 ±0.17 µg at 90 L/min. For engineered lactose, the difference in the emitted dose between 1 L and 2 L inhaled volumes was 7 ±0.41 µg and 4 ±0.04 µg for 60

L/min and 90 L/min respectively. Thus, engineered lactose showed more consistency in the emitted dose compared to Lactohale. This probably was attributed to the difference in the morphological features between Lactohale and engineered lactose. The spherical shape and uniformity of size of engineered lactose might have contributed to the reproducibility of the dose released from the inhaler. With NGI, the variability between low and high inhalation volumes for engineered lactose became even smaller (2 ±0.22 µg) and this was observed when high inhalation flow rate was used (90 L/min). Although the difference in the emitted dose was not significant between 1 L and 2 L inhaled volumes (355.68 ±2.96 µg and 357.58 ±3.18 µg respectively) at 90 L/min, there was a huge and significant increase in the FPD from 75.83 ±1.15 µg to 128.05 ±1.63 µg, suggesting that the inhaled volume has contributed to drug detachment from the surface of the carrier and pulling the detached aerosol to the deepest stages of the impactor.

Irrespective of the impactors, both Lactohale and engineered lactose showed an increase in the FPD with the inhalation flow rate (Tables 4.2, 4.3, 4.4 and 4.5). MacHaler® is a passive device relying on an inspiratory effort to deaggregate powder into particles small enough to reach the deepest stages of the impactors. DPIs have different resistances so the respiratory flow needed to create the pressure drop necessary for optimal delivery differ among DPI devices. For example, MacHaler® has a lower resistance than Turbohaler®, Easyhaler® and Handihaler® which are 0.110, 0.155 and 0.158 $cmH_2O)^{0.5}$ L/min respectively.

Engineered lactose benefited more from the increase in the inhaled volume than Lactohale, as shown from the difference in the FPD between 1 L and 2 L (Tables 4.2, 4.3, 4.4, 4.5). Engineered lactose is hollow and spherical in shape (Figure 4.1.c) and by increasing the inhalation volume this may have provided this lactose with a longer time of flight allowing drug particles to reach the distal part of the impactors.

By combining a forceful inhalation with a prolonged inhalation time (inhaled volume) this does not only allow an increase in the turbulent energy inside the device but also to provide carrier and drug particles with sufficient time of flight to produce drug particles small enough to reach the lungs, as shown from the FPD and MMAD values.

Irrespective of the IFR and Vin for both lactose and impactors the GSD values were higher than 1.2 suggesting the polydispersity of the aerosols.

4.4 Conclusion

This section of work investigated the effect of the lactose carrier particle shape and surface smoothness on the deposition of micronized salbutamol sulphate. The effect of the main inhalation manoeuver parameters such as the inhalation flow rate and inhaled volume were also investigated. Engineered lactose particles resulting from solid state crystallization were produced to have a spherical shape with rougher surface as opposed to the control Lactohale which was tomahawk shape and smooth.

The engineered lactose produced a higher and reproducible salbutamol sulphate emission and fine particle dose after aerosolisation via a MacHaler® tested in both ACI and NGI. It was concluded that choosing carefully the carrier can enhance the potential inhalable fraction of drug from dry powder inhalers, as suggested by the different deposition profiles obtained by the two different lactose carrier particles.

Inhalation flow rate effect has been confirmed in the literature but little has been said with regards to the inhaled volume. This study showed that the inhaled volume is equally important as IFR with regard to dose emission, de-aggregation of the powder formulation and in producing respirable particles for deep lung penetration.

The results obtained suggested that drug delivery to the lungs can be optimized by using a forceful inhalation in combination with a prolonged inhalation time.

Inhalation peak flow vary from patient to patient but the threshold inhalation flow as well as the inhalation time should be mentioned in the patient information leaflet to ensure that drug delivery to the lungs is maximised for the patient.

This study demonstrated evidence of incomplete mass transfer through NGI at a volume (1 L) inferior than the internal dead volume (2.025 L) in contrast to the consistent behaviour of the ACI where the mass transfer had taken place normally even when volume (1 L) which is slightly lower than the internal volume (1.150 L) was used.

The effects of factors such additives in DPI formulation on drug delivery from DPIs require further investigation and will be the basis of the work described in Chapter 5.

Chapter 5

The impact of ternary components on the dose emission characteristics of DPI formulations

5.1 Introduction

5.1.1 Background

Most commercialised DPI products are commonly formulated using a single excipient platform based on a micronised drug substance with an aerodynamic particle diameter of 1 to 5μm and a single excipient which is generally α-lactose monohydrate. Lactose acts as a bulking agent, thus improving handling, dispensing and metering of the drug. Lactose carrier forms the large proportion of DPI formulation, therefore any subtle changes in the carrier particles morphological features such as particle size, shape and surface texture will affect the powder flowability, dosing accuracy and aerodynamic dose emission characteristics of the inhaled aerosol (Larhrib et al., 2003; Larhrib et al., 1999). Therefore, careful selection of lactose carrier with the desired morphological features is a crucial determinant for the overall performance of DPIs.

Attempts were made to improve the dispersibility of cohesive drug particles by adding additives that modify the interparticle forces. This technique has been used by several researchers to improve drug dispersion during aerosolisation in DPI formulation without altering the particle size of the coarse carrier, for example, the mixing of fine carrier particles with a coarse carrier enhanced drug deposition of Salmeterol Xinafoate (Islam et al., 2004), salbutamol sulphate (Tee et al., 2000), and Beclomethasone Dipropionate (Zeng et al., 2000) in the corresponding DPI formulation powder blends. The fine carrier may be a different material from that which comprises the coarse carrier particles. Reducing sugars (glucose) and non-reducing sugars (mannitol and sorbitol) were used to facilitate DPI aerosolisation (Steckel & Bolzen, 2004; Tee et al., 2000; Zeng et al., 1998; Zhou et al., 2013). In addition, other ternary components have been also included to enhance DPI performance such as L-leucine (Chew et

al., 2005) and Magnesium Stearate (Begat et al., 2004; Grosvenor & Staniforth, 1996; Islam, et al., 2004a; Kumon et al., 2006; Young et al., 2005). Magnesium Stearate was effective in improving flowability and dispersibility of powder blends (Zhou et al., 2010). Most ternary components used so far such as L-leucine, fine sugars and Magnesium Stearate (Hazare & Menon, 2009) are fine powders that can reach the lungs when inhaling the formulation, furthermore they are exogenous to the lungs and can be harmful. Parlati et al., (2009) prepared drug solutions with sodium stearate for spray drying and observed micelle formation when this excipient was added in amounts >1%. Amount slightly over >1% exceed the Critical Micelle Concentration (CMC) for this salt, this might happen locally in the lungs with Magnesium Stearate when it exceeds its CMC. The risks of such nanoparticles micelles are still widely unknown. Other researchers opted for the modification of lactose carrier morphological features by modifying lactose surface using crystallization from solution with or without additives such as carbopol (Larhrib et al., 2003; Zeng et al., 2000). The shape modification of lactose was also considered as an option to improve drug deposition by engineering elongated lactose in the form of needle shaped particles (Larhrib et al., 2003).

Drug deposition was improved compared to commercial lactose but drug content uniformity was poor due to poor flow of needle lactose. Co-crystallisation of lactose-mannitol was also considered as an approach to enhance inhalation performance of DPI formulations (Kaialy et al., 2012). Crystallisation from solution has many deficiencies including little control of particle size, shape and surface morphologies. Good fluidity is one of the main requirements for commercial production of a particulate solid into tablet or inhaled solid dosage forms.

Spray drying technique is one of the methods to prepare spherical particles. This process produces particles with narrow size distribution and is also easy to scale-up for commercial production (Pilcer et al., 2012). However, there is still one major disadvantage for spray-drying, such as, production of amorphous material which is physically unstable and the

transformation of amorphous powder to crystalline is a quick process especially in high humidity condition. To improve the spray dried powder characteristics, we processed spray dried lactose particles in the presence of hot ethanol to produce crystalline spherical large particles.

Surface modifiers (such as polyvinylpyrrolidone (PVP), cellulose derivatives, lecithin) can be added in DPI formulations after spray-drying particles to prevent agglomeration of the particles. PVP is a hydrophilic non-ionic polymer that has been extensively used in the formulation of pharmaceuticals. The predominant use of PVP is as a binder in the production of granules and tablets, however it is also used as a polymer coating for granules and tablets, as solubiliser in oral and parenteral formulations and a viscosity modifying agent in topical formulations (Thakur et al., 2016). It has excellent aqueous solubility but is also freely soluble in alcoholic solvents such as ethanol (S. A. Jones, Martin, & Brown, 2004). PVP and NaCl are known to be safe and widely used in various pharmaceutical applications: NaCl is used as a nasal spray, as ophthalmic solutions, in osmotic pumps, in control release.

The inhalation device and the formulation together constitute the DPI. It is important to consider the compatibility between the formulation and the device when developing inhalation products in order to achieve good pharmaceutical performance and to improve patient compliance. DPIs usually rely on the patient's inspiration to deliver the drug, however, this can become an issue for the patient if the activation of the DPI is flow-rate dependent. For example, a study showed that increasing the flow rate from 30 to 60 L/min led to almost double the emitted dose and fine particle mass with Turbuhaler® (Bagherisadeghi et al., 2015). The literature acknowledges the importance of the acceleration of the flow and the pressure change with regards to the de-aggregation of the DPI formulation because the drug is mostly emitted in the first part of an inhalation (Azouz et al., 2015). Manufacturers do not report the threshold at which the inhaler device will be the most efficient, this would make it easier for GPs to

assess whether patients will be able to use a certain device or not. On the other hand, the importance of the inhalation volume has not been clearly reported in the literature. The inhalation volume has to be sufficient enough for the dose to be emptied from the device and also for the drug particles to reach the airways. The volume required varies with different DPI inhalers: some need higher volumes to empty the dose than others. This is due to the difference in the design of the devices: the inhalation channel in each device has a different length and volume. The inhaled volume required for low resistance devices tend to be higher (Azouz et al., 2015), therefore it would be expected for MacHaler® to require a high inhalation volume for maximum delivery of the dose.

The recommended method to obtain the aerodynamic characteristics of the emitted dose is to perform measurements using a pressure drop of 4 kPa and an inhaled volume of 4 L (United States Pharmacopeia, 2014; European Pharmacopeia, 2013). It has been reported in the literature that capsule-based DPI inhalers require 4 L to totally empty the dose (Amirav, Newhouse, & Mansour, 2005; Azouz et al., 2015). This volume is unrealistic from a clinical point of view as some studies have shown that most of the patients were not able to achieve more than 2L (Azouz & Chrystyn, 2012; Buttini et al., 2016). The inhalation manoeuvres when patients use DPIs are different depending on the patient: the inhalation characteristics of children with asthma are lower than those of adults and a bit lower than those of COPD patients. The sampling volume may rise issues to whether we are using ACI or NGI because of their difference in internal dead volume: 1.155 L and 2.025 L respectively (Copley et al., 2005). The sampling time should be sufficient enough to overcome the internal dead volume of the impactor and enable most of the dose to be emitted from the device and capsule. This is why the highest volume chosen in this investigation is 2 L, which is more relevant to asthmatic and COPD patients.

5.1.2 Aim

The aim of this chapter was to co-spray dry lactose with additives namely, either Sodium Chloride (NaCl) or Polyvinylpyrrolidone (PVP) to produce small spherical amorphous particles. Processing said-spherical particles in the presence of hot ethanol that acts as both as an inflating agent to produce large crystalline spherical particles but also as a surface texture modifying agent, the engineered particles were named Processed Spray Dried Lactose (PSDL). The second aim was to characterize the particles using various techniques such as scanning electron microscopy, X-Ray Powder Diffraction and Differential Scanning Calorimetry. The third aim was to formulate separately each lactose carrier (sieved lactose (63-90 μm), PSDL-PVP and PSDL-NaCl) with a model drug micronised Salbutamol Sulphate with a volume mean diameter of 2.4 μm (GSK, Ware, UK). Andersen Cascade Impactor and Next Generation Impactor have different internal dead volumes of 1.150 L and 2.025 L respectively, therefore, NGI may require larger sampling time than ACI and this may affect the aerosol distribution within the impactors. The fourth and the last aim of this chapter was to investigate the deposition of SS profile from a MacHaler® with each carrier using two inertial impactors (NGI and ACI) at 60 L/min using two inhaled volumes 1 L and 2 L.

5.2 Method

5.2.1 Chemicals and solvents

Salbutamol Sulphate was obtained from GSK (UK). Hexane sulfonic acid; glacial acetic acid; methanol (HPLC grade) and absolute ethanol were purchased from Fischer Scientific (UK). Lactose was obtained from DFE Pharma (UK). The water was ultra-purified.

5.2.2 Production of spray-dried particles

Microparticles of Lactohale and PVP or NaCl were prepared by co-spray drying. Pre-calculated amount of Lactohale was solubilised in water to obtain lactose concentration of 10% (w/v). 1% of PVP or NaCl w/w was added. Then the solution was spray dried using a laboratory scale spray dryer (Labplant SD-06, UK) with the following conditions: inlet temperature at 180 °C, solution feed rate at 4 rpm. The product was collected from the collecting chamber and transferred into a glass jar before stored in desiccator before use.

5.2.3 Preparation of Processed Spray dried lactohale

Spray-dried particles were then further processed to obtain Processed Spray dried particles (See Section 4.2.3 for method)

5.2.4 Preparation of coarse lactohale

Lactohale was used as a control. The particle size range was 63-90μm (See section 4.2.4 for method)

5.2.5 Characterisation of particle shape and size using scanning electron microscopy (SEM)

The shape, size and surface texture of Lactohale and PSDL particles were assessed using Scanning Electron Microscopy (See Section 4.2.5 for method).

5.2.6 Characterisation of lactose carriers using differential scanning calorimetry

Differential Scanning Calorimetry (DSC) was used to determine the crystal form of PSDL-PVP and PSDL-NaCl lactose carriers. The experiment was carried out using a Mettler TA 4000 (Mettler, Toledo). Approximately 5mg of each sample was weighed into an aluminium pan (40μl) (Mettler AT 260 delta range weighing balance) and the lid was crimped into place. The samples were then heated from 25 to 250ºC at a heating rate of 10ºC per minute. The DSC was continuously flushed with nitrogen at a flow rate of 50ml/min.

5.2.7 Solid State Characterization of lactose carriers using X-Ray Powder Diffraction (XRPD)

The crystallinity of the carrier particles was assessed using X-Ray diffraction (See section 4.2.7 for method).

5.2.8 Blending lactose carrier particles with salbutamol sulphate

Salbutamol sulphate was mixed separately with PSDL-PVP and PSDL-NaCl in a ratio of 1:67.5, w/w in accordance with the ratio employed in the commercial 'Ventolin®' formulations. Thus, salbutamol sulphate was weighed into a 15 ml vial which was followed by the addition of one spatula full of PSDL-PVP crystals. The powder blend was mixed manually with a spatula. More lactose particles (similar to the amount of the blend) were added to the vial and the blend was mixed manually. This process was repeated until all the PSDL-PVP particles

(2.70 g) had been added into the salbutamol sulphate/lactose blend to obtain a ratio of drug to carrier of 1:67.5, w/w. The same process was done with salbutamol sulphate and PSDL-NaCl. The stoppered vials were then placed in a Turbula mixer and mixed for 30 min. Finally, the samples were stored in a vacuum desiccator over silica gel until required.

Hard gelatine capsules (size 3) were filled with 27.4 mg of the powder mixture so that each capsule contained 400 μg salbutamol sulphate. The filling of capsules was completed manually.

5.2.9 Measurement of the homogeneity of the mixtures

Nine samples were taken randomly from each blend. The sample (approximately 27.4 mg) was weighed accurately and the amount of salbutamol sulphate was measured by HPLC. The coefficient of variation in the drug content was used to evaluate the homogeneity of the mixtures.

5.3 Results and discussion:

5.3.1 Particle shape and surface texture of lactose

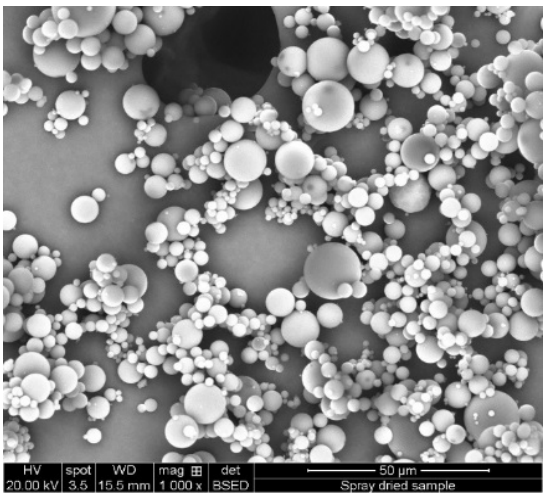

Fig 5.1(A) SDL-NaCl

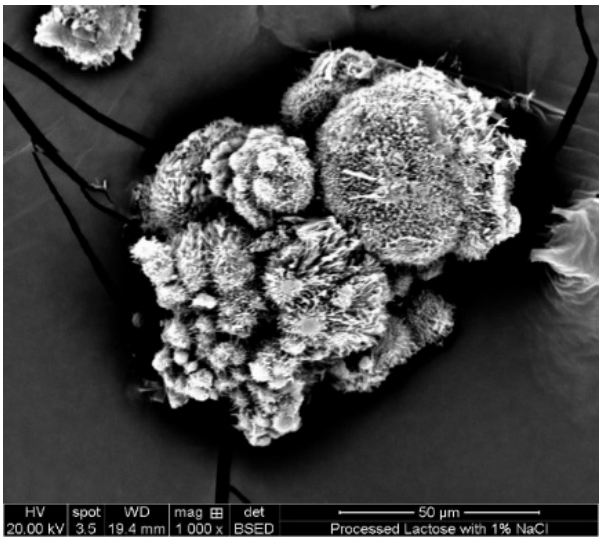

Fig 5.1 (B) PSDL-NaCl

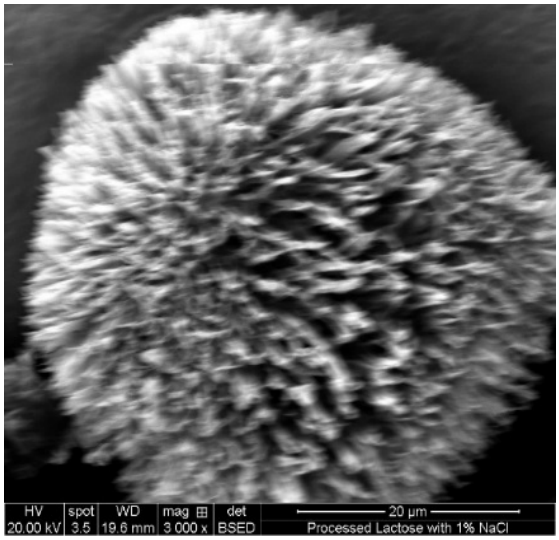

Fig 5.1 (C) PSDL-NaCl

Figure 5.1 Scanning Electron Microscopy images of (A) Spray Dried Lactohale with NaCl, (B-C) close views of PSDL-NaCl

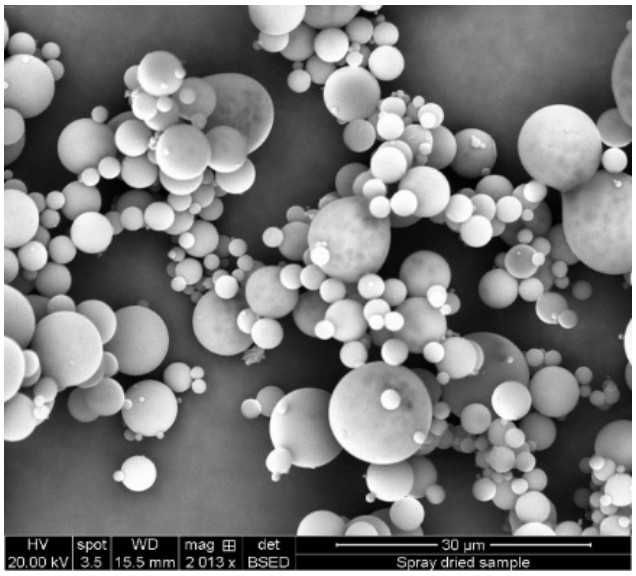

5.2(A) SDL-PVP

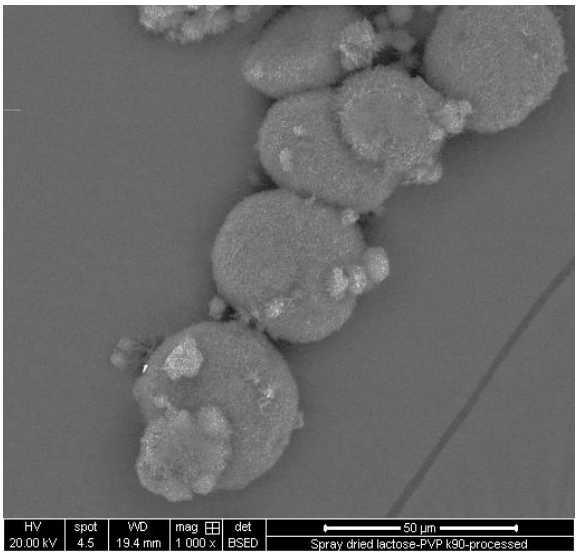

5.2(B) PSDL-PVP-

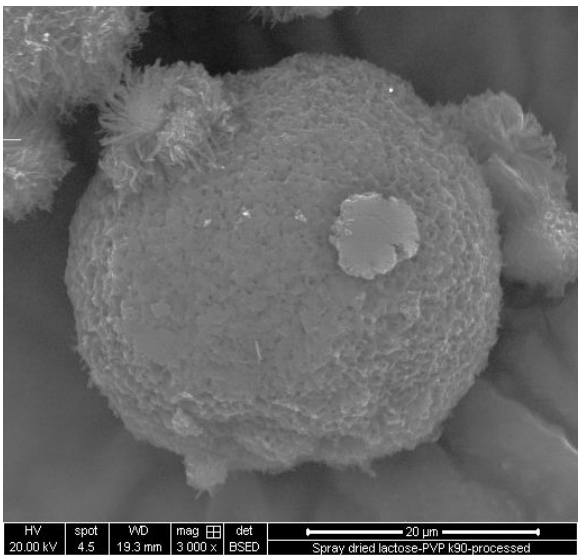

5.2(C)- PSDL-PVP

Figure 5.2 Scanning Electron Microscopy Images of (A) Spray Dried Lactohale with PVP, (B-C) close views of PSDL-PVP

Solid phase crystallisation of co-spray dried lactose-NaCl and lactose-PVP with ethanol produced particles with larger size without changing their spherical shape. Before crystallisation, spray-dried particles were less than 10 µm (Figures 5.1A and 5.2A) with a smooth surface. Crystallisation of particles in the presence of ethanol produced large particles with different surface roughness, depending on the additive.

PSDL-NaCl (Figure 5.1C) appeared to be rougher than PSDL-PVP (Figure 5.2C). Thus, the increase in the particle size with the change in surface texture indicates that lactose particles have undergone some crystallization during the treatment with ethanol. On contact with ethanol, some of the lactose molecules may have dissolved in the ethanol until a saturated solution was formed. Such an ethanolic solution will contain some lactose, although lactose is practically insoluble in ethanol. The solubility could have been enhanced by the presence of amorphous regions in the spray-dried lactose particles, as shown in X-ray diffraction pattern (Figures 5.6 and 5.8).

The dissolved lactose molecules can then be transferred onto the surface of lactose inducing crystal growth, encouraging particle size increase and correcting surface defects produced during spray-drying.

Regions with higher energy such as amorphous regions are more likely to dissolve than those with low energy, thus some of the amorphous regions will diminish or disappear giving place to the formation of crystalline regions (Figures 5.7 and 5.9).

This process of crystallisation used in this thesis is reliable as the particles produced are spherical, irrespective of the type of additive and its solubility in the non-solvent. Surface textures can be modified to produce particles of different surface rugosity and different degrees of crystallinity, depending on the time of exposure to the crystallization medium.

5.3.2 Characterization of lactose particles by DSC and XRPD

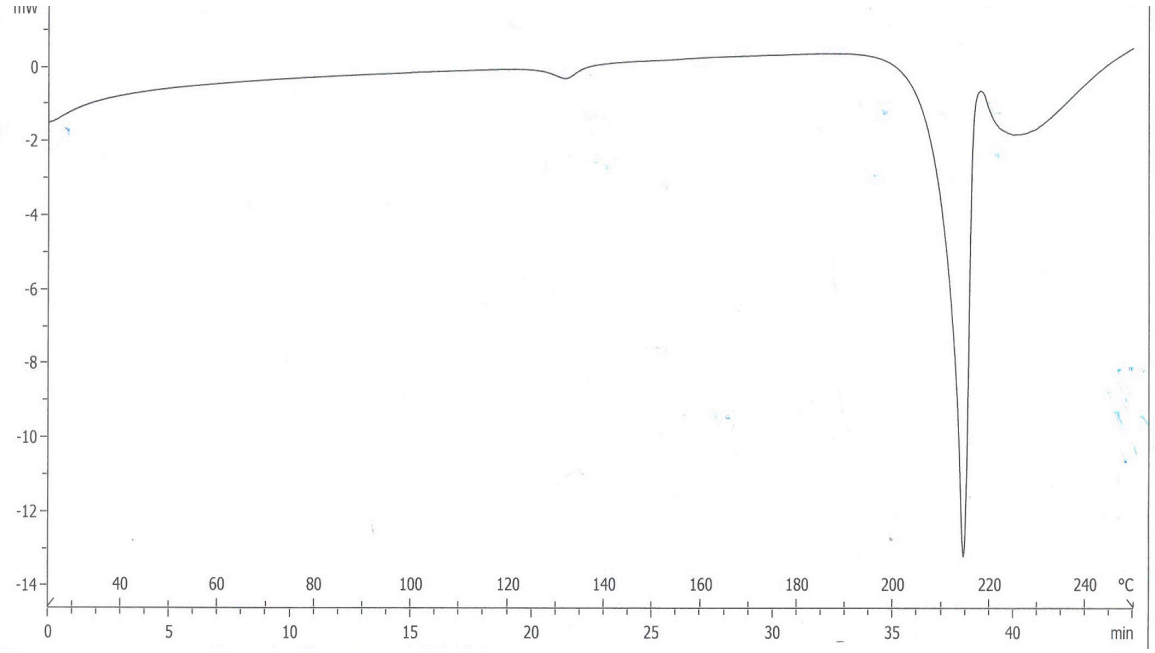

Figure 5.4. DSC thermograph of PSDL-NaCl

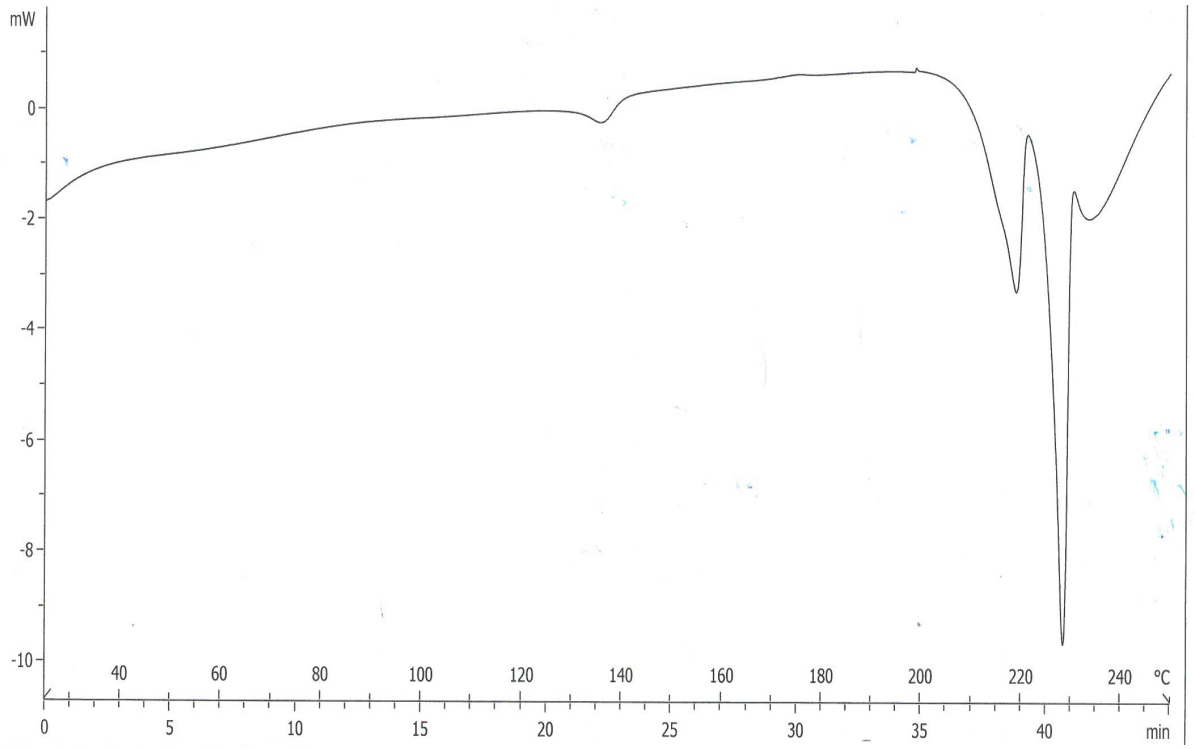

Figure 5.5. DSC thermograph of PSDL-PVP

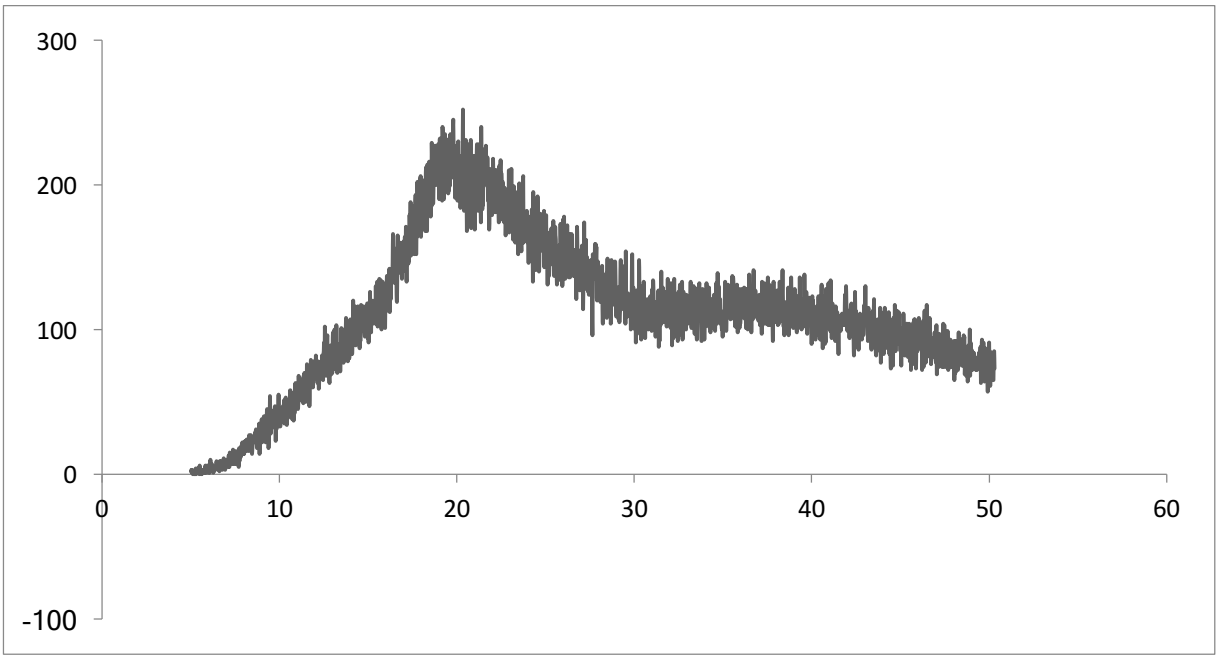

Figure 5.6. X-Ray diffraction pattern of SDL-NaCl

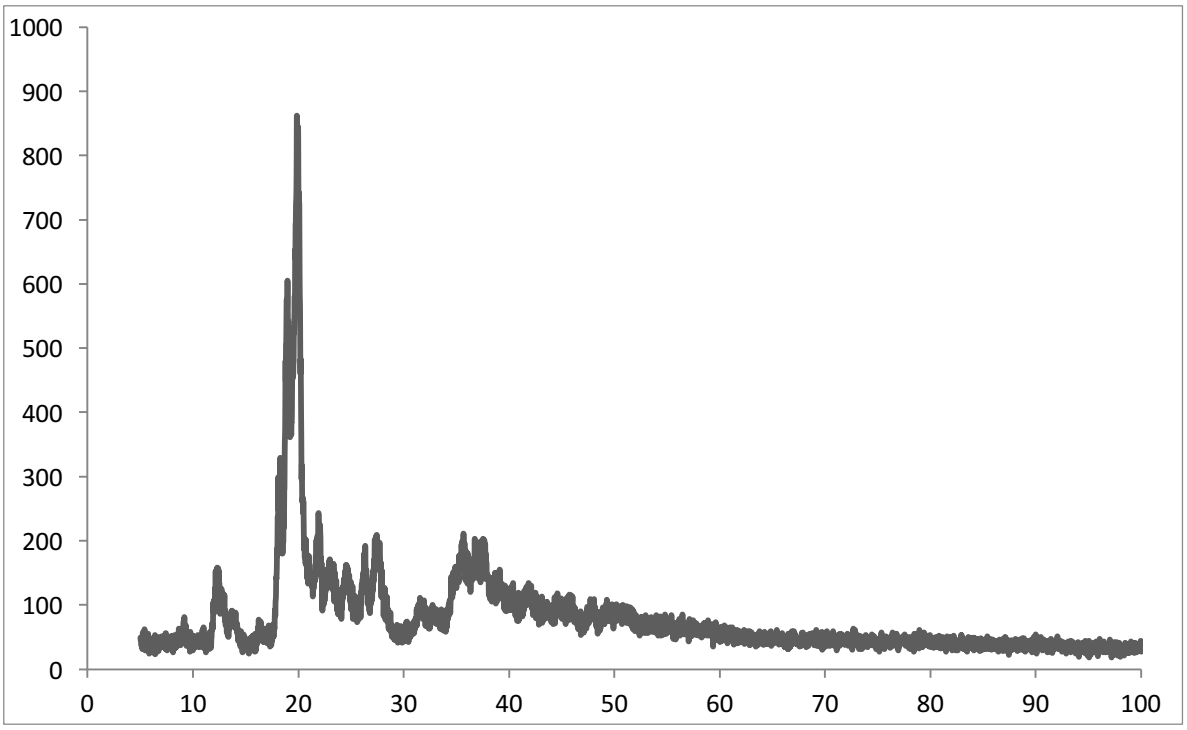

Figure 5.7. X-Ray diffraction pattern of PSDL-NaCl

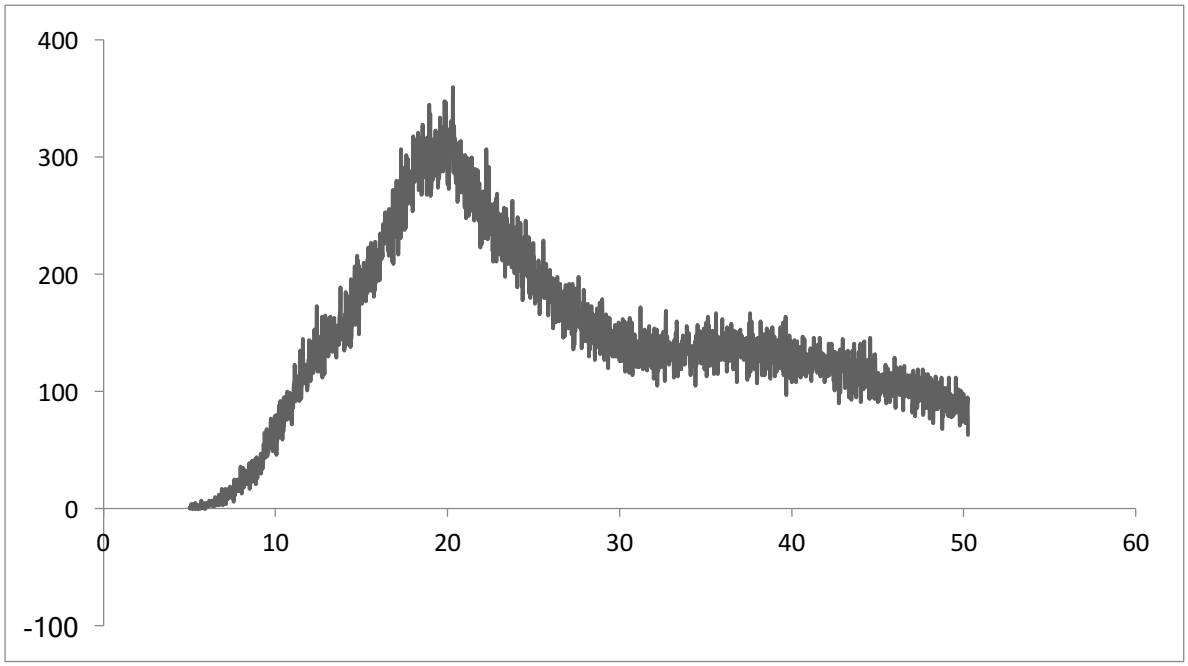

Figure 5.8. X-Ray diffraction pattern of SDL-PVP

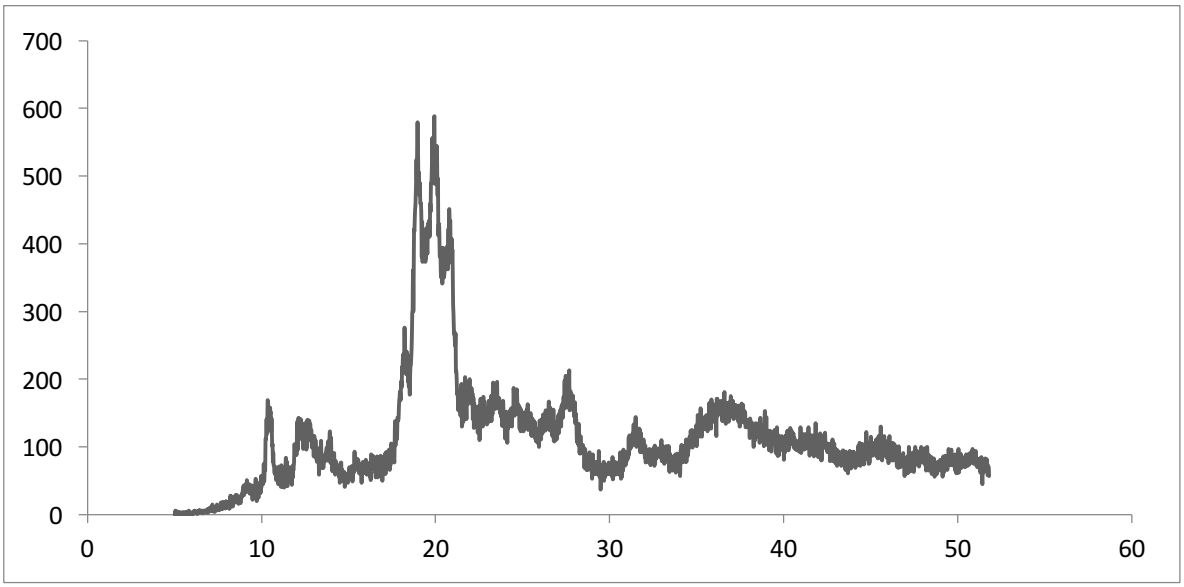

Figure 5.9. X-Ray diffraction pattern of PSDL-PVP

SDL thermogram exhibited three endothermic transitions and an exothermic one. The first transition was a large broad endothermic transition that corresponds to the loss of free water which usually is represented by such transitions at less than 100 °C. The second endothermic

transition at around 120 °C corresponds to the loss of bound water. A strong exothermic transition peaking at around 180 °C suggested the presence of amorphous lactose in the sample, this transition was followed by a sharp endothermic transition corresponding to the melting of α-lactose peaking at around 210 °C.

SDL-PVP showed a similar trend to SDL.

On the other hand, PSDL only displayed one endothermic transition at around 210 °C which corresponded to the melting of α-lactose.

PSDL-PVP thermogram (Figure 5.5) showed three endothermic transitions. The first one occurred at about 135°C followed by two other endothermic transitions around 220°C and 230°C. The first small endothermic transition corresponds to the loss of bound water, the second transition corresponds to the melting of α-lactose whereas the third endothermic transition corresponds to the melting of β-lactose.

SDL with or without PVP produced amorphous material with α-lactose form dominating. However, there is a great difference between PSDL and PSDL-PVP. Only the α- form was apparent in PSDL and both α and β were present in PSDL-PVP (Figure 5.5) with proportions of β form dominating the most.

Both SDL-NaCl (Figure 5.3) and PSDL-NaCl crystallise (Figure 5.4) in α- form. PSDL-NaCl produced a sharper melting peak compared to SDL-NaCl.

The recrystallisation process used in this study enabled the removal of any free water and any amorphous content as suggested by the loss of the exothermic transition that occurred around 180°C. It also affected the polymorphic forms of lactose by producing either α or α-β mixtures.

5.3.3 Aerodynamic dose emission results

Table 5.1. SS dose emissions from NGI at 60 L/min at 1L and 2L for SS-PSDL-NaCl and SS-PSDL-PVP from MacHaler®.

1L-NaCl			1L PVP			2L NaCl			2L PVP		
	mean	SD		mean	SD		mean	SD		mean	SD
S1	24.59	1.18	S1	25.03	1.65	S1	14.93	1.70	S1	20.10	1.56
S2	19.59	0.98	S2	14.38	0.26	S2	21.10	1.93	S2	21.32	0.69
S3	27.56	1.09	S3	14.36	1.08	S3	44.42	2.67	S3	37.27	0.91
S4	26.17	1.27	S4	12.10	0.62	S4	53.24	0.46	S4	45.11	1.28
s5	7.27	0.37	s5	2.43	0.25	s5	21.54	0.04	s5	16.68	1.65
S6	0.00	0.00	S6	0.00	0.45	S6	5.57	0.59	S6	2.86	0.72
s7	0.00	0.00	s7	0.00	0.46	s7	0.00	0.00	s7	0.00	3.54
MOC	0.00	0.00	MOC	16.49	0.05	MOC	0.00	0.00	MOC	15.98	0.18
throat	35.70	1.97	throat	49.58	0.18	throat	30.93	0.71	throat	37.36	2.37
PreSep	183.26	2.68	PreSep	154.86	3.50	PreSep	162.84	2.95	PreSep	121.01	1.38
MP	3.87	0.76	MP	6.36	1.54	MP	3.70	0.81	MP	3.72	0.67
Device	49.46	1.19	Device	42.25	2.54	Device	39.58	1.60	Device	25.78	1.52
Cap	7.50	0.67	Cap	9.36	0.31	Cap	7.43	0.59	Cap	8.83	1.01
TED	328.00	3.60	TED	295.59	4.30	TED	358.27	4.20	TED	321.42	4.33
FPD	80.59	1.62	FPD	59.76	2.18	FPD	145.87	2.04	FPD	139.23	1.87
%FPF	24.57	1.15	%FPF	20.22	1.57	%FPF	40.71	0.48	%FPF	43.32	2.62
RA	56.95	1.34	RA	51.61	1.47	RA	47.01	1.12	RA	34.62	1.75
TRD	384.96	3.60	TRD	347.21	3.15	TRD	405.28	2.97	TRD	356.03	4.25
% Recovery	96.24		% Recovery	86.80		% Recovery	101.32		% Recovery	89.01	
LPM	218.95		LPM	204.44		LPM	193.77		LPM	158.37	
EFPD (<3)	36.69	2.55	EFPD (<3)	32.46	3.04	EFPD (<3)	86.75	1.06	EFPD (<3)	86.01	2.48
MMAD	3.90	0.08	MMAD	4.00	0.12	MMAD	2.85	0.06	MMAD	2.80	0.10
GSD	1.80	0.00	GSD	2.00	0.06	GSD	2.05	0.07	GSD	2.50	0.07

Table 5.2. SS dose emissions from ACI at 60 L/min at 1L and 2L for SS-PSDL-NaCl and SS-PSDL-PVP from MacHaler®.

1L-NaCl			1L PVP			2L NaCl			2L PVP		
	mean	SD		mean	SD		mean	SD		mean	SD
S-2A	7.71	0.05	S-2A	9.81	1.65	S-2A	7.25	0.57	S-2A	7.91	0.56
S-1A	3.03	0.05	S-1A	2.94	0.26	S-1A	1.92	0.19	S-1A	2.21	0.69
S-0	4.18	0.96	S-0	4.11	1.08	S-0	4.28	0.27	S-0	3.42	0.91
S1	12.18	1.44	S1	11.45	0.62	S1	12.62	0.52	S1	11.00	1.28
S2	22.82	2.08	S2	17.59	0.25	S2	25.75	0.92	S2	19.42	1.65
S3	54.97	3.17	S3	40.11	0.45	S3	66.26	0.39	S3	49.07	2.72
S4	27.83	2.84	S4	21.22	0.46	S4	36.98	1.58	S4	31.43	3.54
S5	3.14	0.90	S5	2.96	0.05	S5	3.77	0.49	S5	4.98	0.18
Filter	6.35	0.76	Filter	2.59	0.18	Filter	6.25	0.47	Filter	9.61	0.37
throat	38.02	3.12	throat	44.86	4.50	throat	28.01	3.29	throat	50.82	1.38
PreSep	135.56	5.73	PreSep	131.65	5.47	PreSep	156.55	5.73	PreSep	146.36	2.67
MP	4.68	0.49	MP	4.47	0.54	MP	4.79	1.98	MP	4.08	1.52
Device	50.04	3.08	Device	37.94	2.31	Device	38.69	1.83	Device	33.94	3.01
Cap	9.66	1.26	Cap	18.67	0.99	Cap	6.83	0.84	Cap	12.16	3.92
TED	320.47	4.60	TED	293.77	4.00	TED	354.43	4.10	TED	340.30	3.70
FPD	131.46	3.40	FPD	100.04	2.50	FPD	155.91	3.14	FPD	128.93	3.25
%FPF	41.02	2.52	%FPF	34.05	1.57	%FPF	43.99	2.73	%FPF	37.89	2.62
RA	59.70	1.53	RA	56.61	1.47	RA	45.52	1.68	RA	46.10	1.78
TRD	380.17	4.11	TRD	350.38	4.29	TRD	399.95	3.98	TRD	386.39	3.74
% Recovery	95.04		% Recovery	87.60		% Recovery	99.99		% Recovery	96.60	
LPM	173.58		LPM	176.52		LPM	184.56		LPM	197.18	
EFPD (<3)	110.40	2.10	EFPD (<3)	81.88	1.43	EFPD (<3)	133.92	2.27	EFPD (<3)	104.12	2.64
MMAD	1.65	0.06	MMAD	1.75	0.07	MMAD	1.55	0.09	MMAD	1.55	0.07
GSD	2.30	0.00	GSD	2.60	0.14	GSD	2.15	0.07	GSD	2.35	0.07

Impact of the inhaled volume:

The inhaled volume is a crucial parameter as it can govern the quality of the emitted dose (Abadelah et al., 2018). Inconsistent emitted dose can affect the clinical response (too much drug can cause toxic effects and not enough dose can cause suboptimal treatment) and side effects (Abdelrahim et al., 2010). For dose emission testing, it is recommended by the Pharmacopoeia to use a Vin of 4 L, however most patients with asthma or COPD are usually able to inhale at around 2L (Abadelah et al., 2017) and some patients (children and very severe-case patients) are only able to generate even lower volumes. Additionally, depending on the inhaler device used, dose emission can occur either at the beginning of the inhalation manoeuver (for devices with reservoir or blister based device) or occurs during a more prolonged inspiration (single-dose capsule based devices) (Chrystyn, 2009; Laube et al., 2011).

The aerodynamic characteristics of the emitted dose of SS from MacHaler® was measured at two inhalation volumes 1 litre and 2 litres using both NGI and ACI Tables 5.1 and 5.2 for both formulations PSDL-NaCl and PSDL-PVP. NGI results (Table 5.1) showed that increasing the Vin from 1 L to 2 L resulted in a significant decrease ($p<0.05$) in the amount of SS in the inhaler device, MP, pre-separator, USP throat and stage 1 whilst the amount of SS in stages 2 to 6 has significantly increased. Consequently, resulting in a decrease in the RA left in the inhaler device and an increase in the aerodynamic characteristics of inhaled SS such as TED, FPD, %FPF and EFPD but it should be noted that the MMAD has significantly decreased (Table 5.1) with increasing the inhaled volume. MacHaler® is a low resistance based device and would require a prolonged inhalation time to empty most of the capsule as shown from the results of the RA left in the inhaler at 1 L and 2 L inhaled volume for both formulations. The TED has also significantly increased with the inhaled volume which is in agreement with the literature Chrystyn, 2009; Laube et al., 2011, Azouz et al., 2015; Abdelrahim et al., 2010;

Abadelah et al., 2018). Thus, patients with who are unable to generate sufficient inhaled volume are encouraged to inhale more than once from the inhaler to empty the capsule.

It is generally, recognised that dose emission characteristics from breath activated devices such MacHaler® are associated with inhalation flow rate dependency, the present results suggest that MacHaler® depends also on the inhaled volume. An increase in the inhaled volume from 1 L to 2 L has led to a better device and capsule emptying as shown from the decrease in the total residual amount (TRA). Of the TED, only a fraction of the drug should reach the distal parts of the impactor as a FPD containing particles of clinical relevance smaller than 5 μm and the great majority would deposit as LPM and/or in the proximal stages of the impactor. In real life, the drug particles depositing as LPM are swallowed and do not reach the lungs and providing no therapeutic benefits. Our results showed that a great portion of LPM was converted into FPD smaller than 5 μm when the inhaled volume was increased from 1 L to 2 L (Tables 5.1 and 5.2). MacHaler was capable of producing particles with an MMAD smaller than 5 μm (Tables 5.1 and 5.2). An MMAD < 5 μm is considered to be necessary for sufficient airway deposition (Abadelah et al., 2017). The results shown in Tables 5.1 and 5.2 suggest that inhaled formulation from a MacHaler® should reach the lungs using the present conditions (60 L/min and at least 1 L inhaled volume). An increase in the inhaled volume would have provided particles with sufficient time of flight causing further de-aggregation and dispersion of drug particles in the emitted dose as demonstrated by the shift towards much smaller particles as shown from the MMAD and EFPD (Tables 5.1 and 5.2).

Impact of formulation:

Dry powder formulations have attracted interest in the last decade due to their several advantages over other pulmonary drug delivery platforms. The main goal is to achieve dosing accuracy, minimising dose variability and high pulmonary drug deposition. The carrier is an

important component in the DPI formulation and the ratio of drug to carrier (1:67.5%) w/w being typical according to Ventolin formulation and this ratio of drug to carrier was used by several authors as a reference in formulating DPIs (Larhrib et al., 2003; Larhrib et al., 1999; X Zeng et al., 2001a). Since lactose forms the major proportion in the DPI formulation, any changes in the physico-chemical properties of the carrier can affect the drug deposition profile (Larhrib, Martin, Marriott, et al., 2003). Unsatisfactory drug detachment from the surface of the carrier due to strong inter-particulate forces between drug and carrier may be one of the main reasons of inefficient drug delivery encountered with most DPIs (Zeng et al., 2001a). Adjusted balance between adhesive and cohesive forces to provide sufficient adhesion of drug to carrier producing a long lasting and stable mix with good drug content uniformity and no segregation yet allows for an easy drug detachment from the surface of the carrier during the inhalation manoeuvre. It has been stated that the efficiency of a DPI formulation is extremely dependent on the carrier characteristics and the selection of the carrier is a determinant factor of the overall DPI performance (Pilcer et al., 2012).

It can be seen that the DPI formulations PSDL-NaCl and PSDL-PVP differ in their SS drug deposition profiles (Tables 5.1 and 5.2) when aerosolised under the same conditions. The TRD of SS from all PSDL formulations were in the range of 347.21 ± 3.15 μg to 405.28 ± 2.97 μg (Tables 5.1 and 5.2), these values fall within the acceptable range of 75%-125% of the nominal dose (USP 29, 2006). The satisfactory TRD values for both PSDL indicate that the overall procedures of mixing, sampling, capsule filling, aerosolisation, washing and analysing the drug were accurate and reproducible. At any inhaled volume and irrespective of the impactor used, the TED of SS for PSDL-NaCl were significantly higher ($p<0.05$) than PSDL-PVP (Tables 5.1 and 5.2). When using the same device, such as the case in this study, TED is mainly governed by powder flow. PSDL-NaCl and PSDL-PVP are both spherical in shape but they differ in their surface texture (Figures 5.1C and 5.2C) with PSDL-NaCl rougher and

appears to be more porous than PSDL-PVP. This may have imported some aerodynamicity to the particles compared to non-porous particles, facilitating particle emptying from the device and capsule. The TRA was more or less the same especially with the ACI.

To achieve both a good device and capsule emptying, high drug emission and high drug deposition, the surface characteristics of the carrier is important. Higher TRD and TED for PSDL-NaCl compared to PSDL-PVP indicates that higher amounts of SS is delivered from PSDL-NaCl formulation, thus more drug is expected to be available to the patient when inhaling through the DPI and deposit in the lungs. Percent recovery varied from 86.8 to 101.3% for all formulation suggesting that some drug was lost during the washing procedure but was not substantial and acceptable as discussed above in the TRD.

Both in-vitro and in-vivo deposition studies show that delivered drug fractions in the required aerodynamic size fraction from capsule based DPIs with adhesive mixtures are quite low as shown in Figure 5.10.

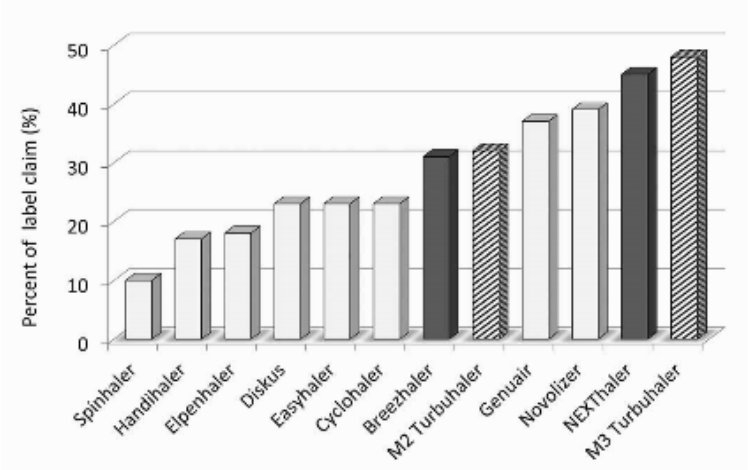

Figure 5.10. In-vitro %FPF of label claim from different DPIs tested at using a next generation impactor (with permission from DeBoer et al. (2016)).

The poor performance of DPIs especially capsule based devices was attributed to the strong inter-particulate forces in the adhesive mixtures and to inefficient dispersion of the powder formulation by the inhaler device. Formulation powder blends containing PSDL as a carrier performed better than most of commercially available DPIs shown in the Figure 5.10. This

indicates that employing engineered lactose in DPI formulations instead of commercially available lactose carrier would result in a high amount of drug reaching the lungs as shown from the %FPF (Tables 5.1 and 5.2).

Comparing PSDL-NaCl with PSDL-PVP, it is clear that PSDL-NaCl performed better than PSDL-PVP as a carrier. Irrespective of the impactor used, the FPD of PSDL-NaCl were greater than PSDL-PVP especially at 1 L inhaled volume (Table 5.1 and 5.2) and the difference in FPD becomes even smaller by increasing the inhaled volume to 2 L. Several factors may have accounted for this, the TED is significantly increased ($p<0.05$) at 2L so more drug was emitted from the inhaler device (Table 1 and 2), secondly the dose emitted from the inhaler was further de-aggregated and dispersed in the airstream by prolonging the time of flight of drug particles as shown from the MMAD values which were further reduced at 2 L inhaled volume. The number of particles smaller than <5 μm as well as the EFPD <3 μm showed a significant increase ($p<0.05$) with inhaled volumes.

The improved SS drug deposition from PSDL-NaCl can be attributed to the surface texture of the PSDL. The solubility of NaCl is much less than that of PVP in ethanol, therefore ethanol may have washed away all PVP or great portion of it from the surface of lactose, whereas, the poor solubility of NaCl in ethanol has led to the formation of microscopic spikes on the surface of spray dried lactose giving some roughness and porosity to lactose particles. Unlike clefts and crevices, these microscopic projections did not accommodate the drug particles and instead enhanced drug detachment from the lactose surface and improved inhalation efficiency.

Comparison of the impactor used:

The cascade impactors are designed to operate at a constant flow rate (Mitchell and Nagel, 2003) and an inhaled volume of 4 L of air is drawn through the DPI to aerosolise the formulation. The 4 L inhaled volume should be sufficient to allow the aerosol cloud to reach

the distal regions of the impactor, thus permitting a complete size fractionation from which the aerodynamic particle size distribution can be determined. Both ACI and NGI are used for assessing the aerosol performance in-vitro, however, they both differ in their internal dead volumes, the latter being 1.155 L for the ACI and 2.025 L for the NGI. The 4 L recommended by the Pharmacopoeia exceeds the internal volumes of both impactors, thus allowing sufficient time for assessing the DPI performance without bias with either impactor.

From a clinical point of view, patients with lung impairment as well as geriatric and paediatric patients with significantly weaker inspiration may however struggle to achieve the 4 L inhaled volume recommended by Pharmacopoeia. Therefore, our study was undertaken to compare the ACI performance with NGI in assessing the aerosol performance from SS DPI formulations containing PSDL-NaCl and PSDL-PVP using an inhalation flow of 60 L/min and an inhaled volume of 1 L and 2L. The experiments were performed with a MacHaler® having a low resistance (0.0189 kPa 0.5 L/min) and the inhalation duration is calculated from the determined flow rate and the specified inhaled volume for aerosol aerodynamic characteristics determination. The flow rate was set to 60 L/min, sampling time was 1 second and 2 seconds for 2 L and 4 L inhaled volumes respectively. The effects of changing inhaled volume on % FPF, EFPD (< 3μm) and LPM are shown in Figures 5.11, 5.12, 5.13, 5.14, 5.15, 5.16.

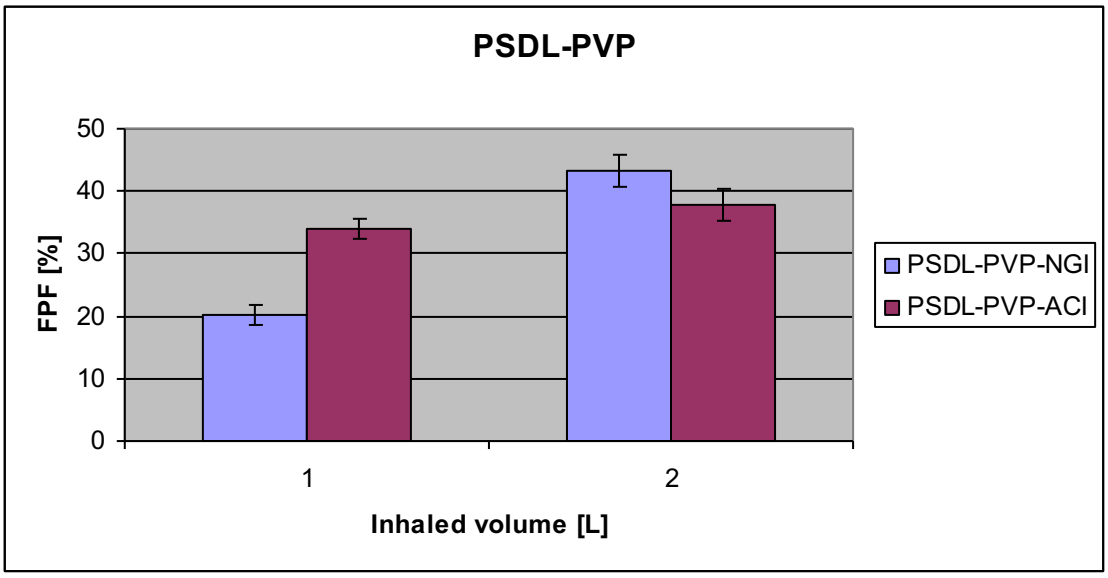

Figure 5.11. The %FPF of SS as a function of inhaled volume for PSDL-PVP using NGI and ACI.

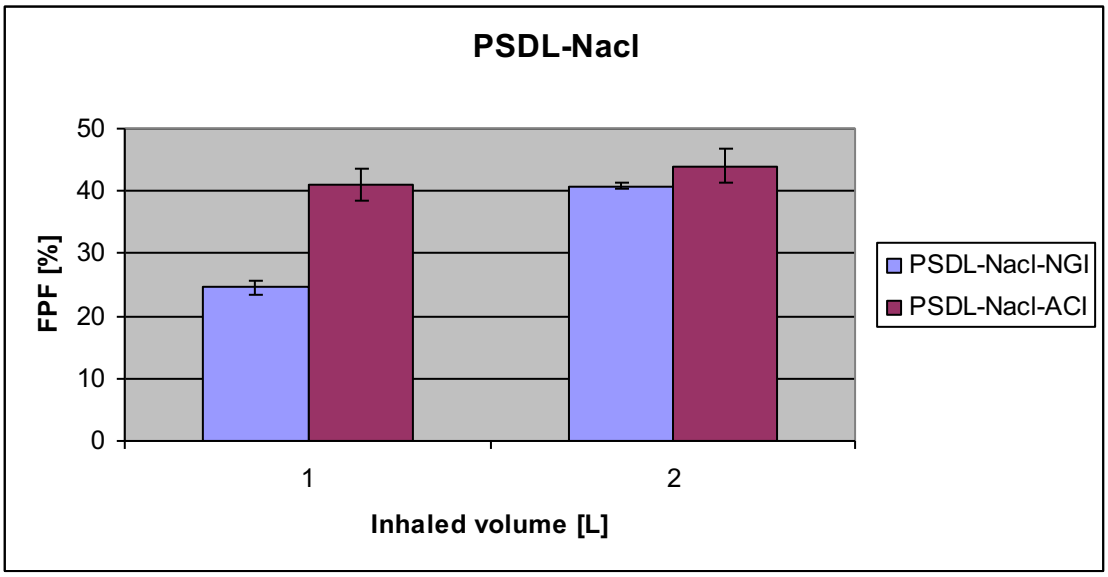

Figure 5.12. The %FPF of SS as a function of inhaled volume for PSDL-NaCl using NGI and ACI.

NGI showed a significant decrease ($p<0.05$) in the %FPF for both PSDL-PVP and PSDL-NaCl when the inhaled volume was reduced to 1 L (Figures 5.11 and 5.12). The 2 L sampling inhaled volume is comparable to that of the dead internal volume of the NGI (2.025 L). The

sampling inhaled volume of 1 L is about 50% of the dead internal volume of the NGI would therefore not have allowed sufficient time for the aerosolised powder formulation to reach the distal regions of the impactor. This explanation is further supported by the marked and significant decrease of EFPD (< 3μm) (Figures 5.13 and 5.14) and the corresponding increase in the mass of the unsized drug captured in the induction port and the pre-separator of the impactor (LPM) when the inhaled volume was reduced to 1 L (Figures 5.15 and 5.16), suggesting premature and substantial drug deposition of the emitted dose in the induction port and pre-separator of the NGI.

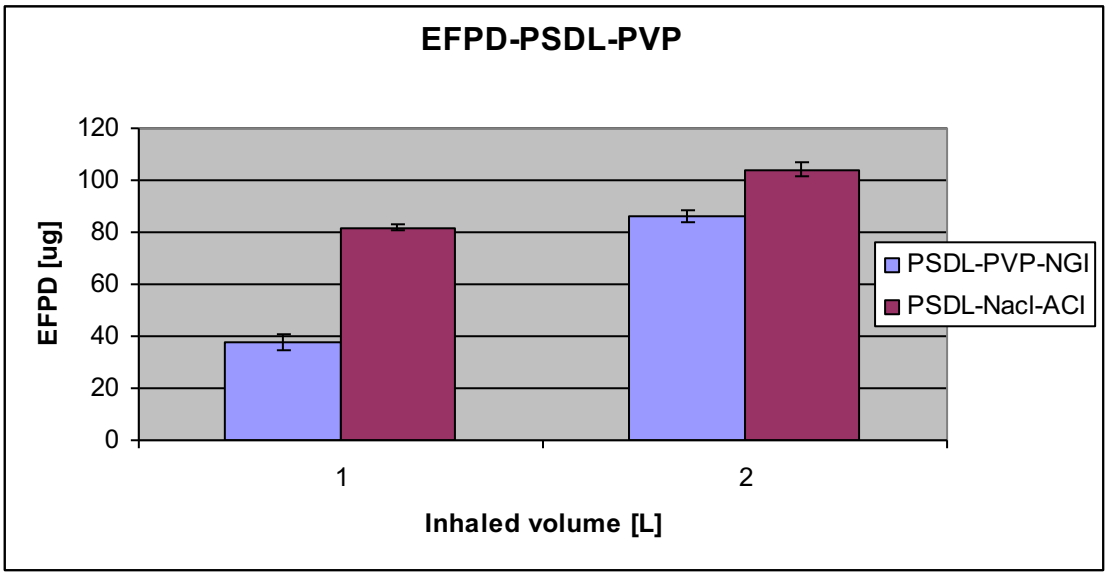

Figure 5.13. The EFPD (< 3 μm) of SS as a function of inhaled volume for PSDL-PVP using NGI and ACI.

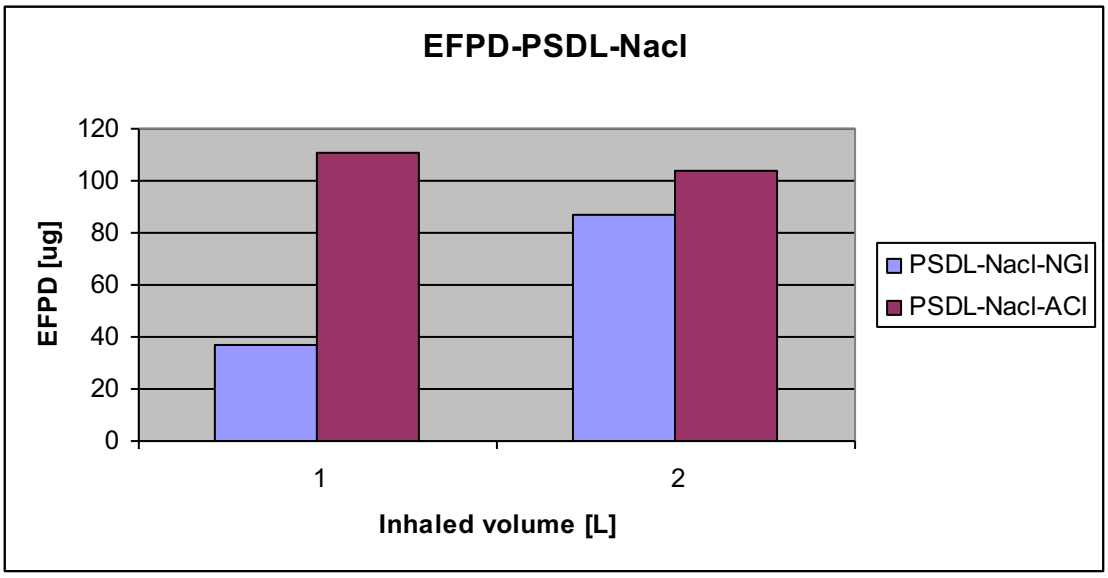

Figure 5.14. The EFPD (< 3 μm) of SS as a function of inhaled volume for PSDL-NaCl using NGI and ACI.

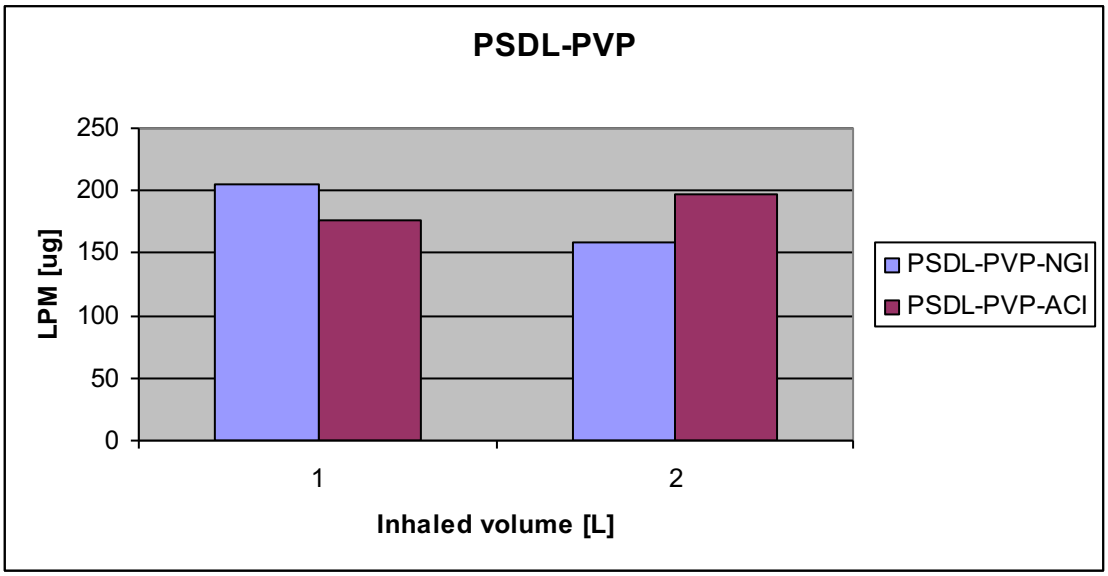

Figure 5.15. The LPM of SS as a function of inhaled volume for PSDL-PVP using NGI and ACI.

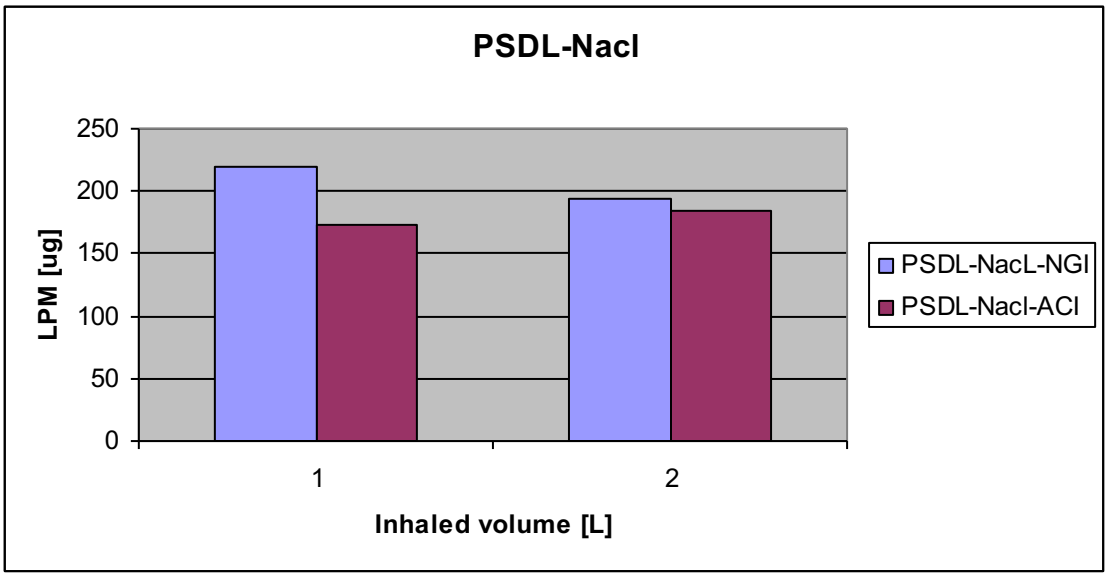

Figure 5.16. The LPM of SS as a function of inhaled volume for PSDL-NaCl using NGI and ACI.

It is also interesting to note the shift towards a reduction in the SS particles deposition with reducing inhaled volume from 2L to 1L for all collection cups beyond stage 1 for PSDL-PVP and stage 3 for PSDL-NaCl as shown in Figure 5.17 and Figure 5.18, respectively. This is consistent with the above explanation of %FPF and EFPD suggesting that less aerosol reached the distal stages of the NGI when the IV was reduced from 2 L to 1 L. There was also a noticeable increase in the SS deposition in the pre-separator for both formulations when the inhaled volume was reduced to 1 L again suggesting a premature deposition of the inhaled aerosol.

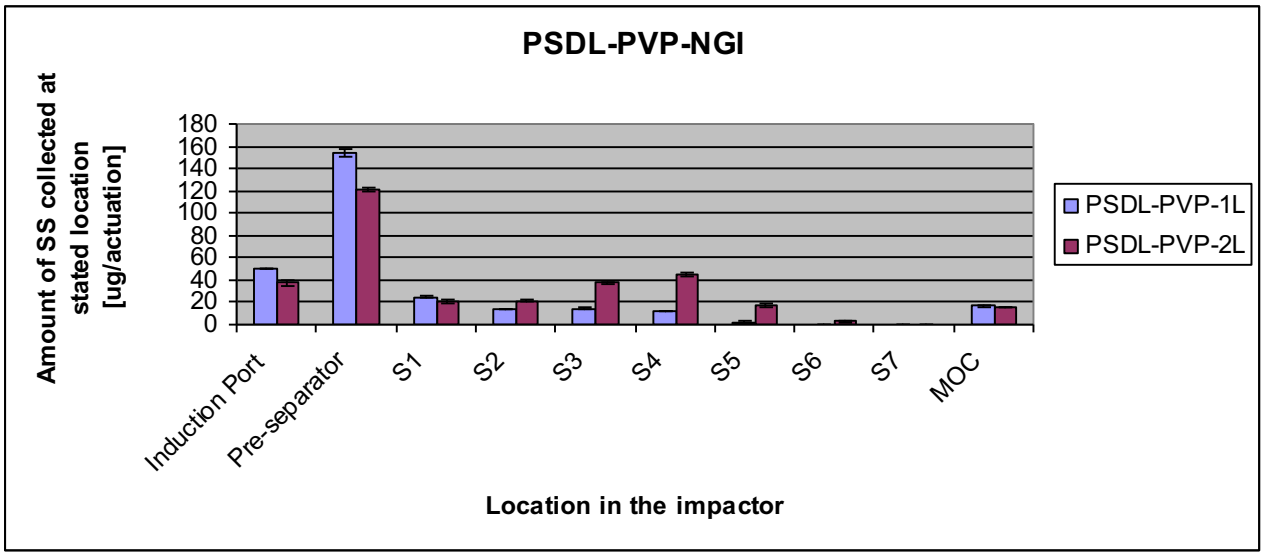

Figure 5.17. Deposition profile of SS from a MacHaler® as a function of inhaled volume after actuation at 60 L/min into an NGI of the DPI formulation containing PSDL-PVP carrier.

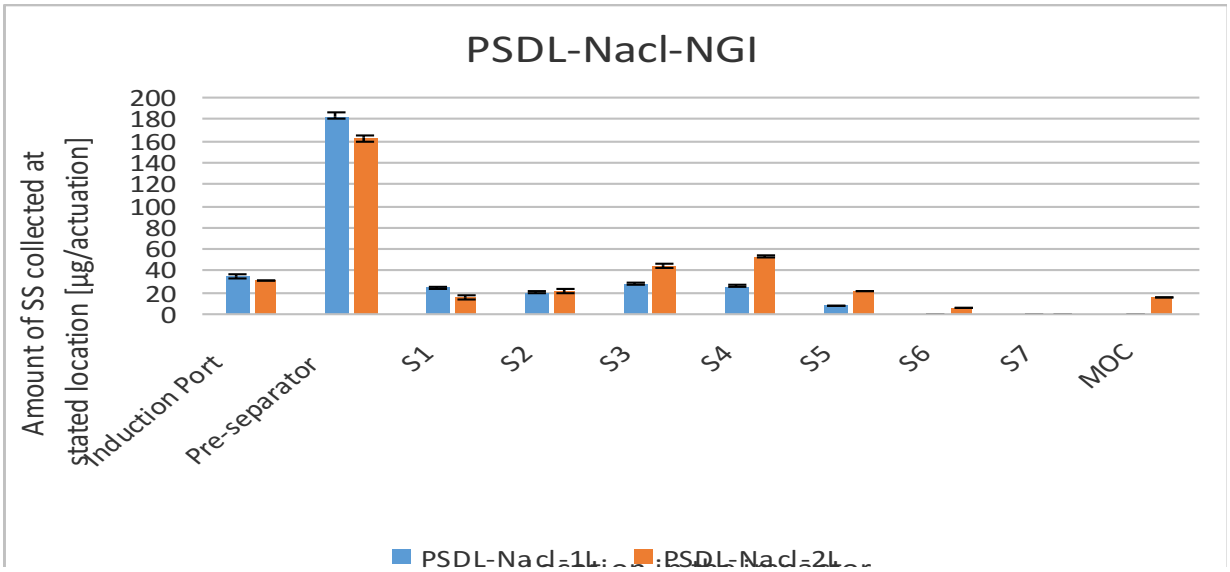

Figure 5.18. Deposition profile of SS from a MacHaler® as a function of inhaled volume after actuation at 60 L/min into an NGI of the DPI formulation containing PSDL-NaCl carrier.

The effect of reducing the inhaled volume from 2 L to 1 L for the NGI was accompanied by a marked and significant increase in the mass median aerodynamic diameter (MMAD) from

2.80 ± 0.10 μm to 4 ± 0.12 μm for PSDL-PVP and from 2.85 ± 0.06 μm 3.90 ± 0.08 μm for PSDL-NaCl (Table 5.1). The NGI was more sensitive to change in the inhaled volume than the PSDL-NaCl (Table 5.1). The NGI was more sensitive to change in the inhaled volume than the ACI as shown in Tables 5.1 and 5.2. The comparison of ACI and NGI was very important in-vitro as to ensure the suitability for ACI or NGI for further study. NGI has a higher dead volume (2.025 L) and some patients might not be able to achieve volumes of 2 L or above (especially when using patient inhalation profiles for COPD patients). Sufficient volume of air has to be drawn through the CI (typically 4 L) so that the finest suspended particles have sufficient time to pass through the entire system and be fractionated. The minimum volume is based on the magnitude of the internal dead volume of the impactor. Recent studies (Mohammed et al., 2012) have demonstrated that decreasing the sample volume when using the NGI at 60 L/min resulted in a lower FPF value which indicated that the finer particles had not enough time to get to the distal stages of the impactor. However, the ACI did not appear to be as sensitive, this is believed to be because of a maldistribution of the flow through the ACI (Mitchell et al., 2013). That is why in the next chapters of this work, it was preferred to use the ACI which has a lower internal dead volume (1.050 L) and patients could easily achieve that volume. Regulatory authorities accept both ACI and NGI however, the data in-vitro might not correlate with in-vivo data because patients might not achieve high volumes and inhalation flow rates.

5.4 Conclusion

The solid phase crystallisation process applied in this work has many advantages compared to crystallisation from solution. The shape, size and surface texture cannot be predicted prior crystallisation when crystallising from a saturated solution on the other hand the physico-chemical properties of the additive used in the crystallization medium may slow, inhibit or promote crystallization. In addition to the stirring speed, the solvent and its volume, shape of the crystallization vessel, temperature can impact on the morphological features of the crystal formed.

The Salbutamol Sulphate dose emissions from the capsule-based MacHaler® device for both formulations PSDL-NaCl and PSDL-PVP demonstrated inhalation volume-dependent dose emissions. The aerodynamic characteristics of Salbutamol sulphate showed MacHaler® was effective in producing respirable particles with an MMAD (<5 μm) irrespective of the formulation used, but the mass fraction of particles with an aerodynamic diameter less than 3 μm was more noticeable at 2 L.

Finally, the results confirm the recommendation of using a prolonged inhalation time when using the MacHaler®.

Chapter 6

The effect of the carrier morphology and mixing time on blend uniformity and drug adhesion in Dry Powder Formulations

6.1 Introduction

6.1.1 Background

Approximately 300 million people worldwide are suffering from asthma and almost 240 million people are affected by COPD. More than half of the patients opt for the use of dry powder inhalers as part of their treatment. DPI devices have shown over the years to deliver reliable drug dose to the patient, with constant evolution in their designs focusing on patient compliance, low cost and ease of use.

From a formulation point of view, DPIs are capable of delivering small and large dosage for a wide range of molecules from traditional asthma drugs, antibiotics to proteins and oligonucleotides. In particular, delivering biological therapeutics deeper into the lungs for systemic delivery offers the most propitious inhalation therapy platform. Drugs for inhalation are often cohesive, due to the high specific surface area (surface area-to-mass ratio) of micron-sized drug particles. Thus, the DPI must be formulated appropriately such that the particles of active ingredient can be easily detached from the surface of the carrier and become easily dispersed into respirable particles upon inhalation. In most DPIs, micron sized drug particles (1-5μm) are adhered to large carrier particles such as lactose via an order mix (Hersey, 1979).

The energy of powder dispersion is usually derived from the inhalation effort applied by the patient. Powders for pulmonary delivery are often cohesive, due to the high specific surface area (surface area-to-mass ratio) of micron-sized particles. Thus, the powders must be formulated appropriately to firstly facilitate drug detachment from the carrier surface and secondly dispersion of drug particles into single particles suitable for deep lung penetration. The extent of drug detachment from the surface of the large carrier is largely dependent upon the interaction between the two components. Stronger adhesion results in lower amounts of drug detaching from carrier particles and is the major cause of low delivery efficiency of drugs from most DPIs. Adhesion forces are mainly composed of van der Waal's and electrostatic

forces (Zimon, 1982). The adhesives forces between fine particles and coarser carrier particles must be strong enough to ensure a good blend homogeneity but on the other hand, the adhesive forces should be weak enough to allow drug detachment from the carrier during the inhalation manoeuvre to allow the drug to enter the lungs. Pharmaceutical powders show a tendency to gain electrical charges during handling, processing (e.g., mixing, milling, spray drying, sieving), transfer of materials from one location to another (Bailey, 1993). All these processes involve high shear forces and can generate electrostatic charges on the powder blends. The impact of these electrical charges on powders in pharmaceutical product development is not fully understood and remains quite unexplored. Drug particles and pharmaceutical excipients can be categorised as electropositive, electronegative or neutral depending on how the powder particles charge. Fig .6.1 shows the examples of commonly used pharmaceutical materials and their electrical behaviour.

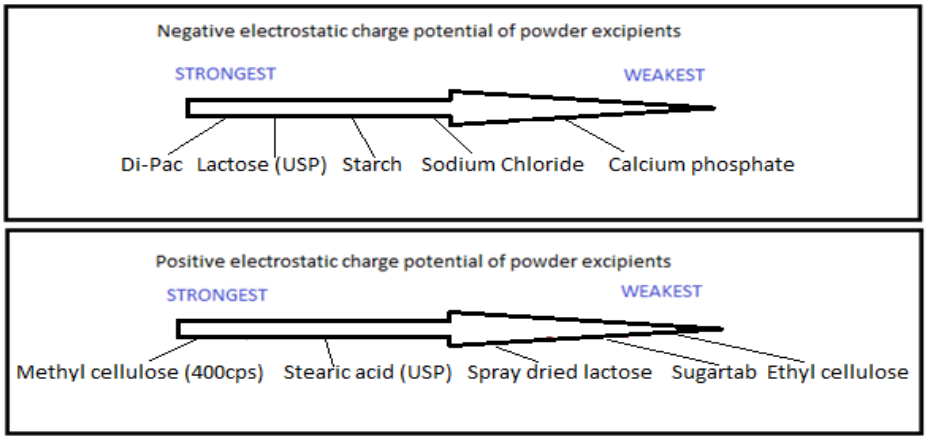

Figure 6.1 Electrical behaviour of selected pharmaceutical excipients

Contact electrification occurs when two different materials make contact and then separate, resulting in a transfer of charge between them (Harper, 1967). Contact electrification is similar to, but distinct to *triboelectrification*, which occurs when two materials collide or are rubbed together, causing a transfer of charge leading up to a build-up of static charge (Dechene & Newton, 1987; Yu & Watson, 2001). The induced charges on the powders may have an effect on the flow behaviour, capsule fill uniformity, drug content uniformity and drug-carrier detachment on actuation (Yu et al.2008).

It is known that tribo-charging (or contact charging) of adhesive mixtures in pharmaceutical processes, such as sieving, mixing, compression, is influenced by several factors such as particle shape (Murtomaa et al., 2004), particle size, electrical properties of each component of the formulation, surface properties of the particles such as surface roughness (Karner et al., 2014), specific surface area, contact area and frequency, purity of the surface and atmospheric conditions (Bailey, 1993; Byron et al., 1995; Kulvanich & Stewart, 1987). Triboelectrification remains a complex phenomenon, as not all materials are sensitive to electrostatic charging at atmospheric conditions and also because triboelectrification can only be characterised if the true area of contact is known (Bailey, 1993). The true area of contact is influenced by the surface roughness of the particles as well as the contact pressure between the particles. Researchers have attempted to modify the contact area between particles by altering the surface roughness of carrier particles in order to reduce tribo-electric charging. Such modifications can be achieved by crystallising lactose particles to produce different surface roughness (Nokhodchi & Martin, 2015). Most pharmaceutical substances are organic materials which behave as insulators under ambient conditions. When two dissimilar particles make contact, a transfer of electrons occurs between the particles in contact due to the difference in their effective work functions (as to equalize the Fermi level energies). The work function of a particle is defined as the difference in the energy state between a reference

material and the outermost electrons (or Fermi level) of the particle. This difference between work functions produce electrostatic charges and it is this adhesion energy, along with electric forces (Van der Waals forces, Coulomb interactions and surface tension interactions) which must be overcome to ensure free movement of particles in pharmaceutical powders.

In order to obtain a high mixing homogeneity and stable DPI formulations, it is crucial that the drug particles are able to attach to the carrier particle surface during contact. During mixing of DPI formulation, particles make repeated contacts with different surfaces, such as the surface of other components in the DPI formulation and the metallic or glass surfaces of the handling and processing equipment. After each contact, the powder particles charge either positively or negatively. The charging behaviour of the particles is highly dependent on the charges present on the particles. Such charged particles are subject to high adhesive forces and drug particles may adhere strongly to the carrier surface, thus compromising drug-carrier particle separation on actuation (Karner et al., 2014). The charges of powder can also affect powder flow and dose uniformity. Karner and Urbantez (2013) have reviewed many factors affecting the magnitude and polarity of particle charges which include particle size and shape, surface roughness, relative humidity and energy of contact. In general, drug particles tend to demonstrate higher levels of charge than excipients (Šupuk et al., 2012). To overcome the high adhesive forces, the addition of antistatic agents can be used to make the surface of the material slightly conductive (Simpkin et al., 1999). Another approach is, when formulating DPI products, the careful selection of the carrier based on the electrical properties of individual components in the DPI formulation so that the final formulation can exhibit neutral charge during powder handling operations.

6.1.2 Aim

This chapter was designed to investigate the effects of mixing time on the homogeneity of the blend, the dispersion performance of DPI formulations and on the electrostatic charges generated during the mixing process of the pharmaceutical materials. Furthermore, it was studied if the surface texture of different lactose carriers (smooth Lactohale and rough PSDL particles) have an effect on the following parameters: the de-agglomeration of the drug during mixing, the effect of drug-carrier adhesion forces and tribo-electrification of lactose carrier and drug particles during formulation. For this purpose, the formulations used in this chapter were made with different types of drugs (hydrophobic and hydrophilic) and lactose carriers having different surface roughness (sieved commercial Lactohale and two types of Processed Spray Dried Lactohale (PSDL) with different surface roughness). Each drug: Salbutamol Sulphate, Fluticasone Propionate or Beclomethasone Dipropionate, was separately mixed for different periods of time with Lactohale or PSDL in a Turbula mixer. The resulting formulations were checked for drug content uniformity. Various analytical techniques were used to characterise the particles. Scanning Electron Microscopy was used to assess the morphological characteristics of the particles qualitatively. XRD was used to assess the crystallinity of the materials. The tribo-electrification arising during the mixing of each formulation component of the DPI was investigated by measuring the net charges of the different lactose carriers as well as the charges of the different drugs using tribo-electrification method detailed in Section 6.2.3.10 of Chapter 6. The dose emission characteristics of each drug from all DPI formulations was determined by aerosolising each formulation from the BreezeHaler® into an Andersen cascade impactor (ACI) at an inhalation flow rate corresponding to a pressure drop of 4 kPa at two inhaled volumes 2 L and 4 L.

6.2 Methodology

6.2.1 Materials

- α-lactose monohydrate (Lactohale™, DFE Pharma UK)
- Salbutamol Sulphate with a VMD of approx. 4.2 μm (GSK, Ware, UK)
- Fluticasone propionate with a VMD of approx. 4.2 μm (GSK, Ware, UK)
- Beclomethasone Dipropionate with a VMD of approx. 4.2 μm (GSK, Ware, UK)
- Absolute ethanol (Fisher Scientific Ltd, UK)
- Ultra-purified water apparatus (Fisher Scientific Ltd, UK)

6.2.2 General laboratory apparatus and equipment

- 500 μm, 125μm, 90 μm and 63 μm sieves with collecting pans (Endecott, UK)
- Hot plate (Cole-Parmer®, UK)
- 20 ml clear glass vials (Sigma Aldrich, UK)
- Volumetric flasks, glass beakers (Fischer Scientific Ltd, UK)
- SD-06 Spray dryer (Labplant, UK)
- Hair dryer (Revlon, UK)
- Ventilated oven (Memmert, Germany)
- Ultrawave U300 benchtop bath (Ultrawave Scienitifc Laboratory Supplies Ltd, UK)
- Turbula mixer T2F (Willy A. Bachofen AG Maschinenfabrik, Switzerland)
- Tribo-Electric Charging Device (Šupuk et al., 2009)
- Scanning Electron Microscope (Jeol, Japan)
- Differential Scanning Calorimeter (Mettler Toledo, UK)
- X-Ray Powder Diffractometer (Bruker AXS, UK)
- High Performance Liquid Chromatography (Shimadzu, UK)
- Onbreez BreezHaler® device (Novartis Pharmaceuticals UK Ltd)

- Hard gelatine capsules, size 3 (Capsugel, France)
- Andersen Cascade Impactor (Copley, UK)

6.2.3 Methods

6.2.3.1 Preparation of lactohale carrier

Lactohale was sieved to obtain relatively narrow size distribution (63-90μm) to match approximately the particle size of PSDL. About 50g of Lactohale was poured into a 90μm sieve which was placed upon a 63 μm sieve. Lactose is known to be brittle, as a result the powder was sieved manually and slowly for about 30 minutes so as to limit particle abrasion, breakage and tribo-charging which can occur during conventional mechanical sieving. The powder was then collected in a sealed glass jar and stored in a desiccator over silica gel until required for further investigation.

6.2.3.2 Production of spray-dried particles

Microparticles of Lactohale were prepared by spray drying. Pre-determined amount of Lactohale was solubilised in ultra-pure water to obtain 10% w/v lactose solution. This lactose solution was spray-dried using a laboratory scale spray dryer (SD-06 spray-drier, Labplant, UK). The following conditions were used from spray-drying: inlet temperature of 180°C, outlet temperature of 102°C, solution feed rate to 4rpm (2ml/min), pressure: (3 bar), 0.5mm nozzle. Following spray-drying, the product was recovered from the collecting jar and transferred into a glass vial before storing in a desiccator containing silica-gel until required for use.

6.2.3.3 Production of Processed Spray dried lactohale

100 ml of absolute ethanol (Fisher, UK) was poured into a 600mL glass beaker and transferred to the fumehood, where ethanol was allowed to boil using a hot plate (Cole-Parmer®, UK). A pre-determined quantity of spray-dried lactose particles (about 10 g) was introduced to the boiling solvent for 10 secs while stirring the lactose suspension at 250 rpm. The beaker was then removed from the hot plate using special laboratory gloves (Delta Plus Grey Cut Resistant Polyethylene-coated cut resistant gloves, RS, UK). The lactose suspension was poured through 500μm sieve into a collecting pan to remove any lumps. The recovered processed spray-dried lactose suspension was dispersed using a cool air generated by a hair drier to avoid polymorphic transformation which can be caused by hot air generated by the hair drier. This step was followed by drying in a ventilated oven at 45°C for 48 hours (Memmert, Germany). The particles were easily removed from the collecting pan as a free-flowing powder and allowed to cool to room temperature for 1 hour before transferring into a clean sealed glass jar and stored in a desiccator over the silica gel until required. The particles resulting from this batch were named $PSDL_{10}$.

The same process was repeated for a second batch however, the spray-dried particles were left on contact with boiling ethanol for a longer time (30 s). The particles resulting from this batch were named $PSDL_{30}$.

6.2.3.4 Preparation of powder blends

Each drug (SS, FP and BDP, Glaxo Smithkline, Ware, UK) 40 ± 1.45 mg was mixed separately with 2.7 g Lactohale and PSDL in a ratio of 1:67.5 w/w, in accordance with the ratio employed in the commercial 'Ventolin®' formulation so that each capsule contains 400 ± 14.5 μg and 27 mg lactose. Thus, each drug with a volume mean diameter of 2.4 μm , was weighed into a 20ml

glass vial to which was added approximately an equivalent amount of lactose carrier either lactohale or PSDL and blended manually using microspatula. Then more lactose carrier was added similar to the amount of the blend contained in the glass vial and mixed manually using the same microspatula. This process was repeated until all the lactose (2.70 g) had been added into the drug/lactose blend to obtain a ratio of drug to carrier of 1:67.5, w/w. The same process was applied to all formulations irrespective of the drug or carrier. The stoppered vials were then placed in a Turbula mixer and mixed for 5 mins, 10 mins, 15 mins and 30 mins. Finally, the samples were stored at room temperature (25 ± 2 ºC) in a vacuum desiccator over silica gel until required for further investigation.

Hard gelatine capsules (size 3) were filled with exactly 27.4 ±0.5 mg of the powder mixture so that each capsule contained 400 ± 14.5µg of the drug. The filling of capsules was completed manually.

6.2.3.5 Measurement of the homogeneity of the mixtures

After each mixing time in the Turbula mixer, the drug content uniformity of SS, FP and BDP were determined by taking randomly 10 aliquots of approximately 27.4 mg each (3 from the top, 3 from the middle, 3 from the bottom and one from anywhere in the blend), Each aliquot was poured into a 100ml volumetric flak and made up to the volume with the HPLC washing solution acetonitrile: water (75:25 v/v). Each solution was assayed for the drug content using a validated HPLC method illustrated in Chapter 3; Section 3.4. The average mean recovery related to the nominal dose were calculated and the percentage coefficient of variation (% CV) was the metric used to access the content uniformity of each powder blend.

6.2.3.6 Characterisation of particle shape and size using Scanning Electron Microscopy (SEM)

SEM was used to assess the lactose carriers (lactohale and PSDL) morphological features: particle size, shape and surface structure. Double-sided carbon adhesive tape (Agar Scientific, UK) was placed on an aluminium stub and after stripping off the upper side of the adhesive, a small amount of lactose particles was firstly dispersed on a glass microscope slide to ensure uniform particle dispersion before mounting them on the adhesive stub. The particles were then coated with approximately 15 to 20 nm gold for one minute using a ion sputter coater (Quorum Technologies Ltd., UK) under vacuum of 0.09 mbar and a current of 40mA. Micrograph Images were produced by scanning fields, selected randomly at several magnifications with a Jeol 6060LV SM Scanning Electron Microscope (JEOL, Japan).

6.2.3.7 Characterisation of lactose carriers using differential scanning calorimetry (DSC)

Differential Scanning Calorimetry (DSC) was used to determine the crystal form of lactose carriers. The experiment was carried out using a Mettler TA 4000 (Mettler, Toledo). Approximately 5 mg of each sample was weighed into an aluminium pan (40µl) (Mettler AT 260 delta range weighing balance) and the lid was crimped into place and the lid of the DSC pans reference and sample were pierced with 0.1 mm needle before transferring to measuring cell. Introducing the pin hole will avoid the increase in the vapour pressure in the sample which can be caused by gas or vapour evolved from the sample. The samples were then heated from 25 to 250ºC at a heating rate of 10ºC per minute. The DSC was continuously flushed with Nitrogen at a flow rate of 50ml/min.

6.2.3.8 Solid State Characterization of lactohale and PSDL using X-Ray Powder Diffraction (XRPD)

X-Ray powder diffraction was used to assess the crystallinity of lactose crystals. Powder X-ray diffraction patterns were recorded after samples were spread uniformly over the sample holder using a D8 Advance powder X-Ray diffractometer with Cu $K_{\alpha l}$ radiation of λ = 1.54Å. (Bruker AXS). The voltage and current applied were 40 kV and 40 mA, respectively. The sample powder was packed into the rotation sample holder and scanned in the 2θ range 5° to 40°. Lactose particles' crystallinity were identified by comparing the characteristic 2θ peaks ("fingerprints") of the XRD pattern.

6.2.3.9 Drug quantification using HPLC method

SS was analysed by HPLC method described in Chapter 3 section 3.4. FP and BDP were analysed using HPLC method containing the mobile phase of acetonitrile and water (75: 25) v/v. The flow rate of the mobile phase was 1 ml min^{-1} and UV detection of BDP and FP was at 230 nm. The HPLC runs for both BDP and FP were run at room temperature but the pressure remained the same at 1050 psi. The Shimadzu HPLC system comprised a liquid chromatograph (LC-20AT), an auto sampler (SIL-20A), a column oven (CTO-10ASVP), a UV-VIS detector (SPD-20A) and an Ascentis RP-Amide column (25 cm x 4.6 mm, 5 µm). The injection volume of the sample was 20 µl. The retention times for FP and BDP were 2.8 and 6.5 minutes, respectively.

6.2.3.10 Measurement of Triboelectric charges

The tribo-electric charge to mass ratio (*Q*/*M*) of the DPI formulation was determined using an electrostatic charge measurement apparatus comprising a Faraday cup, an electrometer and a shaking machine (Šupuk et al., 2009). The Faraday cup consists of two concentric cups made

of a conducting material. The concentring cups differ in size: the outer cup is larger than the inner cup which acts as an electrical shield to prevent impacts of external electric fields. The inner cup was connected to an electrometer (Keithley, model 6514, UK), as shown in Fig. 6.2, as per the method described by Secker and Chubb, 1984.

Each weighed DPI powder (approximately 0.1 g for each run, n=3) was placed in a Retsch stainless steel cylindrical container (10 ml) before being shaken in a horizontal direction using a shaking machine (Retsch MM 400) for 2 minutes at a vibration frequency of 20 Hertz. The measurements were repeated three times. The powder sample was then poured into the Faraday cup. The net charge (C) present on the powder particles were measured on the electrometer. The mean charge per mass of powder was obtained from three replicate measurements.

The mean charge values were presented as nano-coulombs (nC) and the mean charge to mass ratio (Q/M) of each powder was calculated by dividing the final charge with the final mass of the respective powder and was presented as nanoCoulombs/gram (nC/g). The same procedure was followed for all DPI formulations.

The Retsch shaking cylindrical stainless steel container was cleaned thoroughly after each measurement with isopropyl alcohol to ensure the removal of any residual particles and impurities susceptible to invalidate the results. The experiment method was carried in a controlled environment with an ambient temperature of 20-23 °C and relative humidity (RH) of 32-39 %.

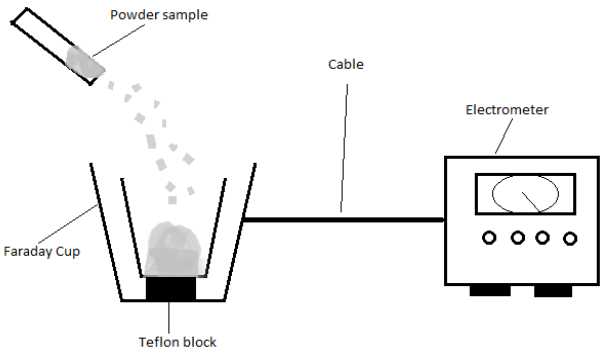

Figure 6.2 Schematic of the experimental set-up for measurement of electrostatic charges for DPI formulations

6.3 Results and discussion

6.3.1 Morphological characterisation of lactose carrier particles by SEM

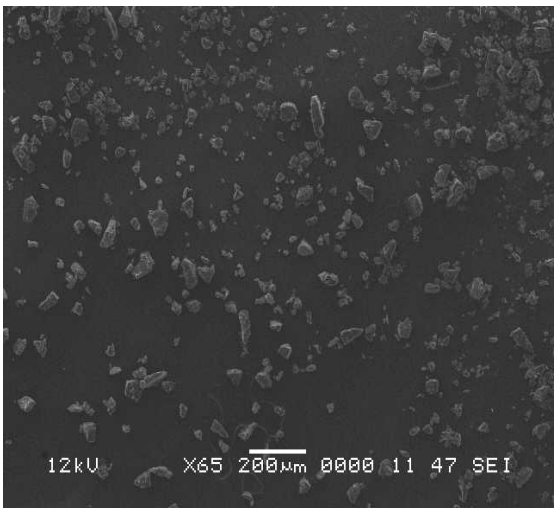

6.3a-General view of Lactohale

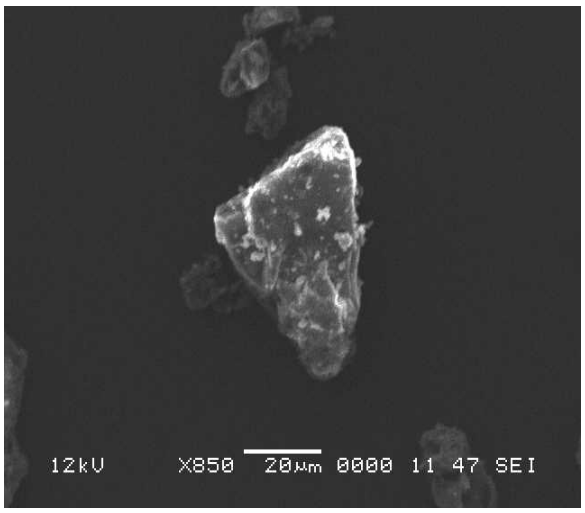

6.3b- Close view of Lactohale

Figure 6.3. SEM micrographs of Lactohale (General view and close view)

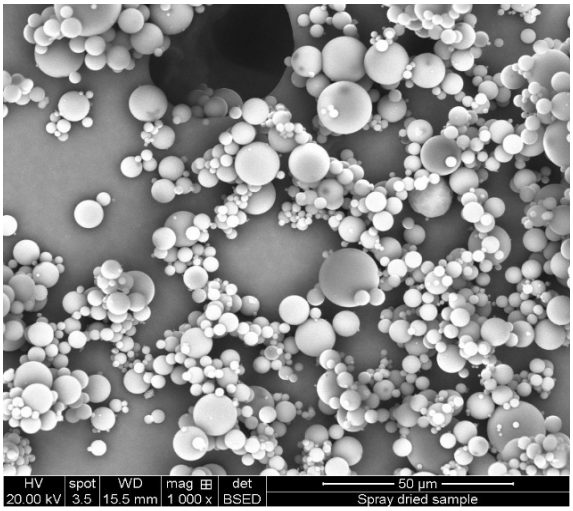

6.4a-General view of Spray Dried Lactohale

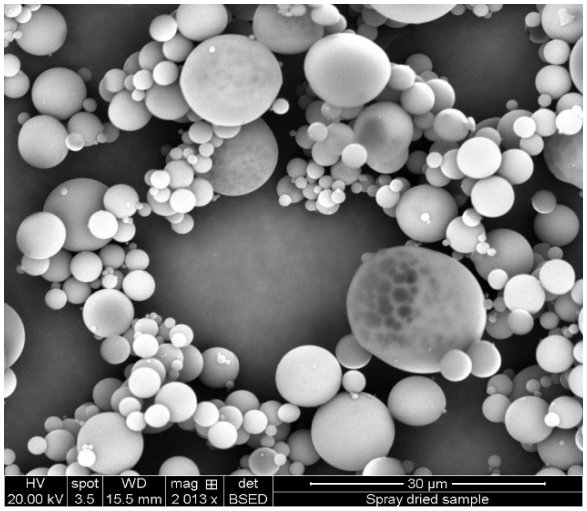

6.4b- Close view of Spray Dried Lactohale

Figure 6.4 SEM micrographs of Spray-Dried Lactohale (General view and close view)

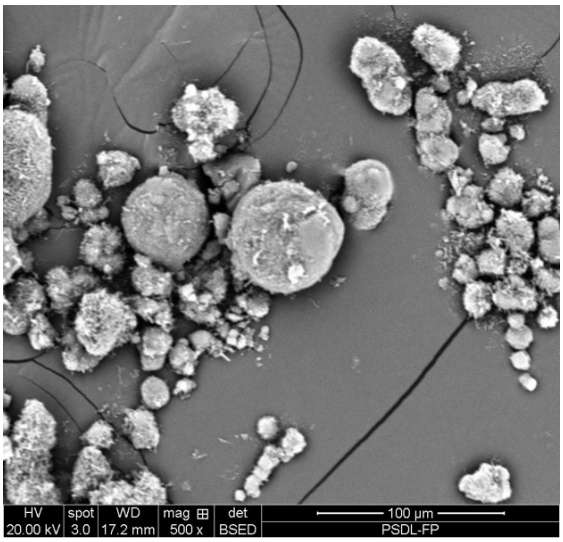

6.5a-General view of $PSDL_{10}$

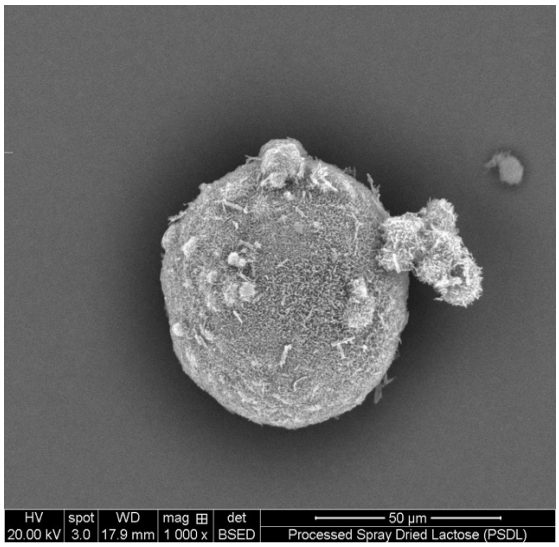

6.5b- Close view of $PSDL_{10}$

Figure 6.5. SEM micrographs of $PSDL_{10}$ (General view and close view)

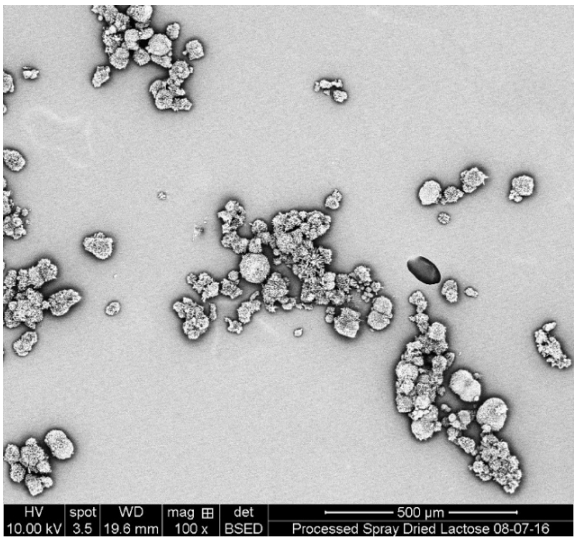

6.6a-General view of $PSDL_{30}$

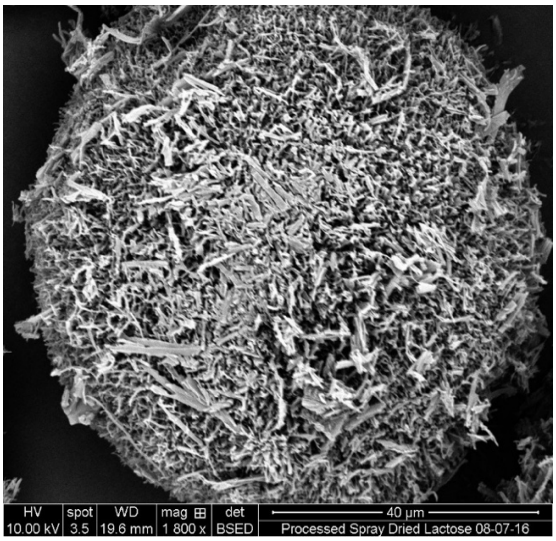

6.6b- Close view of $PSDL_{30}$

Figure.6.6 SEM micrographs of $PSDL_{30}$ (General view and close view)

One of the problems that the development of DPIs faces is that drugs that are fine enough to deposit in the lung are very difficult to handle, measure and meter on their own. Consequently, such drugs have to go through an adhesion or aggregation process, which usually involves binding or adhering the drug to lactose carrier. As the material passes through the device during inhalation manoeuver, a proportion of the drug de-aggregates to create respirable particles. This proportion is typically quite low for BreezHaler®, around 30 % of

label claim (De Boer, 2016) with a significant oropharyngeal deposition of the drug because most of the drug remains associated with large carrier particles. The de-aggregation process is generated by the patient inspiration.

The performance of DPI formulations is highly governed by the drug-carrier adhesion forces. High adhesive forces between drug and carrier particles can hinder drug detachment when the drug is aerosolized, leading to poor drug dispersion (Begat et al., 2004). The literature provides contradictory data on the effect of surface roughness and the aerosolisation performance of DPI formulations. For example, Kaialy et al showed that a better DPI performance was observed when the formulation contained more irregular particles with rougher surfaces, as the carrier particles exhibited smaller adhesion forces with salbutamol sulphate, as opposed to commercial lactose particles.(Kaialy et al., 2012). In contrast, Flament et al., demonstrated that the rougher the lactose particles, the lower the FPF as rough particles have more contacts points with the drug, thus allowing a greater adherence of the terbutaline sulphate to the carrier particles (Flament et al., 2004).

Good adherence of the drug to the carrier usually result in a good homogeneity of the blend, but can lead to less drug de-aggregation from the carrier during aerosolisation.

The morphological features of the particles are also known to influence the aerosol performance. A study by Zellnitz et al. showed that glass beads with rougher surfaces exhibited a higher FPF. This study is in contradiction with the studies from Flament and Kaialy mentioned above. All these studies show in fact that in order to have a higher dose of the drug reaching the deeper lungs, an optimum level of surface roughness is required.

Solid state crystallisation of the spray-dried lactose particles resulted in the formation of spherical particles with a rough surface (Figures.6.5 and 6.6) as opposed to Lactohale particles that had a tomahawk shape with a smoother surface (Figure. 6.3). The PDSL particles can be produced with different surface rugosity without altering size and shape of the particles. The time of exposure of spray-dried particles (Figure 6.4) to hot ethanol was a critical factor in altering surface rugosity as shown in SE micrographs (Figures 6.5 and 6.6). We processed spray dried lactose particles using two exposure times:10 seconds and 30 seconds to produce $PSDL_{10}$ and $PSDL_{30}$ respectively. The longer the exposure time to ethanol the rougher the particles. Therefore, $PSDL_{30}$ was rougher and more porous than $PSDL_{10}$. The performance of DPIs is greatly influenced by the physical properties of the carrier, particularly their particle size, morphology/shape and surface roughness. Because these factors are interdependent, it is difficult to completely understand how they individually influence DPI performance (Peng et al., 2016). Solid-state crystallisation, has been shown to produce spherical particles with any desired size, therefore the impact of particle size on the aerosol performance can be investigated independently without interference from any other morphological features such as shape and surface roughness. The surface roughness can be adjusted using different exposure times to ethanol to produce particles with desired surface rugosity without affecting their shape or size. Thus, the impact of surface rugosity on the aerosol performance can also be studied interdependently from any other morphological features such as the shape and size.

Solid state crystallisation was attempted at room temperature under stirring but there was no change in the particles growth, the particles collapsed when left for long forming a slurry. Increasing the temperature is expected to enhance the solubility of lactose especially very fine particles and amorphous regions within lactose, thus reducing the supersaturation of lactose in the crystallisation medium. Initially, spray dried particles (10g) were introduced in the crystallisation medium and using a solvent in which the solubility of lactose is not substantially

affected to maintain the supersaturation of lactose in the crystallisation medium. Undissolved lactose would act as a seed for crystal growth. It is important to note that the temperature reduces the viscosity of the crystallisation medium, thus facilitating the transfer of the dissolved lactose solution onto the lactose seeds for crystal growth. Increasing the time from 10 secs to 30 secs affected surface texture of the particles forming rough porous spherical particles.

Pharmaceutical powders are generally divided into three categories; plastic, elastic and brittle. Lactose is known to be brittle as shown from its high mean yield pressure derived from Heckel plot (Heckel, 1961; Roberts and Rowe, 1985). During crystal growth, the hollow volume of PSDL increases and reaches a maximum volume after which the particles burst to form needles. The increase in the hollow volume is dictated by the plasto-elasticity of the material. As the growth of the particles progress, the porous structure of the particles facilitates permeation of the solvent inside the hollow space, thus causing an increase in the vapour pressure caused by the evaporation of the solvent. The vapour pressure built inside the hollow space of the particle exerts a radial stress on the shell as shown in the schematic Figure 6.7. If the radial stress exceeds certain limit, the particle will either expand by plastic or elastic deformation or burst if fragmenting. Lactose is a fragmenting material and increasing the exposure time of the particles to the solvents beyond 30 secs caused them to burst as they could not withstand the radial stress applied from inside the particles. The vapour pressure increases in a radial direction and equally so that the spherical shape of the particles is retained (Figure 6.7)

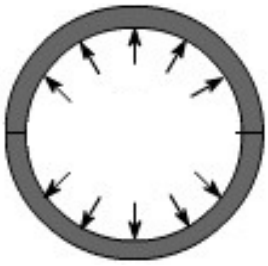

Figure 6.7. Schematic figure representing the direction of the radial stress occurring in a spherical particle as the vapour pressure inside increases.

Both ethanol and heat acted together as inflating and blowing agents to increase the size of the particles but also to modify the particle surface texture to produce light porous particles. The PSDL carrier is hollow and porous, therefore lighter than Lactohale and it is expected that PSDL particles would have a longer time of flight when inhaled in a DPI to allow more time for drug detachment to improve aerosol efficiency.

6.3.2 Crystallinity of the lactose particles by XRPD:

X-ray diffractograms of lactohale, spray-dried lactose, $PSDL_{10}$ and $PSDL_{30}$ were recorded and displayed in figures 6.8, 6.9, 6.10 and 6.11 respectively.

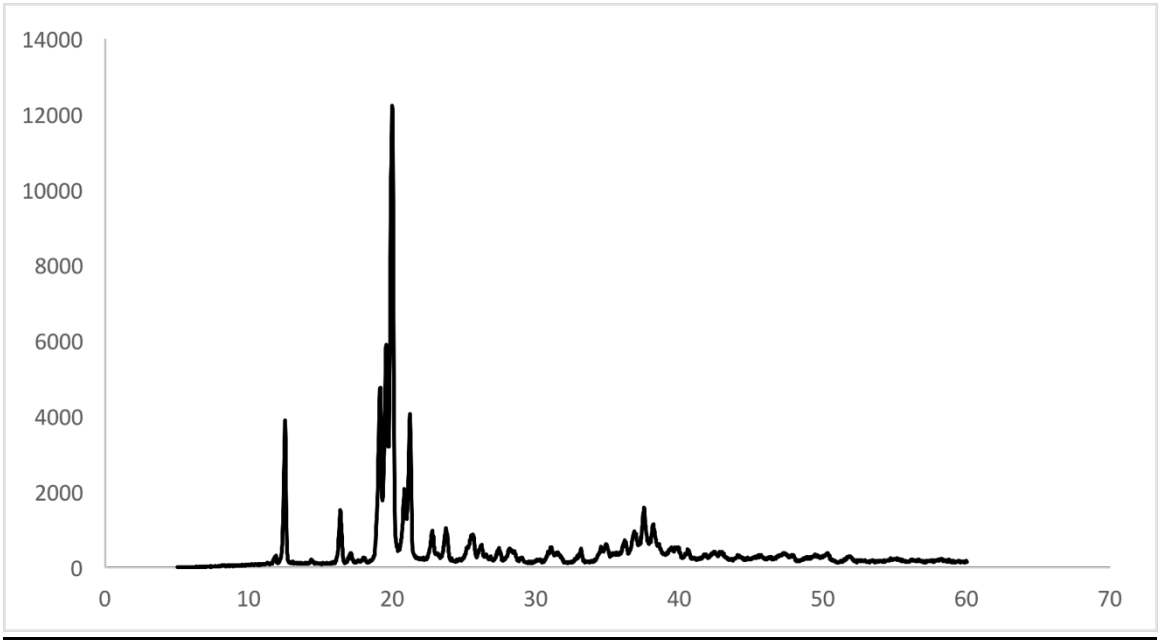

Figure .6.8 XRD pattern of Lactose monohydrate

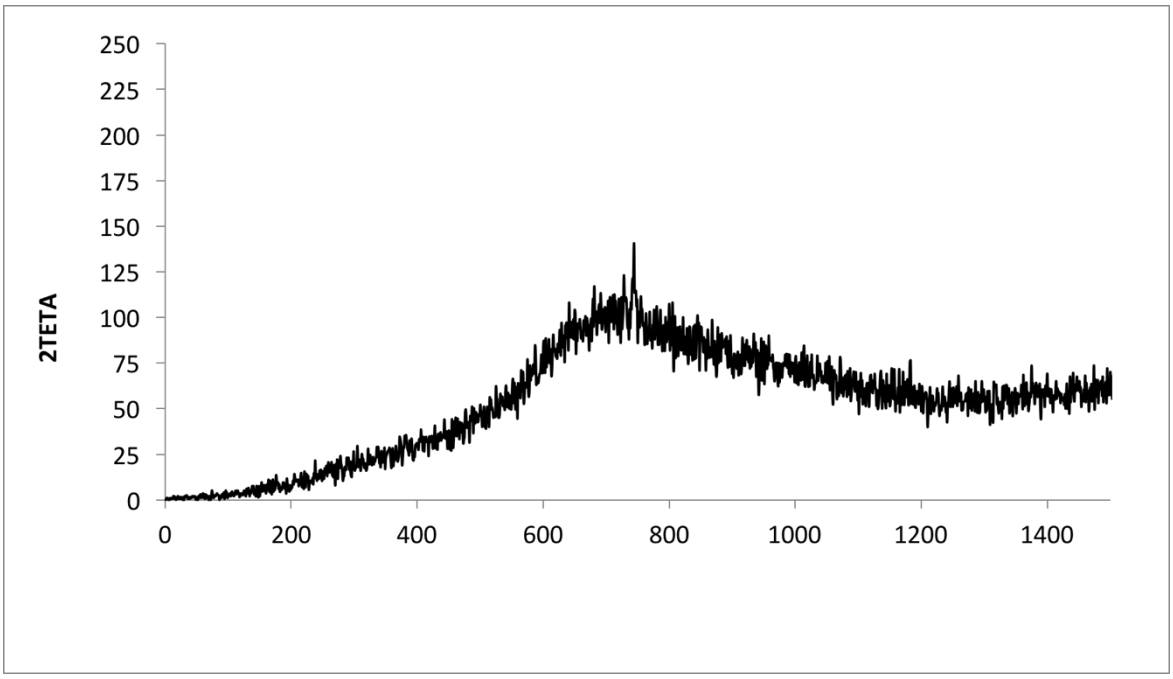

Figure 6.9 XRD pattern of spray-dried lactose

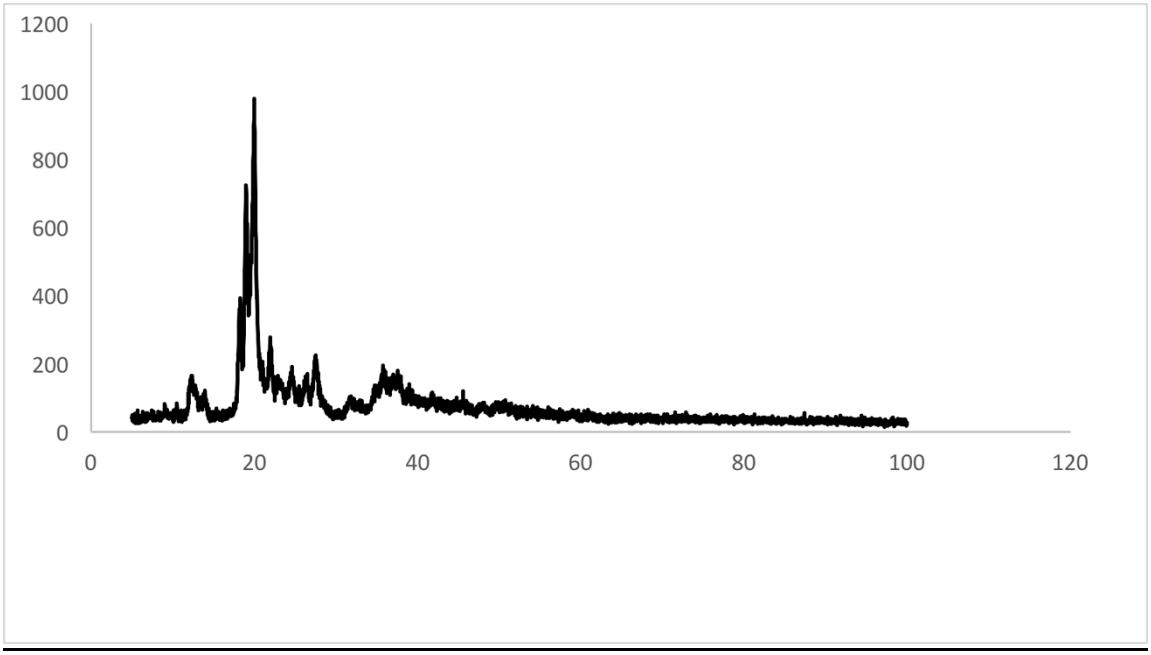

Figure. 6.10 XRD pattern of $PSDL_{10}$

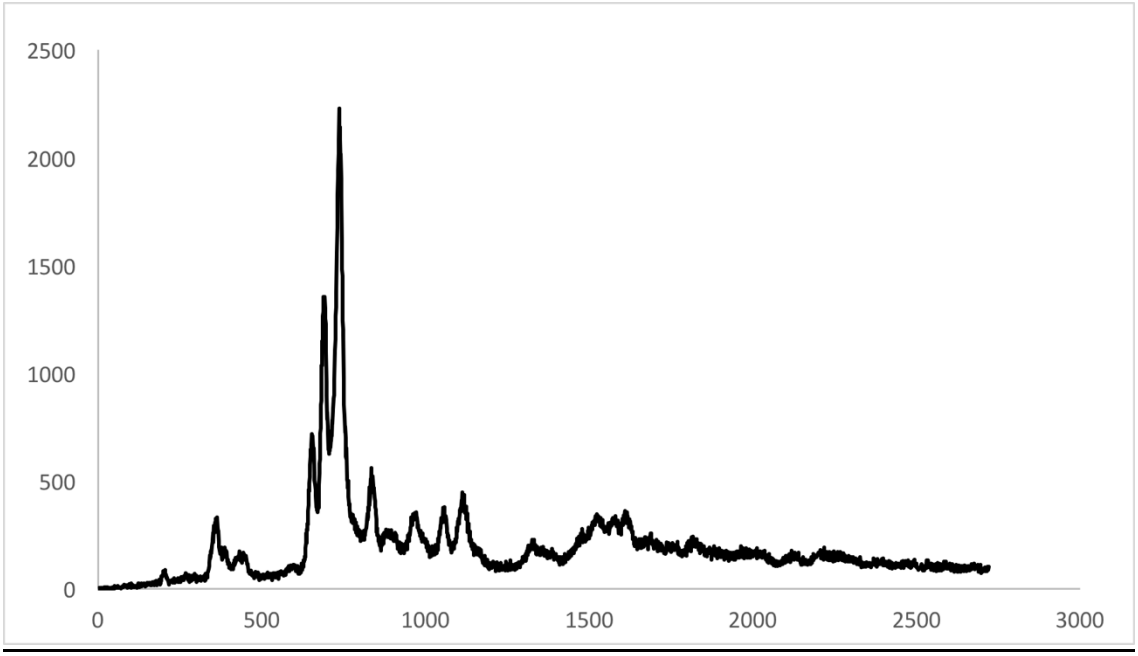

Figure. 6.11 XRD pattern of $PSDL_{30}$

X-Ray powder diffraction is considered to be the most accurate method for the study of crystalline structures (Doff, Brownen, & Corrigan, 1986; Hancock & Zografi, 1997). This

technique is widely used to study the changes in the crystalline states. The reflections of the diffractograms were presented as peaks deviating from the baseline. Crystallinity of materials can be assessed by presuming that broad peaks come from amorphous phase and sharp peaks arise from crystal phase.

Lactohale was found to be crystalline with diffraction peaks at 12°; 16° and 19° (Figure 6.8) representative of the crystalline form of α-lactose monohydrate (Gombas et al., 2002). The principle of spray drying is to disperse drug or excipient solution into very small droplets by the atomizer, then rapidly evaporate the solvent in a hot dry medium like hot air to obtain dry product of powder. This process produces product with narrow particle size distribution, and also is relatively easy to scale up for commercial production (Pilcer et al., 2012). Spray-drying lactose rendered lactose amorphous as suggested by the broad diffuse peaks (Figure 6.9). Spray-drying is known to produce predominantly amorphous material because the transition between the liquid and solid phase is instantaneous, in other words, the rapid drying of the lactose solute droplet did not allow sufficient time for lactose to form a crystalline structure, this is one of the drawbacks of spray drying because the amorphous particles tend to be highly cohesive (Young et al., 2007), have a poor flow and thermodynamically unstable (Shen et al., 2010). In order to improve the handling, metering and flow of DPI drugs, coarse carrier particles are generally used, however spray-dried lactose particles produced are small (Figure 6.4), thus not large enough to be used as carrier particles in DPI formulations. The only advantage of using spray drying in our study was to produce hollow spherical particles, which are considered effective in DPI formulations. This is why a processing method was developed to restore the crystallinity of the particles and to modify their surface texture without affecting their spherical shape. Processing the spray-dried particles in the presence of ethanol restored the crystallinity to lactose particles to form crystalline PSDL particles (Figures. 6.10 and 6.11). The relative degree of crystallinity of different samples of the same crystal form is usually

proportional to the ratio of the peak intensity (Zeng et al., 2000). It is interesting to note that higher peak intensities were observed on $PSDL_{30}$ diffractogram (Figure 6.11) suggesting that $PSDL_{30}$ was more crystalline than $PSDL_{10}$. It is clear that prolonging the exposure time to ethanol has an impact on the crystallinity of the PSDL particles, since it has been reported that the increase in temperature has a linear relationship with the degree of crystallinity of lactose particles (Young et al., 2007).

Operation processes such as sieving, milling, mixing spray-drying and transfer of powder involve frequent interactions between each component of the powder formulation, i.e. the active ingredient and the excipient. Since triboelectrification is a contact phenomenon and pharmaceutical substances are known to gain charges during all the different steps involved in the preparation of dosage forms. The acquired charges associated with DPIs have been recognised to have a significant impact in adhesion/cohesion (Hiestand, 1966). When the patient inhales through a device, the DPI powder blend is fluidized and dispersed; drug particles separate from the surface of the carrier particles and charges are usually exchanged during this process resulting in net particles charges on the particles, which may affect their trajectories and deposition. It is worth mentioning that studies have established a correlation between crystallinity and tribo-charging of particles. Wong et al. (2014) found that SS crystalline particles acquired more charging during tumbling than amorphous SS. The arrangement of SS molecules in the crystal lattice was responsible for the polarity of the charge and the charging. This knowledge should be taken into consideration when optimising formulations for DPIs as the degree of crystallinity has an effect on the electrostatic charges behaviour of the particles which plays an important role in the aerosolisation performance of DPIs.

6.3.3 Impact of mixing time on drug content uniformity of SS, FP, BDP in formulations containing either lactohale or PSDL as a carrier

Table 6.1 Content uniformity of SS, FP and BDP with Lactohale at different mixing times: 5, 10, 15 and 30 min.

	Lactohale					
time	BDP		FP		SS	
	amount(SD)	%CV	amount(SD)	%CV	amount (SD)	%CV
5mins	396.78(24.73)	6.23	412.86 (6.57)	1.59	404.48 (4.23)	1.04
10mins	359.54(15.83)	4.4	406.67 (5.79)	1.42	409.85 (25.53)	6.23
15mins	399(13.65)	3.42	414.27(7.31)	1.76	408.66 (37.95)	9.29
30 mins	405.85(16.55)	4.08	416.78 (15.53)	3.72	410.33 (1.05)	9.69

Table 6.2 Content uniformity of SS, FP and BDP with PSDL30 at different mixing times: 5, 10, 15 and 30 min.

PSDL30					
BDP		FP		SS	
amount(SD)	%CV	amount(SD)	%CV	amount (SD)	%CV
425.1(15.36)	3.61	407.51 (5.20)	1.28	414.64 (14.79)	3.57
412.37(10.32)	2.5	416.92 (8.36)	2	404.80 (9.57)	2.36
404.45(9.87)	2.44	412.32(9.13)	2.21	408.31 (20.61)	5.05
402.93(10.45)	2.59	406.23 (17.84)	4.39	392.23 (19.41)	4.95

Table 6.3 Content uniformity of SS, FP and BDP with PSDL10 at different mixing times: 5, 10, 15 and 30 min.

PSDL10					
BDP		FP		SS	
amount(SD)	%CV	amount(SD)	%CV	amount (SD)	%CV
404.76(11.56)	2.85	409.67 (3.40)	0.83	408.81 (14.56)	3.32
405.21(8.63)	2.13	398.16(6.11)	1.53	413.64 (11.91)	2.88
416.29(15.43)	3.71	398.79(6.24)	1.56	403.42 (11.12)	2.75
406.71(14.73)	3.62	406.06 (14.64)	3.6	398.81 (9.68)	2.28

Various physico-chemical properties of drug substances are affected by their particle size distribution and shapes and it is also known to formulation scientists that very fine pharmaceutical materials such as fine drug particles used for inhalation are difficult to handle. There is a large difference in size between the active component and excipient such as lactose used for inhalation; segregation by percolation can occur, making mixing difficult. The most appropriate mixing method commonly used for DPIs is order mixing to allow fine drug particles to adhere to large carrier particles (63-90 μm) to minimise de-mixing. Not only particle size, but also particle shape and surface texture can influence the flow and mixing efficiency of powder formulations. Adequate distribution of the drug must be demonstrated within the powder blend and also in the final dosage form. The FDA guidelines state that the USP criteria for content uniformity is 85-115% (Berman et al., 1995), but the industry standard for content uniformity is 90-110% (Muselík et al., 2014).

In this chapter, the homogeneity of the blends was assessed using the %CV calculated for each powder blend containing either SS, FP or BDP, which should be less than 5 % (Kaialy, 2016; Larhrib et al., 2003; Zeng et al., 2001a). Homogeneity of the blend is crucial in ensuring that the strength of the drug in the DPI formulation is within the acceptable limits and also gives an indication of the quality of the blend (Williams et al., 2002).

Blend uniformity as demonstrated using procedures described in the parenteral drug association (PDA, 1997). 10 aliquots of 27.4 ± 1mg each were selected from three different depths (3 from the top, 3 from the middle and 3 from the bottom of the blender) and the 10^{th} pulled sample was chosen randomly from the blender. The adequacy of the mix is demonstrated if the mean is between 90-110% of target and %CV is less than 5% (Kaialy et al., 2012; Larhrib et al., 2003; Zeng et al., 2001a).

Blending uniformity of the binary mixtures varied significantly ($p<0.05$) with mixing times, drug types and the type of carrier (Tables 6.1 and 6.2). The mean drug contents varied

between 359.54 ± 15.83 µg and 416.92 ± 8.36 µg for all batches, which are within the acceptable limit of 90-110% of the target weight. However, some mixing times showed a % CV less than 5%. Of the three drugs investigated, SS produced the poorest drug content uniformity with prolonging the mixing time, especially with Lactohale as shown from the highest %CV values exceeding 9% (Table 6.1). A short mixing time of 5 minutes provided a better repartition of SS particles on the surface of Lactohale as shown from the low %CV of 0.31%. The morphological features of particles are known to affect the blend uniformity (Venables & Wells, 2001). Carrier particles with high elongation ratio are disadvantageous in DPI dose metering and processing at handling scale due to their poor flowability (Kaialy et al., 2011; Larhrib et al., 2003).

Furthermore, smooth carrier particles have a low loading capacity which can promote drug segregation especially for high dose drugs. Lactohale has an elongated shape with a smooth surface (Figure 6.3), these morphological features may have affected both the adhesion of drug to the carrier and the flow of powder inside the Turbula mixer, facilitating segregation between drug and carrier particles by prolonging the mixing time.

Both BDP and FP are hydrophobic and showed a similar variability in drug content with prolonged mixing time, as quantified by %CV (Table 6.1), therefore achieved better blend uniformity with Lactohale than hydrophilic SS. SS mixes and de-mixes rapidly and this is shown also with PSDL (Table 6.2), although the %CV observed with PSDL was smaller than with Lactohale (Table 6.2). Hydrophobic drugs such as BDP and FP are highly cohesive and require longer time of mixing and high shear forces to break up drug aggregates before distributing uniformly on the lactose carrier. Thus, hydrophobic drugs can benefit from prolonged mixing times to provide good content uniformity than hydrophilic drugs such as SS with either Lactohale or PSDL.

Pollen shaped carrier particles have low density, therefore they are expected to adhere to the drug for a longer period of time and increase drug deposition in the lungs (Hassan & Lau, 2011; Larhrib et al., 2003). According to Hassan et al. (2011), the use of pollen-shaped carrier particles in formulations resulted in increased FPF.

PSDL was produced to provide pollen-like particles to improve drug content uniformity and to facilitate aerosolisation of drug particles. PSDL particles are spherical in shape with rough surface and gave the highest homogeneity with a very low coefficient of variation than tomahawk shaped smooth Lactohale, whether with SS, FP or BDP.

6.3.4 Impact of mixing process on tribo-charging behaviours of both SS, FP, BDP formulations containing either Lactohale or PSDL as a carrier

Table 6.4. The average final charge to mass ratios of the formulations after tribo-electrification

Formulation	Average final charge: mass ratio (nC g^{-1})
Lactohale	-15.38 ±17.89
PSDL30	5.39 ± 1.23
PSDL10	1.06 ± 2.43
SS	102.79 ± 24.67
FP	-34.52 ± 6.59
BDP	-378.77 ± 80.25
Lactohale-SS	-25.68 ± 2.60
PSDL30-SS	-19.39 ± 4.88
PSDL10-SS	1.75 ± 2.02
Lactohale-FP	-4.51 ± 0.53
PSDL30-FP	-10.93 ± 4.29
PSDL10-FP	2.01 ± 6.40
Lactohale-BDP	-13.35± 3.96
PSDL30-BDP	-8.49 ± 3.14
PSDL10-BDP	3.91± 4.27

In DPI formulations, electrostatic forces have a great impact on the adhesion between drug and carrier particles, consequently affecting the detachment and deposition of drug particles (Staniforth, 1995;Bailey, 1993)

All the individual components that make up the DPI formulation (Carter et al., 1998) and the formulation physicochemical properties (Peart, 1996) will have an effect on the charging behaviour of the powder formulation.

Pharmaceutical processing of materials into dosage forms is usually a multi-step process e.g. sieving, milling, spray-drying, mixing, transfer of the powder blend, compaction (Lachman & Lin, 1968). DPI formulations inevitably undergo tribo-charging during frequent particle-particle physical contacts, particle contacts with the surfaces of the inhaler device, and high impact velocities during their use.

Triboelectrification occurs when particles surfaces' make contact and they gain electrical charges during this multi-step process. The accumulated charges on the particles surface result in 'de-mixing' which can compromise the flowability of powder blends. In order to investigate the effect of triboelectrification during the mixing process of DPI formulations, lactose carriers with different surface morphologies were used: Lactohale, $PSDL_{10}$ and $PSDL_{30}$.

The different components used in the formulations were assessed for electrical properties using a Faraday cup coupled to an electrometer and the results are summarised in Table 6.4. The specific charge (nC/g) was obtained for each component. The tabulated results are represented as a mean and standard deviation of three replicate readings.

Particles that are less than 5μm have large specific surface area and therefore tend to charge very high (Tsai et al., 2006; Grosvenor and Staniforth, 1996). Usually, drugs are known to display higher levels of charge than excipients (Šupuk et al., 2012).

Table 6.4 indicates that different materials have different charging behaviours. The results show that lactose monohydrate showed a specific charge of -15.38 C g^{-1} whereas $PSDL_{30}$ and $PSDL_{10}$ were positively charged with a specific charge of 5.39 C g^{-1} and 1.06 C g^{-1} respectively. Our XRPD data showed that Lactohale is more crystalline than $PSDL_{10}$ (Figures 6.8, 6.10 and 6.11). These results are in agreement with Weng et al. study (2014) and Carter et al. (1998) study which showed that amorphous lactose (such as spray dried lactose) exhibited lower electrostatic charges than crystalline lactose (Carter et al., 1998). This was further confirmed with a study by Murtomaa et al. (2002) which also noticed that the specific charge

of lactose decreases as a function of the amorphous content. To correlate this to our study, the data shows that $PSDL_{30}$ charged slightly higher than $PSDL_{10}$ (5.39 nC/g and 1.06 nC/g respectively). XRD patterns of both $PSDL_{10}$ and $PSDL_{30}$ (Figs. 6.10 and 6.11) showed that $PSDL_{10}$ was less crystalline and indeed more amorphous than $PSDL_{30}$ which explained why $PSDL_{30}$ was more charged than $PSDL_{10}$. Weng et al. (2014) found that crystalline SS acquired more charging during tumbling than amorphous SS. The arrangement of SS molecules in the crystal lattice was responsible for the polarity of the charge and the charging.

The crystallinity of particles can affect how the charge is distributed on the surface of the particles. For example, electrical charges may distribute much quicker for amorphous particles than for crystalline particles. This is due to the mobility of the molecules that can be hindered in crystalline particles due to their crystal lattice. Similarly, charge distribution occurs more evenly on the surface of spherical amorphous particles, whereas the charges on crystalline irregular particles may be mostly distributed on the tips and edges (Figure 2.11) (Zeng et al., 2001a; 2001b).

Since charging behaviour is a surface phenomenon, this will eventually influence the interactions between drugs and carrier particles and could inherently influence adhesion and agglomeration of particles as well as in-vitro drug deposition (Bennett et al., 1999).

Another possible explanation for this difference in charge could be the specific surface area of the particles. Although in this study no experiment was carried out to measure the specific surface area of the particles, it is known from the literature that particles of the same size range but with different surface textures have different surface areas: for example, particles with a rougher surface will result in a larger specific surface area. Such particles will be able to take up more tribo-charges until their surface is charge saturated (Karner & Urbanetz, 2013) as opposed to smooth particles. As shown in Table 6.3, Lactohale alone or in the formulation with SS, FP or BDP always exhibited negative charge. The electronegative charge on Lactohale

increased even more when formulated with SS particles, the charge increased from -15.38 nC/g for Lactohale alone to -25.68 nC/g when formulated with SS. The addition of SS to the carrier particles charged the formulation more negatively, this could be due to de-mixing of the blend, which was supported by drug content uniformity data showing an increase in the %CV with increasing mixing time.

The triboelectrification data also showed that SS remains adhered to the wall of the container, suggesting de-mixing. A similar phenomenon was observed for $PSDL_{30}$ where the addition of a drug seems to increase the negative charge of the blend (Table 6.3). A different phenomenon was observed with $PSDL_{10}$, where not significant change was observed in the charges generated whether $PSDL_{10}$ was alone or in a formulation (Table 6.3). $PSDL_{10}$ was the least crystalline carrier and acquired the least charge, on the other hand, more crystalline particles gained more charges. i.e. were more susceptible to exchange charges which could be attributed to a higher difference in work function between Lactohale, $PSDL_{30}$ and the container.

$PSDL_{30}$ was positively charged when on its own but acquired even more negative charge when in a powder formulation irrespective of the drug SS, FP or BDP (Table 6.3). It is interesting to note that $PSDL_{30}$ with SS blend was the most negatively charged (Table 6.3). This was also reflected in the amount of SS recovered from the walls in $PSDL_{30}$ formulation (Table 6.4). Although $PSDL_{30}$ acquired charge, the amount of drug recovered off the wall for $PSDL_{30}$-SS formulation was only 9% of the blend. Spherical particles have less contact area with adhering surface compared to elongated particles. Lactohale is tomahawk shape and is elongated, therefore it is expected to adhere more in comparison to spherical particles such as PSDL. The data showed that different grades of lactose exhibit different charging behaviours either alone or with different drugs in formulations. Staniforth et al. (1982) showed that contact electrification can be used to develop charges on the surfaces of drug and excipients particles. Such charges can be optimised to render more stable mixes and reduce the tendency of powder

blends to segregate. It is interesting to note that the results obtained in this study showed that $PSDL_{10}$ appeared to have less variation in the charging behaviour of the powder blend, which indicates that the morphological features of $PSDL_{10}$ could potentially be beneficial in DPI formulations as an antistatic effect was observed with this type of carrier and a more stable mix was observed. Anti-static agents can work by reducing the friction between particles or increase the conduction of particle surfaces.

Therefore, it is possible to select carefully components so that the DPI formulation is not prone to high charging.

6.3.5 Assessment of deaggregation of drug particles by measuring drug amounts recovered from the wall of the shaker

Table 6.5. The average drug content of SS, FP and BDP recovered from the wall of the stainless-steel shaker after tribo-charging measurements (n=3)

Formulation	Amount (µg)	SD	% Recovery ± SD
SS-L	1051.31	13.86	71.9 ±0.95
SS-PSDL30	135.21	1.27	9.26 ±0.09
SS-PSDL10	28.56	0.43	1.96 ± 0.03
BDP-L	11.9	2.06	0.8± 0.14
BDP-PSDL30	1.95	0.26	0.13±0.01
BDP-PSDL10	24.93	0.42	1.71 ±0.02
FP-L	8.83	2.94	0.6± 0.2
FP-PSDL30	0.81	0.06	0.05 ±0.0
FP-PSDL10	57.08	0.1	3.9 ±0.0

A strong correlation was found in the present work as Lactohale-SS with high level of net charge required longer mixing time to achieve a good drug content uniformity due to segregation (Supuk et al., 2011), (as shown from %CV within SS-L DPI formulation). This also correlated to the amount adhered to the surface of the stainless-steel container which showed that 71% was adhered to the wall of the stainless-steel shaker (Table 6.5).

Table 6.4 shows the different amounts of drug recovered from the walls of the shaking container after tribo-electrification for all DPI formulation, using HPLC. The results showed a high amount of SS drug was recovered after shaking the formulation containing SS and Lactohale with an average value of 1051.3 ± 13.86 µg corresponding to almost 72% of SS recovered from the wall of the shaker. However, the SS amount recovered when shaking with the $PSDL_{30}$ formulation was significantly lower ($p<0.05$) with an average value of 135.2 ±1.27 µg and even lower ($p<0.05$) for $PSDL_{10}$ formulation with an average of 28.56 ±0.43 µg. $PSDL_{10}$ has a spherical shape and is the least crystalline and exhibited less variations in its charging behaviours, also the amount of SS found on the walls when formulated with PSDL10 was only less than 2% (Table 6.5). This data confirms the tribo-electrification results suggesting that SS de-mixes rapidly in Lactohale formulation, this was also observed in the drug content uniformity results (Tables 6.1 and 6.2). In comparison, the average BDP content recovered from the walls was the lowest with the $PSDL_{30}$ formulation which was 1.95 ±0.26 µg. The same trend was perpetuated with FP (Table 6.4). BDP and FP are both hydrophobic drugs and the impact of the carrier has less effect, this is also shown from the drug content uniformity data (Table 6.1 and Table 6.2). The drug particles found adhered to the wall of the shaker could be either the drug alone or the drug attached to the carrier. In the case of Lactohale, it is more likely that large portion of the drug could adhere alone to the shaker given its tendency to de-mixing. From the drug content uniformity data (Table 6.1), it was observed that

de-mixing is easily occurring with SS, on the other hand, Lactohale is crystalline, highly charged and is prone to adhere to the wall of the shaker. From Table 6.4, the high recovery of the drug from the wall of the container may suggest that high amount of the drug and high amount of the carrier are adhering to the wall, not as a blend but separated from each other.

The drug amounts found on the shaker wall are drug particles that remained attached to the surface of the lactose monohydrate carrier particles, in comparison to PSDL carriers which possess crevices on the surface in which the drug particles can embed within, as well as a lower ability for PSDL on its own to adhere to the walls which in turn reduces the amount of drug left within the shaker after inducing to the motion.

This results from the difference in the surface morphologies and different degrees of crystallinities of the carriers. The surface of Lactohale is smooth whereas both $PSDL_{10}$ and $PSDL_{30}$ are rough (Fig 6.4, 6.5 and 6.6). When comparing Lactohale to PSDL particles, the irregularities present on the surface of PSDL particles allow a higher adhesion between drug and carrier particles as the drug particles got trapped in the crevices of the PSDL surfaces, resulting in a poor drug detachment from the PSDL carrier, as shown in Table 6.5 with the lower amounts of drugs recovered from the PSDL formulations, especially $PSDL_{30}$ which has the roughest surface texture. Lactohale showed a better SS drug release from the carrier due to its smooth surface. Ganderton's data (1992) supports this result, as he showed that reducing the roughness of particles allowed more drug deposition in the lower stages of the lungs. This result is in line with the drug content uniformity results of Lactose-SS formulation which showed that SS was prone to segregation with increasing the mixing time (Table 6.1). A homogeneous mix was rapidly achieved with SS, prolonging the mixing time had a negative impact on the homogeneity of the blend suggesting that there is a weak adhesion between SS and Lactohale particles.

The difference in the degree of crystallinity between all carriers played an important role in the different amounts of SS, FP and BDP being recovered from the formulations. Lactohale is the most crystalline and $PSDL_{10}$ is more crystalline than $PSDL_{30}$ (Figures 6.8, 6.10, 6.11), implying that both PSDL carrier particles have more amorphous contents than Lactohale. Amorphous materials have higher surface energies which facilitate the adhesion between drug and carriers but also prevents the detachment of the drug from the carrier (Saint-Lorant et al., 2006). This justifies the low amounts of drugs retrieved from PSDL formulations. This finding is supported by Saint Lorant et al.'s study (2007) which showed that Lactopress SD 250 which was more amorphous than Pearlitol 100 SD, showed a poor drug deposition compared to Pearlitol 100 SD.

The difference in the physicochemical properties of SS, FP and BDP also contributed to the differences seen in the blend uniformities. From the literature, SS and Lactose are known to be hydrophilic (Harjunen et al., 2003; Berard et al., 2002) whereas FP and BDP are more hydrophobic (Harjunen et al., 2003; Zeng et al., 2000). From the results in Table 6.5, it can be seen that the content uniformity for both FP and BDP were found to be less than that of SS this suggesting that both FP and BDP drug particles were adhering strongly to the carriers. This is in line with the drug content uniformity results which showed that of all three APIs, FP was the least affected by the mixing time as the %CV varied less with the mixing time (Table 6.1 and 6.2), followed by BDP. Both these drugs are hydrophobic and showed a different degree of adhesion to the carrier compared to SS.

The data with BDP and FP were found to be conflicting with the results obtained with SS regarding tribo-charging, drug content uniformity and deposition performance. SS is a hydrophilic drug whereas BDP and FP are hydrophobic. The extend of de-agglomeration of the drug depends on the drug's physicochemical properties (such as hydrophobicity) thus, a direct comparison between hydrophilic and hydrophobic drugs cannot be possible. The

literature showed that the cohesion-adhesion balance (CAB) of Fluticasone with α-lactose monohydrate is 0.22 (Jones et al., 2008; Hooton et al., 2006). It would be expected to have different CAB values depending on the drug used with α-lactose monohydrate. The CAB-value of FP was an indication of a great adhesion to Lactose.

The coarse crystalline Lactohale carrier may have cause higher press-on forces, due to higher contact area, than PSDL spherical particles, leading to a stronger adhesion between BDP and FP with Lactohale than with spherical particles. Spherical particles would therefore exert less press-on forces than elongated particles.

Both BDP and FP have high CAB-values, they tend to adhere strongly to the carrier. Additionally, the drug is more likely to be entrapped in the cavities or valleys of $PSDL_{30}$ surface, hindering drug detachment. The difference in deposition between $PSDL_{30}$ and $PSDL_{10}$ is attributed to the difference in their surface topography. $PSDL_{30}$ is rough and present cavities and valleys on its surface where the drug particles are likely to be entrapped, reducing drug detachment.

$PSDL_{10}$ presented nanoscale surface irregularities. This nanoscale topography may be favourable as it provides sufficient adhesion for the drug to the carrier, ensuring a uniform mix but also facilitates drug detachment upon inhalation as shown by the high FPD (Tables 6.7 and 6.8)

6.3.6 Deposition data obtained from Andersen Cascade impactor:

Table 6.6. In vitro deposition results of SS with Lactohale, $PSDL_{10}$ and $PSDL_{30}$ carriers at 2L and 4L.

SS formulations						
	LACTOHALE		PSDL_30		PSDL_10	
	2L	4L	2L	4L	2L	4 L
Deposition location						
Mouthpiece (MP)	3.18 (0.24)	2.51 (0.36)	5.19 (0.81)	5.22 (0.29)	8.52 (1.65)	16.49 (2.56)
Induction Port (IP)	43.54 (0.46)	41.64 (2.71)	50.01 (1.32)	44.29 (2.90)	132.82 (3.26)	94.77 (2.69)
Pre-separator (PS)	99.21 (5.88)	95.29 (6.44)	168.19 (4.01)	165.96 (3.24)	101.68 (4.08)	136.35 (5.91)
Large Particle Mass (LPM)= (MP+IP+PS)	145.93	139.77	223.39	215.47	243.02	247.61
S-2A	6.17 (0.43)	8.03 (0.89)	7.33 (0.63)	9.32 (0.89)	5.12 (0.62)	8.26 (2.28)
S-1A	3.17 (0.18)	4.96 (0.27)	3.41 (0.99)	3.52 (0.93)	2.32 (0.25)	2.43 (2.65)
S-0	5.37 (0.18)	7.44 (0.27)	4.49 (0.92)	4.24 (0.86)	5.76 (0.45)	3.21 (1.72)
S1	16.35 (0.68)	13.31 (1.22)	12.39 (2.43)	12.53 (2.85)	10.17 (0.46)	14.63 (1.54)
S2	25.50 (0.50)	27.30 (1.41)	17.80 (1.96)	20.11 (4.63)	10.77 (0.05)	15.79 (0.18)
S3	57.76 (1.14)	58.54 (1.47)	36.26 (1.30)	43.70 (3.49)	23.49 (0.18)	28.23 (2.37)
S4	30.59 (1.90)	31.53 (1.91)	14.12 (0.74)	17.19 (3.79)	9.62 (1.00)	11.74 (1.38)
S5	4.85 (0.34)	5.17 (0.81)	1.49 (0.01)	1.75 (0.36)	1.16 (0.10)	3.99 (2.67)
Filter	12.95 (1.09)	9.57 (1.93)	0.74 (0.29)	0.70 (0.34)	0.55 (0.54)	1.79 (1.52)
Fine Particle Dose (FPD)	150.18 (3.78)	156.78 (2.62)	84.02 (2.00)	100.21 (1.61)	61.53 (1.2)	79.48 (1.4)
Extrafine Particle Dose (EFPD) (S4+S5+filter)	102.69	104.82	49.85	63.34	34.82 (0.8)	45.84 (0.7)
Fine Particle Fraction (FPF)	49.11 (2.45)	50.70 (3.05)	26.68 (1.40)	30.50 (2.52)	19.72 (1.4)	23.53 (1.1)
MMAD (um)	1.57 (0.06)	1.60 (0.00)	1.97 (0.06)	1.90 (0.00)	2.1 (0.1)	2.0 (0.1)
GSD	2.30 (0.10)	2.27 (0.06)	2.40 (0.10)	2.47 (0.06)	2.4 (0.0)	2.4 (0.0)
RA caps	10.22 (0.60)	8.22 (2.05)	1.9 (0.45)	1.25 (0.33)	18.66 (2.31)	10.85 (2.01)
RA dev	47.81 (3.72)	44.09 (2.21)	44.6 (2.61)	33.75 (2.24)	34.21 (1.36)	33.67 (1.17)
TRA	58.03	52.31	46.5	35	52.87	44.52
TED	308.66 (3.47)	309.22 (2.97)	321.43 (3.39)	328.52 (3.27)	312.00 (4.7)	337.04 (3.5)
TRD	366.68 (2.98)	361.53 (3.09)	367.98 (2.33)	363.51 (2.67)	364.87 (2.9)	382.31 (3.3)

Table 6.7. In vitro deposition results of FP with Lactohale, $PSDL_{10}$ and $PSDL_{30}$ at 2L and 4L.

FP formulations						
	LACTOHALE		PSDL_30		PSDL_10	
	2L	4L	2L	4L	2L	4L
Deposition location						
Mouthpiece (MP)	6.57 (0.31)	6.75 (0.78)	17.54 (2.29)	17.87 (0.97)	12.27 (0.78)	17.02 (0.48)
Induction Port (IP)	112.37 (7.61)	90.24 (3.49)	118.19 (3.79)	120.89 (4.74)	116.21 (3.36)	84.49 (2.28)
Pre-separator (PS)	129.10 (4.98)	146.89 (5.77)	117.90 (1.65)	109.19 (6.98)	95.37 (4.54)	125.12 (3.62)
Large Particle Mass (LPM)= (MP+IP+PS)	248.04	243.87	253.63	247.95	223.85	226.63
S-2A	8.79 (0.97)	8.52 (0.51)	6.81 (0,85)	9.32 (0.89)	7.66 (1.32)	8.82 (1.25)
S-1A	3.87 (0.38)	4.54 (0.37)	1.92 (0.21)	3.52 (0.93)	2.98 (0.98)	3.51 (1.12)
S-0	7.54 (0.59)	7.83 (0.39)	2.80 (0.25)	4.24 (0.86)	3.91 (1.45)	4.28 (1.62)
S1	17.43 (0.94)	16.86 (2.94)	7.08 (0.57)	12.53 (2.85)	8.01 (0.21)	16.19 (1.01)
S2	13.56 (0.88)	15.39 (1.43)	10.26 (0.75)	20.11 (1.63)	11.15 (0.20)	11.75 (0.24)
S3	22.19 (1.17)	23.40 (1.45)	23.90 (0.44)	43.70 (2.49)	28.31 (0.48)	29.66 (0.68)
S4	7.21 (0.21)	8.41 (1.14)	12.35 (0.44)	17.19 (1.79)	17.36 (1.01)	19.46 (1.69)
S5	1.28 (0.14)	1.12 (0.08)	1.78 (0.10)	1.75 (0.36)	2.90 (2.12)	2.31 (0.45)
Filter	0.94 (0.06)	2.46 (0.36)	1.14 (0.09)	0.70 (0.34)	1.89 (1.63)	0.95 (0.08)
Fine Particle Dose (FPD)	70.17 (2.79)	75.49 (2.90)	57.14 (2.21)	63.47 (1.82)	73.54 (1.2)	84.61 (1.3)
Extrafine Particle Dose (EFPD) (S4+S5+filter)	31.63	35.4	37.4	42.5	50.46 (0.7)	52.38 (0.62)
Fine Particle Fraction (FPF)	21.20 (0.56)	22.71 (1.61)	18.79 (0.50)	20.71 (0.13)	23.87 (0.8)	26.15 (1.2)
MMAD (um)	2.87 (0.12)	2.67 (0.06)	1.80 (0.00)	1.80 (0.00)	2.3 (0.1)	2.3 (0.12)
GSD	2.00 (0.00)	2.17(0.06)	2.77 (0.12)	2.93 (0.06)	2.4 (0.00)	2.5 (0.00)
RA caps	18.15 (3.15)	26.39 (2.43)	14.96 (0.28)	14.61 (1.80)	17.30 (1.29)	14.49 (2.89)
RA dev	35.47 (2.27)	33.39 (1.44)	47.29 (3.14)	44.24 (4.80)	49.08 (3.18)	11.89 (2.76)
TRA	53.62	59.78	62.25	58.85	66.38	26.38
TED	330.88 (3.64)	332.43 (2.52)	321.67 (2.01)	324.36 (1.76)	308.04 (2.1)	323.57 (2.3)
TRD	384.51 (4.87)	392.21 (3.79)	383.92 (3.32)	383.22 (2.17)	374.43 (2.2)	349.95 (2.3)

Table 6.8. In vitro deposition results of BDP with Lactohale, $PSDL_{10}$ and $PSDL_{30}$ at 2L and 4L.

BDP formulations						
	LACTOHALE		PSDL_30		PSDL_10	
	2L	4L	2L	4L	2L	4L
Deposition location						
Mouthpiece (MP)	9.36 (0.49)	12.90 (2.61)	4.64 (0.64)	6.49 (0.41)	17.36 (0.03)	17.74 (0.52)
Induction Port (IP)	92.78 (0.56)	53.41 (6.04)	98.12 (1.85)	100.85 (0.26)	131.95 (2.50)	96.53 (2.64)
Pre-separator (PS)	94.34 (5.26)	132.78 (7.06)	129.24 (1.51)	132.65 (5.51)	88.91 (2.84)	133.26 (3.92)
Large Particle Mass (LPM)= (MP+IP+PS)	196.48	199.09	232.00	239.9	238.22	247.53
S-2A	6.50 (1.21)	4.59 (1.28)	5.10 (0.20)	5.33 (0.28)	6.37 (0.97)	9.89 (0.87)
S-1A	2.94 (0.26)	3.93 (0.46)	2.67 (0.36)	2.97 (0.30)	2.89 (2.14)	3.99 (1.97)
S-0	4.48 (0.17)	2.67 (0.13)	5.25 (0.34)	6.28 (0.31)	4.23 (1.58)	5.06 (1.20)
S1	11.86 (0.52)	12.60 (0.54)	13.34 (1.37)	14.69 (0.34)	10.34 (0.64)	15.81 (0.16)
S2	12.79 (0.23)	13.65 (0.43)	9.56 (0.93)	11.30 (0.45)	13.26 (0.33)	14.35 (0.30)
S3	19.18 (2.50)	20.09 (1.27)	10.99 (1.81)	13.99 (0.47)	24.68 (1.46)	26.26 (0.75)
S4	5.52 (0.30)	6.57 (0.61)	3.74 (0.42)	4.01 (0.31)	8.44 (3.25)	13.59 (2.98)
S5	0.98 (0.48)	0.63 (0.04)	0.33 (0.06)	0.35 (0.08)	0.19 (2.40)	1.35 (2.90)
Filter	9.86 (0.53)	13.43 (2.71)	11.66 (2.41)	8.77 (1.00)	0.03 (3.98)	1.27 (3.69)
Fine Particle Dose (FPD)	61.08 (4.05)	69.66 (2.60)	54.90 (3.02)	59.38 (5.90)	61.18 (1.4)	77.58 (1.20)
Extrafine Particle Dose (EFPD) (S4+S5+filter)	33.5	40.73	26.73	27.11	33.35 (0.7)	42.38 (0.80)
Fine Particle Fraction (FPF)	23.39 (0.94)	25.12 (1.05)	18.63 (1.41)	19.29 (0.47)	19.82 (1.1)	22.77 (1.40)
MMAD (um)	2.23 (0.12)	1.93 (0.06)	2.70 (0.10)	2.67 (0.06)	1.7 (0.1)	2.3 (0.10)
GSD	2.37 (0.06)	2.27 (0.25)	1.93(0.00)	1.90 (0.02)	2.9 (0.00)	2.70 (0.90)
RA caps	25.23 (2.70)	15.29 (0.79)	18.24 (1.91)	29.44 (1.49)	8.03 (0.41)	15.04 (2.02)
RA dev	44.34 (1.24)	36.34 (2.44)	40.31 (1.25)	50.88 (2.39)	58.99 (2.79)	9.09 (3.56)
TRA	69.57	51.63	58.55	80.32	67.03 (0.7)	23.98 (0.90)
TED	270.32 (2.72)	277.27 (1.56)	294.67 (2.58)	307.69 (2.29)	308.66 (2.5)	340.72 (2.70)
TRD	340.16 (2.14)	328.89 (2.37)	353.22 (3.10)	388.02 (2.45)	375.69 (2.3)	364.70 (2.10)

Impact of inhaled volume on the aerodynamic dose emission characteristics

The effects of changing lactose carriers on aerodynamic characteristics for BDP, FP and SS are shown in Tables 6.6, 6.7 and 6.8 respectively.

Tables 6.6, 6.7 and 6.8 summarise the parameters used to calculate the deposition profiles of SS, BDP and FP in an Andersen Cascade Impactor at 2 L and 4 L. Table 6.6 showed that TED for SS varied between 308.66 ± 3.47 to 337.04 ± 3.3 µg, similarly for FP (Table 6.7) where the TED varied between 308.04 ± 2.1 to 332.43 ± 2.52 µg. Finally, TED for BDP (Table 6.8)

varied between 201.88 ± 2.58 to 340.72 ± 2.70 µg. The extent of variation in dose emission was dependent on the active ingredient, the type of carrier and inhaled volume.

In most cases, TED showed an increase with increasing Vin from 2 L to 4 L. For capsule-based DPIs it is recommended to make two separate inhalations for emptying the capsule from each dose, as one inhalation may not be sufficient to fully empty the capsule, especially for patients with low lung capacity as these patients are not capable of prolonging their inhalation time (Laube et al., 2011). This study showed that dose emission increased by increasing the Vin from 2 L to 4 L (Tables 6.6, 6.7 and 6.8)

The TED significantly increased with Vin whilst the TRA, which was calculated as the sum of the amounts left in the capsule and device, decreased with increasing Vin from 2 L to 4 L. It is interesting to note that the amount left in the capsule was generally much lower than that of the device (Tables 6.6, 6.7 and 6.8). The shape of the inhaler device might account for the high residual amount left in the device as Onbrez BreezHaler® has a long inhalation channel (Figure 2.4), which is the distance from the capsule chamber to the end of the mouthpiece. Once the capsule is emptied, the particles are more likely to adhere to the walls of the inhaler device before reaching the patient's mouth.

The FPD, i.e. particles having an aerodynamic diameter less than 5µm, significantly increased with increasing Vin from 2 L to 4 L (Tables 6.6, 6.7 and 6.8). A similar observation was noted with EFPD, i.e. particles having size less than 2 µm. Because TED increased with the Vin, it was expected that a greater portion of that emitted dose would have reached the distal stages of the impactor as shown in Tables 6.6, 6.7 and 6.8. Therefore, increasing the Vin would be beneficial for capsule-based devices, such as BreezHaler®. Not all patients can achieve a high Vin due to the restriction in their lung capacity, in such circumstances they should inhale twice from the same dose to ensure capsule emptying (Abadelah et al., 2017).

Impact of the carrier on the aerodynamics dose emission characteristics

This part of the work aimed to study the physicochemical characteristics that influence the interactions between the drug and carrier particles and their effect on drug dispersion and deposition. In this study, SS, FP and BDP were blended with either Lactohale or PSDL carriers. Drug deposition analysis was based on the influence of the operating conditions (e.g. mixing time, triboelectric forces), the morphological features of the carriers (shape, surface texture), the properties of the drugs (degree of hydrophobicity) and inhalation manoeuver parameter (inhalation volume).

When developing DPI formulations, it is important to take into consideration two types of inter-particulate interactions: drug-drug cohesive forces and drug-carrier adhesive forces (Peng et al., 2016). The performance of DPIs is fundamentally influenced by the drug-carrier adhesive forces since high drug adhesion to the carrier limits drug detachment during aerosolisation, thus decrease drug dispersion (Zellnitz et al., 2013). The carrier is the major component in DPI formulations and it is critical to design a carrier with desired morphological features to provide sufficient adhesion with drug particles to form a stable mix with good drug content uniformity but also to allow drug detachment from its surface during the inhalation manoeuver. For these reasons, we designed two lactose carriers ($PSDL_{30}$ and $PSDL_{10}$), both spherical in shape but with different surface roughness. $PSDL_{30}$ has a rougher surface than $PSDL_{10}$ (as explained in section 6.3.1).

Blades and knives in blenders help in introducing more shear force to break up agglomerates. Particles which have some projections and surface roughness are usually sharper than smooth surfaces and may help de-agglomerating cohesive powders (hydrophobic drug are cohesive and tend to agglomerate more). For cohesive powders, high shear mixing technology is

advised, scientists focus on the nature of the mixer (high shear mixer or low shear blender) but it is also important to take into account the properties of the particles.

Inter-particles interactions are very important in DPI formulations as they govern drug dispersion from carrier particles to allow drug deposition in the lungs. The interactions are dependent on the physicochemical properties of all components in the DPI formulation. The manufacturing process is also a critical step as the blend homogeneity is important when considering the quality of the formulation (FDA, 1998).

Capsule-based DPIs are generally limited by adhesion of the powder in the capsule and the device, which usually result in lower doses of the drug emitted (Vidgren et al., 1988).

For the first determination with BDP, LPM was almost 50% of the total nominal dose, depositing in the MP, IP and PS. This observation is consistent with Mohamad et al. (2012) and Abadalah et al. (2017). The LPM remained almost equal or higher than 50% of the nominal dose irrespective of the Vin, as both volumes used in this work were higher than ACI's internal dead volume (1.155 L), 2 L and 4 L Vins used in this work provided sufficient inhalation time for the aerosol to pass through the entire ACI system.

Both MP and PS showed no trend with increasing Vin irrespective of the carrier and drugs used for all DPI formulations, whereas the amount of the IP generally showed a significant decrease with increasing Vin.

35 to 63 % of the nominal dose was deposited as LPM. The lowest value was observed with Lactohale-SS formulation at a Vin of 4 L and the highest was observed for PSDL30-FP formulation at 2 L Vin. Up to 50% of the nominal dose was observed with ACI in several reports (Mohamad et al., 2012; Abadelah et al., 2017)

The emission of drug particles from the capsule and the device at 4 L were significantly improved when using $PSDL_{10}$ as a carrier as opposed to using Lactohale particles (Tables 6.6, 6.7, 6.8). The $PSDL_{10}$ particles were most effective at emitting the drug particles probably

because of their high surface area, which is expected for rough particles. This finding is in line with a study of Kawashima et al. 1998, who found that lactose particles with higher surface area achieved a higher drug emission and consequently less drug was found in the device and capsule (Kawashima et al., 1998a). Additionally, irrespective of the drug used, the total residual amount (in capsule + device) significantly ($P<0.05$) decreased at 4 L when using $PSDL_{10}$. For this type of device, a deep and prolonged inhalation contributed to a reduction in the TRA.

The inhalation volumes used in this study exceed the internal dead volume of the ACI, which is 1.155 L, to allow sufficient sampling time for the aerosol bolus transfer from the Breezhaler® device to the lowest stages of the ACI. The ACI data shows the importance of the inhalation volume on the aerodynamic characteristics of SS, FP and BDP emitted doses (Tables 6.6, 6.7, 6.8).

There was an opposite trend observed between hydrophilic drugs and hydrophobic drugs. This trend corroborates with the drug content uniformity results (Tables 6.1 and 6.2) and the drug amounts recovered from the walls of the shaker after the tribo-electrification measurements (Table 6.5) where high amounts of SS were recovered from the wall of the container with the SS formulation with Lactohale as opposed to SS-$PSDL_{10}$ and SS-$PSDL_{30}$. The drug content uniformity data showed that SS was prone to segregate from Lactohale with higher mixing times, i.e. more drug is detached from the smooth Lactohale carrier and available for deposition.

In contrast, FP which was strongly adhered to the carrier (Table 6.4) was then allowed to be released from the PSDL carrier when a longer sampling time was generated. The rough surface of PSDL allowed a good blend homogeneity, and allowed hydrophobic drug particles to detach from the carrier surface and deposit in the lower stages of the impactor at higher Vin.

6.4 Conclusion

In this chapter, we discussed a new crystallisation technique from solid state to produce hollow spherical particles with defined surface texture. This crystallisation technique can be used to repair crystal defects and restore the crystallinity to form stable crystalline powder. Furthermore, the final particle size and shape of the particle can greatly depend on the plasto-elasticity of the material composing the particle. Lactose carriers used in this study were characterised in terms of their physicochemical properties, morphological features and aerodynamic properties. Lactohale, $PSDL_{10}$ and $PSDL_{30}$ contrasted in their characteristics: carrier shape (tomahawk/spherical), surface texture (smooth/rough), surface net charges and polarities (positively and negatively charged) and degrees of crystallinity.

In general, the results showed that the content uniformity is affected by the mixing time and is different for each type of drug and each carrier. This study made it possible to demonstrate that surface modification (surface roughness) of the carrier particles through solid phase crystallisation resulted in a dissimilar charging behaviour of the carriers during the mixing of the formulation as opposed to Lactohale. The carrier particles with less roughness charged significantly higher. This was attributed to the difference in contact area between drug and carrier particles as well as particles and the container wall.

Despite Lactohale and PSDL's respective formulations presenting good content uniformity, Lactohale may be considered as the most favourable carrier when used with hydrophilic drugs such as SS as a good content uniformity was achieved with only 5 min of mixing and high doses of SS were emitted and deposited from Lactohale-SS formulation. The amount of drug quantified from the wall of the shaker from tribo-charging analysis with Lactohale-SS formulation was a good indicator of the tendency for SS to segregate from the carrier easily, which was also confirmed by the result obtained with the increase of mixing time and the deposition data for SS-Lactohale formulations. The positive correlation between the different experiments undertaken in this study shows that there is a potential for tribo-electrification

study to be used as a screening tool for DPI formulations instead of using the Andersen Cascade impactor which would be beneficial for researchers as experiments with the ACI are more time consuming and expensive.

On the other hand, $PSDL_{10}$ was considered to be most favourable for hydrophobic drugs where its moderate rough surface was ideal for the drug to adhere to and obtain a stable mix with very good content uniformity irrespective of the mixing time, but the adhesion was weak enough to allow the drug to detach from the carrier during aerosolisation and deposit in the deepest stages of the impactor.

Further optimisation of the PSDL particles should be done and further in-vitro drug deposition studies should to be conducted with different combinations of drugs and different types of carriers in order to discover a better correlation between the tribo-electrification results and the dose emission experiments.

Such results would allow a better selection of carriers and drugs when formulating DPI products as successful carrier selection is crucial in controlling the dose uniformity and the reproducibility of DPIs.

Chapter 7

Study of the difference between two different formulations on the aerodynamic characteristics of emitted dose of salbutamol using patient inhalation profiles from Onbrez Breezhaler®

7.1 Introduction

DPIs are breath-actuated devices and the dose emission from such devices is dependent on different inspiratory parameters, namely maximum inspiratory flow (MIF), inhalation volume and acceleration rate (ACIM) at the start of the inhalation manoeuvre (Abadelah et al., 2017; Dal Negro, 2015; Olsson and Asking, 1994).

The patient inhalation manoeuvre parameters as well as the shape of inhalation profiles (IP) vary depending on the age of the patient, gender, body max index, the type and severity of the disease, as well as the lung geometry (Henry Chrystyn, 2009).These parameters account for the inter-patient variability, thus each patient would receive a different dose when inhaling through the same DPI inhaler device (Hickey et al., 1998; Pasquali et al., 2015; Buttini et al., 2016).

In order to measure the TED and FPD, standard pharmacopoeial methods are used (Council of Europe, 2014; United States Pharmacopeia, 2014). Humans are unable to replicate the square wave generated by a vacuum pump and most of the patients are not able to achieve the inhalation parameters recommended by the pharmacopoeia (Azouz et al., 2015). Recent methods developments by (Chrystyn et al., (2015) and Bagherisadeghi et al. (2017)) led to a method using a patient inhalation profile instead of the vacuum pump measure the TED.

Onbrez Breezhaler® is a low resistance device (0.017 $kPa^{0.5}$ L/min, Dal Negro, 2015) and a MIF of 107 L/min was required to achieve 4kPa pressure drop (Pavkov et al., 2010), patients inhaling through Breezhaler were able to achieve inspiratory parameters of MIF (88 L/min), Vin (2.7 L) and ACIM (5 L/s^2). The experimental set-up used in this study was similar to that used by Bagherisaghi et al., 2017. A mixing inlet was inserted between the pre-separator and the induction port, which allow a complementary air flow to be introduced through the side

arm of the mixing inlet (Figure 7.1). Therefore, the flow at the mouthpiece will be maintained at 0 L/min while keeping constant flow through the impactor (Experimental set-up in details, see Section 4.2.3). In DPI formulations, lactose monohydrate is the most commonly used carrier, several studies have shown that the aerodynamic characteristics and the surface morphology of the lactose particles used in the formulation can affect the overall dose emission from DPIs (Flament et al., 2004; Martin et al., 2012; Kaialy et al., 2012; Kawashima et al., 1998b; Peng et al., 2016; Pilcer et al., 2012; Zellnitz et al., 2015; Zhou et al., 2010). It was showed in the previous chapters that it was possible to engineer lactose carrier particles with or without generally recognised safe additives (GRAS) from spray dried lactose particles produced in-house and in the present chapter it was attempted to apply the same particle engineering technique but using commercially available spray dried lactose (Fisher Scientific Ltd, UK). The latter is commercially available and can be purchased in any batch size from lactose suppliers. Thus, by processing this lactose, a novel form of lactose may be obtained with improved surface morphological features different from the commercially available spray dried lactose and of any batch size. Our engineering technique as reported in the previous chapters (Chapter 4, Chapter 5 and Chapter 6) showed an improvement in the quality of lactose in terms of dose emission and crystallinity. These features are prerequisite for oral solid dosage forms whether, tablets, capsules, powder or dry powder inhalers. Engineered Spray Dried Lactose and Lactohale were separately formulated with SS using an order mix and proportion of lactose to drug. Drug content uniformity from each DPI formulation was assessed using %CV and deposition study was carried out *ex-vivo* using patient inhalation profiles generated *in-vivo*. Among 19 inhalation profiles, only those with the same Vin, ACIM but with different MIFs were selected so as to investigate the impact of the MIF alone on SS drug deposition *ex-vivo* from both DPI formulations containing Lactohale and Engineered spray dried lactose ($PSDL_{com}$) as carriers.

7.2 Material and method

7.2.1 Material

A list of materials and general laboratory apparatus used for the determination of salbutamol dose emission characteristics using *ex-vivo* technique was illustrated in chapter 3 (section 3.1).

7.2.2 Experimental Methods

7.2.2.1 Preparation of PDSL particles

The procedure for generating the PSDL particles used in this study was previously detailed in Chapter 4 (Section 4.2.3).

7.2.2.2 Blending lactose carrier particles with salbutamol sulphate

Salbutamol sulphate was mixed with the carrier particles using an order mix (See Section 4.2.8 for method)

7.2.2.3 Characterisation of particle shape and size using scanning electron microscopy (SEM)

See Chapter 4 (section 4.2.5)

7.2.2.4 Breath simulator with ACI method set-up

Figure 7.1 shows the experimental set-up of the breath simulator (BRS 3000) with ACI. The breath simulator warming profile was carried out (20 cycles) prior to the experiment run.The system warm- up procedure was recommended by the manufacturer (Copley et al., 2014).

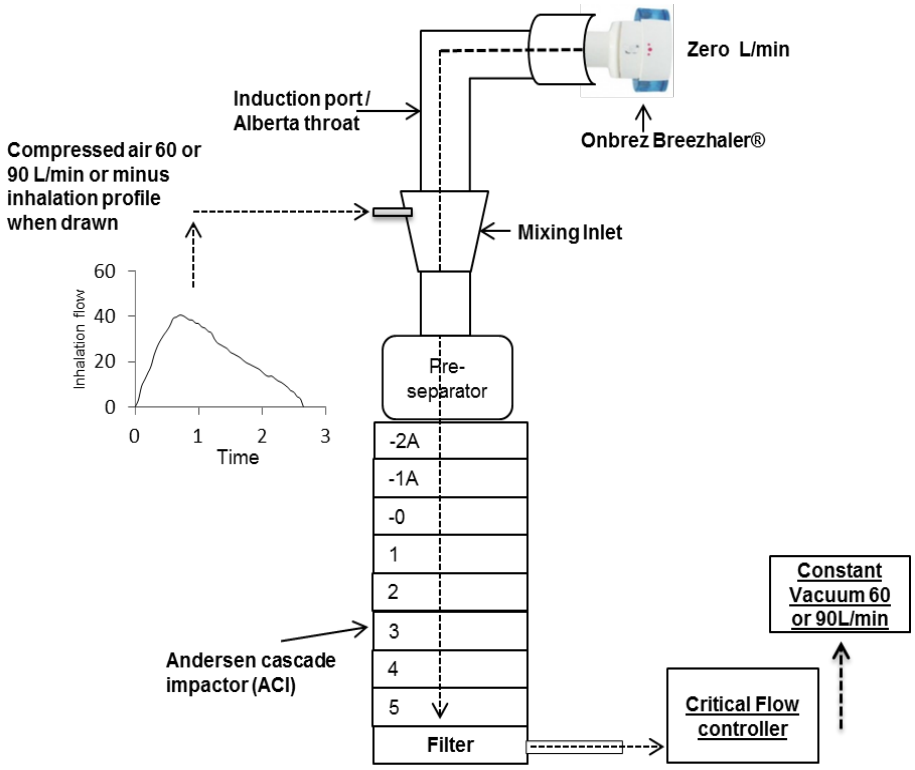

Figure 7.1 Schematic diagram of the methodology set-up (Adpated from Abadelah et al., 2017)

The ACI and the vacuum pump were connected via a critical flow controller (TPK 2000, Copley Scientific Ltd, UK). Then, the breath simulator attached to the impactor using the mixing inlet side arm (Figure 7.1). The additional air cylinder was joined to the breath simulator using a regulatory flow valve. The vacuum pump was allowed to reach flow stability prior to starting the experiment by leaving it on for 20 minutes before the first determination. The airflow through the ACI was set according to the inhalation profile chosen and the flow from the vacuum pump was set while the regulatory flow valve remained closed. The flow meter

(DFM 2000, Copley Scientific Ltd, UK) was used to gauge the flow through the impactor (flow stability P3/P2 ≤ 0.5). When the required flow was achieved, the regulatory valve was then opened to allow the entry of the supplementary air through the mixing inlet side arm. It was important to monitor the flow meter screen to ensure that the incoming supplementary air is equal to that introduced by the vacuum pump, and the flow at the mouthpiece is 0 L/min.

Then, the inhalation profiles were run using the breath simulator software. A constant flow rate was maintained through via the vacuum pump. For the inhalation profiles that are lower than 60 L/min, an operating flow rate of 60 L/min was used and a flow rate of 90 L/min was used for inhalation profiles beyond 60 L/min. ACI stages and collection plates were set-up depending on the flow rate (Discussed in Chapter 3- section 3.3).

The salbutamol sulphate dose emission was performed by using three capsules for each inhalation profile as recommended by the patient information leaflet (PIL) of the Onbrez Breezhaler® (Novartis Pharmaceuticals Ltd, UK) and to ensure the reproducibility of the dose emission. After the aerosolisation of the three capsules, the residual amount left in the capsules and device was assessed.

After aerosolising the dose and before starting the washing procedure, the mouthpiece and the mixing inlet side arm were sealed with parafilm to make sure that no drug loss occurred during while disassembling the set-up.

The washing solution was methanol:water 70:30 % (v/v). Appropriate volumes were used to wash and recover the drug from each part of the set-up: the mouthpiece, the throat, the pre-separator, the ACI stages, the capsule, the device and the filter. The recovered samples were then sonicated for 15 minutes to facilitate drug particle solubility. Finally, all samples were transferred and sealed into 2 mL HPLC amber vials by using a plastic syringe and 0.45 filter tips (Thermo Scientific Ltd, UK). The salbutamol sulphate amounts in each sample were then

quantified using a validated HPLC method (HPLC method validation discussed in Chapter 3 – Section 4).

7.2.2.5 Data analysis

The aerodynamic dose emission parameters were calculated using the Copley Inhaler Data Analysis Software (CITDAS version 2.0, Copley Scientific, UK)

The total emitted dose (TED) was obtained by adding up the amounts of SS collected on the mouthpiece adapter, Alberta-idealised throat, mixing inlet, pre-separator, all the stages of the ACI and finally the filter. The fine particle dose (FPD) was the mass of drug with an aerodynamic particle diameter less than 5 μm, the extra-fine particle dose (EFPD) was the mass of drug with an aerodynamic particle diameter less than 3 μm. The fine particle fraction (FPF) was calculated as a percentage of the FPD divided by the TED. The mass median aerodynamic diameter (MMAD) was represented as the size corresponding to half of the sum of all the recovered amounts of drug deposited on the stages of the ACI.

A validated HPLC method for the determination of Salbutamol in recovered samples was explained in detail in Chapter 3 (Section 3.4). A one and two-way ANOVA were carried out to determine any significant differences in the FPD, TED, MMAD, EFPD. A p value of less than 0.05 ($p<0.05$) corresponded to a significant difference statistically.

7.3 Results and discussion

7.3.1 Characterisation by SEM

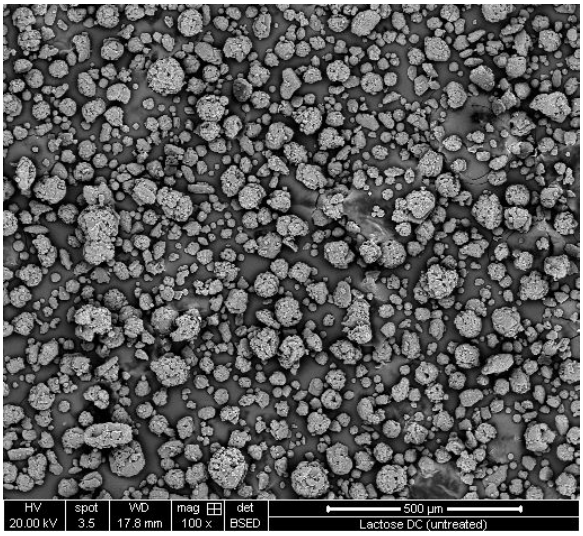

Fig. 7.2.1 General view spherical lactose

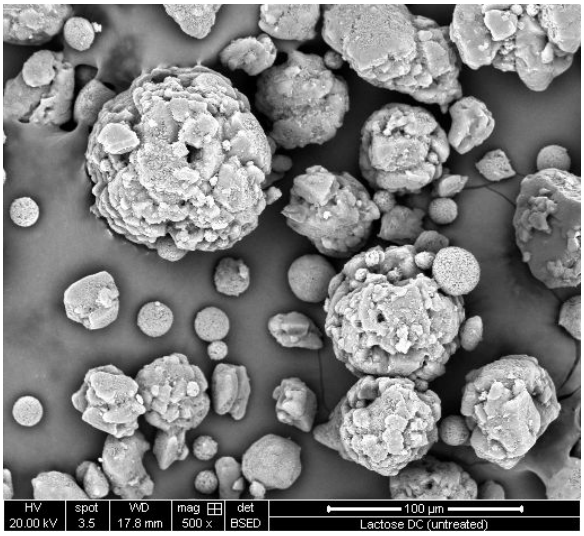

Fig. 7.2.2 General view spherical lactose

Fig. 7.2.3 Close view spherical lactose

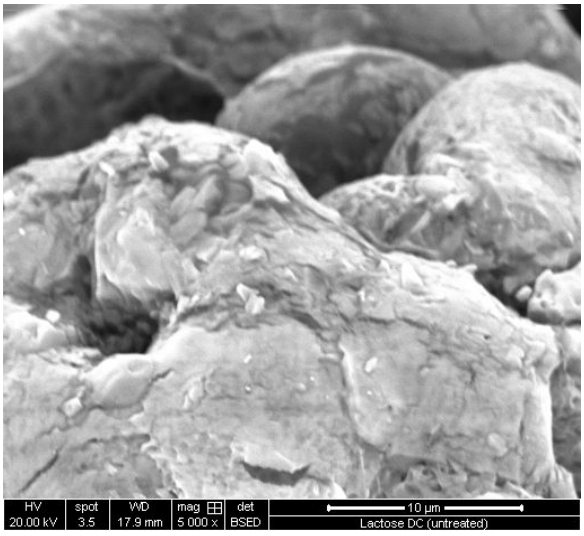

Fig.7.2.4 Surface of spherical lactose

Figure.7.2. SE images of lactose monohydrate particles

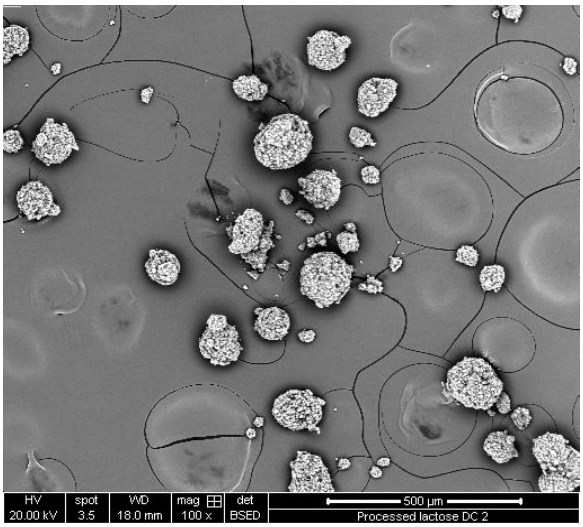

Fig. 7.3.1 General view PSDL

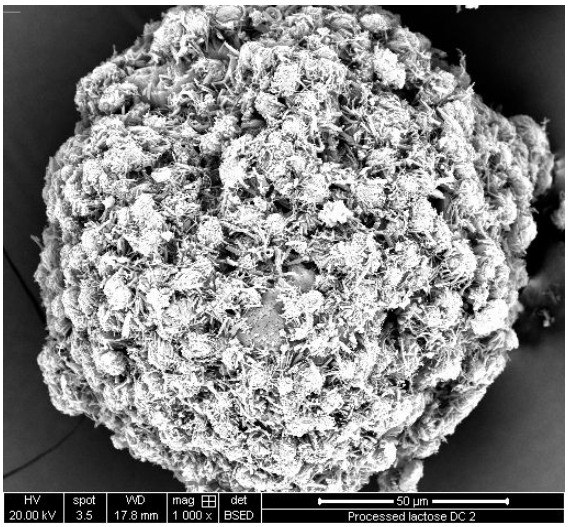

Fig. 7.3.2 General view PSDL

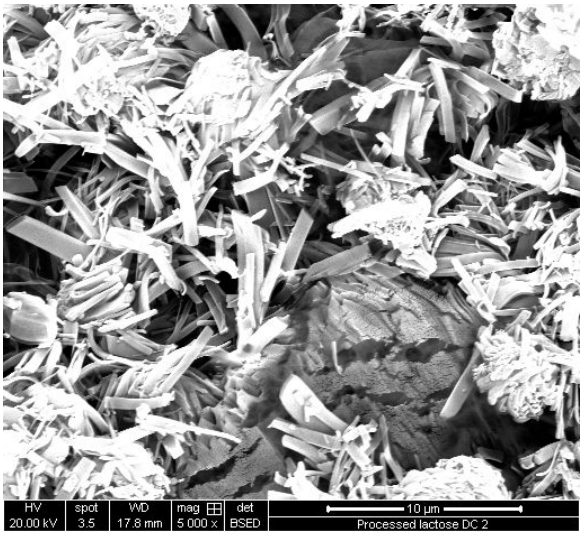

Fig. 7.3.3 Surface of PSDL

Figure. 7.3. SE images of PSDL particles

The mechanism of solid state crystallisation of Spray Dried Lactose particles was fully explained in the previous chapters (Chapter 4, Section 4.2.3) However, in this chapter we tried to expand our understanding on the reliability of our engineering technique using commercially available spray dried particles. In the previous chapters, we processed spray dried lactose produced from solution whereas in this current chapter we processed spray dried lactose produced from a suspension. By looking at the SE micrographs (Fig. 7.2.1 and 7.2.2), it is clear that the spherical spray dried lactose particles were produced by spray drying a lactose

suspension, the individual particles are glued together to form rough spherical particles (Figure 7.2.3). The manufacturer did not mention whether a binder was included in the suspending medium or not.

The SE micrographs displayed the morphological features of the original material (unprocessed commercial spherical lactose) and the processed spray dried lactose ($PSDL_{com}$). The images showed that the integrity of spherical particles was retained after processing the particles in hot ethanolic solution. By comparing Figure 7.2.1 before processing and Figure 7.3.1 after processing, the processing imparted to the particles new features making them rougher, as shown in Figure 7.3.2. The particles discussed in the previous chapter (Chapter 6, Figure 6.5 and 6.6) have a different surface texture compared to the present particles (Figure 7.3.2). The former particles were initially produced from a spray dried solution forming a continuous shell (Chapter 6, Figure 6.4) whilst, the latter was initially spray dried from a suspension and discontinuities are apparent between particles as shown in Figure 7.2.3. During processing in hot ethanol, the crystal growth was somehow taking place on each single particle as observed in Figure 7.3.2 and 7.3. 3. This is due to the discontinuity presents between particles, the growth of the crystal was not able to close the gap between the particles to propagate to the neighbouring particles. It seems like the particles were growing independently of each other and upwards (Fig. 7.3.3). Thus, providing a high surface roughness (Figures 7.3.2 and 7.3.3) compared to those particles processed from spray dried lactose solution (Chapter 6, Figures 6.5 and 6.6).

7.3.2 Aerodynamic dose emission characteristics using in-vivo method

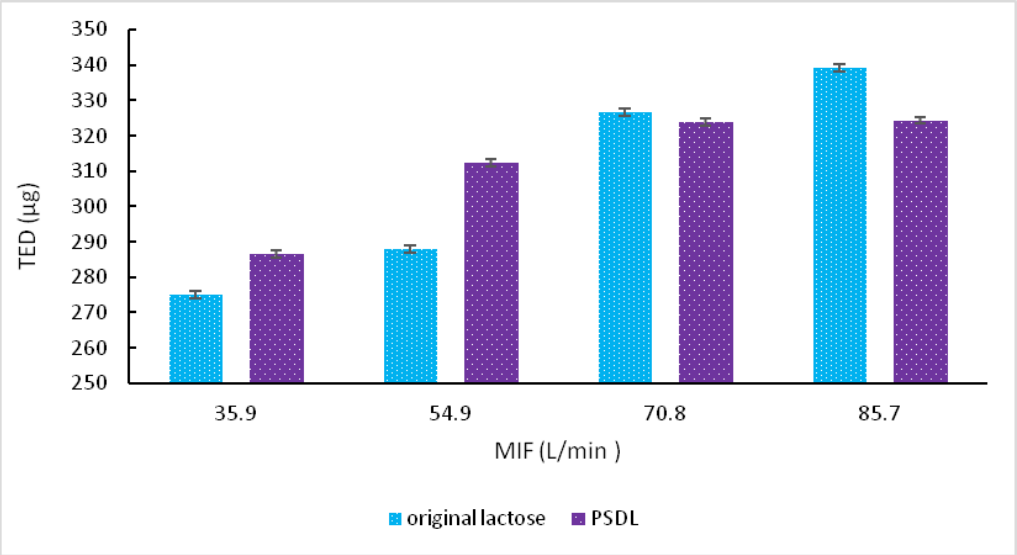

Figure 7.4. Total emitted dose of SS from Lactohale and PSDL formulations at different MIFs (L/min)

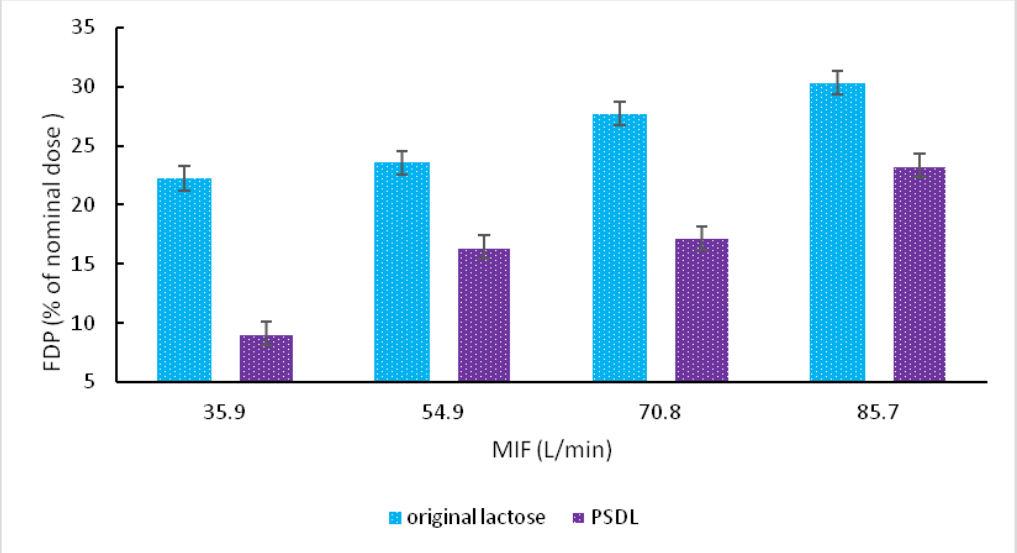

Figure. 7.5. Fine particle dose for both Lactohale and PSDL formulations at different MIFs (L/min)

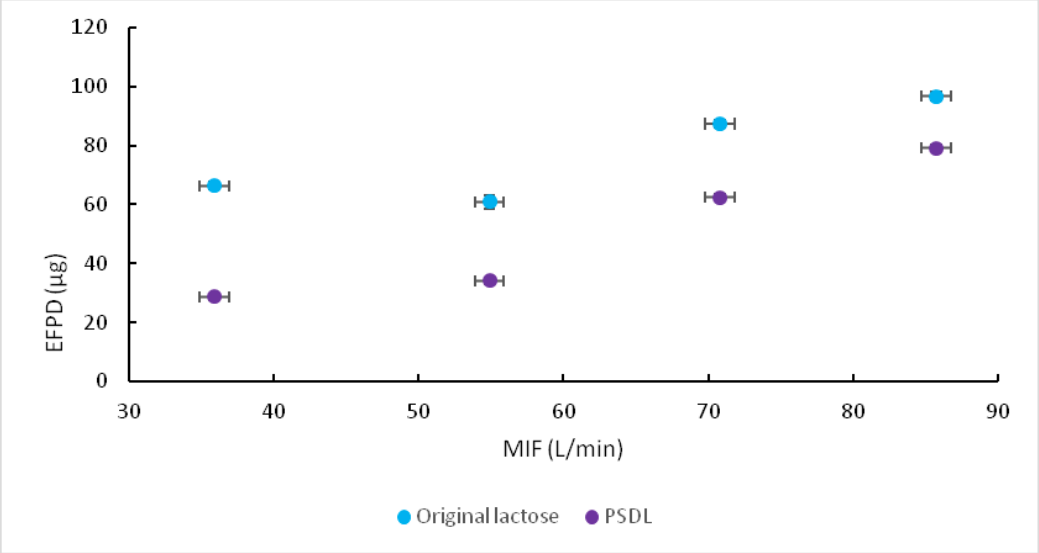

Figure. 7.6. EFPD for both Lactohale and PSDL formulations at different MIFs (L/min)

Table 7.1 Summary of SS deposition from Lactose-SS formulations at different MIF

	35.9L/min			54.9L/min			70.8L/min			85.7L/min	
	mean	SD		mean	SD		mean	SD		mean	SD
S-1	2.83	0.03	S-1	3.50	0.52	S-2A	6.53	0.78	S-2A	5.60	0.48
S-0	3.95	0.50	S-0	4.35	0.64	S-1A	2.24	0.36	S-1A	2.97	0.28
S1	7.65	0.84	S1	11.33	0.92	S-0	5.00	0.54	S-0	5.83	0.62
S2	13.47	0.97	S2	13.73	0.87	S1	14.63	1.32	S1	14.36	1.25
S3	35.88	2.14	S3	41.80	1.97	S2	19.46	0.98	S2	21.81	1.12
S4	16.95	1.58	S4	19.22	1.20	S3	37.10	1.45	S3	47.53	1.62
S5	2.47	0.64	S5	2.62	0.16	S4	14.66	0.21	S4	20.80	1.01
S6	0.00	0.00	S6	0.39	0.00	S5	1.52	0.00	S5	2.49	0.24
Filter	12.52	1.46	Filter	5.20	0.75	Filter	18.50	0.48	Filter	8.51	0.68
throat	79.00	3.25	throat	88.62	2.98	throat	90.36	4.01	throat	95.33	3.69
MI	12.38	2.40	MI	14.42	2.98	MI	14.57	2.12	MI	13.50	2.45
PreSep	84.53	3.98	PreSep	78.09	3.69	PreSep	98.16	4.63	PreSep	97.50	4.29
MP	3.29	0.41	MP	4.61	1.02	MP	3.87	1.29	MP	2.96	2.89
Device	67.50	2.79	Device	63.34	3.56	Device	43.62	3.18	Device	32.49	2.76
Cap	38.64	2.52	Cap	21.82	1.12	Cap	20.42	2.26	Cap	22.09	3.56
TED	**274.94**	**3.92**	**TED**	**287.90**	**2.97**	**TED**	**326.59**	**3.17**	**TED**	**339.19**	**2.85**
FPD	**88.95**	**1.25**	**FPD**	**94.30**	**1.16**	**FPD**	**110.88**	**2.90**	**FPD**	**121.32**	**1.30**
%FPF	**32.35**	**1.42**	**%FPF**	**32.75**	**1.83**	**%FPF**	**33.95**	**1.26**	**%FPF**	**35.77**	**1.98**
TRA	**106.14**	**2.15**	**TRA**	**85.16**	**1.97**	**TRA**	**64.04**	**1.47**	**TRA**	**54.59**	**1.10**
TRD	**381.07**	**3.75**	**TRD**	**373.06**	**3.38**	**TRD**	**390.63**	**2.89**	**TRD**	**393.77**	**2.78**
%			**%**			**%**			**%**		
Recovery	**95.27**		**Recovery**	**93.27**		**Recovery**	**97.66**		**Recovery**	**98.44**	
LPM	**175.92**	**2.10**	**LPM**	**181.14**	**2.47**	**LPM**	**203.08**	**2.54**	**LPM**	**206.34**	**2.54**
			EFPD								
EFPD (<3)	**66.34**	**1.32**	**(<3)**	**60.88**	**2.24**	**EFPD (<3)**	**87.30**	**1.13**	**EFPD (<3)**	**96.67**	**1.13**
MMAD	**2.60**	**0.07**	**MMAD**	**2.70**	**0.18**	**MMAD**	**1.70**	**0.02**	**MMAD**	**1.70**	**0.02**
GSD	**1.90**	**0.00**	**GSD**	**1.80**	**0.01**	**GSD**	**2.00**	**0.07**	**GSD**	**2.30**	**0.07**

Table 7.2 Summary of SS deposition from PSDL-SS formulations at different MIF

	35.9L/min			54.9L/min			70.8L/min			85.7L/min	
	mean	**SD**		**mean**	**SD**		**mean**	**SD**		**mean**	**SD**
S-1	0.14	0.02	**S-1**	0.73	0.12	**S-2A**	1.96	0.23	**S-2A**	2.71	0.08
S-0	0.58	0.07	**S-0**	0.35	0.07	**S-1A**	0.39	0.04	**S-1A**	0.99	0.05
S1	2.89	0.13	**S1**	3.67	0.23	**S-0**	0.82	0.08	**S-0**	1.52	0.12
S2	5.01	0.26	**S2**	6.33	0.41	**S1**	5.40	0.12	**S1**	7.38	0.34
S3	17.96	1.07	**S3**	15.64	1.25	**S2**	9.21	0.35	**S2**	13.38	0.76
S4	8.03	0.98	**S4**	5.72	0.75	**S3**	17.09	0.89	**S3**	26.38	0.98
S5	0.00	0.00	**S5**	0.00	0.00	**S4**	5.01	0.21	**S4**	9.02	0.34
S6	0.00	0.00	**S6**	0.00	0.00	**S5**	0.00	0.00	**S5**	0.66	0.04
Filter	6.12	0.34	**Filter**	35.03	1.69	**Filter**	31.26	1.45	**Filter**	34.89	1.37
throat	82.91	2.42	**throat**	61.17	1.89	**throat**	42.23	1.37	**throat**	59.22	1.34
MI	9.60	0.99	**MI**	9.33	1.14	**MI**	5.89	0.78	**MI**	5.06	0.96
PreSep	151.13	2.89	**PreSep**	170.21	2.23	**PreSep**	196.54	1.95	**PreSep**	160.44	2.14
MP	2.97	0.42	**MP**	5.04	0.68	**MP**	7.99	1.04	**MP**	2.71	0.58
Device	56.84	1.09	**Device**	38.71	1.32	**Device**	34.02	1.10	**Device**	32.83	1.52
Cap	5.32	0.12	**Cap**	7.18	0.56	**Cap**	9.26	0.78	**Cap**	9.15	0.68
TED	**287.36**	**2.45**	**TED**	**313.22**	**2.74**	**TED**	**323.79**	**1.98**	**TED**	**324.37**	**2.32**
FPD	**37.13**	**1.20**	**FPD**	**66.39**	**1.45**	**FPD**	**68.79**	**1.36**	**FPD**	**93.23**	**1.75**
%FPF	**12.92**	**1.14**	**%FPF**	**21.20**	**1.25**	**%FPF**	**21.24**	**1.08**	**%FPF**	**28.74**	**1.17**
TRA	**62.16**	**1.32**	**TRA**	**45.89**	**1.27**	**TRA**	**43.29**	**1.10**	**TRA**	**41.98**	**1.27**
TRD	**349.53**	**3.12**	**TRD**	**359.12**	**2.96**	**TRD**	**367.07**	**2.81**	**TRD**	**366.35**	**3.13**
% Recovery	**87.38**		**% Recovery**	**89.78**		**% Recovery**	**91.77**		**% Recovery**	**91.59**	
EFPD (<3)	**28.60**	**1.64**	**EFPD (<3)**	**34.12**	**1.41**	**EFPD (<3)**	**62.42**	**1.85**	**EFPD (<3)**	**79.11**	**1.34**
MMAD	**2.50**	**0.12**	**MMAD**	**2.60**	**0.14**	**MMAD**	**0.90**	**0.07**	**MMAD**	**1.20**	**0.00**
GSD	**1.50**	**0.02**	**GSD**	**1.50**	**0.00**	**GSD**	**1.20**	**0.00**	**GSD**	**1.20**	**0.00**

The in-vitro aerodynamic parameters and resulting particle size distributions from a DPI are usually measured using standard pharmacopeial methodology which is widely accepted by the regulatory authorities (Chrystyn, 2015; Council of Europe, 2014; USP 2014). The procedure involves generating a flow using a vacuum pump to simulate an inhalation profile through an inhaler to emit the dose and collect it in a cascade impactor. However, humans cannot replicate the square wave generated by a vacuum pump and majority of patients are unable to achieve the inhalation parameters recommended by the Pharmacopoeia (4 kPa pressure drop and 4L inhaled volume) (USP, 2014) when they inhale through Breezhaler® (Azouz et al., 2015).

This becomes more challenging for paediatric patients whose lung capacities are usually less than that of an adult. Ex-vivo method with patient inhalation profiles was used in this chapter to replace the vacuum pump used with pharmacopeial methods. This would provide us with experimental aerodynamic parameters (TED, FPD and MMAD) being more realistic and closer to what patients would have achieved in real life. The Breezhaler® has a low resistance (0.017

$kPa^{0.5}$ min/L) and the patient needs to exceed 100 L/min to generate the 4 kPa pressure drop in the device (Section 7.1).

Drug de-aggregation, dispersion and emission relies highly on the patient's inspiratory flow rate, the volume and the acceleration (how fast he inhales) (Abadelah et al., 2017; Chrystyn et al., 2015).

The performance of salbutamol sulphate using a Breezhaler® was determined using real life recorded patients' IPs. These profiles were generated in-vivo and were re-played ex-vivo using a breath simulator (BRS) to determine dose emission characteristics of SS.

The results obtained from the ex-vivo deposition tests are shown in Fig. 7.4, 7.5, 7.6 are represented as total emitted dose, fine particle dose, extra fine particle dose of SS for both lactose formulations.

The dose emission of Salbutamol from two different formulations using inhalation profiles were determined. The two formulations showed difference in the dose emission depending on the MIF.

The results indicated that TED increased significantly ($p< 0.05$) with increasing the MIF of the inhalation profiles from 274.94 ± 3.92 μg to 339.19 ± 2.85 μg when SS-Lactohale was used (Table 7.1). A similar trend was observed with SS-PSDL formulation, where TED ranged from 287 ± 2.45 μg to 324 ±2.32 μg with increasing the MIF (Table 7.2). FPD also improved as MIF increased with both formulations, however the values were significantly higher with SS-Lactohale than SS-PSDL (Figure 7.5). On the other hand, MMAD showed a dissimilar trend as MMAD values decreased with increasing MIF with SS-Lactohale formulation, the MMAD obtained at 35.9L/min was 2.60 ± 0.07 and at 85.7L/min it was found to be 1.70 (Table 7.1 and 7.2). The MMAD obtained with SS-PSDL formulation was 2.50 at 35.9 L/min and was 1.20 at 85.7 L/min.

The dose emission from Lactohale was more flow-rate dependent than engineered particles, especially at low MIFs. $PSDL_{com}$ showed more flow rate dependency in the dose emission at low flow rates (Tables 1 and 2) whereas more dose emission in comparison to engineered lactose was observed only at high MIFs (i.e. 85.7 L/min).

The difference in the particle shape between these carriers may have accounted for the difference in dose emission results for PSDL. The high dose emission at low flow rate for PSDL may have been promoted by the spherical shape of the carrier particles, in comparison to elongated tomahawk shape Lactohale carrier particles.

FPD was calculated as a percentage of the total delivered dose obtained from drug content uniformity (Table 7.1 and 7.2). FPD of SS from both carriers increased with increasing the MIF, suggesting a portion of the TED was delivered as a fine particle mass (<5μm) (Figure 7.5).

FPD was found to vary between approximately 9% to 30% depending on the flow rate and the type of carrier used (smooth or rough carrier) (Figure 7.5).

Although TED was higher at low MIF (35.9 and 54.9 L/min) for $PSDL_{com}$, the corresponding FPD was found to be lower than for Lactohale. This probably was caused by the surface roughness of the PSDLcom particles (Figures 7.3.2 and 7.3.3), allowing less drug detachment from its rough surface. A great proportion (≥ 50% of the total delivered dose) of SS was deposited prematurely as LPM (Table 7.2). The present study confirms the superiority for Lactohale for delivering SS in comparison to PSDL observed in the previous chapters (Chapter 1, Chapter 3). Therefore, SS is better delivered from smooth surface than from rough carrier surface. The increase of LPM associated with the increase in MIF is typical for DPI devices especially those having a low resistance such as BreezHaler®. Most drug will impact in the oropharyngeal region due to an increase in the particle-particle momentum and the high MIF.

As previously mentioned, a carrier which performs better with one drug might not perform better with another drug, depending on the physicochemical characteristics of the drug, as shown with BDP and FP which performed better with a carrier ($PSDL_{10}$) with moderate surface roughness (Chapter 3). Therefore, there is no ideal universal carrier that performs well with all drugs, which may explain why drug delivery to the lungs from DPIs is still low despite the effort made by DPI formulators and device engineers (<30% as confirmed by de Boer et al., 2016). This novel finding would be useful for inhalation formulation scientists that moderate surface roughness may be useful more for hydrophobic drugs than hydrophilic drugs. The PSDLcom has excessively rough surface, which could further hinder drug deposition compared to $PSDL_{10}$ (produced in Chapter 3) or Lactohale.

A plot of the TED from the two formulations at different MIF is presented in Fig. 7.3. This plot suggests that as the MIF increased from 35.9 to 85.7 L/min, irrespective of the formulation used, SS was significantly ($p<0.05$) more emitted from the device. It is known that capsule-based DPIs tend to retain drugs as residual amounts (in capsule and device) which could lead to less dose being emitted (Abadelah et al., 2018)

It is interesting to note that less SS was retained in the device when PSDL formulation was used as opposed to lactose formulation.

Furthermore, irrespective of the formulation used, the incomplete dose emptying can be seen from the values of TRA retained in the capsule and device which appear to be higher at low MIF (35.9 and 54.9 L/min). Thus, inhaling forcefully would contribute to the reduction in the TRA.

The results of the FPD as a function of the nominal dose at different MIFs for both formulations are shown in Fig. 7.4. The FPD significantly ($p < 0.05$) increased with the MIF irrespective of the formulation used.

The results suggest that SS-lactose dose emission characteristics showed very good results with maximum dose emitted from the device at 70.8 L/min and above. When low MIFs of 35.9 L/min and 54.9 L/min were used, the turbulence energy generated inside the Breezhaler® was not enough to efficiently de-aggregate the dose, consequently less dose was emitted from the device. The formulation with untreated lactose showed a very good correlation with the MIF used in the dose emission characteristics. The Breezhaler® has been previously reported to show a flow-dependent dose emission for Indacaterol formulations (Pavkov et al., 2010), SS dose emission showed similar results with flow dependency of the formulation. There are three main reasons for successful dose emission: the inhaler device, the inhalation manoeuvre by the patient and finally the formulation with the active ingredient. The above results showed high doses would reach the patient lungs when MIF of 60 L/min and above was used. 60 L/min could be considered as a threshold MIF to manoeuvre the Breezhaler®, this MIF can be easily achieved as this inhaler has a low resistance. These results are in line with Abadelah et al. (2018) study which also showed that the rate of increase in the FPD with BreezHaler® was higher when reaching 60 L/min. In our study, almost 30% fine particle dose was generated at high flow rate with untreated lactose formulation as opposed to almost 25% with PSDL formulation (Fig. 7.4), suggesting that the inter-particle forces were stronger between PSDL particles and SS particles than between untreated lactose and SS particles. These results are in line with the results found in Chapter 6 where SS was found to be more easily emitted from Lactohale smooth particles than from PSDL rough particles. One of the reasons was the physico-chemical properties of the drug, SS being hydrophilic, had a weaker adhesion force to the Lactohale particles than the PSDL particles.

The results of the EFPD for both formulations with increasing MIFs are shown in Fig. 7.6. EFPD significantly increased ($p<0.05$) when increasing the MIFs. Irrespective of the

formulation used, the steepest increase in the EFPD was observed when MIF value was above 60 L/min. The increase in EFPD was combined with a significant ($p < 0.05$) decrease in the MMAD (Table 7.1 and 7.2) when the MIF value above 60 L/min was used. High values of EFPD would correspond to higher amounts of drug deposited in the peripheral airways in the lungs, which is favourable in treating COPD patients (Grasmeijer & De Boer, 2014). High MIFs generated higher turbulence energy inside the device to be able to de-aggregate the particles, thus favouring drug particles detachment from the carrier particles, particle dispersion and allowed single drug particles to reach the deepest regions of the impactor.

When PSDL-SS was used, MMAD was low and more drug was recovered in the filter (Table 7.2), suggesting that in real life use, the patient might get more therapeutic effect despite less dose emitted compared to untreated lactose formulations data.

A possible reason for that could be that in constricted airways, particles within the range of 2μm (1-3μm) have more tendency to produce vaso-relaxation effect and better asthma and COPD management (Heyder, 2004; Morén, 1987). An MMAD of less than 5 μm is thought to be required to achieve an efficient deposition of the drug in the airways (Roche et al., 2013).

7.4 Conclusion

The dose emission study of SS from the capsule-based Breezhaler® appeared to show inhalation flow-dependency, irrespective of the formulation used. The aerodynamic characteristics of SS from the lactose-SS formulation showed that using a carrier with a smooth surface when using a hydrophilic drug such as SS was effective in producing respirable particles with a low MMAD (less than 5μm) irrespective of the MIF used. This chapter also showed the importance of the MIF to maximise the fraction of SS particles less than 3μm (EFPD). The results showed that the increase in EFPD was more noticeable above 54.9 L/min. These results confirm the recommendation of using a forceful inhalation when using Onbrez

Breezhaler®. This chapter showed that the solid phase crystallisation method was promising and successful in achieving spherical particles with rough surface, however the method needs to be further optimised to achieve the right degree of rugosity depending on the API used to achieve optimum adhesion forces between the particles. Using ex-vivo study as opposed to Pharmacopoeial method provided us with more accurate results that reflect more realistically the dose inhaled from individual patients.

Chapter 8

General conclusion and future work

8.1 General conclusions

Drug delivery to the lungs via dry powder inhalers (DPIs) is becoming increasingly popular. The most important component of the DPI formulation is the carrier particle, as the ratio of drug to carrier is usually 1:67.5, thus any changes in the physicochemical properties of the carrier will have a great impact on the formulation and lung deposition. Carrier particles should have a number of key physicochemical properties to obtain both a successful formulation and an efficient delivery of the drug to the lungs. Lactose is most commonly used in DPI formulations, it should be of a suitable particle size to be used as carriers, the particles should also be crystalline to allow the formulation to be stable during shelf life and also to ensure the reproducibility of the particle morphology. The overall objective of this thesis was to produce a carrier particle with suitable properties to be used in DPI formulations. Hence, this thesis was more focused on the formulation development of DPIs.

The use of commercially available lactose in DPI formulations poses many challenges in dispersing the drug from the lactose carrier surface. The latter only allows 20-30% of the total dose to reach the lungs. Such low efficiency of current DPIs emphasises the need for DPI formulations to be optimised. The most common technique used to modify the morphological features of lactose particles is crystallisation from solutions. However, this technique has many disadvantages that limit the opportunity to optimise and control the physicochemical properties of the engineered particles. The final product is usually complex and unpredictable as inter- and intra-batch variations are likely to occur. Also, this technique requires the use of toxic solvents (e.g. hexane, chloroform) which are not environmental-friendly. Therefore, it would be preferable to develop a crystallisation method that controls particle size, shape, crystallinity and surface texture of the carrier particle so that desirable features are obtained.

Many studies in the literature suggest the use of spherical shaped particles as an alternative to the traditional irregular lactose. Spherical carriers have been shown to improve drug deposition to the lungs. This is why, this project suggested the use of spherical engineered lactose particles to be used as carriers in DPI formulations.

The first step in this project was to engineer the lactose particles (PSDL) from commercially available Lactohale®, characterise them with various analytical techniques then formulate both Lactohale and PSDL with Salbutamol Sulphate and finally assess their performance in DPI formulations.

The engineering process involved few steps: the first step was to spray dry lactose particles to obtain spherical particles. The spherical particles were then introduced to the inflating agent (ethanol), when the particles came in contact with the inflating agent, the amorphous regions on the surface of the spray-dried particles partially dissolved, allowing ethanol to form pores and permeate into the hollow space of the particles. As the vapour pressure of the inflating agent increased, the pressure inside the particles increased, inflating the particles until it reached a certain point. The engineering process allowed the particles to have increased in size reaching more than 80 μm without deviating from the spherical shape. Ethanol acted as an inflating agent promoting an increase in the lactose particle size. The engineering process also allowed to modify the surface of the particles to engineer rough surfaces. The rough surface of the PSDL particles contributed to the stability of the powder blend against segregation.

The engineered lactose was found to be crystalline as opposed to the spray-dried lactose which was amorphous. The engineering process helped repairing the defects present in the spray-dried lactose. One of the advantages resulting from this process was that the product was made to be more stable due to its crystallinity being restored.

Spherical shape, rough surface and crystalline particle are desirable features in order to produce a stable and performant solid dosage form. With regards to inhalation, the engineered particles contributed to a better dose emission of the DPI formulation and to a better drug delivery consistency.

In a general aspect, the engineering process provided a reliable method of producing suitable sized carrier particles, with a rougher surface while retaining the spherical shape of the spray-dried material which could potentially enhance drug deposition into deep lungs.

When comparing the deposition profiles of both DPI formulations, there was less drug (SS) dispersed from PSDL formulation in comparison to Lactohale®. This was because the adhesion forces between PSDL and SS were stronger than the forces between Lactohale and SS.

The deposition studies were performed with a MacHaler® device, the results showed that this device has a threshold at 60L/min. Above the threshold, a little change has been observed in TED when the inhalation flow rate increased from 60 to 90 L/min suggesting that TED reached its maximum value at 60 L/min. Both ACI and NGI were compared in this study and it is interesting to note that the highest TED values irrespective of the impactor were obtained at the highest inhaled volume coupled with the highest inhalation flow rate (90L/min; 2 L) suggesting that a forceful inhalation coupled with deep breath are helpful in maximizing drug delivery to the lungs, as shown from the highest FPD values.

The results suggest that an inhaled volume of 1L was not sufficient to pull the aerosol to deep stages of the NGI. These results are in agreement with Mohammed et al. (2012) study which showed that 1L was not generating sufficient turbulent airflow within the device to de-aggregate the powder and to overcome the dead volume of NGI. PSDL showed more consistency in the emitted dose compared to Lactohale. The spherical shape and uniformity of

size of engineered lactose might have contributed to the reproducibility of the dose released from the inhaler. Engineered lactose benefited more from the increase in the inhaled volume than Lactohale, as shown from the difference in the FPD between 1 L and 2 L. Engineered lactose is hollow and spherical in shape and by increasing the inhalation volume this may have provided this lactose with a longer time of flight allowing drug particles to reach the distal part of the impactors. By combining a forceful inhalation with a prolonged inhalation time (inhaled volume) this does not only allow an increase in the turbulent energy inside the device but also to provide carrier and drug particles with sufficient time of flight to produce drug particles small enough to reach the lungs, as shown from the FPD and MMAD values obtained.

The engineered lactose produced a more reproducible Salbutamol Sulphate emission and Fine Particle Dose after aerosolisation via a MacHaler® tested in both ACI and NGI.

This study showed that Vin is equally important as MIF with regard to dose emission, de-aggregation of the powder formulation and in producing respirable particles for deep lung penetration.

The results obtained suggested that drug delivery to the lungs can be optimised by using a forceful inhalation in combination with a prolonged inhalation time.

Inhalation peak flow vary from patient to patient but the threshold inhalation flow as well as the inhalation time should be mentioned in the patient information leaflet to ensure that drug delivery to the lungs is maximised for the patient.

This study demonstrated evidence of incomplete mass transfer through NGI at a volume (1 L) inferior than the internal dead volume (2.025 L) in contrast to the consistent behaviour of the ACI where the mass transfer had taken place normally even when volume (1 L) which is slightly lower than the internal volume (1.150 L) was used.

Secondly this project investigated the effect of incorporating a ternary component to the formulation and assess the effect they have on the surface properties of the resulting particles. The effect of V_{in} and the difference between the two impactors (ACI and NGI) was further studied in this chapter. NaCl and PVP were used for this purpose.

Solid-phase crystallisation of co-spray dried lactose-NaCl and lactose-PVP with ethanol produced particles with larger size compared to the spray-dried particles, without changing their spherical shape. PSDL-NaCl appeared to have a rougher surface than PSDL-PVP. This method showed that the surface roughness can be adjusted, depending on the solubility of the additive to ethanol. This method also affected the polymorphic forms of lactose by producing either α or α-β mixtures.

This process of crystallization is reliable as the particles produced are spherical, irrespective of the type of additive and its solubility in the non-solvent. Surface textures can be modified to produce particles of different surface rugosity and different degrees of crystallinity, depending the solubility and the time of exposure to the crystallization medium.

Formulation powder blends containing PSDL as a carrier performed better than most of commercially available DPIs at higher volumes, as suggested by the %FPF obtained >30%, in comparison to the %FPF of commercial DPIs. This indicates that employing engineered lactose in DPI formulations instead of commercially available lactose carrier would result in a high amount of drug reaching the lungs. The improved SS drug deposition from PSDL-NaCl can be attributed to the surface texture of the PSDL. The solubility of NaCl is much less than that of PVP in ethanol, therefore ethanol may have washed away all PVP or great portion of it from the surface of lactose, whereas, the poor solubility of NaCl in ethanol has led to the formation of microscopic spikes on the surface of spray dried lactose giving some roughness and porosity to lactose particles. Unlike clefts and crevices, these microscopic projections did not

accommodate the drug particles and instead enhanced drug detachment from the lactose surface and improved inhalation efficiency.

The NGI was more sensitive to change in the inhaled volume than the ACI as the latter did not appear to be as sensitive, this is believed to be because of a maldistribution of the flow through the ACI

Thirdly, a comprehensive investigation on some of the process parameters (e.g. processing time, mixing time, triboelectrification, use of hydrophobic/hydrophilic drugs) was done. Determining the degree of adhesive forces of the carrier helped correlate the aerosolisation results with the morphological features, especially the surface roughness of the carrier.

The PDSL particles could be produced with different surface rugosity without altering size and shape of the particles. The time of exposure of spray-dried particles to hot ethanol was a critical factor in altering surface rugosity: the longer the particles were in contact with ethanol, the rougher they were.

Lactohale, $PSDL_{10}$ and $PSDL_{30}$ contrasted in their characteristics: carrier shape (tomahawk/spherical), surface texture (smooth/rough), surface net charges and polarities (positively and negatively charged) and degrees of crystallinity.

The data showed that different grades of lactose exhibit different charging behaviours either alone or with different drugs in formulations.

$PSDL_{10}$ appeared to have less variation in the charging behaviour of the powder blend, which indicates that the morphological features of $PSDL_{10}$ could potentially be beneficial in DPI formulations as an antistatic effect was observed with this type of carrier and a more stable mix was observed.

In general, the results showed that the content uniformity is affected by the mixing time and is different for each type of drug and each carrier.

Despite Lactohale and PSDL's respective formulations presenting good content uniformity, Lactohale may be considered as the most favourable carrier when used with hydrophilic drugs such as SS as a good content uniformity was achieved with only 5 mins of mixing and high doses of SS were emitted and deposited from Lactohale-SS formulation.

On the other hand, PSDL was considered to be most favourable for hydrophobic drugs where its rough surface was ideal for the drug to adhere to and obtain a stable mix with very good content uniformity irrespective of the mixing time, but the adhesion was weak enough to allow the drug to detach from the carrier during aerosolisation and deposit in the deepest stages of the impactor.

In the last part of the study, we wanted to ensure that the engineering method was reliable in retaining the spherical shape of the particles while modifying their surface texture, commercially available spray-dried lactose (which was spherical) was processed to obtain rough particles. It is interesting to note that the commercial available lactose used was initially spray-dried from a suspension, in comparison to the PSDL particles engineered in Chapter 4, 5 and 6 which were spray-dried from a solution. The results showed that processing lactose particles obtained from a spray-dried suspension resulted in much rougher particles than when processed from spray-dried solution. These results suggest that the surface roughness of the particle can be adjusted by either spray drying from a lactose solution or a suspension.

With regards to SS, there was no improvement in drug dispersion when using PSDLcom, however the results showed that more drug was emitted from the device at low MIFs (<60L/min) with PSDL formulations, this was due to the spherical shape of the PSDLcom particles, allowing a better flow of the powder formulation out of the device. The last part of the study showed that there is no ideal universal carrier that performs well with all drugs, which may explain why drug delivery to the lungs from DPIs is still low despite the effort made by DPI formulators and device engineers (<30%). As previously mentioned, a carrier which

performs better with one drug might not perform better with another drug, depending on the physicochemical characteristics of the drug, as shown with BDP and FP which performed better with a carrier with moderate surface roughness (Chapter 6). SS was shown to be better delivered from smooth surface than from rough carrier surface. (Chapter 6 and Chapter 7).

8.2 Future work

- Further tuning of the engineering method should be done, i.e. use of different inflating agents, different contact times with the crystallisation medium to be able to achieve different particle sizes.
- Use of different starting material with different plasto-elasticity to produce novel particle shapes (e.g. use of a material that is both fragmentating and plastic could form unsymmetrical particles which are not yet in the literature). Scientists have been crystallising using various material but there has been no mention about the plasto-elasticity of the material which play an important role in the inflating mechanism in the crystallisation process.
- Use of different additives (with different solubility to the crystallisation medium) to establish a better correlation between the physicochemical properties of the additive and the surface roughness of the carrier particles.
- Work in parallel with computer simulations programs to be able to predict all new crystals forms.

References

1) Abadelah, M., Chrystyn, H., Bagherisadeghi, G., Abdalla, G., & Larhrib, H. (2018). Study of the Emitted Dose After Two Separate Inhalations at Different Inhalation Flow Rates and Volumes and an Assessment of Aerodynamic Characteristics of Indacaterol Onbrez Breezhaler® 150 and 300 µg. *AAPS PharmSciTech*, *19*(1), 251–261.

2) Abadelah, M., Hazim, F., Chrystyn, H., Bagherisadeghi, G., Rahmoune, H., & Larhrib, H. (2017). Effect of maximum inhalation flow and inhaled volume on formoterol drug deposition in-vitro from an Easyhaler® dry powder inhaler. *European Journal of Pharmaceutical Sciences*. https://doi.org/10.1016/j.ejps.2017.03.035

3) Abdelrahim, M. E., Plant, P., & Chrystyn, H. (2010). In-vitro characterisation of the nebulised dose during non-invasive ventilation. *Journal of Pharmacy and Pharmacology*. https://doi.org/10.1111/j.2042-7158.2010.01134.x

4) Adi, H., Larson, I., & Stewart, P. J. (2007). Adhesion and redistribution of salmeterol xinafoate particles in sugar-based mixtures for inhalation. *International Journal of Pharmaceutics*. https://doi.org/10.1016/j.ijpharm.2007.01.007

5) Adi, H., Traini, D., Chan, H. K., & Young, P. M. (2008). The influence of drug morphology on the aerosolisation efficiency of dry powder inhaler formulations. *Journal of Pharmaceutical Sciences*. https://doi.org/10.1002/jps.21195

6) Alaboud, A., Assi, K. H., & Chrystyn, H. (2010). In vitro characterization of the emitted dose from the foradil aerolizer to identify the influence of inhalation flow, inhilation volume and the number of inhalations per dose. In *Respiratory drug delivery* (Vol. 3, pp. 803–806).

7) Alyami, H., Dahmash, E., Bowen, J., & Mohammed, A. R. (2017). An investigation into the effects of excipient particle size, blending techniques & processing parameters

on the homogeneity & content uniformity of a blend containing low-dose model drug. *PLoS ONE*. https://doi.org/10.1371/journal.pone.0178772

8) Amirav, I., Newhouse, M. T., & Mansour, Y. (2005). Measurement of peak inspiratory flow with in-check dial device to simulate low-resistance (Diskus) and high-resistance (Turbohaler) dry powder inhalers in children with asthma. *Pediatric Pulmonology*. https://doi.org/10.1002/ppul.20180

9) Atkins, P. J. (2005). Dry powder inhalers: an overview. *Respiratory Care*.

10) Azouz, W., Chetcuti, P., Hosker, H. S. R., Saralaya, D., Stephenson, J., & Chrystyn, H. (2015). The inhalation characteristics of patients when they use different dry powder inhalers. *Journal of Aerosol Medicine and Pulmonary Drug Delivery*. https://doi.org/10.1089/jamp.2013.1119

11) 11)Azouz, W., & Chrystyn, H. (2012). Clarifying the dilemmas about inhalation techniques for dry powder inhalers: Integrating science with clinical practice. *Primary Care Respiratory Journal*. https://doi.org/10.4104/pcrj.2012.00010

12) B. Laube et al., (2002). Advances in treating diabetes with aerosolized insulin. *Diabetes Technology and Therapeutics*.

13) Bagherisadeghi, G., Larhrib, E. H., & Chrystyn, H. (2017). Real life dose emission characterization using COPD patient inhalation profiles when they inhaled using a fixed dose combination (FDC) of the medium strength Symbicort®Turbuhaler®. *International Journal of Pharmaceutics*. https://doi.org/10.1016/j.ijpharm.2017.02.057

14) Bagherisadeghi, G., Larhrib, H. E., & Chrystyn, H. (2015). In-vitro emitted dose characteristics of combination budesonide / formoterol tubuhaler using patient inhalation profiles. *Eur. Respir. J.*

15) Bailey, A. G. (1993). Charging of Solids and Powders. *Journal of Electrostatics*. https://doi.org/10.1016/0304-3886(93)90072-F

16) Balásházy, I., & Hofmann, W. (1995). Deposition of aerosols in asymmetric airway bifurcations. *Journal of Aerosol Science*. https://doi.org/10.1016/0021-8502(94)00106-9

17) Begat, P., Morton, D. A. V., Staniforth, J. N., & Price, R. (2004). The cohesive-adhesive balances in dry powder inhaler formulations I: Direct quantification by atomic force microscopy. *Pharmaceutical Research*.

18) Begat, P., Morton, D. A. V, Shur, J., Kippax, P., Staniforth, J. N., & Price, R. (2009). The role of force control agents in high-dose dry powder inhaler formulations. *Journal of Pharmaceutical Sciences*, *98*(8), 2770–2783.

19) Begat, P., Price, R., Harris, H., Morton, D. A. V., & Staniforth, J. N. (2005). The influence of force control agents on the cohesive-adhesive balance in dry powder inhaler formulations. *KONA Powder and Particle Journal*. https://doi.org/10.14356/kona.2005014

20) Bennett, F. S., Carter, P. A., Rowley, G., & Dandiker, Y. (1999). Modification of electrostatic charge on inhaled carrier lactose particles by addition of fine particles. *Drug Development and Industrial Pharmacy*. https://doi.org/10.1081/DDC-100102148

21) Berkenfeld, K., Lamprecht, A., & McConville, J. T. (2015). Devices for dry powder drug delivery to the lung. *AAPS PharmSciTech*, *16*(3), 479–490.

22) Brocklebank, D., Ram, F., Wright, J., Barry, P. W., Cates, C., Davies, L., ... White, J. (2001). Comparison of the effectiveness of inhaler devices in asthma and chronic

obstructive airways disease: a systematic review of the literature. *Health Technology Assessment*. https://doi.org/10.3310/hta5260

23) Buhl, R., & Banerji, D. (2012). Profile of glycopyrronium for once-daily treatment of moderate-to-severe COPD. *International Journal of Chronic Obstructive Pulmonary Disease*, *7*, 729.

24) Bunnag, C., Fuangtong, R., Pothirat, C., & Punyaratabandhu, P. (2007). A comparative study of patients' preferences and sensory perceptions of three forms of inhalers among Thai asthma and COPD patients. *Asian Pacific Journal of Allergy and Immunology*.

25) Butt, H. J., & Kappl, M. (2009). Normal capillary forces. *Advances in Colloid and Interface Science*. https://doi.org/10.1016/j.cis.2008.10.002

26) Buttini, F., Brambilla, G., Copelli, D., Sisti, V., Balducci, A. G., Bettini, R., & Pasquali, I. (2016). Effect of Flow Rate on In Vitro Aerodynamic Performance of NEXThaler(®) in Comparison with Diskus(®) and Turbohaler(®) Dry Powder Inhalers. *Journal of Aerosol Medicine and Pulmonary Drug Delivery*. https://doi.org/10.1089/jamp.2015.1220

27) Buttini, F., Pasquali, I., Brambilla, G., Copelli, D., Alberi, M. D., Balducci, A. G., ... Sisti, V. (2016). Multivariate Analysis of Effects of Asthmatic Patient Respiratory Profiles on the in Vitro Performance of a Reservoir Multidose and a Capsule-Based Dry Powder Inhaler. *Pharmaceutical Research*. https://doi.org/10.1007/s11095-015-1820-1

28) Carter, P. A., Rowley, G., Fletcher, E. J., & Stylianopoulos, V. (1998). Measurement of electrostatic charge decay in pharmaceutical powders and polymer materials used in

dry powder inhaler devices. *Drug Development and Industrial Pharmacy*. https://doi.org/10.3109/03639049809089953

29) Chan, H.-K. (2006). Dry powder aerosol delivery systems: current and future research directions. *Journal of Aerosol Medicine*, *19*(1), 21–27.

30) Chan, H.-K., & Chew, N. Y. K. (2003). Novel alternative methods for the delivery of drugs for the treatment of asthma. *Advanced Drug Delivery Reviews*, *55*(7), 793–805.

31) Chew, N. Y., & Chan, H. K. (2001). In vitro aerosol performance and dose uniformity between the Foradile Aerolizer and the Oxis Turbuhaler. *Journal of Aerosol Medicine*. https://doi.org/10.1089/08942680152744703

32) Chew, N. Y. K., Shekunov, B. Y., Tong, H. H. Y., Chow, A. H. L., Savage, C., Wu, J., & Chan, H. K. (2005). Effect of amino acids on the dispersion of disodium cromoglycate powders. *Journal of Pharmaceutical Sciences*. https://doi.org/10.1002/jps.20426

33) Chougule, M. B., Padhi, B. K., Jinturkar, K. A., & Misra, A. (2007). Development of dry powder inhalers. *Recent Patents on Drug Delivery & Formulation*. https://doi.org/10.2174/187221107779814159

34) Chougule, M. B., Padhi, B. K., & Misra, A. (2006). Nano-liposomal dry powder inhaler of amiloride hydrochloride. *Journal of Nanoscience and Nanotechnology*. https://doi.org/10.1166/jnn.2006.405

35) Chow, K. T., Zhu, K., Tan, R. B. H., & Heng, P. W. S. (2008). Investigation of electrostatic behavior of a lactose carrier for dry powder inhalers. In *Pharmaceutical Research*. https://doi.org/10.1007/s11095-008-9651-y

36) Chrystyn, H. (2003). Is inhalation rate important for a dry powder inhaler? Using the In- Check Dial to identify these rates. *Respiratory Medicine*. https://doi.org/10.1053/rmed.2003.1351

37) Chrystyn, H. (2006). Closer to an "ideal inhaler" with the Easyhaler®: An innovative dry powder inhaler. *Clinical Drug Investigation*. https://doi.org/10.2165/00044011-200626040-00001

38) Chrystyn, H. (2007). The DiskusTM: A review of its position among dry powder inhaler devices. *International Journal of Clinical Practice*. https://doi.org/10.1111/j.1742- 1241.2007.01382.x

39) Chrystyn, H. (2009). Effects of device design on patient compliance : Comparing the same drug in different devices. In *RDD Europe 2009*.

40) Chrystyn, H., Safioti, G., Keegstra, J. R., & Gopalan, G. (2015). Effect of inhalation profile and throat geometry on predicted lung deposition of budesonide and formoterol (BF) in COPD: An in-vitro comparison of Spiromax with Turbuhaler. *International Journal of Pharmaceutics*. https://doi.org/10.1016/j.ijpharm.2015.05.076

41) Clark, A. R., & Hollingworth, A. M. (1993). The relationship between powder inhaler resistance and peak inspiratory conditions in healthy volunteers—implications for in vitro testing. *Journal of Aerosol Medicine*, *6*(2), 99–110.

42) Coates, M. S., Fletcher, D. F., Chan, H.-K., & Raper, J. A. (2004). Effect of Design on the Performance of a Dry Powder Inhaler Using Computational Fluid Dynamics. Part 1: Grid Structure and Mouthpiece Length. *Journal of Pharmaceutical Sciences*. https://doi.org/10.1002/jps.20201

43) Colombo, M., Carregal-Romero, S., Casula, M. F., Gutiérrez, L., Morales, M. P., Böhm, I. B., ... Parak, W. J. (2012). Biological applications of magnetic nanoparticles. *Chemical Society Reviews*. https://doi.org/10.1039/c2cs15337h

44) Colthorpe, P., Voshaar, T., Kieckbusch, T., Cuoghi, E., & Jauernig, J. (2013). Delivery characteristics of a low-resistance dry-powder inhaler used to deliver the long-acting muscarinic antagonist glycopyrronium. *Journal of Drug Assessment*. https://doi.org/10.3109/21556660.2013.766197

45) Copley, M. (2008). Cascade impactors: Theory, design, and practical information for optimal testing. *Inhalation*, *2*(1), 19–23.

46) Copley, M., Director, S., & Scientific, C. (2014). Using breathing simulators to enhance inhaled product testing. *Accessed Jul*, *28*.

47) Copley, M., Smurthwaite, M., Roberts, D. L., & Mitchell, J. P. (2005). Revised internal volumes of cascade impactors for those provided by Mitchell and Nagel. *Journal of Aerosol Medicine*, *18*(3), 364–366.

48) Corrigan, D. O., Corrigan, O. I., & Healy, A. M. (2006). Physicochemical and in vitro deposition properties of salbutamol sulphate/ipratropium bromide and salbutamol sulphate/excipient spray dried mixtures for use in dry powder inhalers. *International Journal of Pharmaceutics*. https://doi.org/10.1016/j.ijpharm.2006.05.022

49) Crowder, T. M., Louey, M. D., Sethuraman, V. V., Smyth, H. D. C., & Hickey, A. J. (2001). 2001: An odyssey in inhaler formulation and design. *Pharmaceutical Technology*.

50) Dal Negro, R. W. (2015). Dry powder inhalers and the right things to remember: A concept review. *Multidisciplinary Respiratory Medicine*. https://doi.org/10.1186/s40248- 015-0012-5

51) De Boer, A. H., Dickhoff, B. H. J., Hagedoorn, P., Gjaltema, D., Goede, J., Lambregts, D., & Frijlink, H. W. (2005). A critical evaluation of the relevant parameters for drug redispersion from adhesive mixtures during inhalation. *International Journal of Pharmaceutics*. https://doi.org/10.1016/j.ijpharm.2005.01.035

52) De Boer, A. H., Hagedoorn, P., Gjaltema, D., Goede, J., & Frijlink, H. W. (2003). Air classifier technology (ACT) in dry powder inhalation: Part 1. Introduction of a novel force distribution concept (FDC) explaining the performance of a basic air classifier on adhesive mixtures. *International Journal of Pharmaceutics*. https://doi.org/10.1016/S0378-5173(03)00250-3

53) De Boer, A. H., Hagedoorn, P., Gjaltema, D., Goede, J., Kussendrager, K. D., & Frijlink, H. W. (2003). Air classifier technology (ACT) in dry powder inhalation Part 2. The effect of lactose carrier surface properties on the drug-to-carrier interaction in adhesive mixtures for inhalation. *International Journal of Pharmaceutics*. https://doi.org/10.1016/S0378-5173(03)00264-3

54) De Boer, A. H., Hagedoorn, P., Gjaltema, D., Lambregts, D., Irngartinger, M., & Frijlink, H. W. (2004). The mode of drug particle detachment from carrier crystals in an air classifier-based inhaler. *Pharmaceutical Research*. https://doi.org/10.1007/s11095-004- 5171-6

55) Dechene, R. L., & Newton, R. E. (1987, December 22). Flow measuring apparatus with analog, essentially linear output. Google Patents.

56) Decramer, M., Gosselink, R., Bartsch, P., Löfdahl, C. G., Vincken, W., Dekhuijzen, R., ... Troosters, T. (2005). Effect of treatments on the progression of COPD: Report of a workshop held in Leuven, 11-12 March 2004. In *Thorax*. https://doi.org/10.1136/thx.2004.028720

57) Dickhoff, B. H. J., de Boer, A. H., Lambregts, D., & Frijlink, H. W. (2006). The effect of carrier surface treatment on drug particle detachment from crystalline carriers in adhesive mixtures for inhalation. *International Journal of Pharmaceutics*. https://doi.org/10.1016/j.ijpharm.2006.07.017

58) Doff, D. H., Brownen, F. L., & Corrigan, O. I. (1986). Determination of α-impurities in the β-polymorph of inosine using infrared spectroscopy and X-ray powder diffraction. *Analyst*, *111*(2), 179–182.

59) Dunbar, C. A., Morgan, B., M, V. O., & Hickey, A. J. (2000). A comparison of dry powder inhaler dose delivery characteristics using a power criterion. *PDA J Pharm Sci Technol*.

60) Dunber, C. A., Hickey, A. J., & Holzner, P. (1998). Dispersion and characterization of pharmaceutical dry powder aerosols. *KONA Powder and Particle Journal*. https://doi.org/10.14356/kona.1998007

61) El-Sabawi, D., Edge, S., Price, R., & Young, P. M. (2006). Continued investigation into the influence of loaded dose on the performance of dry powder inhalers: Surface smoothing effects. *Drug Development and Industrial Pharmacy*. https://doi.org/10.1080/03639040600712920

62) Elversson, J., Millqvist-Fureby, A., Alderborn, G., & Elofsson, U. (2003). Droplet and particle size relationship and shell thickness of inhalable lactose particles during spray drying. *Journal of Pharmaceutical Sciences*. https://doi.org/10.1002/jps.10352

63) Fatnassi, M., Jacquart, S., Brouillet, F., Rey, C., Combes, C., & Girod Fullana, S. (2014). Optimization of spray-dried hyaluronic acid microspheres to formulate drug-loaded bone substitute materials. *Powder Technology*. https://doi.org/10.1016/j.powtec.2013.08.027

64) Feeley, J. C., York, P., Sumby, B. S., & Dicks, H. (1998). Determination of surface properties and flow characteristics of salbutamol sulphate, before and after micronisation. *International Journal of Pharmaceutics*. https://doi.org/10.1016/S0378-5173(98)00179-3

65) Flament, M. P., Leterme, P., & Gayot, A. (2004). The influence of carrier roughness on adhesion, content uniformity and the in vitro deposition of terbutaline sulphate from dry powder inhalers. *International Journal of Pharmaceutics*. https://doi.org/10.1016/j.ijpharm.2004.02.002

66) Fowkes, F. M. (1964). Attractive forces at interfaces. *Industrial & Engineering Chemistry*, *56*(12), 40–52.

67) French, D. L., Edwards, D. A., & Niven, R. W. (1996). The influence of formulation on emission, deaggregation and deposition of dry powders for inhalation. *Journal of Aerosol Science*. https://doi.org/10.1016/0021-8502(96)00021-3

68) Frijlink, H. W., & de Boer, A. H. (2005). Trends in the technology-driven development of new inhalation devices. *Drug Discovery Today: Technologies*. https://doi.org/10.1016/j.ddtec.2005.05.020

69) Gilani, K., Najafabadi, A. R., Darabi, M., Barghi, M., & Rafiee-Tehrani, M. (2004). Influence of formulation variables and inhalation device on the deposition profiles of cromolyn sodium dry powder aerosols. *DARU Journal of Pharmaceutical Sciences*.

70) Gómez-Gaete, C., Fattal, E., Silva, L., Besnard, M., & Tsapis, N. (2008). Dexamethasone acetate encapsulation into Trojan particles. *Journal of Controlled Release*. https://doi.org/10.1016/j.jconrel.2008.02.008

71) Grasmeijer, F., & De Boer, A. H. (2014). The dispersion behaviour of dry powder inhalation formulations cannot be assessed at a single inhalation flow rate.

International Journal of Pharmaceutics. https://doi.org/10.1016/j.ijpharm.2014.02.024

72) Groneberg, D. a, Witt, C., Wagner, U., Chung, K. F., & Fischer, a. (2003). Fundamentals of pulmonary drug delivery. *Respiratory Medicine*. https://doi.org/10.1053/rmed.2002.1457

73) Grosvenor, M. P., & Staniforth, J. N. (1996). The influence of water on electrostatic charge retention and dissipation in pharmaceutical compacts for powder coating. *Pharmaceutical Research*. https://doi.org/10.1023/A:1016409227565

74) Hamishehkar, H., Emami, J., Najafabadi, A. R., Gilani, K., Minaiyan, M., Mahdavi, H., & Nokhodchi, A. (2010a). Effect of carrier morphology and surface characteristics on the development of respirable PLGA microcapsules for sustained-release pulmonary delivery of insulin. *International Journal of Pharmaceutics*, *389*(1–2), 74–85.

75) Hamishehkar, H., Emami, J., Najafabadi, A. R., Gilani, K., Minaiyan, M., Mahdavi, H., & Nokhodchi, A. (2010b). Influence of carrier particle size, carrier ratio and addition of fine ternary particles on the dry powder inhalation performance of insulin-loaded PLGA microcapsules. *Powder Technology*. https://doi.org/10.1016/j.powtec.2010.04.017

76) Hancock, B. C., & Zografi, G. (1997). Characteristics and significance of the amorphous state in pharmaceutical systems. *Journal of Pharmaceutical Sciences*, *86*(1), 1–12.

77) Harjunen, P., Lehto, V. P., Martimo, K., Suihko, E., Lankinen, T., Paronen, P., & Järvinen, K. (2002). Lactose modifications enhance its drug performance in the novel multiple dose Taifun® DPI. *European Journal of Pharmaceutical Sciences*. https://doi.org/10.1016/S0928-0987(02)00126-4

78) Harper, W. R. (1967). *Contact and frictional electrification*. Clarendon Press.

79) Hassan, M. S., & Lau, R. (2010a). Feasibility study of pollen-shape drug carriers in dry powder inhalation. *Journal of Pharmaceutical Sciences*. https://doi.org/10.1002/jps.21913

80) Hassan, M. S., & Lau, R. (2010b). Inhalation performance of pollen-shape carrier in dry powder formulation with different drug mixing ratios: Comparison with lactose carrier. *International Journal of Pharmaceutics*. https://doi.org/10.1016/j.ijpharm.2009.10.047

81) Hassan, M. S., & Lau, R. (2011). Inhalation performance of pollen-shape carrier in dry powder formulation: Effect of size and surface morphology. *International Journal of Pharmaceutics*. https://doi.org/10.1016/j.ijpharm.2011.04.033

82) Hatch, T. F., & Gross, P. (1964). Pulmonary deposition and retention of inhaled particles. *New York, Academic Press. Landahl, HD (1950). Bull. Math. Biophys*, *12*(43), 161–174.

83) Haynes, A., Shaik, M. S., Chatterjee, A., & Singh, M. (2003). Evaluation of an aerosolized selective COX-2 inhibitor as a potentiator of doxorubicin in a non-small-cell lung cancer cell line. *Pharmaceutical Research*. https://doi.org/10.1023/A:1025774630993

84) Hazare, S., & Menon, M. (2009). Improvement of Inhalation Profile of DPI Formulations by Carrier Treatment with Magnesium Stearate. *Indian Journal of Pharmaceutical Sciences*, *71*(6), 725–727. 85. Heckel, R. W. (1961). Density-Pressure Relationships in Powder Compaction. *Transactions of the Metallurgical Society of AIME*.

85) Heng, P. W., Chan, L. W., & Lim, L. T. (2000). Quantification of the surface morphologies of lactose carriers and their effect on the in vitro deposition of salbutamol sulphate. *Chemical & Pharmaceutical Bulletin*. https://doi.org/10.1248/cpb.48.393

86) Hersey, J. A. (1974). Powder Mixing by Frictional Pressure: Specific Example of Use of Ordered Mixing. *Journal of Pharmaceutical Sciences*, *63*(12), 1960–1961. https://doi.org/10.1002/JPS.2600631233

87) Hersey, J. A. (1975). ORDERED MIXING: A NEW CONCEPT IN POWDER MIXING PRACTICE. *Powder Technology*. https://doi.org/10.1016/0032-5910(75)80021-0

88) Hertel, M., Schwarz, E., Kobler, M., Hauptstein, S., Steckel, H., & Scherließ, R. (2018). Powder flow analysis: A simple method to indicate the ideal amount of lactose fines in dry powder inhaler formulations. *International Journal of Pharmaceutics*. https://doi.org/10.1016/j.ijpharm.2017.10.052

89) Heyder, J. (2004). Deposition of Inhaled Particles in the Human Respiratory Tract and Consequences for Regional Targeting in Respiratory Drug Delivery. *Proceedings of the American Thoracic Society*. https://doi.org/10.1513/pats.200409-046TA

90) Hickey, A. J., Mansour, H. M., Telko, M. J., Xu, Z., Smyth, H. D. C., Mulder, T., ... Papadopoulos, D. (2007). Physical characterization of component particles included in dry powder inhalers. I. Strategy review and static characteristics. *Journal of Pharmaceutical Sciences*. https://doi.org/10.1002/jps.20916

91) Hiestand, E. N. (1966). Powders: Particle-particle interactions. *Journal of Pharmaceutical Sciences*. https://doi.org/10.1002/jps.2600551202

92) Hinds (1982). Current management of patients after cardiopulmonary bypass. *Anaesthesia*. https://doi.org/10.1111/j.1365-2044.1982.tb01058.x

93) Hinds, W. C. (1999). Properties, Behavior, and Measurement ofAirborne Particles. *Journal of Aerosol Science*. https://doi.org/10.1016/0021-8502(83)90049-6

94) Hussain, M., Madl, P., & Khan, a. (2011). Lung deposition predictions of airborne particles and the emergence of contemporary diseases, Part-I. *The Health*.

95) Iida, K., Hayakawa, Y., Okamoto, H., Danjo, K., & Leuenberger, H. (2003). Preparation of Dry Powder Inhalation by Surface Treatment of Lactose Carrier Particles. *CHEMICAL & PHARMACEUTICAL BULLETIN*. https://doi.org/10.1248/cpb.51.1

96) Iida, K., Inagaki, Y., Todo, H., & Okamoto, H. (2004). Effects of surface processing of lactose carrier particles on dry powder inhalation properties of salbutamol sulfate. *Chemical and ...*. https://doi.org/10.1248/cpb.52.938

97) Ikegami, K., Kawashima, Y., Takeuchi, H., Yamamoto, H., Isshiki, N., Momose, D. I., & Ouchi, K. (2002). Improved inhalation behavior of steroid KSR-592 in vitro with Jethaler® by polymorphic transformation to needle-like crystals (β-form). *Pharmaceutical Research*. https://doi.org/10.1023/A:1020492213172

98) Islam, N., & Cleary, M. J. (2012). Developing an efficient and reliable dry powder inhaler for pulmonary drug delivery – A review for multidisciplinary researchers. *Medical Engineering & Physics*. https://doi.org/10.1016/j.medengphy.2011.12.025

99) Islam, N., & Rahman, S. (2008). Pulmonary drug delivery: Implication for new strategy for pharmacotherapy for neurodegenerative disorders. *Drug Discov Ther*.

100) Islam, N., Stewart, P., Larson, I., & Hartley, P. (2004a). Effect of Carrier Size on the Dispersion of Salmeterol Xinafoate from Interactive Mixtures. *Journal of Pharmaceutical Sciences*. https://doi.org/10.1002/jps.10583

101) Islam, N., Stewart, P., Larson, I., & Hartley, P. (2004b). Lactose surface modification by decantation: Are drug-fine lactose ratios the key to better dispersion of salmeterol xinafoate from lactose-interactive mixtures? *Pharmaceutical Research*. https://doi.org/10.1023/B:PHAM.0000019304.91412.18

102) Jashnani, R. N., Byron, P. R., & Dalby, R. N. (1995). Testing of dry powder aerosol formulations in different environmental conditions. *International Journal of Pharmaceutics*. https://doi.org/10.1016/0378-5173(94)00197-D

103) Jones, M. D., Harris, H., Hooton, J. C., Shur, J., King, G. S., Mathoulin, C. A., ... Price, R. (2008). An investigation into the relationship between carrier-based dry powder inhalation performance and formulation cohesive-adhesive force balances. *European Journal of Pharmaceutics and Biopharmaceutics*. https://doi.org/10.1016/j.ejpb.2007.11.019

104) Jones, M. D., Young, P. M., Traini, D., Shur, J., Edge, S., & Price, R. (2008). The use of atomic force microscopy to study the conditioning of micronised budesonide. *International Journal of Pharmaceutics*. https://doi.org/10.1016/j.ijpharm.2008.01.042

105) Jones, S. A., Martin, G. P., & Brown, M. B. (2004). Determination of polyvinylpyrrolidone using high-performance liquid chromatography. *Journal of Pharmaceutical and Biomedical Analysis*. https://doi.org/10.1016/j.jpba.2004.01.024

106) Kaialy, W. (2016). A review of factors affecting electrostatic charging of pharmaceuticals and adhesive mixtures for inhalation. *International Journal of Pharmaceutics*. https://doi.org/10.1016/j.ijpharm.2016.01.076

107) Kaialy, W., Alhalaweh, A., Velaga, S. P., & Nokhodchi, A. (2011). Effect of carrier particle shape on dry powder inhaler performance. *International Journal of Pharmaceutics*. https://doi.org/10.1016/j.ijpharm.2011.09.010

108) Kaialy, W., Alhalaweh, A., Velaga, S. P., & Nokhodchi, A. (2012a). Influence of lactose carrier particle size on the aerosol performance of budesonide from a dry powder inhaler. *Powder Technology*. https://doi.org/10.1016/j.powtec.2012.03.006

109) Kaialy, W., Martin, G. P., Larhrib, H., Ticehurst, M. D., Kolosionek, E., & Nokhodchi, A. (2012b). The influence of physical properties and morphology of crystallised lactose on delivery of salbutamol sulphate from dry powder inhalers. *Colloids and Surfaces B: Biointerfaces*. https://doi.org/10.1016/j.colsurfb.2011.08.019

110) Kaialy, W., & Nokhodchi, A. (2013). Engineered Mannitol Ternary Additives Improve Dispersion of Lactose–Salbutamol Sulphate Dry Powder Inhalations. *The AAPS Journal*. https://doi.org/10.1208/s12248-013-9476-4

111) Kalman, H. (2000). Attrition of powders and granules at various bends during pneumatic conveying. *Powder Technology*, *112*(3), 244–250.

112) Karhu, M., Kuikka, J., Kauppinen, T., Bergström, K., & Vidgren, M. (2000). Pulmonary deposition of lactose carriers used in inhalation powders. *International Journal of Pharmaceutics*. https://doi.org/10.1016/S0378-5173(99)00450-0

113) Karner, S., Littringer, E. M., & Urbanetz, N. A. (2014). Triboelectrics: The influence of particle surface roughness and shape on charge acquisition during aerosolization and the DPI performance. *Powder Technology*. https://doi.org/10.1016/j.powtec.2014.04.025

114) Karner, S., Maier, M., Littringer, E., & Urbanetz, N. A. (2014). Surface roughness effects on the tribo-charging and mixing homogeneity of adhesive mixtures used in dry powder inhalers. *Powder Technology*. https://doi.org/10.1016/j.powtec.2014.03.040

115) Karner, S., & Urbanetz, N. A. (2013). Triboelectric characteristics of mannitol based formulations for the application in dry powder inhalers. *Powder Technology*. https://doi.org/10.1016/j.powtec.2012.10.034 117.

116) Katainen, J., Paajanen, M., Ahtola, E., Pore, V., & Lahtinen, J. (2006). Adhesion as an interplay between particle size and surface roughness. *Journal of Colloid and Interface Science*. https://doi.org/10.1016/j.jcis.2006.09.015

117) Kawashima, Y., Serigano, T., Hino, T., Yamamoto, H., & Takeuchi, H. (1998a). A new powder design method to improve inhalation efficiency of pranlukast hydrate dry powder aerosols by surface modification with hydroxypropylmethylcellulose phthalate nanospheres. *Pharmaceutical Research*. https://doi.org/10.1023/A:1011916930655

118) Kawashima, Y., Serigano, T., Hino, T., Yamamoto, H., & Takeuchi, H. (1998b). Effect of surface morphology of carrier lactose on dry powder inhalation property of pranlukast hydrate. *International Journal of Pharmaceutics*. https://doi.org/10.1016/S0378- 5173(98)00202-6

119) Kho, K., & Hadinoto, K. (2013). Dry powder inhaler delivery of amorphous drug nanoparticles: effects of the lactose carrier particle shape and size. *Powder Technology*, *233*, 303–311.

Kitaigorodsky, A. I., & Ahmed, N. A. (1972). Theoretical determination of the geometrical form of the crystal of anthracene. *Acta Crystallographica Section A*. https://doi.org/10.1107/S0567739472000439

120) Kou, X., Chan, L. W., Steckel, H., & Heng, P. W. S. (2012). Physico-chemical aspects of lactose for inhalation. *Advanced Drug Delivery Reviews*. https://doi.org/10.1016/j.addr.2011.11.004

121) Kulvanich, P., & Stewart, P. J. (1987). An evaluation of the air stream Faraday cage in the electrostatic charge measurement of interactive drug systems. *International Journal of Pharmaceutics*. https://doi.org/10.1016/0378-5173(87)90161-X

122) Kumon, M., Machida, S., Suzuki, M., Kusai, A., Yonemochi, E., & Terada, K. (2008). Application and mechanism of inhalation profile improvement of DPI formulations by

mechanofusion with magnesium stearate. *Chemical & Pharmaceutical Bulletin*. https://doi.org/10.1248/cpb.56.617

123) Kumon, M., Suzuki, M., Kusai, A., Yonemochi, E., & Terada, K. (2006). Novel approach to DPI carrier lactose with mechanofusion process with additives and evaluation by IGC. *Chemical & Pharmaceutical Bulletin*. https://doi.org/10.1248/cpb.54.1508

124) Labiris, N. R., & Dolovich, M. B. (2003). Pulmonary drug delivery. Part II: The role of inhalant delivery devices and drug formulations in therapeutic effectiveness of aerosolized medications. *British Journal of Clinical Pharmacology*. https://doi.org/10.1046/j.1365-2125.2003.01893.x

125) Lachman, L., & Lin, S. (1968). Electrostatic characteristics of pharmaceutical solids and packaging materials I. Design of testing equipment and preliminary findings. *Journal of Pharmaceutical Sciences*, *57*(3), 504–510.

126) Larhrib, H., Martin, G. P., Marriott, C., & Prime, D. (2003). The influence of carrier and drug morphology on drug delivery from dry powder formulations. *International Journal of Pharmaceutics*. https://doi.org/10.1016/S0378-5173(03)00156-X

127) Larhrib, H., Martin, G. P., Prime, D., & Marriott, C. (2003). Characterisation and deposition studies of engineered lactose crystals with potential for use as a carrier for aerosolised salbutamol sulfate from dry powder inhalers. *European Journal of Pharmaceutical Sciences*. https://doi.org/10.1016/S0928-0987(03)00105-2

128) Larhrib, H., Zeng, X. M., Martin, G. P., Marriott, C., & Pritchard, J. (1999). The use of different grades of lactose as a carrier for aerosolised salbutamol sulphate. *International Journal of Pharmaceutics*. https://doi.org/10.1016/S0378-5173(99)00164-7

129) Laube, B. L., Janssens, H. M., De Jongh, F. H. C., Devadason, S. G., Dhand, R., Diot, P., ... Chrystyn, H. (2011). What the pulmonary specialist should know about the new

inhalation therapies. *European Respiratory Journal*. https://doi.org/10.1183/09031936.00166410

130) Lavorini, F., Pistolesi, M., & Usmani, O. S. (2017). Recent advances in capsule-based dry powder inhaler technology. *Multidisciplinary Respiratory Medicine*. https://doi.org/10.1186/s40248-017-0092-5

131) Lee, S. H., Heng, D., Ng, W. K., Chan, H. K., & Tan, R. B. H. (2011). Nano spray drying: A novel method for preparing protein nanoparticles for protein therapy. *International Journal of Pharmaceutics*. https://doi.org/10.1016/j.ijpharm.2010.10.012

132) Li, H. Y., Seville, P. C., Williamson, I. J., & Birchall, J. C. (2005). The use of amino acids to enhance the aerosolisation of spray-dried powders for pulmonary gene therapy. *Journal of Gene Medicine*. https://doi.org/10.1002/jgm.654

133) Li, Q., Rudolph, V., & Peukert, W. (2006). London-van der Waals adhesiveness of rough particles. *Powder Technology*. https://doi.org/10.1016/j.powtec.2005.10.012

134) Louey, M. D., Razia, S., & Stewart, P. J. (2003). Influence of physico-chemical carrier properties on the in vitro aerosol deposition from interactive mixtures. *International Journal of Pharmaceutics*. https://doi.org/10.1016/S0378-5173(02)00621-X

135) Lucas, P., Anderson, K., Potter, U. J., & Staniforth, J. N. (1999). Enhancement of small particle size dry powder aerosol formulations using an ultra low density additive. *Pharmaceutical Research*. https://doi.org/10.1023/A:1011981326827

136) Lucas, P., Anderson, K., & Staniforth, J. N. (1998). Protein deposition from dry powder inhalers: Fine particle multiplets as performance modifiers. *Pharmaceutical Research*. https://doi.org/10.1023/A:1011977826711

137) Malcolmson, R. J., & Embleton, J. K. (1998). Dry powder formulations for pulmonary delivery. *Pharmaceutical Science and Technology Today*. https://doi.org/10.1016/S1461- 5347(98)00099-6

138) Marple, V. A., Roberts, D. L., Romay, F. J., Miller, N. C., Truman, K. G., Van Oort, M., ... Hochrainer, D. (2003). Next generation pharmaceutical impactor (a new impactor for pharmaceutical inhaler testing). Part I: Design. *Journal of Aerosol Medicine*, *16*(3), 283– 299.

139) Martini & Nath, J. (2009). *Fundamentals of Anatomy and Physiology*. *Learning*. https://doi.org/612

140) Masters, K. (1988). Drying of droplets/sprays. *Spray Drying Handbook, Wiley, New York*, 298–342.

141) Matsusaka, S., Chìn, K., Ogura, M., Suenaga, M., Shinozaki, E., Mishima, Y., ... Hatake, K. (2010). Circulating tumor cells as a surrogate marker for determining response to chemotherapy in patients with advanced gastric cancer. *Cancer Science*. https://doi.org/10.1111/j.1349-7006.2010.01492.x

142) McPolin, O. (2009). *Validation of analytical methods for pharmaceutical analysis*. Lulu. com.

143) Meyer, T., Brand, P., Ehlich, H., Köbrich, R., Meyer, G., Riedinger, F., ... Scheuch, G. (2004). Deposition of {Foradil} {P} in human lungs: comparison of in vitro and in vivo data. *Journal of Aerosol Medicine: The Official Journal of the International Society for Aerosols in Medicine*. https://doi.org/10.1089/089426804322994451

144) Morén, F. (1987). Dosage forms and formulations for drug administration to the respiratory tract. *Drug Development and Industrial Pharmacy*. https://doi.org/10.3109/03639048709105214

145) Mullin, J. W. (2001). *Crystallization*. Elsevier.

146) Mullins, M. E., Michaels, L. P., Menon, V., Locke, B., & Ranade, M. B. (1992). Effect of geometry on particle adhesion. *Aerosol Science and Technology*. https://doi.org/10.1080/02786829208959564

147) Murtomaa, M., Mellin, V., Harjunen, P., Lankinen, T., Laine, E., & Lehto, V. P. (2004). Effect of particle morphology on the triboelectrification in dry powder inhalers. *International Journal of Pharmaceutics*. https://doi.org/10.1016/j.ijpharm.2004.06.002

148) Murtomaa, M., Ojanen, K., Laine, E., & Poutanen, J. (2002). Effect of detergent on powder triboelectrification. *European Journal of Pharmaceutical Sciences*. https://doi.org/10.1016/S0928-0987(02)00167-7

149) Murtomaa, M., Savolainen, M., Christiansen, L., Rantanen, J., Laine, E., & Yliruusi, J. (2004). Static electrification of powders during spray drying. *Journal of Electrostatics* https://doi.org/10.1016/j.elstat.2004.05.001

150) Muselík, J., Franc, A., Doležel, P., Goněc, R., Krondlová, A., & Lukášová, I. (2014). Influence of process parameters on content uniformity of a low dose active pharmaceutical ingredient in a tablet formulation according to GMP. *Acta Pharmaceutica*, *64*(3), 355–367.

151) Nadarassan, D. K., Assi, K. H., & Chrystyn, H. (2010). Aerodynamic characteristics of a dry powder inhaler at low inhalation flows using a mixing inlet with an Andersen Cascade Impactor. *European Journal of Pharmaceutical Sciences*. https://doi.org/10.1016/j.ejps.2010.01.002

152) Newman, S. P., & Busse, W. W. (2002). Evolution of dry powder inhaler design, formulation, and performance. *Respiratory Medicine*. https://doi.org/10.1053/rmed.2001.1276

153) Nielsen, K. G., Skov, M., Klug, B., Ifversen, M., & Bisgaard, H. (1997). Flow-dependent effect of formoterol dry-powder inhaled from the Aerolizer®. *European Respiratory Journal*. https://doi.org/10.1183/09031936.97.10092105

154) Nokhodchi, A., & Martin, G. P. (2015). *Pulmonary Drug Delivery: Advances and Challenges*. John Wiley & Sons.

155) Olsson, B. O., & Asking, L. (1994). A model for the effect of inhalation device flow resistance on the peak inspiratory flow rate and its application in pharmaceutical testing. *Journal of Aerosol Medicine*, *7*(2), 201–204.

156) Patton and Byron (1994). Drug delivery via the respiratory tract. *Journal of Aerosol Medicine: Deposition, Clearance, and Effects in the Lung*.

157) Palander, A., Mattila, T., Karhu, M., & Muttonen, E. (2000). In vitro Comparison of Three Salbutamol-Containing Multidose Dry Powder Inhalers. *Clinical Drug Investigation*. https://doi.org/10.2165/00044011-200020010-00004

158) Parlati, C., Colombo, P., Buttini, F., Young, P. M., Adi, H., Ammit, A. J., & Traini, D. (2009). Pulmonary Spray Dried Powders of Tobramycin Containing Sodium Stearate to Improve Aerosolization Efficiency. *Pharmaceutical Research*. https://doi.org/10.1007/s11095-009-9825-2

159) Pasquali, I., Merusi, C., Brambilla, G., Long, E. J., Hargrave, G. K., & Versteeg, H. K. (2015). Optical diagnostics study of air flow and powder fluidisation in Nexthaler®—Part I: Studies with lactose placebo formulation. *International Journal of Pharmaceutics*, *496*(2), 780–791.

160) Pavkov, R., Mueller, S., Fiebich, K., Singh, D., Stowasser, F., Pignatelli, G., ... Rietveld, I. (2010). Characteristics of a capsule based dry powder inhaler for the delivery of indacaterol. *Current Medical Research and Opinion*. https://doi.org/10.1185/03007995.2010.518916 163. Peart, J. (1996). Electrostatic charge interactions in pharmaceutical dry powder aerosols. University of Bath.

161) Peng, T., Lin, S., Niu, B., Wang, X., Huang, Y., Zhang, X., ... Wu, C. (2016). Influence of physical properties of carrier on the performance of dry powder inhalers. *Acta Pharmaceutica Sinica B*. https://doi.org/10.1016/j.apsb.2016.03.011 165.

Pharmacopeia, U. S., & Revision, X. (1995). US Pharmacopeial convention. *Inc., Rockville, MD*, 1161–1162.

162) Pilcer, G., & Amighi, K. (2010). Formulation strategy and use of excipients in pulmonary drug delivery. *International Journal of Pharmaceutics*. https://doi.org/10.1016/j.ijpharm.2010.03.017

163) Pilcer, G., Wauthoz, N., & Amighi, K. (2012). Lactose characteristics and the generation of the aerosol. *Advanced Drug Delivery Reviews*. https://doi.org/10.1016/j.addr.2011.05.003 168.

164) Podczeck, F. (1999). The Influence of Particle Size Distribution and Surface Roughness of Carrier Particles on the in vitro Properties of Dry Powder Inhalations. *Aerosol Science and Technology American Association for Aerosol Rese Arch*. 169. Prime, D. (1997). Review of dry powder inhalers. *Advanced Drug Delivery Reviews*. https://doi.org/10.1016/S0169-409X(97)00510-3

165) Rabbani, N. R., & Seville, P. C. (2005). The influence of formulation components on the aerosolisation properties of spray-dried powders. *Journal of Controlled Release*. https://doi.org/10.1016/j.jconrel.2005.09.004

166) Rahimpour, Y., & Hamishehkar, H. (2012). Lactose engineering for better performance in dry powder inhalers. *Advanced Pharmaceutical Bulletin*. https://doi.org/10.5681/apb.2012.028

167) Raula, J., Thielmann, F., Naderi, M., Lehto, V. P., & Kauppinen, E. I. (2010). Investigations on particle surface characteristics vs. dispersion behaviour of l-leucine coated carrier-free inhalable powders. *International Journal of Pharmaceutics*. https://doi.org/10.1016/j.ijpharm.2009.10.036

168) Roberts, R. J., & Rowe, R. C. (1985). The effect of punch velocity on the compaction of a variety of materials. *Journal of Pharmacy and Pharmacology*. https://doi.org/10.1111/j.2042-7158.1985.tb03019.x

169) Roche, N., Chrystyn, H., Lavorini, F., Agusti, A., Virchow, J. C., Dekhuijzen, R., & Price, D. (2013). Effectiveness of Inhaler Devices in Adult Asthma and Copd. *Citation: EMJ Respir*.

170) Sahane, S. P., Nikhar, A. K., Bhaskaran, S., & Mundhada, D. R. (2012). Dry powder inhaler : An advance technique for pulmonary drug delivery system. *International Journal of Pharmaceutical and Chemical Science*.

171) Saleki-Gerhardt, A., Ahlneck, C., & Zografi, G. (1994). Assessment of disorder in crystalline solids. *International Journal of Pharmaceutics*. https://doi.org/10.1016/0378- 5173(94)90219-4

172) Schoubben, A., Blasi, P., Giovagnoli, S., Ricci, M., & Rossi, C. (2010). Simple and scalable method for peptide inhalable powder production. *European Journal of Pharmaceutical Sciences*, *39*(1–3), 53–58.

173) Sebhatu, T., Angberg, M., & Ahlneck, C. (1994). Assessment of the degree of disorder in crystalline solids by isothermal microcalorimetry. *International Journal of Pharmaceutics*. https://doi.org/10.1016/0378-5173(94)90188-0

174) Shekunov, B. Y., Feeley, J. C., Chow, A. H. L., Tong, H. H. Y., & York, P. (2003). Aerosolisation behaviour of micronised and supercritically-processed powders. *Journal of Aerosol Science*. https://doi.org/10.1016/S0021-8502(03)00022-3

175) Shen, S. C., Ng, W. K., Chia, L., Dong, Y. C., & Tan, R. B. H. (2010). Stabilized amorphous state of ibuprofen by co-spray drying with mesoporous SBA-15 to enhance dissolution properties. *Journal of Pharmaceutical Sciences*. https://doi.org/10.1002/jps.21967

176) Siddiqui, M. A. A., & Plosker, G. L. (2005). The Novolizer®: A multidose dry powder inhaler. *Treatments in Respiratory Medicine*. https://doi.org/10.2165/00151829-200504010-00007

177) Simpkin, G. T., Trunley, R., & Leighton, A.-M. (1999, June 1). Inhalation powder containing antistatic agent. Google Patents.

178) Smith, I. J., & Parry-Billings, M. (2003). The inhalers of the future? A review of dry powder devices on the market today. *Pulmonary Pharmacology and Therapeutics*. https://doi.org/10.1016/S1094-5539(02)00147-5

179) Sosnik, A., & Seremeta, K. P. (2015). Advantages and challenges of the spray-drying technology for the production of pure drug particles and drug-loaded polymeric carriers. *Advances in Colloid and Interface Science*. https://doi.org/10.1016/j.cis.2015.05.003

180) Srichana, T., Martin, G. P., & Marriott, C. (1998). Dry powder inhalers: The influence of device resistance and powder formulation on drug and lactose deposition in vitro. *European Journal of Pharmaceutical Sciences*. https://doi.org/10.1016/S0928-0987(98)00008-6

181) Ståhl, K., Claesson, M., Lilliehorn, P., Lindén, H., & Bäckström, K. (2002). The effect of process variables on the degradation and physical properties of spray dried insulin intended for inhalation. *International Journal of Pharmaceutics*. https://doi.org/10.1016/S0378-5173(01)00945-0

182) Staniforth, J. N. (1995). Performance-modifying influences in dry powder inhalation systems. *Aerosol Science and Technology*. https://doi.org/10.1080/02786829408959752

183) Staniforth, J. N. (1997). Improvements in or relating to powders for use in dry powder inhalers. *WO*, *97*, 3649.

184) Staniforth, J. N., Rees, J. E., Lai, F. K., & Hersey, T. L. J. A. (1982). Interparticle forces in binary and ternary ordered powder mixes. *Journal of Pharmacy and Pharmacology*. https://doi.org/10.1111/j.2042-7158.1982.tb04210.x

185) Steckel, H., & Bolzen, N. (2004). Alternative sugars as potential carriers for dry powder inhalations. *International Journal of Pharmaceutics*. https://doi.org/10.1016/j.ijpharm.2003.10.039

186) Steckel, H., & Müller, B. W. (1997). In vitro evaluation of dry powder inhalers II: Influence of carrier particle size and concentration on in vitro deposition. *International Journal of Pharmaceutics*. https://doi.org/10.1016/S0378-5173(97)00115-4

187) Šupuk, E.,Seiler C., and Ghadiri, M. (2009). Analysis of a simple test device for Tribo-Electric charging of bulk powders, particles and particle system characterisation, 26 (1-2), 7-16

188) Šupuk, E., Zarrebini, A., Reddy, J. P., Hughes, H., Leane, M. M., Tobyn, M. J., Ghadiri, M. (2012). Tribo-electrification of active pharmaceutical ingredients and excipients. *Powder Technology*. https://doi.org/10.1016/j.powtec.2011.10.059

189) Tarsin, W. Y., Pearson, S. B., Assi, K. H., & Chrystyn, H. (2006). Emitted dose estimates from Seretide® Diskus® and Symbicort® Turbuhaler® following inhalation by severe asthmatics. *International Journal of Pharmaceutics*. https://doi.org/10.1016/j.ijpharm.2006.02.040

190) Tee, S. K., Marriott, C., Zeng, X. M., & Martin, G. P. (2000). The use of different sugars as fine and coarse carriers for aerosolised salbutamol sulphate. *International Journal of Pharmaceutics*. https://doi.org/10.1016/S0378-5173(00)00553-6

191) Telko, M. J., & Hickey, A. J. (2005). Dry powder inhaler formulation. *Respiratory Care*. https://doi.org/10.2165/00128413-200615470-00016

192) Telko, M. J., Kujanpää, J., & Hickey, A. J. (2007). Investigation of triboelectric charging in dry powder inhalers using electrical low pressure impactor (ELPITM). *International Journal of Pharmaceutics*. https://doi.org/10.1016/j.ijpharm.2006.12.018

193) Thakur, R. R. S., Tekko, I. A., Al-Shammari, F., Ali, A. A., McCarthy, H., & Donnelly, R. F. (2016). Rapidly dissolving polymeric microneedles for minimally invasive intraocular drug delivery. *Drug Delivery and Translational Research*. https://doi.org/10.1007/s13346-016-0332-9

194) Thibert, R., & Tawashi, R. (1999). Micronization of pharmaceutical solids. *MML SERIES*, *1*, 327.

195) Thomas, S. H. L., O'Doherty, M. J., Graham, A., Page, C. J., Blower, P., Geddes, D. M., & Nunan, T. O. (1991). Pulmonary deposition of nebulised amiloride in cystic fibrosis: Comparison of two nebulisers. *Thorax*. https://doi.org/10.1136/thx.46.10.717

196) Tian, Y., Klegerman, M. E., & Hickey, A. J. (2004). Evaluation of microparticles containing doxorubicin suitable for aerosol delivery to the lungs. *PDA J Pharm Sci Technol*.

197) Timsina, M. P., Martin, G. P., Marriott, C., Ganderton, D., & Yianneskis, M. (1994). Drug delivery to the respiratory tract using dry powder inhalers. *International Journal of Pharmaceutics*. https://doi.org/10.1016/0378-5173(94)90070-1

198) Tsai, C. J., Lin, J. S., Deshpande, C. G., & Liu, L. C. (2006). Electrostatic charge measurement and charge neutralization of fine aerosol particles during the generation process. *Particle and Particle Systems Characterization*. https://doi.org/10.1002/ppsc.200500961

199) Vehring, R. (2008). Pharmaceutical particle engineering via spray drying. *Pharmaceutical Research*. https://doi.org/10.1007/s11095-007-9475-1

200) Venables, H. J., & Wells, J. I. (2001). Powder mixing. *Drug Development and Industrial Pharmacy*. https://doi.org/10.1081/DDC-100107316

201) Vidgren, M., Kärkkäinen, A., Karjalainen, P., Paronen, P., & Nuutinen, J. (1988). Effect of powder inhaler design on drug deposition in the respiratory tract. *International Journal of Pharmaceutics*. https://doi.org/10.1016/0378-5173(88)90177-9

202) Voss, A., & Finlay, W. H. (2002). Deagglomeration of dry powder pharmaceutical aerosols. *International Journal of Pharmaceutics*, *248*(1–2), 39–50.

203) Waldron, J. (2007). *Asthma Care in the Community*. John Wiley & Sons.

204) Weibel, E. R. (1963). Geometric and Dimensional Airway Models of Conductive,

205) Transitory and Respiratory Zones of the Human Lung. In *Morphometry of the Human Lung* (pp. 136–142). Berlin, Heidelberg: Springer Berlin Heidelberg. https://doi.org/10.1007/978-3-642-87553-3_11

206) Welte, T. (2009). Optimising treatment for COPD - New strategies for combination therapy. *International Journal of Clinical Practice*, *63*(8), 1136–1149. https://doi.org/10.1111/j.1742-1241.2009.02139.x

207) Weuthen, T., Roeder, S., Brand, P., Müllinger, B., & Scheuch, G. (2002). In vitro testing of two formoterol dry powder inhalers at different flow rates. *Journal of Aerosol Medicine : The Official Journal of the International Society for Aerosols in Medicine*. https://doi.org/10.1089/089426802760292636

208) Williams, R. L., Adams, W. P., Poochikian, G., & Hauck, W. W. (2002). Content uniformity and dose uniformity: Current approaches, statistical analyses, and presentation of an alternative approach, with special reference to oral inhalation and nasal drug products. *Pharmaceutical Research*. https://doi.org/10.1023/A:1015114821387

209) Wolff, R. K., & Dorato, M. A. (1993). Toxicologic testing of inhaled pharmaceutical aerosols. *Critical Reviews in Toxicology*. https://doi.org/10.3109/10408449309104076

210) Yamamoto, H., Kuno, Y., Sugimoto, S., Takeuchi, H., & Kawashima, Y. (2005). Surface- modified PLGA nanosphere with chitosan improved pulmonary delivery of calcitonin by mucoadhesion and opening of the intercellular tight junctions. *Journal of Controlled Release*. https://doi.org/10.1016/j.jconrel.2004.10.010

211) Yang, M. Y., Chan, J. G. Y., & Chan, H.-K. (2014). Pulmonary drug delivery by powder aerosols. *Journal of Controlled Release*, *193*, 228–240.

212) Yang, T., Mustafa, F., Bai, S., & Ahsan, F. (2004). Pulmonary delivery of low molecular weight heparins. *Pharmaceutical Research*. https://doi.org/10.1023/B:PHAM.0000048191.69098.d6

213) Yawn, B. P. (2009). Differential assessment and management of asthma vs chronic obstructive pulmonary disease CME. *MedGenMed Medscape General Medicine*, *11*(1). Retrieved from http://www.embase.com/search/results?subaction=viewrecord&from=export&id=L354 133914%5Cnhttp://journal.medscape.com/viewprogram/18776_pnt

214) Yeomans, A. H., Rogers, E. E., & Ball, W. H. (1949). Deposition of Aerosol Particles. *Journal of Economic Entomology*, *42*(4), 591–596. Retrieved from http://dx.doi.org/10.1093/jee/42.4.591

215) Young, P. M., Chiou, H., Tee, T., Traini, D., Chan, H. K., Thielmann, F., & Burnett, D. (2007). The use of organic vapor sorption to determine low levels of amorphous content in processed pharmaceutical powders. *Drug Development and Industrial Pharmacy*. https://doi.org/10.1080/03639040600969991

216) Young, P. M., Cocconi, D., Colombo, P., Bettini, R., Price, R., Steele, D. F., & Tobyn, M. J. (2002). Characterization of a surface modified dry powder inhalation carrier

prepared by “particle smoothing”. *The Journal of Pharmacy and Pharmacology*. https://doi.org/10.1211/002235702760345400

217) Young, P. M., Edge, S., Traini, D., Jones, M. D., Price, R., El-Sabawi, D., ... Smith, C. (2005). The influence of dose on the performance of dry powder inhalation systems. *International Journal of Pharmaceutics*. https://doi.org/10.1016/j.ijpharm.2005.02.004

218) Yu, Z.-Z. G., & Watson, K. (2001). Two-step model for contact charge accumulation. *Journal of Electrostatics*, *51*, 313–318.

219) Yue, B., Yang, J., Wang, Y., Huang, C. Y., Dave, R., & Pfeffer, R. (2004). Particle encapsulation with polymers via in situ polymerization in supercritical CO2. *Powder Technology*. https://doi.org/10.1016/j.powtec.2004.07.002

220) Zellnitz, S., Redlinger-Pohn, J. D., Kappl, M., Schroettner, H., & Urbanetz, N. A. (2013). Preparation and characterization of physically modified glass beads used as model carriers in dry powder inhalers. *International Journal of Pharmaceutics*. https://doi.org/10.1016/j.ijpharm.2013.02.044

221) Zellnitz, S., Schroettner, H., & Urbanetz, N. A. (2015). Influence of surface characteristics of modified glass beads as model carriers in dry powder inhalers (DPIs) on the aerosolization performance. *Drug Development and Industrial Pharmacy*. https://doi.org/10.3109/03639045.2014.997246

222) Zeng, X. M., Martin, G. P., Marriott, C., & Pritchard, J. (2000). The effects of carrier size and morphology on the dispersion of salbutamol sulphate after aerosolization at different flow rates. *The Journal of Pharmacy and Pharmacology*. https://doi.org/10.1211/0022357001777342

223) Zeng, X. M., Martin, G. P., Marriott, C., & Pritchard, J. (2000). The influence of carrier morphology on drug delivery by dry powder inhalers. *International Journal of Pharmaceutics*. https://doi.org/10.1016/S0378-5173(00)00347-1

224) Zeng, X. M., Martin, G. P., Marriott, C., & Pritchard, J. (2001a). Lactose as a carrier in dry powder formulations: The influence of surface characteristics on drug delivery. *Journal of Pharmaceutical Sciences*. https://doi.org/10.1002/jps.1094

225) Zeng, X. M., Martin, G. P., Marriott, C., & Pritchard, J. (2001b). The use of lactose recrystallised from carbopol gels as a carrier for aerosolised salbutamol sulphate. *European Journal of Pharmaceutics and Biopharmaceutics*. https://doi.org/10.1016/S0939-6411(00)00142-9

226) Zeng, X. M., Martin, G. P., Tee, S. K., & Marriott, C. (1998). The role of fine particle lactose on the dispersion and deaggregation of salbutamol sulphate in an air stream in vitro. *International Journal of Pharmaceutics*. https://doi.org/10.1016/S0378-5173(98)00300-7

227) Zeng, X. M., Pandhal, K. H., & Martin, G. P. (2000). The influence of lactose carrier on the content homogeneity and dispersibility of beclomethasone dipropionate from dry powder aerosols. *International Journal of Pharmaceutics*. https://doi.org/10.1016/S0378-5173(99)00400-7

228) Zhou, Q., Qu, L., Gengenbach, T., Larson, I., Stewart, P. J., & Morton, D. A. V. (2013). Effect of Surface Coating with Magnesium Stearate via Mechanical Dry Powder Coating Approach on the Aerosol Performance of Micronized Drug Powders from Dry Powder Inhalers. *AAPS PharmSciTech*. https://doi.org/10.1208/s12249-012-9895-z

229) Zhou, Q. T., & Morton, D. A. V. (2012). Drug-lactose binding aspects in adhesive mixtures: Controlling performance in dry powder inhaler formulations by altering lactose carrier surfaces. *Advanced Drug Delivery Reviews*. https://doi.org/10.1016/j.addr.2011.07.002

230) Zhou, Q. T., Qu, L., Larson, I., Stewart, P. J., & Morton, D. A. V. (2010). Improving aerosolization of drug powders by reducing powder intrinsic cohesion via a mechanical

dry coating approach. *International Journal of Pharmaceutics*. https://doi.org/10.1016/j.ijpharm.2010.04.032

231) Zimon, A. (1982). Adhesion of Dust and Particles. *Consultants Bureau, NY*, 154.

232) https://www.pdhpe.net/the-body-in-motion/how-do-the-musculoskeletal-and-cardiorespiratory-systems-of-the-body-influence-and-respond-to-movement/respiratory-system/structure-and-function, accessed October 2017

233) (NHS improvement program asthma, available at https://www.pharmaceutical-journal.com/learning/learning-article/knowing-the-differences-between-copd-and-asthma-is-vital-to-good-practice/11085597.article